
THE UNIVERSITY
*of* EDINBURGH

This thesis has been submitted in fulfilment of the requirements for a postgraduate degree (e.g. PhD, MPhil, DClinPsychol) at the University of Edinburgh. Please note the following terms and conditions of use:

This work is protected by copyright and other intellectual property rights, which are retained by the thesis author, unless otherwise stated.
A copy can be downloaded for personal non-commercial research or study, without prior permission or charge.
This thesis cannot be reproduced or quoted extensively from without first obtaining permission in writing from the author.
The content must not be changed in any way or sold commercially in any format or medium without the formal permission of the author.
When referring to this work, full bibliographic details including the author, title, awarding institution and date of the thesis must be given.

# Large-scale neuroimaging studies of major depressive disorder, associated traits and polygenic risk

Xueyi Shen


THE UNIVERSITY *of* EDINBURGH

Doctor of Philosophy

The University of Edinburgh

2018

## Abstract

Major depressive disorder (MDD) is a highly prevalent and disabling condition with a heritability of around 37%. Key symptoms of MDD include low mood and psychological distress, but the mechanisms underlying MDD and its symptoms are unclear. Genetic and neuroimaging techniques are important methods with which to better understand the aetiology and mechanisms of depression. Recently, through the availability of the UK Biobank and ENIGMA datasets, it has been possible to conduct well-powered imaging studies of heterogeneous traits like MDD, with genome-wide genetic data. These genetic data can act as causal instruments and can be utilised to identify differences in neurobiological mechanisms.

The current thesis presents neurobiological associations with depressive symptoms and genetic risk for MDD using data from the UK Biobank imaging project (N range from 5,000 to 12,000). My overall aims were to investigate the neurobiological basis of MDD status, depressive symptoms and MDD polygenic risk.

First, MDD case-control differences in subcortical volumes and white matter microstructure indexed by fractional anisotropy and mean diffusivity, are presented using the largest structural neuroimaging samples to date. MDD was associated with worse white matter microstructure in the thalamic-radiation subset and forceps major (posterior corpus callosum). No group difference was found for the volume of any subcortical structure.

Next, associations between depressive symptom severity (including longitudinal and cross-sectional measures) with white matter microstructure were tested. Over 8,000 participants had repeated measure of depressive symptoms assessed on 2-4 occasions across 5.89 to 10.69 years. I found several novel associations between measures of depressive symptom severity (at the time of imaging, their variance within individuals over time, and with longitudinal increasing depression severity) all associated with lower white matter microstructure in the thalamic radiations. This was the first study of this size looking at imaging associations with longitudinal symptom measures and demonstrates consistent findings implicating thalamocortical connections.

The third study presents results of phenotype wide association ('PheWAS') analysis of polygenic risk for MDD, including imaging and other available phenotypes. In

total, 1,744 phenotypes were tested, covering sociodemographic, physical health, mental health, subcortical volumes, white matter microstructure assessed with FA and MD (mean diffusivity) and resting-state connectivity. I found that MDD polygenic risk was associated with MDD-related phenotypes including severity of depression and neuroticism, sleep, smoking, subjective well-being as well as neurobiological phenotypes including white matter microstructure and resting-state connectivity.

In my final data chapter, neurobiological associations with cognition, as an important risk factor of major depressive disorder, were also reported. I found that higher connectivity related to the default mode network was associated with better cognitive performance.

These studies suggest two features of neurobiology related to MDD traits and genetic risk. First, they implicate microstructure of thalamic white matter connections as an important biomarker for MDD risk, psychological distress and genetic risk, as reflected by its consistent associations with depressive status, depressive symptoms, within-subject variability of depression and MDD polygenic risk. Secondly, the aberrant connections within the default mode network were related to MDD phenotypes and polygenic risk. These findings, therefore, provide evidence that these features may play a key role in MDD-related neuroarchitecture.

## Lay Summary

Major Depressive Disorder (MDD) is the leading cause of disability worldwide. Approximately 322 million people worldwide live with depression, affecting all age ranges, ethnicities and countries. Genetic studies of psychiatric disorders including MDD have indicated the importance of large sample sizes for such complex disorders. Until recently, however, due to the expense, neuroimaging studies have been largely restricted to sample sizes of often less than 200 people, which has led to inconsistent and contradictory findings.

This thesis has therefore used the largest neuroimaging cohort currently available, (initially n=5,000, then 12,000 people with further releases of data), to explore differences in brain structure and function in individuals with and without depression. Other advantages of this cohort data include longitudinal assessment of depressive symptoms and the availability of genetic data.

The main findings indicate that in white matter, the structural connections between the thalamus and other parts of the brain are associated with having major depression, with higher level of psychological distress, and with greater genetic risk. In terms of functional brain changes, ‘over connectedness’ of regions within a circuit called the ‘default mode network’ was also associated with higher genetic risk of depression. The default mode network has greater synchrony of activity at rest and is involved in internalized thought processing, rumination and negative thoughts.

In conclusion, imaging findings may be important biomarkers for depression, which can potentially give clinical insights into its mechanisms, eventually leading to potentially more informative early diagnosis.

## Declarations

I declare that this thesis has been composed by myself. Except where otherwise stated, the work presented is entirely my own.

Two published papers are included in this thesis in Chapter 2 and Chapter 5 respectively:

**Shen, X**., Reus, L. M., Cox, S. R., Adams, M. J., Liewald, D. C., Bastin, M. E., Smith, D. J., Deary, I. J., Whalley, H. C. and McIntosh, A. M. (2017) 'Subcortical volume and white matter integrity abnormalities in major depressive disorder: Findings from UK Biobank imaging data', Scientific Reports. Springer US, 7(1), pp. 1–10. doi: 10.1038/s41598-017-05507-6.

**Shen, X**., Cox, S. R., Adams, M. J., Howard, D. M., Lawrie, S. M., Ritchie, S. J., Bastin, M. E., Deary, I. J., McIntosh, A. M. and Whalley, H. C. (2018) 'Resting-state connectivity and its association with cognitive performance, educational attainment, and household income in UK Biobank', Biological Psychiatry: Cognitive Neuroscience and Neuroimaging. Elsevier Inc, pp. 1–9. doi: 10.1016/J.BPSC.2018.06.007.

Xueyi Shen

October 2018

## Acknowledgements

First and foremost, I would like to thank my supervisors, Dr Heather C Whalley and Prof. Andrew M McIntosh. Dr Whalley has been a really good supervisor that I can hardly say there is anything I can ask more from her. She is able to help us challenge ourselves and at the same time make us feel supported. She is also a willing helper and a generous friend, all while remaining entirely modest. The most important thing I have learnt from her is to be self-aware of the need to find out the most efficient and correct solution in a complex situation, which is undeniably priceless for both research and life. She helped me to learn the importance of doing research that is replicable, robust, clinically transferrable and interpretable. It is indeed my privilege to be her student. Prof. McIntosh has been an excellent example of what a dedicated researcher looks like. He is very persuasive, energetic and passionate about research. I highly appreciate both the flexibility and support he has provided, as well as opportunities of collaborations and access to really exciting data. I am thankful for all the valuable challenges and exciting opportunities I have had while Andrew has been supervising me.

I would like to also thank my parents, aunt and uncle. My dad wants me to like studying, my mom wants me to know how to study without liking it, and my aunt and uncle want me to have a fun life. Regardless of whether any of them have succeeded or not, I appreciate all the influences they tried to have had on me, and each is all indeed valuable.

I would also like to thank all my friends in Buccleuch free church. They have been extremely supportive. Special thanks to Daniel and Marion Sladek and their boys Conrad, Addison and Jacob, who have given me lots of love, protection and support. Thanks to my dear friends Eric, Moira, Wei, Rebecca & Jon, Heather & Bob, Mary & Neil for all the love and kindness they have shown unconditionally.

Huge thanks to my colleague Laoni (also Yanni). She has been a role model. She has never hesitated to help and thankfully never turned down my late night phone calls even

when it was about work. Many thanks to my colleagues Mark, Dave, Mat, Toni, Emma, Ella, Jude, Miruna, Laura(s), Dom, Julie, Aleks, Eileen, Andriano, Foteini, Clara and all the others not mentioned here who have supported me throughout my PhD.

In general, I am sure that I am very lucky. I enjoyed what I have been doing and hopefully will continue to enjoy it.

Xueyi Shen

October 2018

# Table of Contents

# Chapter 1: Introduction

## Major Depressive Disorder (MDD)

### 1 Epidemiology of MDD

MDD is one of the most crucial health concerns in the world (Vigo et al. 2018). In a recent report by World Health Organization in 2015 conducted on 138, 602 people interviewed in 10 low-income and 14 high-income countries across five continents, the prevalence of lifetime MDD was 11.2% (Kessler et al. 2015), ranking at a high tier of prevalence among major psychiatric illnesses (Sullivan et al. 2012). Approximately 322 million people worldwide are living with depression, with wide coverage across age ranges and ethnicities (World Health Organization 2017). The reported prevalence for lifetime depression has had a significant increase over the last two decades. Taking the statistics for United States as an example, the rate of lifetime depression was 5.2% in 1996 (Weissman 1996), 16.2% in 2003 (Kessler et al. 2014), and 20.6% in 2018 according to the most recent national survey of 36,309 US adults (Hasin et al. 2018). This could due to a true increase in the number of affected individuals, or a higher level of awareness of the disease.

MDD is severe in terms of its impact on educational attainment (Ritsher et al. 2001; Bulik-Sullivan et al. 2015), job performance (Ritsher et al. 2001; Gavin et al. 2010), mental health of off-spring (Ensminger et al. 2003; Lewinsohn et al. 2005), and even mortality (Kessler et al. 1996). By the year 2017, suicide deaths caused by MDD has reached a number close to 800,000 per year (World Health Organization 2017). According to the most up-to-date national survey of the US published in 2018, mean age of onset for depression was 29.05 years, indicating that a large proportion of MDD cases suffer from the negative impacts of the disorder impacting long-term life course trajectories (Hasin et al. 2018).

According to a systematic review by Geddes et al. (2003), 16-18% of patients relapse in a year after one to six months' treatment, with the relapse rate increasing to 24-33% after two years (Geddes et al. 2003). A very recent meta-analysis by Cipriani et al. (2018) reportedly analysed the responses of 21 anti-depressant drugs on 116,477 adult patients. Low to moderate odds ratio for response rate for active drugs versus placebo were reported (ranged from 1.37 to 2.13), and high variability of treatment efficiency was observed for all anti-depressants. Among all the major anti-depressant, only Fluoxetine and Agomelatine showed lower dropout rates than placebo (Cipriani et al. 2018). These findings reflect the uncertainty in MDD treatment. One of the major causes for the uncertainty is the individual variations among MDD cases, which is reflected on both drug response and depressive symptomology. Various reasons such as side effects and individual differences of drug response hinder individual-level interventions. The first step to meet the imminent need for effective treatment is to find reliable empirical evidence to help us understand the underlying mechanism of MDD.

One big challenge for understanding MDD is its inherent heterogeneity. According to the definitions for MDD in DSM-V (Diagnostic and Statistical Manual of Mental Disorders, 5th Edition) and ICD-10 (International Classification of Diseases: 10th revision), MDD can be diagnosed if five of nine symptoms were met. However, some of those symptoms are antagonistic. For example, psychomotor retardation, hypersomnia and weight gain are opposite to psychomotor agitation, insomnia and weight loss. This may result in having people with almost opposite symptoms diagnosed under the same category. There are two approaches that can potentially empower the interpretations for the underlying mechanism of MDD, bearing with the difficulties brought by its heterogeneity. First, we need to have reliable, replicable findings on case-control differences to help understand the general aetiology of MDD, because the heterogeneity of the trait hinders drawing confident conclusions based on small samples. Large cohort studies are therefore needed to find neurobiological and genetic associations of MDD, of which small effect sizes are expected due to a variety of manifestations in the sample. Second,

stratification of subtypes of depression having different biological mechanisms would largely benefit future studies to test whether specifying subtypes would help to undertake personalised treatments. The second approach again would require large statistic power to allow subgrouping populations that have MDD.

## 2 Definition of MDD and its major risk factors

MDD is a clinical status that is marked by depressed mood with excessive severity, assessed according to the impact and duration. According to major diagnostic criteria such as DSM-V, MDD is expressed in mainly four categories (Fava and Kendler 2000; Sullivan et al. 2012). (i) Declined mood health, reflected by constant and prolonged psychological distress, higher mood variability. (ii) Disrupted neurogenerative functions, mainly observed as a rapid and substantial change of appetite or sleep. (iii) Irrational cognition, such as unnecessary guilt, shame and worthlessness. Finally, (iv) abnormal psychomotor activity, presented as either overly active (agitation) or lack of activity (tiredness).

The onset of MDD is contributed by mixed effects from genetic, neurobiological and social factors (Yirmiya et al. 2015). One of the most consistently found risk factor is family history, which incorporates variances contributed by genetic variants (Wray et al. 2018) and familial environment (Ensminger et al. 2003). Higher prevalence of MDD is also found in females (Kessler et al. 2014), people with childhood trauma (Heim, Newport, et al. 2008), social deprivation (World Health Organization 2017), people with lower educational attainment (Ensminger et al. 2003), cardiovascular conditions (Davidson et al. 2005) and obesity (Heo et al. 2006),

Biological factors include genetic risk and neurobiological disruptions. For neurobiological factors, various mood disorders, including MDD, have been reported by some studies to be the outcome of brain tumours/lesions, especially in emotion-related

brain regions (Starkstein et al. 1987; Sharpe et al. 1990; Fornito et al. 2015) – a summary of the neuroimaging literature is described below. In terms of genetic risk, the latest genome-wide association studies (GWAS) found 44 genetic loci associated with lifetime onset of depression, most of which are associated with neural development and have high levels of expression in brain tissues (Wray et al. 2018). In the remainder of this chapter, major biological models for MDD are introduced.

## 3 Biological mechanisms

In this section, four main models/mechanisms are introduced. The first and second described are neurobiological models underpinning emotional processing and emotion regulation respectively. Vulnerable brain regions and network utilities involved in these two types of processes in MDD are discussed. The third is the Hypothalamic-Pituitary-Adrenal-axis (HPA-axis) model. HPA-axis through its role in neuroendocrine function is particularly involved in the stress response and regulation of other physiological responses including immune function and circadian timing. The interaction and possible mediation effect of HPA-activity with brain development and behaviour patterns (such as circadian rhythm) are discussed. Finally, the fourth mechanism introduced is the polygenic model relating to the genetic effects contributed by common genetic variants. This part describes the causal relationship between genetic risk and the presence of MDD, as well as and the overlapping genetic aetiology between MDD and other heritable traits. I have selected these main models to introduce key concepts underlying studies presented in the thesis.

### 3.1 Cognitive models for emotion processing (Model 1) and emotion regulation (Model 2) in MDD

Emotion is cognitive, subjective and highly associated with brain and hormonal activities (Etkin et al. 2015). Normally, emotion is a responsive activity, elicited by given

environmental stimuli (Dolan 2002). A positive stimulus triggers positive emotional processes and leads to repetitive behaviour to continue seeking similar stimuli, and a negative stimulus processed by negative emotional systems, triggers a “fight-or-flee” response, in order to either eliminate or avoid future negative stimuli. Emotional processing thereby involves a complex series of steps including an established past memory of the environment, the evaluation of current input stimuli, the regulation and response to current inputs, and finally the updating of memory and cognitive systems associated with emotional processing (Etkin et al. 2015).

One important network associated with emotion processing is the limbic system. It includes regions involved in negative emotion processing like amygdala, thalamus, insula, and regions that relate to emotional memory including hippocampus and para-hippocampus, and finally, positive-emotion/reward-related areas include caudate, ventral striatum and nucleus accumbens (Dalgleish 2004). These have a key role in primary emotion evaluation for negative or positive stimuli and attention allocation (Dalgleish 2004). Prefrontal and cingulate cortex are also important regarding executive control and down-stream regulation (Bush et al. 2000; Etkin et al. 2015). These regions have complex interactions and often work in a synchronous network manner (Etkin et al. 2015). These networks can be roughly categorised into: networks within the limbic system itself for processing of different attributes of emotions (Dalgleish 2004; Russo and Nestler 2013), and networks involving anatomically distant regions including high-level integrative and regulative regions like prefrontal and cingulate cortex, connecting to the limbic system (Etkin et al. 2015) (see Figure 1).

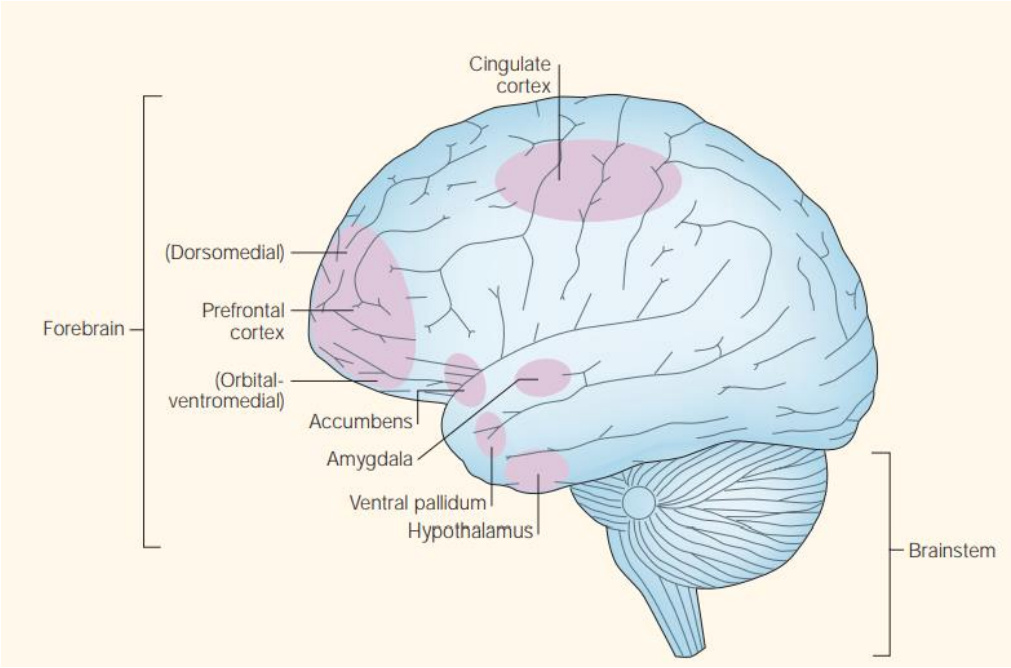


Figure 1. Brain regions related to emotional processing and emotional regulation in the brain (Dalgleish 2004).

In terms of MDD, aberrance of emotional processing often manifests in two ways: (1) biased cognitive processing of emotional stimuli (Disner et al. 2011), and (2) aberrant emotion regulation (Etkin et al. 2015). Though these two aspects may have different behavioural expressions, they could involve similar neural pathways. For example, the attention regulation pathway that mainly involves the activity of dorsal lateral prefrontal cortex (DLPFC) and limbic system, may be activated in paradigms like reappraisal that require spontaneous emotion regulation to deactivate negative emotional processing (Wager et al. 2008). Also, when discussing the neural basis of these two networks, although the regionally segregated functions are important for interpretation, network integration (functional/structural connectivity) is important for forming a complete behavioural pattern. More details about how networks could associate with emotion processing and regulation are described and discussed below in the sections for each model.

### 3.1.1 Model 1: Biased cognitive processing of emotional stimuli in MDD

In many studies, MDD cases typically show pessimistic processing of emotional stimuli, expressed as hypersensitivity to negative stimuli and an attenuated response to positive ones. This could be explained by biased attention, biased evaluation, and biased memory (see Figure 2).

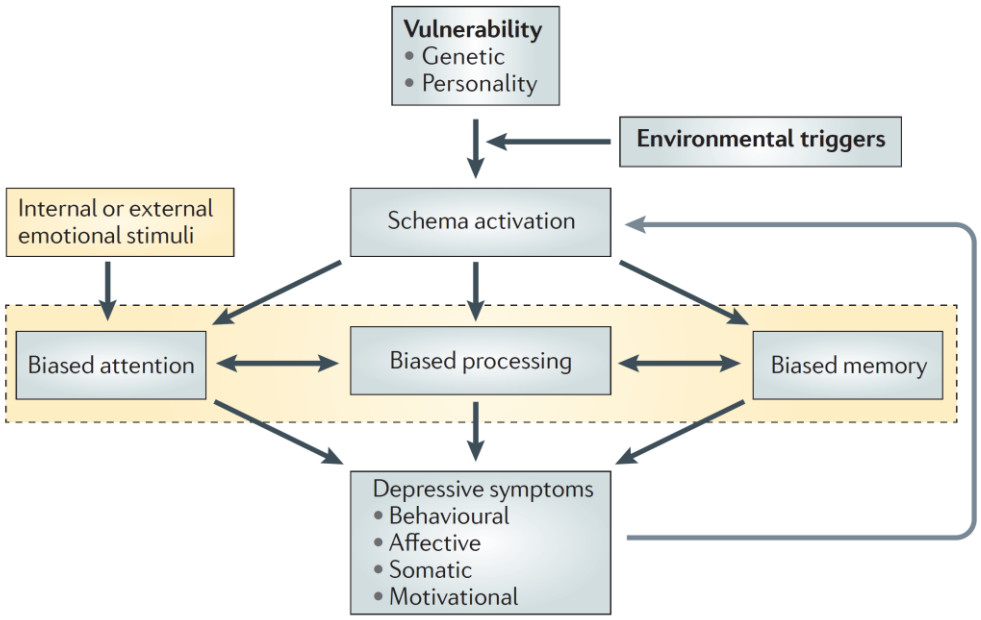


Figure 2. The cognitive model of emotional processing in MDD (Disner et al. 2011).

#### 3.1.1.1 Biased attention in MDD

Biased attention in MDD could be explained by (1) over-loaded allocation of attention to negative stimuli (Posner and Rothbart 2000; Gotlib and Krasnoperova 2004), and/or (2) or a lack of ability to detach attention from negative stimuli (Mitterschiffthaler et al. 2008; Eugène et al. 2010). Behaviourally, individuals with MDD typically show much faster reaction time and higher recall rate of negative stimuli compared with positive/neutral ones (Mitterschiffthaler et al. 2008).

On the neuronal level, activations in the superior parietal cortex (involved in coordinating

shifts in gaze), ventral lateral prefrontal cortex (allocating attention), anterior cingulate cortex (conflict detection and executive regulation to downstream brain regions), and dorsal lateral prefrontal cortex (executive control and integrating sensory information from downstream brain regions) have been reported to be the main putative regions that may have key roles in such biased attention (Corbetta et al. 1998; Kastner et al. 1998). In addition, reduced functional connectivity between the regions has been found associated with the inability of balancing attention allocation and disengaging from negative stimuli, which has been found as one of the major funcitonal deficits in patients with MDD (Fales et al. 2008).

#### 3.1.1.2 Biased emotion processing in MDD

Biased emotional processing, which is also referred to as 'biased evaluation' of emotional stimuli in some articles, is mainly expressed in patterns of: biased valence, abnormal arousal levels, and unusual durations (Dolan 2002; Bressler and Menon 2010; Etkin et al. 2015). Behaviourally, individuals with MDD have higher ratings for negative visual stimuli and pain (Leppa 2006; Bylsma et al. 2008), and higher neuronal arousal to negative scenarios revealed by a greater N2 component in event-related potential (Proudfit et al. 2015). MDD patients are also more likely to interpret ambiguous or neutral inputs as negative in various experimental contexts, such as short scenarios and emotional pictures (Mogg et al. 2006; Moser et al. 2012).

Brain regions found to be associated with biased evaluations of emotional stimuli include those involved in reaction to negative stimuli (amygdala, thalamus and subgenual cingulate (Dalgleish 2004) and those associated with reward processing (ventral tegmental area, ventral striatum and putamen (Dalgleish 2004; LeDoux 2012)). In individuals with MDD, it is typically reported that there is hyperactivity of negative systems along with blunted activation in the reward system (Grimm et al. 2011). The negatively biased process is presented in both self-related scenarios, and other-related circumstances, which is reflected by, for instance, stronger empathy with other people's

physical and emotional pain (Schreiter and Pijnenborg 2013; Fujino et al. 2014). Blunted reward-response has also been abundantly found to be associated with treatment response (Dichter et al. 2012; Pechtel et al. 2013). Balanced evaluations of emotional stimuli also require sufficient regulation from dorsal lateral prefrontal cortex (DLPFC) and dorsal anterior cingulate cortex (ACC). Both DLPFC and ACC receive inputs from the limbic system and give mainly suppressive feedback when cognitive regulation is necessary (Bush et al. 2000; Bae et al. 2006; Kolling et al. 2016).

#### 3.1.1.3 Biased ruminative thoughts in MDD

Previous studies have found that MDD demonstrates negative-biased memory and excessive self-referent cognition of negative stimuli. These lead to rumination of negative thoughts seen clinically in patients with MDD patients (Spasojević and Alloy 2001).

Putative brain regions involved in these biased processings include: (1) hippocampus, related to memory, (2) amygdala and subgenual cingulate, responsible for negative emotion processing, especially for stressful stimuli, (3) medial prefrontal cortex (MPFC), involved in self-related cognition, and finally (4) DLPFC and ventral lateral prefrontal cortex (VLPFC), responsible for executive control and information integration (Denson et al. 2009; Cooney et al. 2010). Hyperactivity of the hippocampus, amygdala, subgenual cingulate and MPFC would therefore be hypothesised in patients with MDD (Ray  Ochsner, K.N., Cooper, J.C., Robertson, E.R., Gabrielle, J.D.E. & Gross, J.J. 2000; Denson et al. 2009; Cooney et al. 2010). The activity of DLPFC and VLPFC and attenuated connectivity between these regions and limbic system were found associated with recalls of negative memories and self-referent rumination in MDD under episodic memory paradigms (Gusnard et al. 2001; Cooney et al. 2010).

To summarise, therefore, the above neurocognitive models of MDD mainly imply the involvement of two main brain systems: (1) the limbic system, responsible for primary

emotional processes, and (2) the executive system located in DLPFC and ACC, providing down-stream regulation to the limbic system. The above model gives insights into the main cognitive components of MDD and gives a broad summary based on numerous cognitive paradigms for MDD. However, this model gives a very limited explanation of down-stream regulation and the complex structural and functional connectivity between DLPFC/ACC and limbic system. Emotion regulation is complex because it is not always explicit and whether consciousness processing is involved may indicate different patterns of neuronal connectivity. More details of emotion regulation will be explained in the next section where the emotion regulation model proposed by Etkin et al. is introduced and discussed (Etkin et al. 2015).

### 3.1.2 Model 2: Emotion regulation model

Emotion regulation involves in chains of decisions, which can be either conscious (explicit) or unconscious (implicit), to achieve desired emotional status (Etkin et al. 2015).

Explicit emotion regulation is top-down, conscious, effort-demanding and relatively slow compared to primary sensory processing and implicit emotion regulation (Etkin et al. 2015). Main regions involved in this process include the DLPFC, ventral lateral prefrontal cortex, parietal cortex and pre-supplementary motor area. The DLPFC, in particular, has been most consistently found associated with executive control (Wagner et al. 2001). Anatomically, DLPFC is connected to the limbic system through cortico-cortical white matter tracts, for instance, superior longitudinal fasciculus and anterior thalamic radiation (see Figure 3) (Mori et al. 2002). Functionally, activity in DLPFC connects to the thalamus, and DLPFC studies found that enhanced activity in DLPFC leads to higher activations in limbic systems such as amygdala and thalamus (Meyer-lindenberg et al. 2005; Fox et al. 2012).

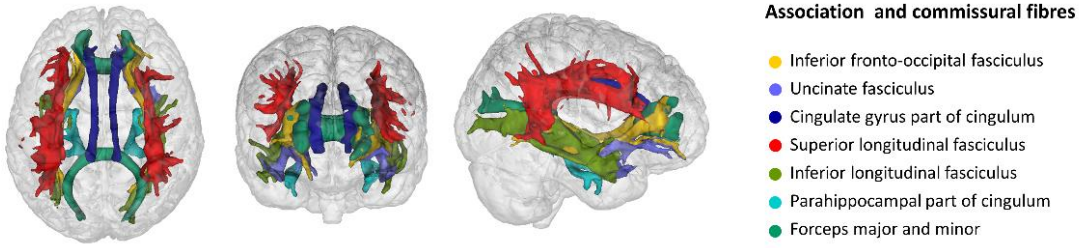


Figure 3. Demonstration of association and commissural fibres. White matter tract maps were generated based on the first release of UK Biobank imaging data.

The importance of the DLPFC to MDD patients has been emphasised by studies on treatment and treatment prediction (Meyer-lindenberg et al. 2005; Fox et al. 2012). For example, some recent studies reported that anti-depressant treatment and Cognitive Behavioural Therapy for MDD patients results in strengthened regulatory functional connectivity from DLPFC to limbic regions (Rosenblau et al. 2012; Shou et al. 2017). Further, a meta-analysis of 60 studies in which 1,569 MDD cases were included showed that antidepressant medication increased the activity in DLPFC (Ma 2015). Enhancing effects of transcranial manipulation such as transcranial direct current stimulation and transcranial magnetic stimulation on DLPFC have also been used to strengthen emotional regulation, showing a behavioural improvement of emotion regulation and stronger regulatory connectivity between DLPFC and amygdala (Rosenblau et al. 2012; Shou et al. 2017). Improvements were also surprisingly shown in drug-resistant patients using these transcranial methods to enhance activity in the DLPFC (Palm et al. 2012). The above studies suggest that DLPFC may serve as the emotion stabiliser in subjects that particularly suffer from excessively variable mood (Brunoni et al. 2013). Aberrant functions and connectivity related to this region, either in white matter or grey matter, indirectly influences downstream regulation. The structural changes may be hypothesised to be caused by various factors such as early developmental deficits of maturation of myelination, degeneration of cortical functionality and structure due to

premature or accelerated ageing, and excessive neuronal pruning (Dolan 2002; Bressler and Menon 2010).

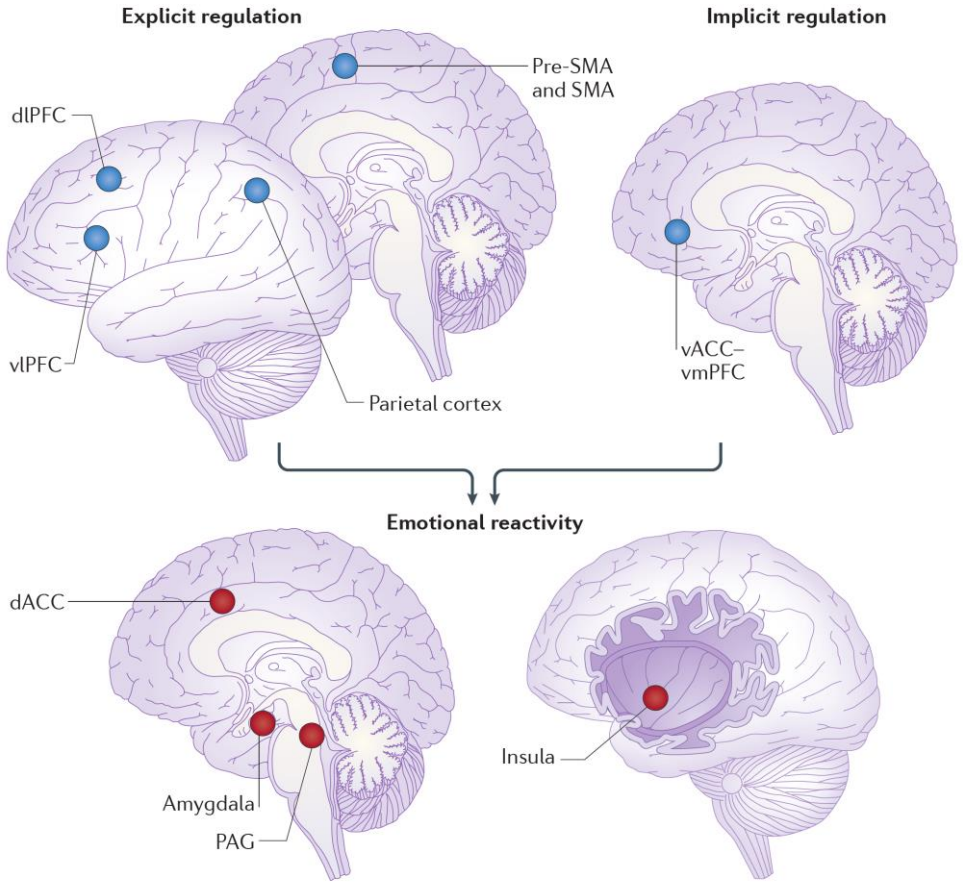


Figure 4. The explicit and implicit emotional regulation model proposed by Etkin et al., 2014 (Etkin et al. 2015).

Implicit emotion regulation indicates non-conscious modulation in emotional processing areas. Important regions for this type of emotional regulation are anterior cingulate cortex (ACC) and ventral medial prefrontal cortex (VMPFC) (Etkin et al. 2015). They are responsible for the detection of emotion evaluation, integrating conflicting inputs, monitoring unexpected stimuli (Botvinick et al. 2004). All these functions are mainly conducted in an automated, relatively fast, bottom-up manner. Another important role for implicit emotion regulatory regions is to moderate between DLPFC and primary sensory processing system in limbic areas (Rosenblau et al. 2012). ACC integrates the upstream

regulatory signal from DLPFC and downstream inputs from primary processing systems. Therefore, activity in ACC helps neurobiological response to antidepressants to expand across neural networks (Ho et al. 2017).

Functions of the above brain regions and pathways are not restrictively associated to processes involves in emotion, but also highly important in broader aspects such as decision making (Glimcher and Rustichini 2004; Fehr and Camerer 2007), in which the involvement of emotions is much more implicit and subtle compared with classical emotion regulation paradigms. Healthy performance in these regions ensures optimal goal-directed decisions, which enables the inference for the functionality of emotion regulation system to reach to a much broader context (Glimcher and Rustichini 2004; Fehr and Camerer 2007). Social decision making takes place on a daily basis. Quality of decisions broadly influences whether subjects have desirable social interactions and whether they are able to maintain a reciprocal inter-personal environment. Many studies suggest that social support is one of the most important interventions of MDD (Leskelä et al. 2006).In addition, the symptoms of depression, including decreased enthusiasm and poor social decision making in MDD patients, contribute to a reduction of social support, leading to a spiral of negative influences (Meyer-Lindenberg and Tost 2012). Improvements in emotion regulation may, therefore, help to break away from the effect of the vicious spiral caused by impaired social interactions in MDD patients.

The above two models mainly intend to explain the affective abnormalities associated with MDD. However, MDD is far more complex than mere affective symptomology. Cognitive and somatic symptoms may be strong contributors to MDD condition, but their roles are not explained in the above models. For some somatic symptoms, such as weight gain, are not well studied in the field of neuroscience. Take body mass index as an example, which has been consistently found associated linearly with MDD condition, showed linear association with white matter microstructure in some studies (Xu et al. 2013; Mazza et al. 2017), but also showed a non-linear association in some others,

indicating that high body mass index may be protective of brain integrity in some groups (Stanek et al. 2011). These unclear associations may indicate that some of the somatic symptoms may have contributions to the presence of MDD, independent from direct neurobiological mechanism or having regulatory influence to the association between brain phenotypes and the presence of MDD.

Another limitation of these two models is that psychological factors may not be the only reasons for brain alterations. Functional signals have local heterogeneity in the brain, largely defined by the vascular localisation in some areas of the brain heavier than the other regions. One example is posterior cingulate cortex (PCC), although has been found involved in psychological activities, has a naturally high level of BOLD signal (especially at a low frequency) even without explicit tasks. It has been suggested that the dense vessel layout in this region may contribute to this phenomenon (Szikla et al. 2012), which can potentially reflect individual differences of cardiovascular conditions (Szikla et al. 2012).

In general, the above limitations suggest a need for other models that give explicit explanations about the behavioural patterns and physical conditions that associate with MDD symptomology. One of the most well studied of these models is the HPA-axis model, which will be introduced in the following section.

### 3.2 Model 3: the HPA-axis model

The hypothalamic pituitary adrenal (HPA) axis is the central stress response system and therefore of key importance to MDD since onset is often linked with stressful life events (Pariante and Lightman 2008). Compared with other biological models, since HPA axis is highly associated and sensitive to behavioural patterns such as sleep, the model gives particular insights for linking behavioural patterns with neurobiological activities and the presence of mood disorder. The activity of HPA axis consists of the release of adrenocorticotrophic hormone releasing factor and vasopressin from the hypothalamus,

adrenocorticotrophic hormone from the pituitary (regulated by adrenocorticotrophic hormone releasing factor), and glucocorticoids from the adrenal cortex (regulated by adrenocorticotrophic hormone) (see Figure 5). One such glucocorticoid in humans is cortisol. Secretion of cortisol has a negative feedback mechanism to hypothalamic and pituitary activities therefore to remain homeostasis within the system (Pariante and Lightman 2008).

HPA axis has an anatomical basis in the brain and is also highly associated with hormonal activities in the peripheral nervous system. Cortisol, in particular, is one of the few hormones that can pass the brain-blood barrier. HPA axis forms a key component linking psychiatric symptoms and physiological patterns like sleep, appetite and addiction (Nemeroff and Vale 2005). Compared with previous brain functional models which were found mainly in specific behavioural paradigms, the activity in HPA axis is broadly associated with various complex behavioural patterns (Yehuda et al. 2004; Heim, Newport, et al. 2008). This system has rapid response to acute stress stimuli and has a circular regulate-feedback mechanism to sustain allostasis. Allostatic overload is often considered to contribute to the pathophysiology of mood disorders, particularly when the overloaded status remains unsustainably long/strong (Pariante and Lightman 2008; Rilling 2013).

There is substantial evidence to suggest that elevated activation of the HPA axis is presented in MDD patients, consistently supported by evidence of high cortisol level (Brown et al. 2004). Though HPA axis is directly associated with acute stress response, exposure to stressful life events such as childhood trauma/early adversity can cause aberrantly hypersensitive HPA-axis activity, with long-term consequences extending into adolescence and adulthood (Heim, Mletzko, et al. 2008). These indicate that aberrant HPA-axis activity may not only be a feature of MDD but also a vulnerability factor (Heim and Nemeroff 2002).

Dysfunction in the negative feedback pathway from cortisol to hypothalamus and pituitary

is the most consistently found contributor of HPA-axis hyperactivity (Pariante 2006). This failed inhibition mechanism can be caused by insufficient binding between cortisol and glucocorticoid/mineralocorticoid receptor (Pariante 2006) and lack of affinity of cortisol to P-glycoprotein as the carrier of cortisol and antidepressant across the blood-brain barrier (Uhr et al. 2008). Deficit in these mechanisms overlay with metabolic and immune system abnormality as expressed as peripheral inflammation (Gordon et al. 2015) and disrupted circadian and ultradian rhythm (Stetler and Miller 2011; Scheiermann et al. 2013).

Neurobiologically, glucocorticoid and mineralocorticoid receptors are located mainly in the limbic system and particularly enriched in hypothalamus and hippocampus (Gordon et al. 2015). Abnormality of these receptors is often associated with abrupted regional functions of these brain regions, which could explain the behavioural patterns in depressed individuals, expressed as impaired spatial memory in rodents, and worsened verbal and episodic memory in human MDD patients (Vythilingam et al. 2004; Gandy et al. 2017). This is supported by a recent meta-analysis from the ENIGMA consortium project (Enhancing Neuro Imaging Genetics Through Meta-Analysis, http://enigma.ini.usc.edu/), incorporating 15 international studies of 1,728 MDD cases and 7,199 controls, which found that, in the eight major subcortical structures, only hippocampal volume was associated with lifetime MDD (Schmaal et al. 2017). This study further supports that the brain alterations which may suggest HPA-axis abnormality could be an important biomarker expressed in neurogenesis and neural development.

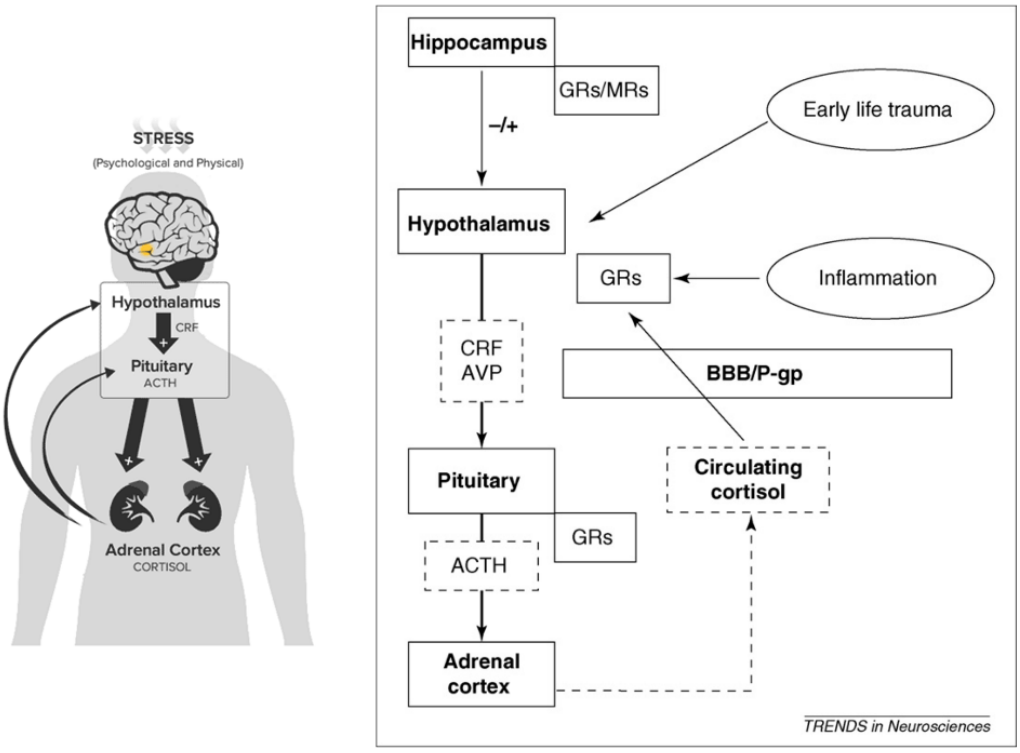


Figure 5. HPA-axis system and its hormonal regulations, adapted from Pariante et al., 2008 (Pariante and Lightman 2008).

The main brain regions associated with HPA-axis model, to some extent, overlap with models for emotional processing, because the limbic system is important for both types of models (HPA-axis hormones are enriched in the limbic system, and limbic system is important for primary emotional processing). However, compared with models for emotional processing, HPA-axis model gives more insight into how depression is related to lifestyle, cardiovascular and metabolic traits like sleep patterns and activity in the immune system such as inflammation, and how these factors may associate with the limbic system. Therefore, the additional information provided by HPA-axis model may give further insights into how shared genetic architecture between MDD, HPA-axis and metabolic/immune system interact, and enrich understandings of possible biological pathways between neural development and MDD genetic risk, and how this pathway can be mediated by HPA-axis related physical and behavioural patterns, such as circadian rhythm and cardiovascular conditions.

### 3.3 Model 4: Polygenic model

Genome-wide association studies (GWAS) has made great contributions to the understandings of genetic markers for MDD (Wray et al. 2018). However, variance explained by single SNPs is small, therefore the potential of using those significant hits to predict and understand the genetic contribution of predicting MDD based on common variances is limited (Wray et al. 2014). Gandal *et al.* summarised that the genetic variance of MDD is mainly contributed by common genetic variants. Also, the effects of the genetic variants are largely additive (Gandal et al. 2016). Therefore another approach was introduced as “polygenic risk profiling”, which takes whole-genome variances into account, at a less stringent significance level compared to that of traditional genome-wide level studies (Wray and Maier 2014; Bulik-Sullivan et al. 2015; Wray et al. 2018). To calculate polygenic risk scores, summary statistics of a GWAS conducted on a training sample of a given trait is applied on genomic profile for each individual in a test sample, and the effect sizes of each genetic variants were treated as weights. The weighted sum of whole-genome variances is the polygenic risk score of the trait. A higher score for a person indicates a higher whole-genome-level genetic risk (Wray et al. 2014). Transferability of the technique was also successfully validated by a cross-ethnicity study which successfully used a European training sample to predict MDD status of Han Chinese woman (Edwards et al. 2018). The increased sample sizes of MDD GWAS have significantly contributed to the increased accuracy of MDD polygenic risk profiling, as many more genome-wide significant genetic risk variants have been found in recent studies (Wray et al. 2018), which indicate increasingly better estimates for the effects of MDD compared than smaller samples used previously (Wray et al. 2013).

Polygenic risk of MDD is associated with various traits, such as neuroticism (Navrady et al. 2018), psychological distress (Musliner et al. 2015), comorbidity for/with and childhood trauma (Peyrot et al. 2018). Higher risk scores of MDD is also associated with physical conditions like pain (McIntosh et al. 2016) and body mass index (Clarke et al.

2015), cognitive performance and educational attainment (Hagenaars et al. 2016).

However, very little literature has investigated the relationship between MDD polygenic risk score and wider phenotypes including brain measures. There are several reasons for this: first, under-powered training samples may introduce a significant amount of uncertainty for the estimation of SNP effects, (Wray et al. 2013); and second, only recently, large neuroimaging cohorts that also include genetic data have been available (Elliott et al. 2018); finally, though meta-analyses had significantly larger power compared with traditional small-sample studies, more flexible phenotypes such as resting-state connectome data would be extremely hard to merge based on inconsistent protocols between sites. However, biologically, it is extremely important to investigate this association, as most of the depressive symptoms like sleep, anhedonia and mood variability may be more relevant to contemporaneous brain activity, along with the less temporally fluctuating structural brain changes. Many of the top hits found in a recent GWAS were associated with brain phenotypes and some directly expressed in brain tissue (Wray et al. 2018), along with the evidence that many structural and functional brain phenotypes can have heritability up to 80% (Elliott et al. 2018), these facts together suggest that potentially there is an association between brain features and genetic risk for MDD.

## 4 Limitations of the above models and questions to ask in the present thesis

The biggest limitation of the above neurobiological models is the inconsistency of previous findings. Although MDD is one of the most severe and disabling diseases, its aetiology is largely ambiguous, not simply because of the paucity of data, but results are heterogeneous or even contradictory. A massive number of regions, including the lateral and medial side of the prefrontal cortex, sensorimotor regions, parietal cortex that associate with attention and finally visual cortex in the occipital cortex have all been found in some studies associating with MDD case-control differences. If all these results were true associations, the conclusion may be that MDD is related to whole-brain

disturbance, which has no specific neurobiological basis and is contradictory to the nature of the brain with regional functionality. A very likely explanation for the overly wide coverage of brain structure and activities appeared in previous studies, is that there may be a very large number of false positive results. It is likely due to the fact that most of the previous studies are underpowered, limited to sample sizes of less than 50 MDD cases (Linden 2012). MDD is highly prevalent and heterogeneous. It would be extremely difficult to represent the overall population of MDD well enough if only less than 50 people were selected. It is likely that a small number of severe cases in such studies may be able to drive the effects to reach statistical significance, nonetheless, noise may be introduced as those individuals that brought the largest effects may only be a particular subtype of MDD, therefore the results would reflect their own particular symptoms only. Despite these hypothetic inferences that previous findings may contain many false positive findings, previous findings have indeed shown results in opposite directions. For example, Eijndhoven *et al.* tested the differences in cortical thickness between medication-naïve patients and medication-free remitted patients. They found that patients with current symptoms had greater thickness in the temporal pole and anterior cingulate cortex (van Eijndhoven et al. 2009). Some found the depressive symptoms were exclusively associated with the limbic system (Nebes et al. 2001), whereas others report associations in lateral prefrontal cortex only (Taylor et al. 2004). In addition to these studies, Lenze et al. found no significant group difference either in white matter hyperintensity or grey matter volume (Lenze et al. 1999). Previous heterogeneous findings, to some extent, led the hypothesis overly broad and spread across the whole brain, as can be seen in the models introduced above. Though the models above give detailed descriptions of MDD-related cognition/affection biases, genetic factors and hormonal reactivities, an overall additive effect of biased attention, evaluation and rumination on the brain is needed to build up learn-able models to help predict symptoms, liability and treatment outcomes. As a first step however, reliable estimation of the associations between depressive symptoms and brain structures and functions are

required.

Second, investigations and models for mood variability is needed. The above biased emotional processing is often investigated based on one-shot trials (i.e. unrelated events). Studies of cognitive learning models, which describe the dynamics of updating emotional inputs based on previous history of both negative and positive stimuli (Forbes and Dahl 2012; Whitton et al. 2015), show that longitudinal mood variation could be another important component of MDD symptoms. Longitudinal variation can be presented in different forms such as longitudinal linear progression and over-time variability. Studying the fluctuating nature of mood status may therefore give particular insights into emotion-reaction dynamics in MDD in the long run (McFarland and Klein 2009; Forbes and Dahl 2012; Pechtel et al. 2013).

Another limitation is that it is unclear whether structural and functional connectivity is associated with genetic risk of depression. Previous studies have provided evidence that using genetic risk of a brain-related disorder to directly predict brain phenotypes is a reasonable path. For example, the latest GWAS by Wray et al. and Howard et al. revealed that top genome-wide significant SNPs (Single-nucleotide polymorphism) associated with MDD condition were expressed in brain regions (Howard, Adams, Shirali, et al. 2018; Wray et al. 2018). Other examples are family studies that found some evidence that corticolimbic connectivity was altered in people with familial risk, although whether it remains true when only genetic effect is taken into account needs further investigation (Pariante 2009; Huang et al. 2011; Meyer-Lindenberg and Tost 2012). The above evidence is not yet enough, because the brain is highly integrated as a network, a single alteration that can be potentially caused by gene expression associated with a disorder may not result in a single region (Bressler and Menon 2010). Also, compensatory mechanisms against neurobiological deficits, such as enhanced activity in DLPFC in high-functioning groups (Cabeza et al. 2002), can be found in people that show disease resilience, therefore gene expression may not necessarily end up having

phenotypic impact on the phenotypes in a matured brain. The gap of understanding of genetic risk factor to brain structural and functional connectivity associated with emotion regulation is mainly due to a lack of samples that contain both genetic and neuroimaging data. The opinion of this thesis is that the linkage between the brain and genetic risk of depression may enrich the interpretation of the genetic architecture of MDD and lead to better understandings of the multifactorial relationship between behavioural patterns, brain phenotypes and MDD condition. According to previous studies using polygenic risk of MDD to predict physical/behavioural traits such as smoking and body mass index (BMI), a sample of at least thousands of participants were used in these studies (Wray et al. 2013; Musliner et al. 2015; Mistry et al. 2018). This scale of sample sizes, however, has been rarely seen in neuroimaging studies.

To investigate the above challenges, I have used data from UK Biobank project and particularly focused on brain phenotypes such as white matter microstructure, resting-state connectivity and their associations with behavioural and genotyping data. UK Biobank is a project that was established in 2006 (Matthews and Sudlow 2015), between then and 2010, 500,000 volunteers from 40 to 70 years old were recruited (Muñoz et al. 2016; Bycroft et al. 2017a). To date, over 90% of all participants have been genotyped and part of the sample was selected to attend imaging assessments. The imaging project started in 2015, and data collection is still on-going (Miller et al. 2016). The first release covered approximately 5,000 people, and the most up-to-date release in 2018 covered around 12,000 people. Behavioural and part of physical measures were assessed both at the initial assessment and at the same time with the later imaging assessment. This cohort has several advantages despite its impressive sample size. Genetic and neuroimaging data were quality-checked under standard protocols, and the biology data was in general assessed in depth, as revealed by a larger number of genetic variants assessed compared to other large cohorts such as PGC and 23andMe (Howard *et al.*, 2018), and a large range of different types of neuroimaging data was collected, including T1, DTI (diffusion tensor imaging), T2, and resting-state functional data (Miller et al.

2016). Especially the imaging data has exceptionally good data quality compared with other big cohorts because all data were collected in a single scanner. Homogeneity of imaging data, on the other hand, is expected to be able to provide larger statistic power. Another advantage is the longitudinal clinical data. A large proportion of the self-reported physical and mental health conditions were assessed at multiple time points, which makes UK Biobank a unique dataset with large-scale longitudinal assessments that may cover up to thousands of people. For other features of the dataset, details will be introduced in the data chapters.

# White Matter Microstructure and MDD

## 1 White Matter Microstructure

Early developments of neuroimaging techniques, especially MRI, have largely enriched our understanding of the brain maps for regional functions (Soares and Mann 1997). However, more recent studies found that many psychiatric diseases are ‘connectome disorders’. Rather than the structural deficit of a single segregated region, the lack of healthy integrated connections is proposed to contribute to disrupted psychological functions (Rubinov and Bullmore 2013).

White matter (WM) fibres construct the structural bridges within the brain. The most popular method to test the integrity of these structures is diffusion tensor imaging (DTI), which captures the diffusion of water molecules. In oriented environments such as WM, diffusion is anisotropic (see Figure 6). Reduced directionality of diffusion is, in general, associated with worse psychiatric symptoms and worse connectome caused by lesions (Denk et al. 2012).

Conventional DTI measures include FA (fractional anisotropy) and MD (mean diffusivity) (see Figure 6). These two measures are both derived from direct observations of diffusion in three spatial axes (L1 to L3). FA describes the fractional directionality, and MD is the mean diffusion of L1 to L3. By definition, higher FA would usually be interpreted as better/increased white matter integrity, whereas lower MD would be interpreted and decreased integrity. These two measures are both sensitive to white matter microstructure, and each of them has its own advantages and limitations. FA is much more restricted to the variances in WM (see Figure 6), whereas MD is comparatively more easily influenced by partial-volume contamination and the boundaries between WM and grey matter. The generalised sensitivity over all tissues for MD has its advantage however for areas of cross-over fibres, where FA is typically less sensitive (Jones et al. 2013). Therefore, although FA and MD usually have opposite directions, it does not

necessarily mean that they are measures that only differ in polarisation, but rather two validated methods for representing white matter microstructural variations. In the present thesis, both FA and MD results were reported for transparency.

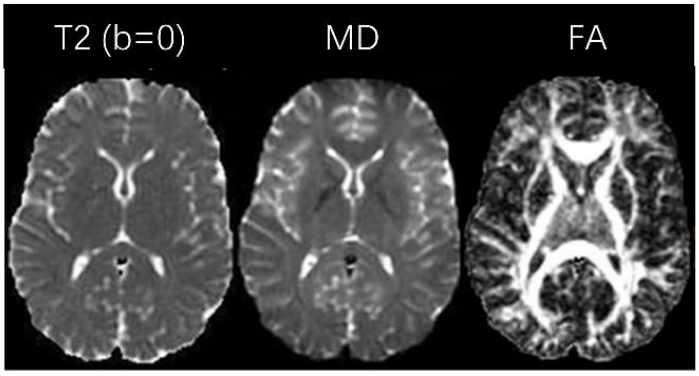


$$MD = \frac{\lambda_1+\lambda_2+\lambda_3}{3}$$

$$FA = \sqrt{\frac{3}{2}}\ \frac{\sqrt{(\lambda_1-MD)^2+(\lambda_2-MD)^2+(\lambda_3-MD)^2}}{\sqrt{\lambda_1{}^2+\lambda_2{}^2+\lambda_3{}^2}}$$

Figure 6. Comparison of whole brain maps between T2W, FA and MD images.

FA and MD are general microstructure variances that describe the pathway features of white matter tracts. However, different structural changes could contribute independently to FA and MD variation, such as intensity loss which contributes to white matter disconnection, the proportion of myelin, which has different diffusive attributes compared with neurons (Jones et al. 2013).

The newly developed neurite orientation dispersion and density imaging (NODDI) measures provide complementary data to explore cellular contributors of FA and MD differences analysis (see Figure 7). These include ICVF (intercellular volume fraction, describing neurite density), ISOVF (isotropic of free water volume fraction, i.e. extracellular water proportion describing the proportion of water outside of cellular space)

and OD (orientation dispersion index, describes morphology of tract organisation, for instance, fanning and bending of axon bundles) (Zhang et al. 2012). There is increasing interest in the use of NODDI measures as complementary dMRI measures, in addition to FA and MD, since these measures depict additional sources of FA and MD variations which conventional DTI measures cannot distinguish (Beaulieu 2002). These NODDI measures are relatively new but are encouragingly robust (Zhang et al. 2012), and importantly have been shown to demonstrate distinct sensitivity to different biological processes, for example in relation to healthy aging (Cox, Ritchie, et al. 2016) and between clinical samples (Rae et al. 2017). The analysis in this thesis therefore incorporates these NODDI measures along with the traditional FA and MD variables to provide deeper insights into the pathophysiology of MDD.

## 2 White Matter Microstructure and MDD

Higher FA and lower MD in structural connections between prefrontal cortex and limbic system have been associated with MDD (Liao et al. 2013). For specific tracts categorised in this subset, worse FA microstructure in anterior thalamic radiation has been observed in MDD patients according to a meta-analytic study (Liao et al. 2013). This tract connects thalamus and bilateral dorsal prefrontal cortex. Functional connection between them involves in top-down emotional regulation and executive control (Mamah et al. 2010; Coenen et al. 2012). Other prefrontal-cortex-related tracts include superior and inferior longitudinal fasciculus (Huang et al. 2011). These structures also show significant associations with cognition, which implies that these regions may have associations concerning MDD-related cognitive deficit (Karlsgodt et al. 2008; Mamah et al. 2010; Cox, Bastin, et al. 2015). However, it is not always the case that white matter microstructure linking prefrontal cortex is found. For example, Gutman et al. found FA changes in MDD only located in limbic regions (Gutman et al. 2009).

NODDI measures have been used in clinical studies but the number of studies is limited as it is a relatively new technique. Recent studies on mental illness, such as first-episode

psychosis and dementia, revealed that for mood disorders, neurite density, as measured by ICVF, is the main contributor for microstructural variances (Mahoney et al. 2014; Rae et al. 2017). On the other hand, neurodegenerative mental illnesses, such as Parkinson's, has been associated with poorer ISOVF (Kamagata et al. 2017). So far there is no study that directly investigates MDD-related NODDI changes, and this topic will be studied and discussed in the present thesis (chapter 3).

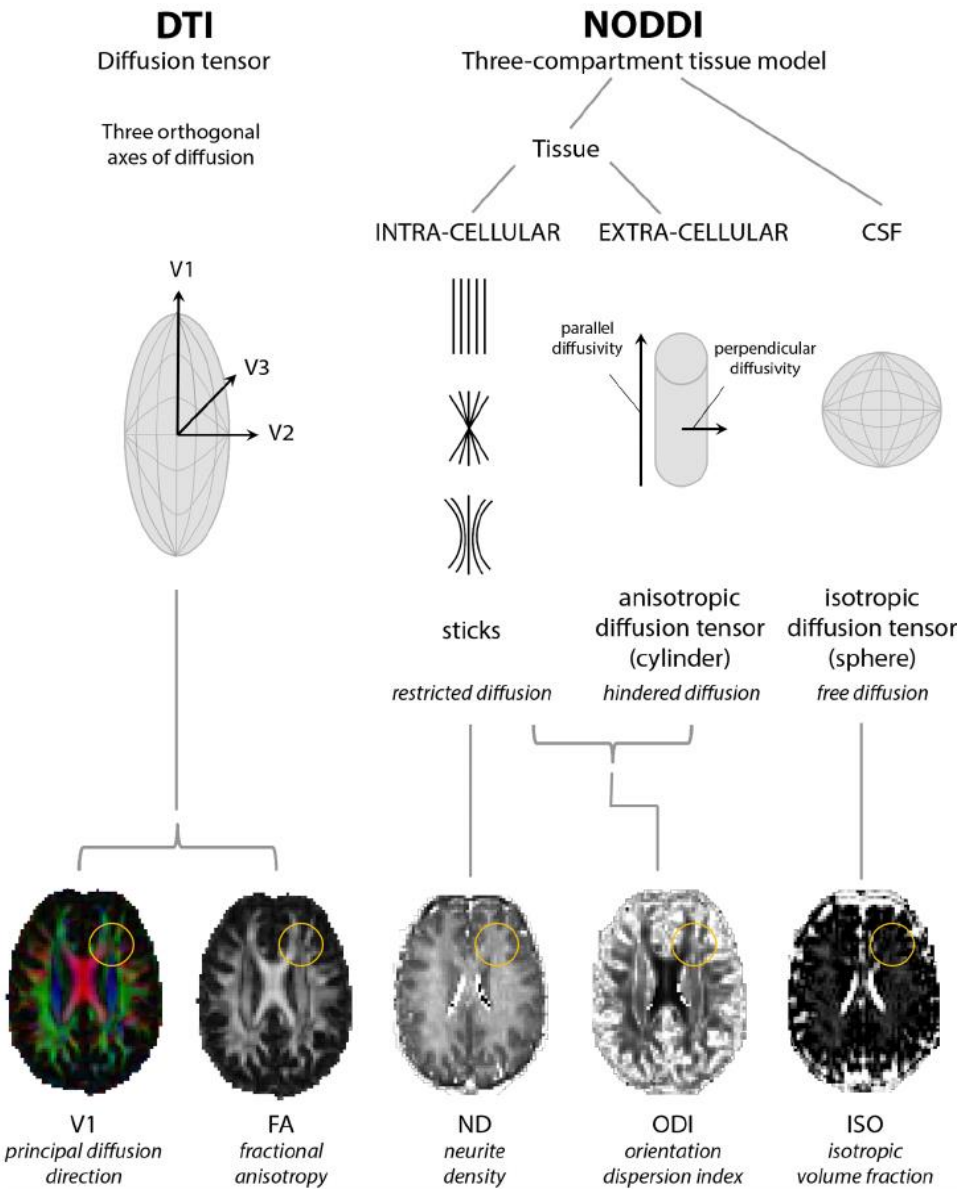


Figure 7. Comparison between FA and neurite orientation dispersion and density imaging (NODDI) measures. NODDI measures described here include: ICVF (intercellular volume fraction, describing neurite density, therefore also referred to as ND in the figure), ISOVF (isotropic of free water volume fraction, referred to as ISO in the figure) and OD (orientation dispersion index, referred to as ODI in the figure). The figure was adapted from Rae et al., (Rae et al. 2017).

## Resting-state connectivity and MDD

### 1 Resting-state fMRI

Structural and event-related fMRI studies have consistently identified prefrontal brain regions as having the strongest associations with general cognitive ability (Kievit et al. 2014; Rosenberg et al. 2016). These regions play a crucial role in executive control (Koechlin and Summerfield 2007) and multisensory integration (Wunderlich et al. 2011), and can be assessed using various task-based paradigms (MacDonald et al. 2000; Weissman et al. 2006; Goldin et al. 2008). However, it has recently been demonstrated that the brain is highly active in the absence of experimental stimuli, i.e. when it is in 'resting state'. The activity of the brain under resting state is metabolically demanding and topologically efficient; it has been proposed that this actively maintains neural signalling in preparation for quick adaptions (Bullmore and Sporns 2012; Hahn et al. 2012). Such spontaneous modulations at rest are temporally correlated between distant brain regions, forming the linkage known as functional connectivity.

The spatial patterns of functional connectivity are known as resting-state networks (RSN). It is well established that these RSN can be robustly extracted from fMRI data (Power et al. 2011), and they have been consistently verified in several independent cohorts (Fox et al. 2006; van den Heuvel et al. 2008; Braun et al. 2012). The RSN approach provides a non-invasive, task-free way of studying such a distributed functional dynamics of the brain (Turk-Browne 2013). In addition to its broad practicability, functional networks found under resting-state are spontaneous, and they are therefore free from confounding effects due to external input (Sporns 2014). This approach therefore provides the possibility of examining the simultaneous involvement of multiple networks, whose temporal organisation is relevant to MDD which is associated with various high-level, integrative mechanisms that involve in emotional and cognitive processing (Cocchi et al. 2013; Sporns 2014).

Major RSN include the default mode network (DMN) and various of task-relevant networks such as the salience, executive control, sensorimotor, dorsal attention and visual networks (see Figure 8) (Buckner and Krienen 2013). The DMN is a network mainly consist of medial prefrontal cortex, posterior cingulate cortex and temporal-parietal junction, was first discovered to be deactivated while the brain is engaged in a goal-directed task and activated under resting-state (Raichle 2015). This network has been hypothesised to be associated with thought rumination and various automated processes (Raichle 2015). The task-relevant networks, on the other hand, were found associated with the functions that they were named after (Buckner and Krienen 2013).

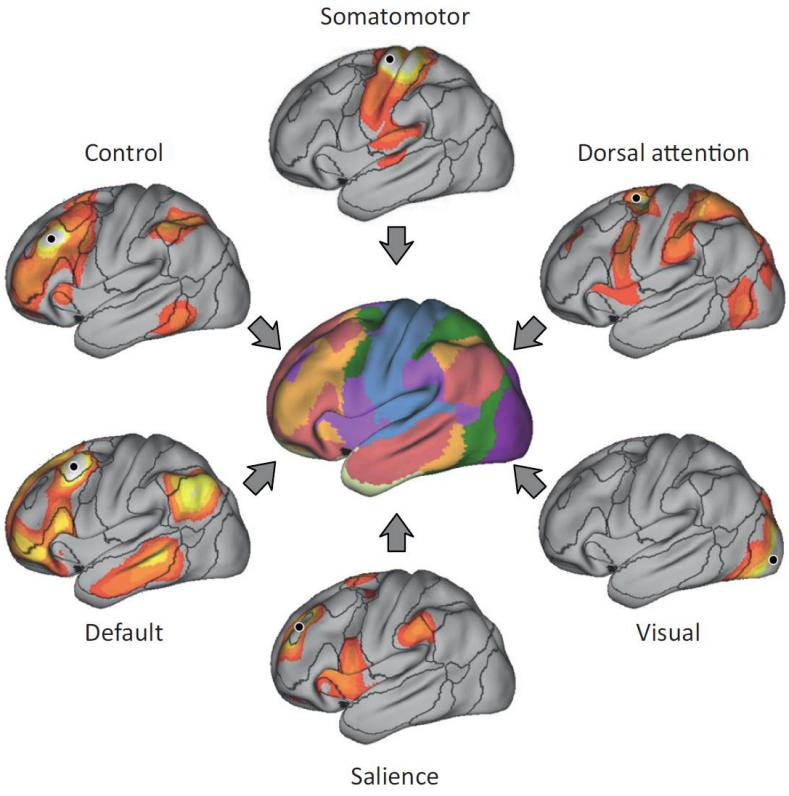


Figure 8. Major resting-state networks (Buckner and Krienen 2013).

## 2 Resting-state networks and MDD

Early studies of resting-state networks involved largely the low-frequency BOLD-signal (blood-oxygen-level dependent) amplitudes in networks of interest (Zou et al. 2008; Han et al. 2011). MDD patients typically showed hyperactivity in DMN in task-related phase when DMN activity is normally suppressed (Sambataro et al. 2014). Inference for the abnormally active DMN is that the network involves spontaneous processes, such as rumination of negative thoughts (Hamilton et al. 2011). Studies about cognition have shown that DMN deactivation in resting-state is associated with lower global network efficiency (Hearne et al. 2016). Therefore the activity of DMN is essential for remaining whole-brain alertness (Greicius et al. 2008), and overly activated DMN may lead to disrupted performance in task-related networks (Bartova et al. 2015).

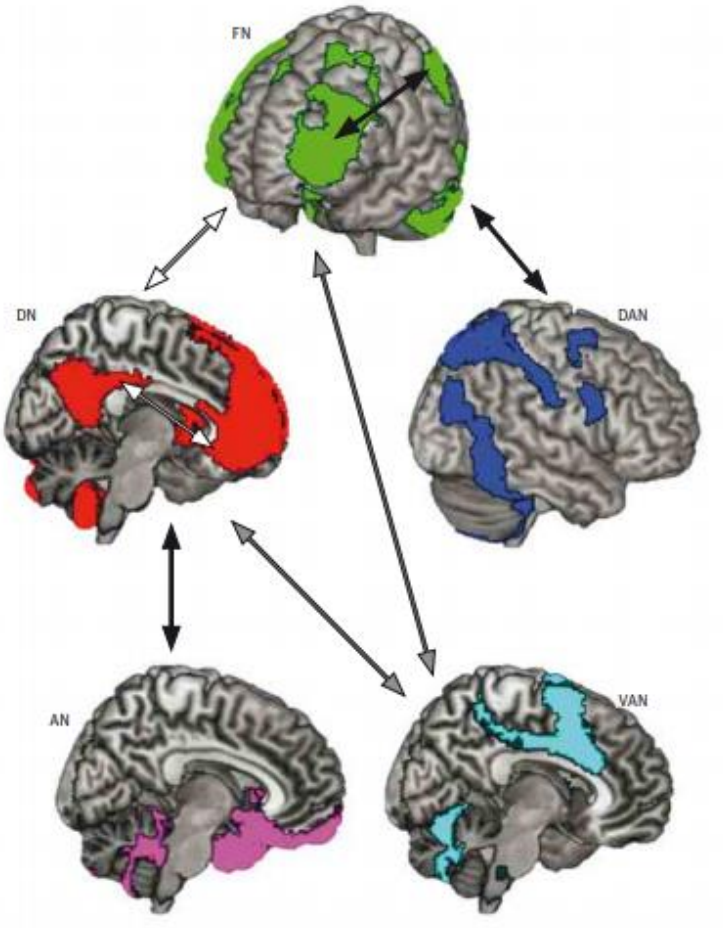


Figure 9. Connectivity between bulk resting-state networks that associate with the onset of MDD

based on a meta-analysis of resting-state connectivity (Kaiser et al. 2015). In the figure, FN=frontoparietal network, DAN=dorsal attention network, DN=default mode network, AN=affective network, and VAN=ventral attention network. The white arrow means hyper-connectivity in MDD, black arrows indicate weaker connections in MDD, and grey arrows represent inconsistent weakening/strengthening in MDD from different studies.

Other than early discussions about arousal level of resting-state networks, topology of functional connectivity in resting-state brings much more dynamic and biologically interpretable phenomenon that can implicate clinically significant inferences.

Resting-state network properties can be presented in several ways. The most widely used measure is functional connectivity, which describes the temporal correlation between remote brain regions (van den Heuvel and Hulshoff Pol 2010) (see Figure 9). MDD case versus control differences has been shown in bulk network connections between DMN and salience network (Bressler and Menon 2010). Studies suggest that the salience network has a mediating role in facilitating the dynamic switch between DMN and the executive control network (see Figure 11). Aberrant connection between DMN and salience network may indicate impaired ability to suppress DMN when goal-directed tasks are involved, therefore hyper-activation in DMN may become a counter-active lever for task-positive networks (Bressler and Menon 2010).

Other properties of resting-state include regional homogeneity (Zhu et al. 2008) and graph-theory topologies, such as small-worldness and global degree (van den Heuvel et al. 2008; Braun et al. 2012). Higher regional homogeneity and global degree were shown in dorsal lateral prefrontal network and temporal-parietal networks in healthy people compared with MDD, which may indicate higher efficiency within networks themselves, and it serves for better functionality (Wu et al. 2011). Previous resting-state studies about MDD suffer from common disadvantages like structural studies that lack statistic power. An additional gap is the extremely limited understanding between the activity of

functional network and genetic risk of MDD, which so far, to our knowledge, has not been investigated in cohort data.

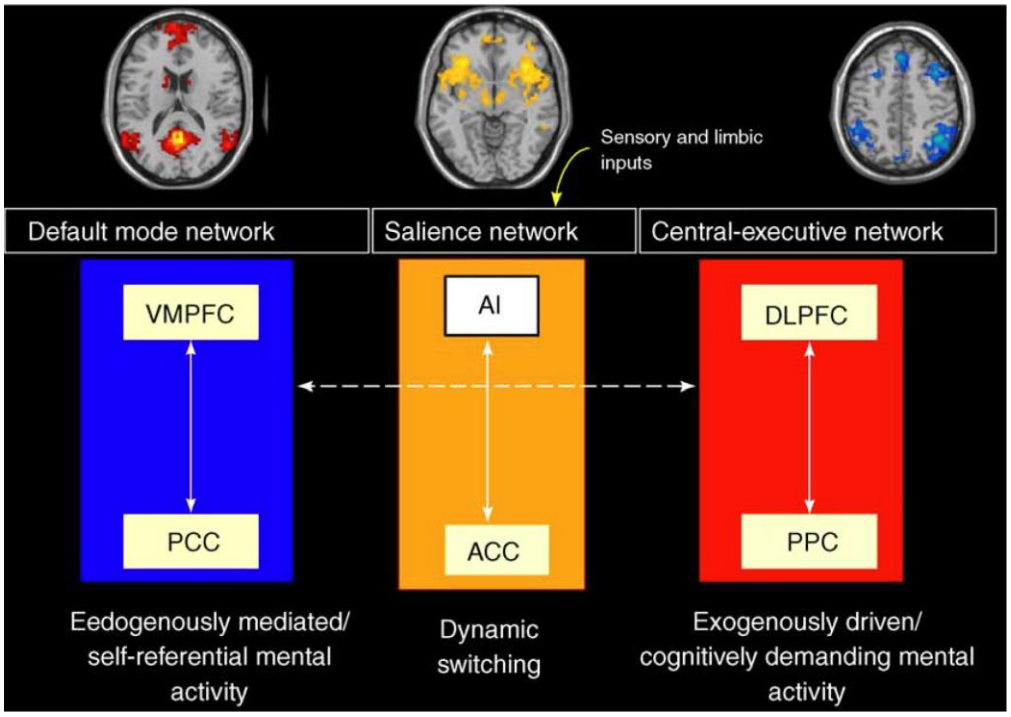


Figure 10. The counterbalanced relationship between DMN and central-executive network, and the lever-like role of salience network (Bressler and Menon 2010).

# Chapter 2:

## Subcortical volume and white matter integrity abnormalities in major depressive disorder: findings from UK Biobank imaging data

## 1 Chapter introduction

This chapter presents a study of group differences between MDD cases and controls in subcortical volumes and white matter microstructure, using the first release of UK Biobank imaging data that includes 1,157 and 1,089 people for subcortical and white matter microstructural measures respectively. Previous studies on MDD case-control differences often used small samples (N<100), therefore led to heterogeneous results. This study aimed to employ a very large sample and investigate the MDD case-control differences, which has been summarised in a published paper entitled, “Subcortical volume and white matter integrity abnormalities in major depressive disorder: findings from UK Biobank imaging data” (Shen et al. 2017), in which I was the first author. I conceived the hypotheses, conducted data analyses and wrote the manuscript under supervision.

## 2 Paper

### 2.1 Abstract

Previous reports of altered grey and white matter structure in Major Depressive Disorder (MDD) have been inconsistent. Recent meta-analyses have, however, reported reduced hippocampal grey matter volume in MDD and reduced white matter integrity in several brain regions. The use of different diagnostic criteria, scanners and imaging sequences may, however, obscure further anatomical differences. In this study, we tested for differences in subcortical grey matter volume (n=1157) and white matter integrity (n=1089) between depressed individuals and controls in the subset of 8590 UK Biobank Imaging study participants who had undergone depression assessments. Whilst we found no significant differences in subcortical volumes, significant reductions were found in depressed individuals versus controls in global white matter integrity, as measured by fractional anisotropy (FA) (β=-0.182, p=0.005). We also found reductions in FA in association/commissural fibres (β=-0.184, $p_{corrected}$=0.010) and thalamic radiations (β=-0.159, $p_{corrected}$=0.020). Tract-specific FA reductions were also found in the left superior longitudinal fasciculus (β=-0.194,

$p_{corrected}$=0.025), superior thalamic radiation (β=-0.224, $p_{corrected}$=0.009) and forceps major (β=-0.193, $p_{corrected}$=0.025) in depression (all betas standardised). Our findings provide further evidence for disrupted white matter integrity in MDD.

## 2.2 Introduction

Major Depressive Disorder (MDD) is a common psychiatric illness, affecting between 5 and 30% of the population which accounts for around 10% of all days lived with disability(Marcus et al. 2012). There is therefore an urgent need to identify the mechanisms underlying MDD and human *in vivo* MRI has been widely applied in this search(Gamazon et al. 2015).

Many brain imaging studies have measured grey matter volume differences between healthy individuals and, predominantly clinically ascertained, individuals with MDD. Prefrontal cortex and limbic areas are fundamental to emotion processing and mood regulation(DeRubeis et al. 2008), and these areas have also been consistently implicated in imaging studies of MDD(Bora et al. 2012; Maller et al. 2014; Meng et al. 2014). As the use of automated methods such as voxel-based morphometry(Soriano-Mas et al. 2011; Wagner et al. 2011) and Freesurfer(Sacchet et al. 2015) have increased, this has expanded the search across the whole brain. In general, structural abnormalities have been reported across diverse brain networks in MDD. Regions including the thalamus(Nugent et al. 2013), amygdala(Bora et al. 2012), insula(Soriano-Mas et al. 2011), caudate(Sacchet et al. 2015), anterior cingulate cortex(Bora et al. 2012), along with prefrontal areas such as orbital prefrontal cortex (OFC)(Fried and Kievit 2015) and dorsal lateral prefrontal cortex (PFC)(Amico et al. 2011) have been reported to be smaller in MDD versus healthy controls. However, other studies have found conflicting results(Kong et al. 2014; Sacchet et al. 2015), or have reported null findings(Wagner et al. 2011). This inconsistency may be due to limited sample sizes and other sources of heterogeneity such as sample characteristics, recruitment criteria, data acquisition and image processing(Arnone et al. 2012).

The lack of a single anatomically circumscribed abnormality in MDD has led many to suggest that the disorder might be due to abnormalities of brain networks affecting connections between several regions. In support of this, findings from individual studies of white matter structure in MDD have shown patterns of alteration using diffusion

tensor imaging (DTI). Proxy measures of white matter integrity, including fractional anisotropy (FA) and mean diffusivity (MD), have been used to infer connectivity differences between groups. Decreased FA indicates lower directionality of water molecule diffusion along fibre pathways and is a proxy of decreased tract integrity, whilst increased MD indicates less constrained water molecule diffusion and a proxy for lower integrity.

White matter integrity of frontal-limbic tracts have been suggested to underlie clinical features in MDD due to a lack of frontal cortical control over brain regions that involve in emotion processing(Korgaonkar et al. 2014). Studies have reported altered water diffusivity of white matter tracts in MDD compared to healthy controls, but the tracts identified are often inconsistent. Some studies reported decreased white matter integrity in tracts that connect prefrontal areas (e.g. fronto-occipital fasciculus, superior longitudinal fasciculus) (Sexton et al. 2012) . While some studies using similar sample sizes also found consistent results (Liao et al. 2013), other groups reported FA deficits in limbic areas (e.g. posterior thalamic radiation, posterior corona radiata) (Korgaonkar et al. 2014). Similar to the studies of subcortical volumes described above, DTI investigations of MDD have often used relatively small sample sizes (Murphy and Frodl 2011; Liao et al. 2013).

Meta-analytic methods may help to overcome issues related to small sample sizes and are also able to quantify and test for between-study heterogeneity. A recent meta-analysis of subcortical structures by Schmaal *et al.* tested over 1650 MDD patients and around 7000 healthy controls across 15 studies, and reported hippocampal grey matter volume reductions in MDD. No other case-control differences were found (Schmaal et al., 2016a). Meta-analyses of white matter integrity measures in MDD have also reported FA reductions in superior longitudinal fasciculus, fronto-occipital fasciculus, and thalamic radiations (Murphy and Frodl 2011; Liao et al. 2013). These studies, however, often require the combination of imaging data from different scanners, using different ascertainment criteria and methodology, different clinical instruments and have differing levels of phenotypic data to pursue further research questions. Meta-analytic findings therefore highlight the pressing need to measure brain structural abnormalities in MDD using larger single-scanner samples where robust conclusions can be made in the absence of differing study methodologies.

In the current study, we examined the volumetric structural imaging data of subcortical brain structures and tract-specific white matter integrity measures from the UK Biobank imaging study. UK Biobank is a study of 500,000 subjects recruited from across the United Kingdom (Sudlow et al. 2015). The dataset used in the current study is the latest release of imaging data on 8590 participants who participated in the brain imaging assessment (Miller et al. 2016). For our current purposes this included 354/342 MDD and 803/762 controls respectively who provided usable for T1-weighted/DTI data from a single scanner, along with available data regarding diagnostic and phenotypic information. The scanning protocol and pre-processing pipelines were devised by UK Biobank, with consistent, compatible setting of scanner parameters and participant-friendly experimental procedures. This data therefore allowed us to explore structural changes associated with depression in a single large population-based sample using data from an individual study source with unified depression classification, and with scanning sequences and image processing procedures applied consistently across all subjects, all of whom were imaged on a single MRI scanner.

## 2.3 Methods

### Participants

In the latest release of imaging data from UK Biobank, 5797 people completed the subcortical brain structural MRI measurements and 5171 completed DTI assessment (Fig S1). The study has been approved by the National Health Service (NHS) Research Ethics Service (approval letter dated 17th June 2011, reference: 11/NW/0382), and by the UKB Access Committee (Project #4844). Written informed-consent was obtained from each subject. All assessments were performed in accordance with the regulations and protocols from the committees.

Individuals from the initial pilot phase of imaging using different acquisition parameters were excluded from the current study, as were those that did not complete pre-processing quality checks conducted by UK Biobank. In addition, scans from individuals that were identified by our internal quality check as having a structural measure that lay more than three standard deviations from the sample mean were excluded (Appendix 1: Fig S2, S3, Table S1). Any participants that had a diagnosis of

Parkinson's Disease, bipolar disorder, multiple personality disorder, schizophrenia, autism or intellectual disability were also excluded from the current analysis (ICD-10/9 or self-report). This resulted in data from 5397 participants with T1-weighted subcortical volumes and 4590 participants with DTI measures. Mean ages were 55.47 +/- 7.49 years for those with T1-weighted, grey matter data and 55.46 +/- 7.41 years for those with DTI, white matter integrity. The proportions of male participants are were similar in both datasets (45.78% for those providing T1-weighted data and 47.12% for those with DTI measures). Details of data exclusions are detailed within supplementary materials (Method, Participants; Fig S1).

**MDD definitions**

The definition of MDD used in the current study was generated based on the putative MDD category summarized previously by Smith *et al.*, as presented in supplementary materials (Fig S4) (Smith et al. 2013). They generated the criteria of single episode major depression, recurrent major depression (moderate), recurrent major depression (severe) and those who were absent of depression. This category was benchmarked by testing its prevalence in the sample, and by testing for association with a number of traits, such as neuroticism (Jylha et al. 2009), that have previously been associated with MDD (Kendler et al. 2004). However, since the category is based on hospital admission data and depressive symptoms, which were both self-reported, rather than more formal ICD/SCID criteria, cases should be considered 'probable' MDD rather than operationally defined on the basis of an interview.

We generated two definitions of probable MDD. One was the principal MDD definition that compared all MDD patients (recurrent and single episode) with healthy controls, while the other was based on recurrence and compared recurrent MDD patients with non-recurrent and non-MDD individuals.

The principal MDD definition therefore included those who were categorised in single and multiple episode major depression as cases. The corresponding control group contained participants that were absent of depression according to the putative MDD category described by Smith *et al* (Smith et al. 2013). For the recurrent MDD definition, the case group only included recurrent major depression. The corresponding control group therefore referred to the participants without recurrent MDD, which included single episode major depression, those who were absent of depression and those who

reported depressive symptoms but not enough to be specified as MDD. Participants who did not answer one or more of the questions necessary for classification were excluded from this analysis.

For each definition of probable MDD, the participants with subcortical volume data consisted of 354 MDD cases and 803 controls and 261 MDD cases and 1196 controls respectively for principal and recurrent definitions. Participants with DTI data consisted of 335 MDD cases and 754 controls and 242 MDD cases and 1113 controls for principal and recurrent definitions respectively. Method used to derive the samples into analyses were presented in supplementary materials, Fig S1.

The descriptions and demographic characteristics of each MDD definition are shown in supplementary materials (Appendix 1: Table S2, S3). For the purposes of the current analysis, we used the principal definition of depression as the main definition as it most closely resembles the general application of typical clinical criteria. We also report results of the recurrent definition of MDD to highlight differences associated with a more severe recurrent MDD diagnosis. (Appendix 1: Supplementary materials, Table S3).

**MRI acquisition and analyses**

We used the imaging-derived phenotypes (IDPs) generated by UK Biobank. The MRI acquisition, pre-processing and imaging analysis for subcortical volumes and FA values of white matter tracts were all conducted by UK Biobank using standard protocols(Miller et al. 2016), see supplementary material. Briefly, all imaging data was collected on a Siemens Skyra 3T scanner (https://www.healthcare.siemens.com/magnetic-resonance-imaging) and was preprocessed using FSL packages. For T1-weighted data, segmentation of brain was conducted in two steps: firstly, a tissue-type segmentation using FAST (FMRIB's Automated Segmentation Tool)(Zhang et al. 2001) was applied to extract cerebrospinal fluid, grey matter and white matter; then subcortical structures are extracted using FIRST (FMRIB's Integrated Registration and Segmentation Tool)(Patenaude et al. 2011). For DTI data, parcellation of tracts were conducted using AutoPtx (De Groot et al. 2013).

The summary data contained volumes of grey matter, white matter, cerebrospinal fluid, thalamus, putamen, pallidum, hippocampus, caudate, brain stem, amygdala and accumbens (Fig S2). DTI data provided tract-averaged FA for 27 major tracts (12 bilateral tracts in both hemispheres and 3 tracts that pass across brain): (a) association and commissural fibres: forceps major and minor, inferior fronto-occipital fasciculus, uncinate fasciculus, cingulum bundle and superior longitudinal fasciculus; (b) thalamic radiations: anterior, superior and posterior thalamic radiations; (c) projection fibres: corticospinal tract, acoustic radiation, medial lemniscus, middle cerebellar peduncle.

Scans with severe and obvious normalization problems were excluded by UK Biobank. In addition we also excluded observations that were more than three standard deviation from the sample mean for the analysis of subcortical volumes. For DTI measures, participants with at least one outlier of tract-averaged FA from the sample mean were excluded for that measure. Descriptions of the sample were reported in supplementary materials (Method, MRI preprocessing; Fig S1-3). For transparency, the results without excluding outliers are also presented in the supplementary materials.

**Statistical methods**

Subcortical volumes: First, differences in global intracranial volume (ICV) associated with a probable MDD diagnosis were examined by modelling ICV as dependent variable, controlling for age, age$^2$, sex and assessment centre. ICV was measured by adding up volumes of white matter (WM), grey matter (GM) and cerebrospinal fluid (CSF). For bilateral subcortical volumes, age, age$^2$, sex, hemisphere, assessment centre and ICV were set as covariates in a repeated-effect linear model to test for an association between both probable MDD definitions on subcortical volumes, adjusted for whole brain size. For unilateral structures, a general linear model was applied as above, without controlling for hemisphere. We also examined the interaction of hemisphere and MDD definitions on bilateral structures. Where there was a significant MDD by hemisphere interaction, analyses on both lateralised structures were conducted separately. All subcortical volumes were rescaled into zero mean and unitary standard deviation in order that effect sizes represent standardized scores. False Discovery Rate (FDR) multiple comparison correction was applied for tests of the 8 subcortical volumes plus additional tests on ICV, conducted separately for the two probable MDD definitions (Fig 1, Table 1, S5).

White matter integrity: In order to test for an association between probable MDD and FA, as above we used a general linear model with age, age$^2$, sex and assessment centre as covariates and the definition of MDD as a fixed factor. First we examined for the effects of diagnosis on global whole brain white matter integrity. The brain's white matter tracts have been shown to share a considerable proportion of variance in their microstructural properties in this (Cox, Ritchie, et al. 2016) and other samples (Penke et al. 2010, 2012). Global integrity was determined using standardised approaches by applying principal component analysis (PCA) on the 27 tracts to extract a latent measure (Cox, Ritchie, et al. 2016). Scores of the first un-rotated component of FA were extracted and set as the dependent variable of the general linear model to test the effect of probable MDD diagnosis (variance explained=36.5%). Then we separately examined three subsets of white matter tracts: (a) association and commissural fibres which include tracts connecting cortex to cortex, (b) projection fibres which consist of tracts connecting cortex to spinal cord and brainstem, as well as sensory tracts that connect cortex to thalamus and (c) thalamic radiations that connect thalamus with cortical areas (Cox, Ritchie, et al. 2016). Scores of the principal un-rotated component for each subset was extracted (variance explained=44.1%, 60.1% and 38.1% respectively for A/CF, TR and PF) for further general linear modelling as with the global latent measure. Loadings and scree plot of PCA analyses are in supplementary materials (Appendix 1: Table S10, Fig S5). Finally, we examined the effects of depression on each tract individually. Repeated-effect linear models were used for the measures of bilateral white matter tracts correcting for hemisphere as above, while random-effect general linear models were used for the unilateral midline tracts. Both the main effect of MDD definition and its interaction with hemisphere were tested. Where the interaction was significant, tests were applied individually for left and right sides separately. FDR correction was individually applied over the three subsets of white matter tracts as well as individual tracts (Benjamini et al. 1995).

## 2.4 Results

### The effect of MDD definitions on subcortical volumes

We found no significant group effect for ICV based on the principal definition of MDD ($\beta$=-0.046, $p_{uncorrected}$=0.341). There were also no significant differences between groups based on the principal definition of MDD for any of the subcortical brain regions,

including the hippocampus (βs=-0.050~0.064, $ps_{uncorrected}$>0.199, $ps_{corrected}$>0.834); see Fig. 1, Table 1. No region demonstrated significant interaction of hemisphere, therefore no region was examined separately on different hemispheres.

The same models were also applied to compare recurrent MDD and controls, see above. No subcortical regions reached significance in this definition of recurrent cases versus controls. The largest nonsignificant effect size was observed for the caudate (β=0.064, $p_{uncorrected}$=0.231).

Figure 1. (A) Subcortical structures of interest in left, inferior and anterior view. (B) The effect of principal definition of probable MDD on subcortical volumes. Linear models were conducted, controlling the effect of age, age$^2$, sex, assessment centre and intracranial volume (and hemisphere for the regions that have bilateral values). The x-axis shows the standardised effect size of MDD definition, and y-axis is the layout of the subcortical structures. The error bar represents standard deviation of mean.

(A)

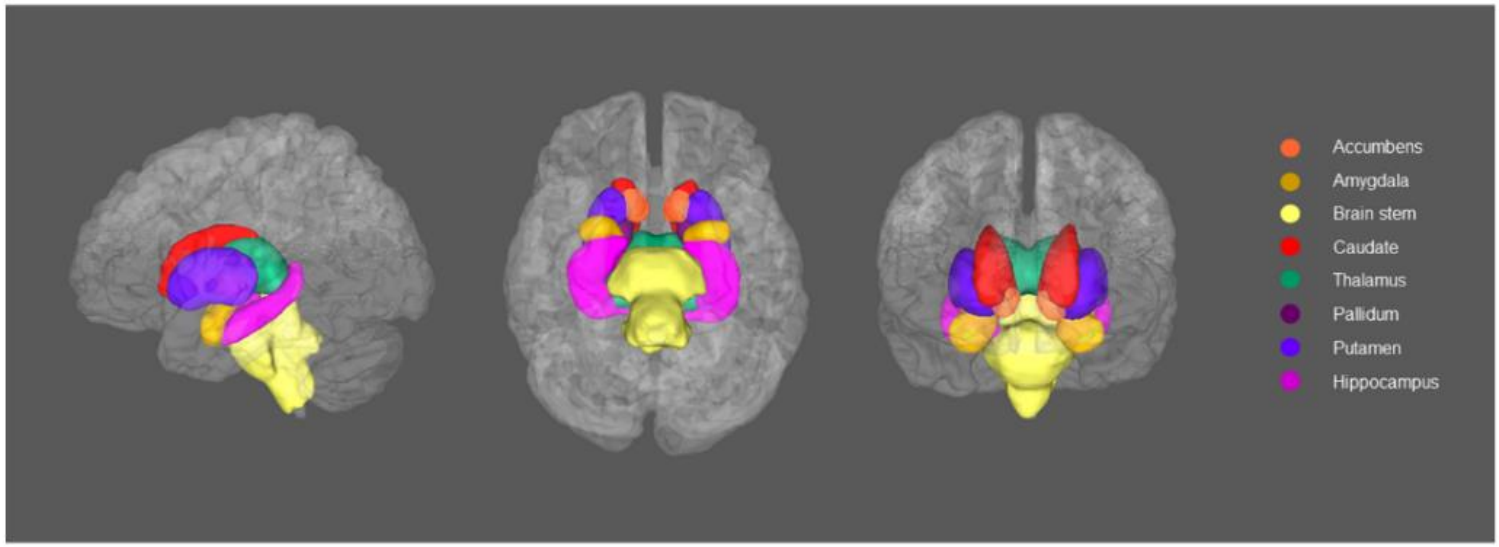
Accumbens
Amygdala
Brain stem
Caudate
Thalamus
Pallidum
Putamen
Hippocampus

(B)

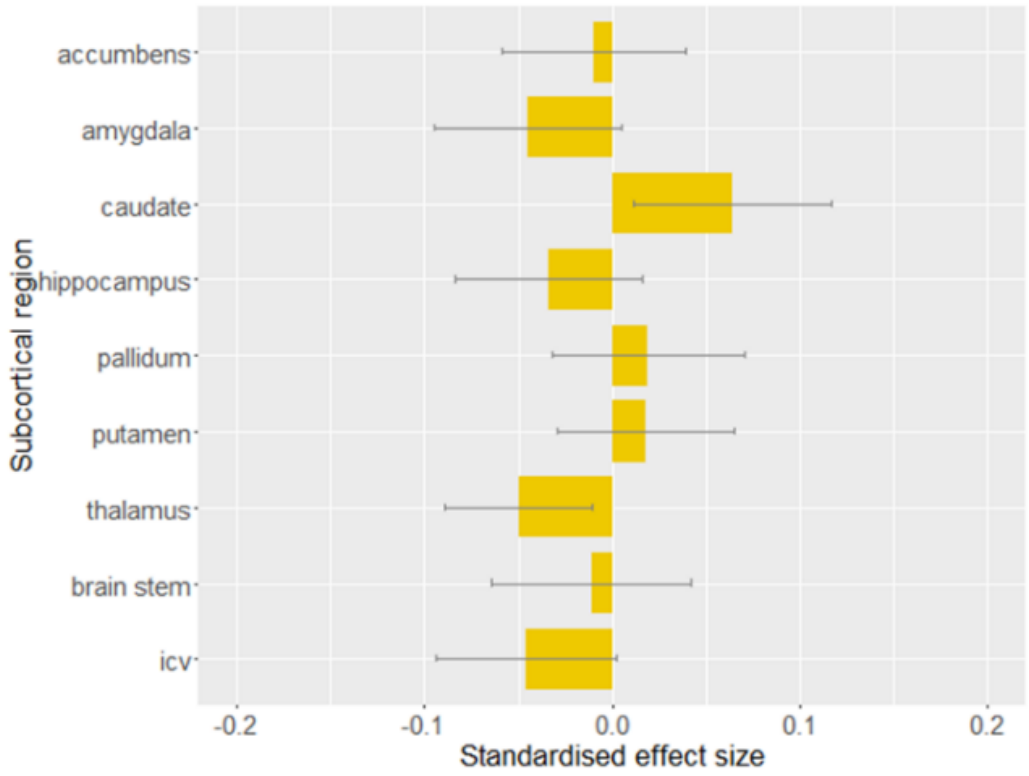
accumbens
amygdala
caudate
hippocampus
pallidum
putamen
thalamus
brain stem
icv
Subcortical region
-0.2
-0.1
0.0
0.1
0.2
Standardised effect size

**The effect of probable MDD on measures of white matter integrity**

Firstly we tested the effect of probable MDD on general white matter FA (gFA). For both the principal and recurrent definitions, gFA was lower in probable MDD cases versus controls (β=-0.182, p=0.005; β=-0.160, p=0.022 respectively).

We then examined tracts categorised into association/commissural fibres (gAF), thalamic radiations (gTR) and projection fibres (gPF). We found effects of probable MDD on measures of FA in two of the three groups of tracts. Probable MDD at principal and recurrent definitions showed smaller values in gAF (Probable MDD: β=-0.184, $p_{corrected}$=0.010; Recurrent MDD: β=-0.170, $p_{corrected}$=0.045) and gTR (Probable MDD: β=-0.159, $p_{corrected}$=0.020; Recurrent MDD: β=-0.141, $p_{corrected}$=0.068). No effect was found for gPF (Probable MDD: β=-0.115, $p_{corrected}$=0.073; Recurrent MDD: β=-0.057, $p_{corrected}$=0.401). The above findings were checked in self-declare depression, and the results were found to be similar (see supplementary materials, MDD definitions).

We then proceeded to compare FA values in the individual tracts between cases and controls. Initially, we tested the tracts controlling for hemisphere effects. Then we tested the interaction of hemisphere and probable MDD definitions on bilateral tracts to identify any lateralised effects. There was a significant interaction of hemisphere in superior longitudinal fasciculus for recurrent definition of probable MDD (β=0.117, $p_{corrected}$=0.026). The left and right superior longitudinal fasciculi were therefore tested separately.

We found reduced FA in the left superior longitudinal fasciculus for both definitions of MDD versus controls (Probable MDD: β=-0.194, $p_{corrected}$=0.025; Recurrent MDD: β=-0.221, $p_{corrected}$=0.025) (Fig. 2, Table 2). No significant association was found with right superior longitudinal fasciculus (Principal MDD: Probable MDD: β=-0.057, $p_{corrected}$=0.379; Recurrent MDD: β=-0.029, $p_{corrected}$=0.684). Significant FA decrease was found in superior thalamic radiation and forceps major, but only for principal MDD definition (Probable MDD: β=-0.224, $p_{corrected}$=0.009; β=-0.193, $p_{corrected}$=0.025. Recurrent MDD: β=-0.179, $p_{corrected}$=0.080; β=-0.133, $p_{corrected}$=0.150 respectively for the two tracts). In order to check whether the decreased FA in the above tracts was due to global changes in gFA, the effect of MDD definitions was tested again with gFA

included as a covariate (Appendix 1: Table S6). Left superior longitudinal fasciculus remained significant in both definitions (Probable MDD: β=-0.194, $p_{corrected}$=0.038; Recurrent MDD: β=-0.221, $p_{corrected}$=0.025). Forceps major showed decreased FA in probable MDD definition (β=-0.193, $p_{corrected}$=0.038) but not in recurrent MDD (β=-0.133, $p_{corrected}$=0.350). The effect MDD definitions on superior thalamic radiation didn't reach significance after correcting for gFA (Probable MDD: β=-0.110, $p_{corrected}$=0.162; Recurrent MDD: β=-0.077, $p_{corrected}$=0.568). The above results of individual tracts turned null if outliers weren't excluded, but the standard effect sizes were in similar trend (Appendix 1: Table S7).

Figure 2 (see the next page). (A) White matter tracts in each anatomical subset in left, posterior and anterior view. (B) The effect of principal definition of probable MDD on FA value of tracts. Linear models were conducted, controlling the effect of age, age$^2$, sex and assessment centre (and hemisphere for the tracts that have bilateral values). Left superior longitudinal fasciculus was presented because there was a significant interaction between recurrent MDD definition and hemisphere. Follow-up analysis showed a lateral effect of probable MDD definition on left superior longitudinal fasciculus. The x-axis shows the standardised effect size of MDD definition, and y-axis is the layout of the white matter tracts. The error bar represents standard deviation of mean.

(A)

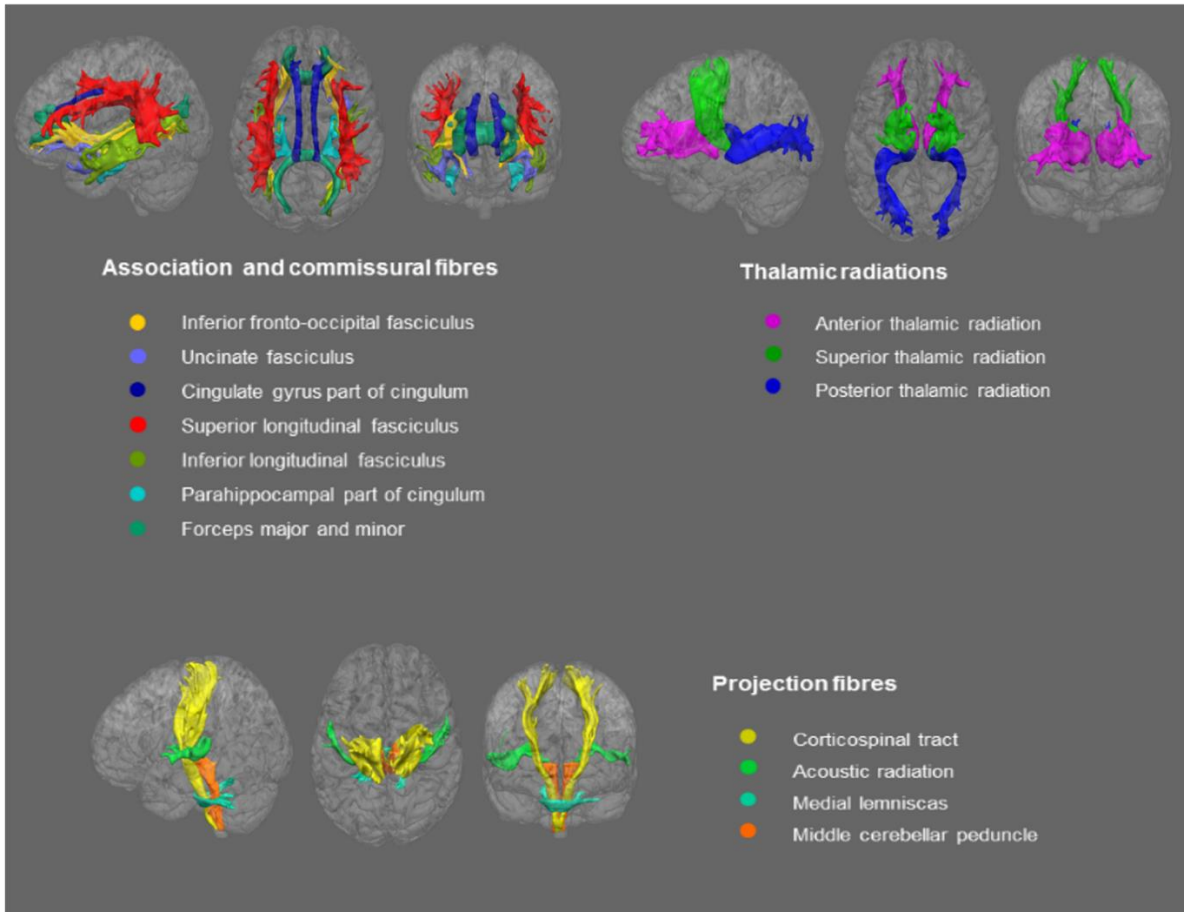
Association and commissural fibres
Inferior fronto-occipital fasciculus
Uncinate fasciculus
Cingulate gyrus part of cingulum
Superior longitudinal fasciculus
Inferior longitudinal fasciculus
Parahippocampal part of cingulum
Forceps major and minor
Thalamic radiations
Anterior thalamic radiation
Superior thalamic radiation
Posterior thalamic radiation
Projection fibres
Corticospinal tract
Acoustic radiation
Medial lemniscas
Middle cerebellar peduncle

(B)

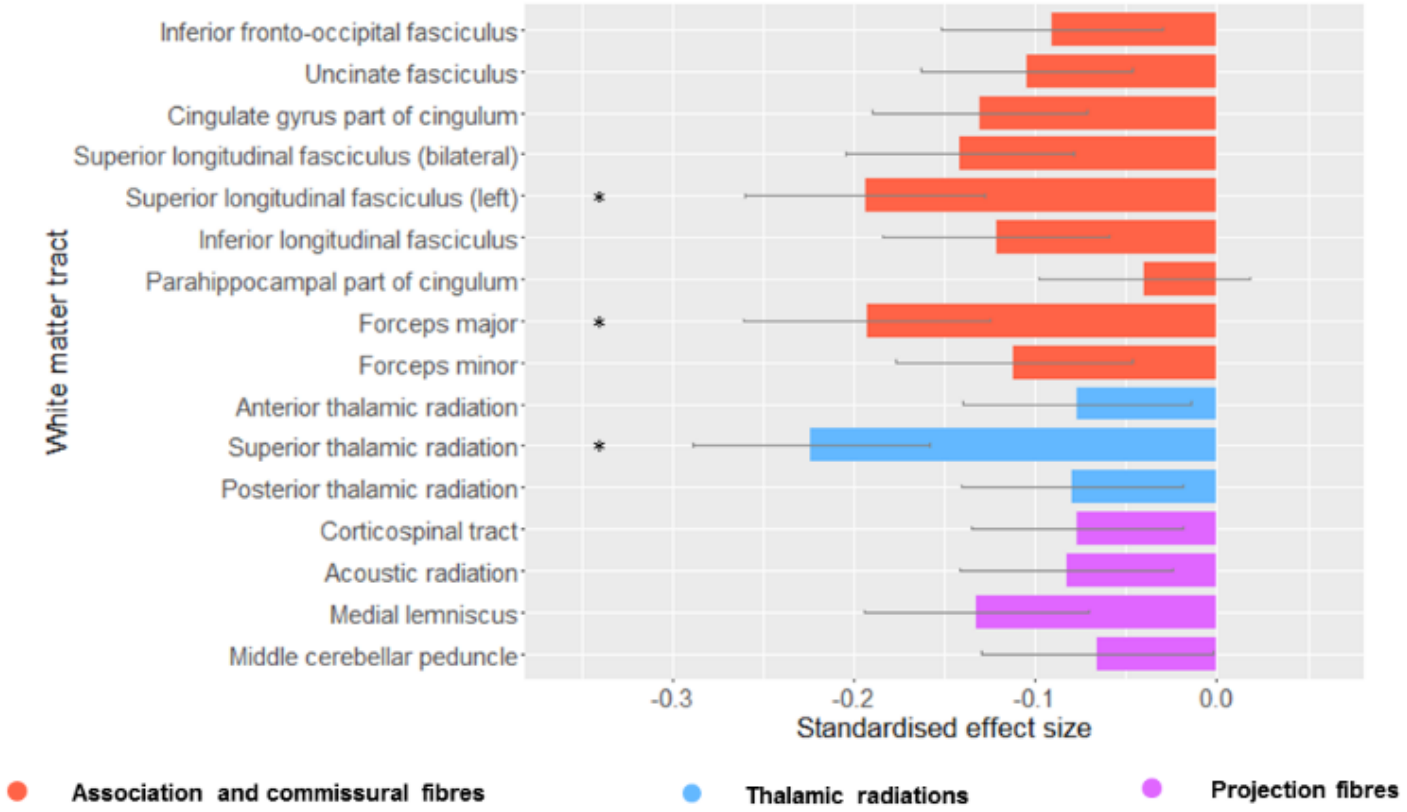
Inferior fronto-occipital fasciculus
Uncinate fasciculus
Cingulate gyrus part of cingulum
Superior longitudinal fasciculus (bilateral)
Superior longitudinal fasciculus (left)
Inferior longitudinal fasciculus
Parahippocampal part of cingulum
Forceps major
Forceps minor
Anterior thalamic radiation
Superior thalamic radiation
Posterior thalamic radiation
Corticospinal tract
Acoustic radiation
Medial lemniscus
Middle cerebellar peduncle
*
*
*
White matter tract
-0.3
-0.2
-0.1
0.0
Standardised effect size
Association and commissural fibres
Thalamic radiations
Projection fibres

## 2.5 Discussion

In the current study, we sought to determine whether MDD was associated with differences in subcortical grey matter volume or white matter integrity in a large imaging dataset from a single scanner of more than 8000 people, and among them over 1000 were included as cases and controls in the analyses for the present study. The sample sizes of MDD cases and controls included in the analysis of white matter integrity is by far the largest to our knowledge. Also, the present study considered two important brain structural modalities in two highly overlapping samples. Whilst we did not find any statistically significant subcortical volumetric differences between unaffected participants and individuals with probable MDD (using any of the definitions with increasing severity), we did find substantial evidence of reduced white matter integrity in MDD. This was seen globally, in two of the three categories of tracts (association/commissural fibres and thalamic radiation tracts), and in individual tracts (bilateral superior thalamic radiation, forceps major and left superior longitudinal fasciculus). Similar patterns of findings were seen for both principal and recurrent definition of depression with generally greater effect sizes in recurrent cases, with the exception of the localised differences in the superior thalamic radiation and forceps major.

Our study notably did not find evidence for bilateral hippocampal volume reduction as previously reported in the large collaborative meta-analysis of MDD(Schmaal et al. 2016). We also did not find evidence of reductions in hippocampal volume when looking at recurrent MDD as published in the same study. The lack of subcortical volumetric differences associated with probable MDD diagnoses in the current study therefore does not support the widely held belief that there are subcortical volumetric changes associated with the disorder. There are several potential explanations for this. Firstly, the UK Biobank dataset included only community-dwelling, ambulant individuals who could independently complete the health and cognitive assessments, and attend the follow-up imaging assessments. This approach arguably selected MDD groups that were more well/better functioning but equally more representative of the general population than purely clinically ascertained samples. We also used a composite ‘probable’ MDD diagnosis that was based on self-report symptoms and hospital admission statistics, and the cases were selected based on self-report lifetime experience of probable depression. In contrast, many other studies previously used a

structured clinical interview schedule, such as the Structured Clinical Interview for DSM-IV (SCID), to define MDD according to standard criteria. Some studies have specifically studied people who were certainly experiencing depression at the time of imaging assessment(Turner et al. 2012). Whilst the probable MDD definitions used in the current paper were not based on an interview, they showed many of the same epidemiological and risk-factor associations as clinically defined cases (Smith et al. 2013; Okbay et al. 2016).

Although we do not report subcortical volume differences, we did find substantive evidence for robust deficits in both global and local white matter integrity. We found that MDD patients had global loss of FA which was also found to be reduced in association and commissural fibres as well as in thalamic radiations, but not in projection fibres. FA in these structures was also more severely reduced in the recurrent MDD patients. The above results indeed reflect previous findings from previous small-sample and meta-analytic studies (Sexton et al. 2009; Liao et al. 2013; Chen et al. 2016), while extending them to a more generalizable population-based cohort excluding potential methodological confounds as associated with the previous studies. A previous meta-analytic study that compared 231 MDD patients with 261 healthy participants found reduced FA in inferior longitudinal fasciculus, inferior fronto-occipital fasciculus, posterior thalamic radiation and corpus callosum, which belong to the association/commissural fibres and thalamic radiations(Liao et al. 2013). Following the above study, another two recent meta-analyses found integrity reductions in the same categories, i.e. dorsal lateral PFC area, commissural fibres (Wen et al. 2014; Chen et al. 2016). The global loss of FA in these regions could be the result of general neurodevelopmental alterations in MDD patients (Korgaonkar et al. 2011), and findings within defined subsets of white matter tracts could reflect the neurological basis of MDD as a disconnection within an integrated network of cortex-cortex and cortical-limbic pathways (Veer 2010). The general FA reductions in groups of tracts is also consistent with findings from resting-state fMRI studies, which reported abnormalities in MDD populations in regional networks rather than just individual regions or structures (Greicius et al. 2007; Meng et al. 2014). The networks that derive from prefrontal cortex and thalamus has been found largely contribute to emotional and social cognition processes (Korgaonkar et al. 2011). The reduced integrity in these groups of tracts may therefore reflect the repeatedly found impairment of emotion regulation (Kanske et

al. 2012; Heller et al. 2013), reward processing (Gradin et al. 2011) and executive control (Snyder 2013) in MDD populations.

In the tests of single white matter tracts, we found significantly altered integrity in left superior longitudinal fasciculus and superior thalamic radiation both in the overall MDD population and recurrent MDD patients. Reduction of left superior longitudinal fasciculus was notably larger in recurrent MDD patients. Reduction of integrity in forceps major was also found in MDD compared with healthy subjects, however showed no specific change of FA in recurrent MDD.

Superior longitudinal fasciculus, as a part of association fibres, connects prefrontal cortex and other lobes (Huang et al. 2011). Small-sample studies have specifically reported reduced integrity in superior longitudinal fasciculus in various depressive samples, including elderly patients with depression (Sheline et al. 2008; Korgaonkar et al. 2011), depressive adolescents (Cullen et al. 2010) and adolescents with familial risk for depression (Huang et al. 2011), compared with controls. Meta-analytic studies (de Schotten et al. 2011; Chen et al. 2016) and a review (Sexton et al. 2009) also ascertained that the reduction of white matter integrity specifically in superior longitudinal fasciculus may be an important biomarker of the presence of depression. A recent study combined genetic and neuroimaging techniques found that people with higher polygenic risk of depression have greater loss of FA in superior longitudinal fasciculus (Whalley et al. 2013), suggesting that it may also therefore be a useful trait-related marker of risk. Loss of integrity in superior longitudinal fasciculus has also previously been reported to be associated with various cognitive dysfunctions, like working memory (Karlsgodt et al. 2008) and attention (de Schotten et al. 2011). Severity of depressive symptoms was also found correlate with FA loss in superior longitudinal fasciculus (Lai and Wu 2014). There is increasingly convincing evidence therefore that reduced integrity in superior longitudinal fasciculus might be an important feature of the neurobiology of MDD and may underlie impaired emotional process and cognitive abilities in MDD population (Murphy and Frodl 2011).

Another strength of the present study is that cross-modality assessment was conducted on both subcortical volumes and white matter integrity. Though the findings were largely found in white matter integrity instead of subcortical volumes, this is consistent with another cross-modality study by Sexton et al.(2012), which presented that no significant group difference was found between late-life depression and healthy

control, whereas white matter integrity was reduced in many regions (Sexton et al. 2012). Another study on 358 people similarly found that depressive symptoms of elderly subjects also showed significant deficit in white matter, but not in grey matter measures (Allan et al. 2016). The age range for the present study is from 40 to 70, which covers a notable range of elderly participants. This feature of our sample could be the reason why it showed similar contrast of findings between white matter and grey matter measurements.

Potential limitations of the current study should be considered, these include the absence of a face-to-face structured diagnostic interview schedule and the lack of hospital-based sampling. The large sample size may, however, overcome some of these difficulties and community based population sampling may yield more generalizable findings than those based on clinically ascertained samples alone (Benedetti et al. 2011; Soriano-Mas et al. 2011). The current investigation, by avoiding the combination of clinically and methodologically diverse samples, may also have ameliorated several important confounds such as differences due to different healthcare systems and illness related conditions including age of onset and duration of illness. Another factor of interest for future studies is the effect of hospital treatment. As studies have reported changes of depressive symptoms caused by medication or cognitive treatment (DeRubeis et al. 2008), investigates on the neurological effect of treatment should be conducted. The prevalence of the present study is lower than 10%, which is less than the prevalence of ~20% in overall sample of the cohort in the study by Smith et al. (2013) (Smith et al. 2013). This was mainly due to the difference of sizes between the two samples. There were ~5500 participants in the sample with T1-weighted/DTI data, whereas over 30 times of people were included in the full cohort (N=172,751). This difference therefore supports the necessity of studying MDD in a large sample to minimise the bias of selecting study sample. A further potential limitation is that for the volumetric analysis we only focused on the subcortical volumes in the current study. We can therefore not exclude the possibility of cortical differences in MDD, including regional volume differences, as well as measures of cortical thickness and gyrification for example.

Our study presents a comprehensive comparison of brain structural changes related to MDD using the largest single sample available to date from a single scanner with uniform methodologies for clinical categorisation and scanning. We mainly report

reductions of white matter FA in general latent measures of association and commissural fibres as well as thalamic radiations, and in left superior longitudinal fasciculus both in MDD and recurrent MDD. Future work would be potentially focusing on structural changes in cortical areas as well as richer stratification of MDD into informative biologically-based subgroups.

Table 1. The effect of MDD definition on the volumes of subcortical regions and brain matters.

| Subcortical regions | Principal definition | | | | | Recurrent definition | | | | |
|---|---|---|---|---|---|---|---|---|---|---|
| | Effect size | Standard deviation | t value | p value | $p_{corrected}$ | Effect size | Standard deviation | t value | p value | $p_{corrected}$ |
| **Accumbens** | -0.010 | 0.049 | -0.211 | 0.833 | 0.838 | -0.018 | 0.052 | -0.348 | 0.728 | 0.819 |
| **Amygdala** | -0.045 | 0.050 | -0.896 | 0.371 | 0.834 | 0.038 | 0.053 | 0.711 | 0.477 | 0.819 |
| **Caudate** | 0.064 | 0.053 | 1.198 | 0.231 | 0.834 | 0.025 | 0.056 | 0.453 | 0.650 | 0.819 |
| **Hippocampus** | -0.034 | 0.050 | -0.682 | 0.495 | 0.838 | -0.040 | 0.053 | -0.758 | 0.449 | 0.819 |
| **Pallidum** | 0.019 | 0.051 | 0.372 | 0.710 | 0.838 | -0.022 | 0.054 | -0.414 | 0.679 | 0.819 |
| **Putamen** | 0.018 | 0.047 | 0.386 | 0.700 | 0.838 | -0.008 | 0.049 | -0.162 | 0.871 | 0.871 |
| **Thalamus** | -0.050 | 0.039 | -1.284 | 0.199 | 0.834 | -0.059 | 0.041 | -1.428 | 0.154 | 0.819 |
| **Brain stem** | -0.011 | 0.053 | -0.205 | 0.838 | 0.838 | 0.045 | 0.056 | 0.794 | 0.428 | 0.819 |
| **ICV** | -0.046 | 0.048 | -0.953 | 0.341 | 0.834 | -0.049 | 0.051 | -0.959 | 0.338 | 0.819 |

Table 2. The effect of MDD definition on FA values of DTI tracts.

| DTI tracts | Principal definition | | | | | Recurrent definition | | | | |
|---|---|---|---|---|---|---|---|---|---|---|
| | Effect size | Standard deviation | t value | p value | $p_{corrected}$ | Effect size | Standard deviation | t value | p value | $p_{corrected}$ |
| **Acoustic radiation** | -0.083 | 0.059 | -1.410 | 1.59E-001 | 0.231 | -0.094 | 0.063 | -1.485 | 1.38E-001 | 0.221 |
| **Anterior thalamic radiation** | -0.077 | 0.063 | -1.221 | 2.22E-001 | 0.254 | -0.065 | 0.067 | -0.973 | 3.31E-001 | 0.441 |
| **Cingulate gyrus part of cingulum** | -0.131 | 0.059 | -2.213 | 2.71E-002 | 0.085 | -0.102 | 0.064 | -1.601 | 1.10E-001 | 0.195 |
| **Corticospinal tract** | -0.077 | 0.058 | -1.321 | 1.87E-001 | 0.236 | -0.049 | 0.062 | -0.795 | 4.27E-001 | 0.488 |
| **Inferior fronto-occipital fasciculus** | -0.091 | 0.061 | -1.489 | 1.37E-001 | 0.219 | -0.059 | 0.065 | -0.901 | 3.68E-001 | 0.453 |
| **Inferior longitudinal fasciculus** | -0.122 | 0.062 | -1.983 | 4.76E-002 | 0.109 | -0.124 | 0.066 | -1.891 | 5.89E-002 | 0.150 |
| **Medial lemniscus** | -0.133 | 0.062 | -2.148 | 3.19E-002 | 0.085 | -0.141 | 0.066 | -2.155 | 3.14E-002 | 0.100 |
| **Parahippocampal part of cingulum** | -0.040 | 0.058 | -0.683 | 4.94E-001 | 0.494 | -0.018 | 0.060 | -0.304 | 7.61E-001 | 0.761 |
| **Posterior thalamic radiation** | -0.080 | 0.061 | -1.306 | 1.92E-001 | 0.236 | -0.089 | 0.065 | -1.373 | 1.70E-001 | 0.247 |
| **Superior longitudinal fasciculus (bilateral)** | -0.142 | 0.063 | -2.246 | 2.49E-002 | 0.085 | -0.151 | 0.068 | -2.229 | 2.60E-002 | 0.100 |
| **Superior longitudinal fasciculus (left)** | -0.194 | 0.066 | -2.951 | 3.23E-003 | 0.025 | -0.221 | 0.070 | -3.165 | 1.59E-003 | 0.025 |
| **Superior thalamic radiation** | -0.224 | 0.065 | -3.461 | 5.58E-004 | 0.009 | -0.179 | 0.069 | -2.580 | 9.99E-003 | 0.080 |
| **Uncinate fasciculus** | -0.105 | 0.058 | -1.810 | 7.06E-002 | 0.141 | -0.107 | 0.062 | -1.718 | 8.60E-002 | 0.172 |
| **Forceps major** | -0.193 | 0.068 | -2.834 | 4.69E-003 | 0.025 | -0.133 | 0.072 | -1.842 | 6.57E-002 | 0.150 |
| **Forceps minor** | -0.112 | 0.065 | -1.723 | 8.52E-002 | 0.152 | -0.159 | 0.070 | -2.266 | 2.36E-002 | 0.100 |
| **Middle cerebellar peduncle** | -0.066 | 0.064 | -1.024 | 3.06E-001 | 0.326 | 0.039 | 0.068 | 0.576 | 5.65E-001 | 0.602 |

## 3 Chapter conclusion

We found that MDD case-control differences were mainly shown in white matter microstructure measured by FA in general variance of thalamic radiations, the tract-specific variance in superior longitudinal fasciculus, forceps major and superior thalamic radiation. The results provided evidence that significant MDD case-control difference has a moderate Cohen's d of 0.1 to 0.3 in a population-based sample. This very large sample confirmed the important role of white matter connecting to connecting to the prefrontal cortex.

# Chapter 3:

## White matter microstructure is related to the mean and within-subject variance of depressive symptoms

## 1 Chapter introduction

Following the findings of MDD case-control differences in white matter microstructure, the study in this chapter investigated how white matter microstructure was associated with depressive symptoms measured at multiple time points, of which the importance has been discussed in Chapter 1. The longitudinal measures of depressive symptoms were assessed on 2-4 occasions across 5.89 to 10.69 years. Over 8,000 people had data for two or more assessments. Using the longitudinal data, three types of longitudinal measures were derived: (1) variability of depressive symptoms, (2) mean depressive level over time and (3) longitudinal trajectory of depressive symptoms. The neurobiological associations in white matter microstructure with these different cross-sectional measures were assessed, and the differences and similarities across measures of depressive symptoms were discussed.

This study is presented as a paper entitled, “White matter microstructure is related to the mean and within-subject variance of depressive symptoms”. It is now ready for submission. As the first author of the paper, I conceived the idea, ran the data analyses, and wrote the manuscript independently under supervision.

## 2 Paper

### 2.1 Abstract

Background: Assessments of white matter integrity in depression typically show reductions in depressed individuals but are frequently limited by small sample sizes and the absence of longitudinal measures of depressive symptoms. We sought to test if greater levels of depressive symptoms or an individual’s propensity to emotional variability over time are associated with reductions in white matter microstructure.

Methods: We sought to address the cross-sectional and longitudinal relationships between depressive symptoms and white matter microstructure using the UK Biobank Imaging Study. Depressive symptoms were assessed on 2-4 occasions using the

PHQ-4 across 5.89 to 10.69 years and imaging data was collected at a single time point. Depressive symptom measures were available in approximately 8,660 individuals on at least two occasions, and in approximately 1,940 individuals on 4 occasions. We tested the associations between depressive symptoms (cross-sectional, mean and within-subject variability in depressive symptoms over time) with white matter microstructure (Fractional Anisotropy, FA; Mean Diffusivity; MD) in 27 major tracts.

Results: We found that greater mean diffusivity (MD) of the thalamic radiations was associated with increased depressive symptom levels measured at the imaging assessment, increased variability of depressive level, and also with increasing depressive symptoms over time ($\beta>0.024$, $p_{corr}<0.043$). Greater MD in association fibres that connect prefrontal areas was associated with increasing levels of depression over time ($\beta=0.050$, $p_{corr}=0.034$). In contrast, increased projection fibre MD in the brain stem, cortex and connected limbic areas ($\beta=0.045$, $p_{corr}=0.001$) was associated with greater variability in depressive symptoms. No association was found in FA ($p_{corr}>0.11$).

Conclusions: Our results provide evidence that higher MD in thalamic radiations is associated with a higher number, variability and increasing trajectory of depressive symptoms. Variability and longitudinal change showed separate associations with projection fibres and association fibres, respectively. This suggests that white matter microstructure may be selectively important for aspects of the pathophysiology and progression of depressive symptoms.

## 2.2 Introduction

Major depressive disorder (MDD) is a disabling disorder with a high heritability (Sullivan et al. 2000; Vos et al. 2012) and prevalence (Kessler et al. 2003). It is a heterogeneous illness (Howard, Clarke, et al. 2017; Whalley et al. 2018), often studied in modest sample sizes (Liao et al. 2013). These limitations have led to diverse findings (Fava and Kendler 2000) and to an uncertain relationship between quantitative measures of depressive symptoms and associated neurobiology.

A possible contributor to the heterogeneous imaging findings in MDD is the longitudinal variability of depressive symptoms (Kendler and Gardner 2011). Although MDD is often

diagnosed based on a single assessment in most studies, depressive symptoms are inherently dynamic (Kendler and Gardner 2016). For instance, some people may have a highly variable mood state but have a low mean level of depressive symptoms, whereas others may show higher mean levels of depressive symptoms, or a progressively increasing level of symptoms over time. Observations based on multiple assessments of depressive symptoms would therefore allow the mean, variance and longitudinal pattern of depressive symptoms to be assessed. Recent studies found data-driven clusters based on different patterns of trajectories of depressive symptoms, suggesting a possibility of stratifying depression according to dissociated patterns on the basis of fluctuations over time (Lin et al. 2016).

Recent cohort studies found emerging evidence for the association between mood disorders and reductions of white matter microstructure in thalamic radiations (Shen et al. 2017; Barbu et al. 2018), which contains important tracts involved in emotional processing (Hall et al. 2008) and regulation (Phillips et al. 2008). Deficits in these functions is associated with the onset and severity of MDD (Leppa 2006). However, these studies used diagnosis limited to one occasion or lifetime diagnosis (Liao et al. 2013). The present study aims to use so far the largest neuroimaging cohort with longitudinal depressive symptoms assessed, to test whether measures of the mean, variability, and longitudinal pattern of depressive symptoms show shared or different associations with white matter microstructure, and thereby to provide a better understanding of the neurobiological mechanisms of depression based on prospectively collected longitudinal data.

In this study, depressive symptoms were assessed on up to four separate occasions and across a maximum time span of 5.89 to 10.69 years. One depressive symptom assessment coincided with an MRI imaging assessment. Based on these repeated measurements, we generated four measures, which include an assessment of depressive symptoms at the same time as the imaging assessment, the mean level of depressive symptoms and their variance (i.e. variability of depressive symptoms), and finally, the slope of depressive symptoms within individuals over time, as a measure of longitudinally worsening of depressive symptoms.

In the current study, we tested for associations between these 4 depressive symptom measures and white matter microstructure in the UK Biobank Imaging Study of 8,837 people(Miller et al. 2016). Within this database, more than 8,000 people provided

useable data for at least one time point for both depressive symptoms and white matter microstructure.

## 2.3 Methods

### Participants

The UK Biobank team recruited ~500,000 people across the United Kingdom (Sudlow et al. 2015) and an ongoing imaging assessment was undertaken for a subset of 11,293 participants (Miller et al. 2016). For the current analyses, the most recent release of imaging data was used which included 8,837 individuals who provided data that passed the quality check performed by UK Biobank imaging team after data preprocessing(Alfaro-Almagro et al. 2018). In this total sample, the mean age was 62.53 years (standard deviation=7.42) and 47.52% were men. We then conducted further data quality control of the removing outliers, and then the imaging data was merged with other data (steps listed below and presented in Figure S1).

UK Biobank data acquisition was approved by Research Ethics Committee (reference 11/NW/0382). The analysis and data acquisition for the present study were conducted under application #4844. Written consent was obtained for all participants. All the imaging preprocessing was undertaken under the protocol released from UK Biobank (https://biobank.ctsu.ox.ac.uk/crystal/docs/brain_mri.pdf).

### Depressive symptoms

Depressive symptoms were measured by a 4-item physical health questionnaire (PHQ-4)(Batty et al. 2016). PHQ-4 has an AUC (area under the curve) of 0.79 for its correlation with depression diagnosis (Khubchandani et al. 2016). This measure also shows association with measures of disability (Kroenke et al. 2009) and risk factors for depression (Löwe et al. 2010; Batty et al. 2016). See more details in the URL: http://biobank.ctsu.ox.ac.uk/crystal/label.cgi?id=100060, and items in supplementary methods.

PHQ-4 was assessed repeatedly up to a maximum of four times. Time points included: (a) the first assessment visit (2006-2010, N=8,782), (b) a repeat visit on a sub-sample (2012-2013, N=2663), (c) the imaging visit (2014-2017, N =8,309) and finally the (d)

online follow-up (2015-2017, N =6,676). Further details can be found on UK Biobank website: http://biobank.ctsu.ox.ac.uk/crystal/label.cgi?id=100060.

Based on the repeated PHQ-4 measures, we generated four measures of depressive symptoms (Figure 1, S2): (i) First, a single PHQ-4 score measure acquired at the same time as the imaging assessment. (ii & iii) Then the mean and variability of depressive symptoms across all available assessments, where the mean depressive level was the average of PHQ-4 over at least two time points, and variability of depressive symptoms was the standard deviation of PHQ-4 scores over a minimum of three time points. (iv) Finally, we estimated the longitudinal slope of depressive symptoms within each individual with all four PHQ-4 assessments, using a linear growth curve model. A positive slope indicated depressive symptoms becoming more severe over time, and a negative slope when they reduced over time. Details of the growth curve model estimation are detailed in the supplementary methods. Descriptive statistics for the above PHQ-4 measures were presented in Figure S1, Table S1 and supplementary results.

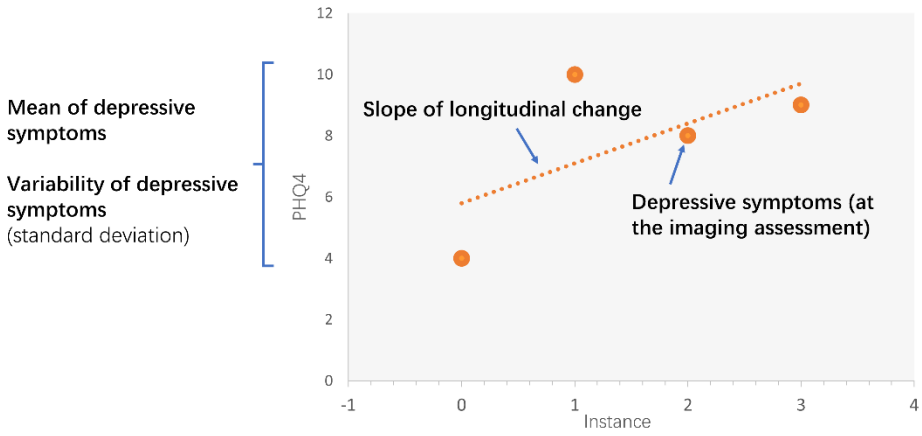


Figure 1. The measures for depressive symptoms generated for this study. There were four measures generated: (1) fundamental one-time measurement for depressive symptoms acquired with imaging assessment, (2) mean of depressive symptoms generated based on at least two multiple assessments, (3) variability of depressive symptoms which was the standard deviation of at least three time-points, and finally (4) linear growth curve denoting longitudinal trajectory of depressive symptoms derived from all four time-points.

**Imaging data**

We used IDPs (imaging-derived phenotypes) for DTI data release by UK Biobank Imaging Study. Data acquisition, data preprocessing, estimation of white matter microstructure and quality check after the above steps were conducted by UK Biobank imaging team using a standard protocol described in the Primary Brain Imaging Documentation (URL: https://biobank.ctsu.ox.ac.uk/crystal/docs/brain_mri.pdf) and two protocol papers(Miller et al. 2016; Alfaro-Almagro et al. 2018). The major procedures are described in brief below.

All imaging data were acquired using a 3T Siemens Skyra (software platform VD13) machine, using a standard ("monopolar") Stejskal-Tanner pulse sequence. FSL packages were used for data preprocessing and microstructure estimation (Andersson et al. 2007b). Preprocessing included correction for eddy currents, head-motion and gradient distortion, using the Eddy tool(Andersson and Sotiropoulos 2015a). Five dMRI microstructure measures were estimated after preprocessing. DTI measures including FA and MD were generated using DTIFIT (Anthofer et al. 2015). These are the measures that were used as main proxies and reported in the main text. Three newly developed neurite orientation dispersion and density imaging (NODDI) measures were also generated using AMICO tool (Daducci et al. 2015). These measures depict additional sources of variation to FA and MD such as neurite density, extracellular water proportion, and morphology of tract organization. For completeness, findings using these measures are detailed in the supplementary materials and briefly discussed where necessary (Appendix 2: Figures S3 and S4).

The processed data was then fed into AutoPtx package from FSL (https://fsl.fmrib.ox.ac.uk/fsl/fslwiki/AutoPtx), which uses probabilistic-tractography based method to map 27 major tracts over the whole brain(Miller et al. 2016). The processed tracts included 12 bilateral and 3 unilateral tracts (Figure 2 and Appendix 2: supplementary methods). FA data was used for mapping and the masks of tracts for each individual were used to locate the tracts on MD and NODDI measures. Weighted means of DTI measures for each tract were generated.

Figure 2. Illustration of WM tracts. The tracts were defined by tractography mapping on FA

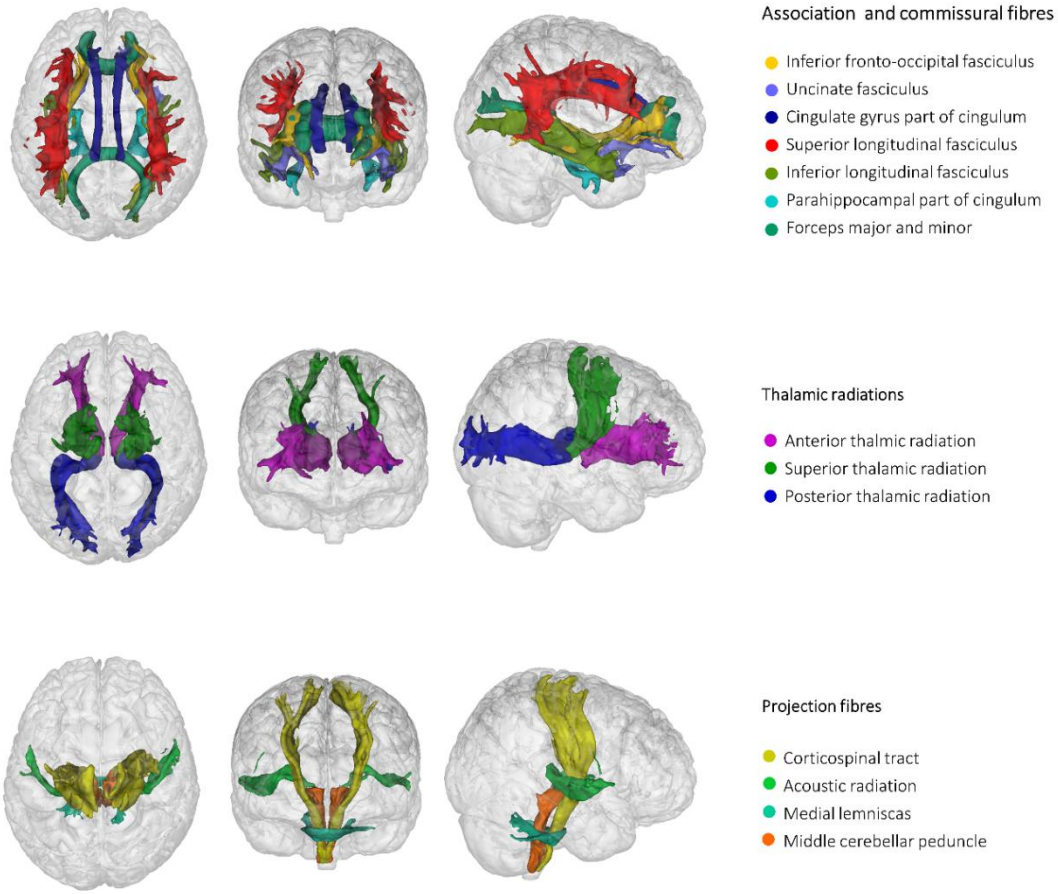


(fractional anisotropy) data using AutoPtx (https://fsl.fmrib.ox.ac.uk/fsl/fslwiki/AutoPtx). They were categorised into three subsets as shown in the figure. Forceps major, forceps minor and uncinate fasciculus are unilateral structures and the rest are bilateral. For the purpose of clear illustration, bilateral structures were shown identically in both hemispheres.

## Statistical methods

Before any analysis was performed, outliers were first removed (Shen et al. 2017). This was achieved by performing separate PCA for each DTI measure on the overall sample of 8,837 people, and those who were outside of +/- 3 standard deviations from mean were removed (Shen et al. 2017). This resulted in ~8,780 people remaining (see Appendix 2: Figure S1) for further analysis. Results for the sample without outliers removed can be found in Appendix 2: Figure S5.

First, we tested the associations between the measures for depressive symptoms i) quantified at the imaging assessment as a single time point, ii) as the overall mean depressive level, (iii) as the variability of depressive level and (iv) as the slope of

longitudinal trajectory with global WM microstructure changes (trajectory modelled by a growth curve model, see supplementary methods). For each of the DTI measures, we performed PCA on all the tracts and three major subsets of WM tracts that included association and commissural fibres, thalamic radiations and projection fibres (Shen et al. 2017). These three subsets are distinct in both anatomy and function (Cox, Ritchie, et al. 2016). Association fibres are the tracts that connect cortical areas, thalamic radiations connect thalamus with other parts of the brain, and finally projection fibres are the tracts associated with subcortical/spinal cord. Categorisation of the subsets can be found in Figure 2. The scores of the first un-rotated principal component for each microstructural metric were then extracted to index the common properties of white matter microstructure shared across tracts, denoted as gTotal, gAF, gTR and gPF. In our previous published papers on the same cohort (Cox, Ritchie, et al. 2016; Shen et al. 2017), there was a substantial component of shared variance across white matter tracts for each microstructural parameter (Appendix 2: Figure S6 and Table S2). Following the analysis of the g variations, we tested the associations of microstructure of individual tracts and four types of measures for depressive symptoms.

We used “glm” function in R to test the above associations (Chatfield et al. 2010). Age, age$^2$, gender were set as covariates. Other covariates include: head position in the scanner (on x, y and z axis) to control for systematic unevenness of static field in the scanner, smoking status and alcohol consumption at the time of imaging assessment to control for depression-related behaviour patterns that may influence brain structure, and finally stressful life events occurring within 2 years before imaging test to control for response bias to PHQ-4. Each of the covariates are described in supplementary materials (Appendix 2: supplementary methods and Table S1, S5 and S6). For completeness, we also reported results that did not control for smoking status, alcohol consumption, stressful life events (Figure S7). FWE correction was applied on each set of measures with a whole brain as a unit by using “p.adjust” function using FDR method in R (q-value<0.05) (Benjamini et al. 1995). The effect sizes reported are all standardised.

## 2.4 Results

### Associations between white matter microstructure and depressive symptoms at the imaging assessment

Global differences (g) of MD over all tracts (gTotal), and tracts separated into the categories of association fibres (gAF) and thalamic radiation (gTR) were positively associated with depressive symptoms measured at the time of imaging assessment (β ranged from 0.023 to 0.029, $p_{corr}$<0.032, see Appendix 2: Figure 3, Table S3). In individual tracts, higher MD in the anterior thalamic radiation (β=0.036, $p_{corr}$=0.002), cingulate part of cingulum (β =0.027, $p_{corr}$=0.025), corticospinal tract (β =0.031, $p_{corr}$=0.022) and superior thalamic radiation (β =0.024, $p_{corr}$=0.030) were all associated with higher depressive symptoms at the imaging assessment. No significant associations were found either globally ($p_{corr}$>0.114), or regionally in individual tracts ($p_{corr}$>0.148) between FA and depressive symptoms at the time of the imaging assessment.

**Associations between white matter microstructure and mean and variability of longitudinal depressive symptoms**

No association was found between global or subset measures of MD (all $p_{corr}$>0.126) and mean depressive symptoms. However, MD in thalamic radiations (β=0.024, $p_{corr}$=0.043) and in projection fibres (β=0.045, $p_{corr}$=0.001) were both positively associated with within-subject measures of variability in depressive symptoms.

For specific tracts, higher MD in anterior thalamic radiation was significantly associated with higher mean depressive symptoms (β=0.032, $p_{corr}$=0.013). Higher MD in anterior thalamic radiation (β=0.032, $p_{corr}$=0.015), and middle cerebellar peduncle (β=0.045, $p_{corr}$=0.003) were associated with greater variability of depressive symptoms.

No association was found for FA (all $p_{corr}$>0.199) in any global or tract-specific measure and any measure of depressive symptoms.

**Associations between the longitudinal slope of depressive symptoms and WM microstructure**

Higher global, association fibres and thalamic radiations MD were each associated with progressively increasing levels of depressive symptoms (β ranged from 0.050 to 0.056, $p_{corr}$<0.031). No significant individual tract-wise analysis reached significance after multiple correction. However, forceps major (β=0.053, $p_{corr}$=0.073), superior thalamic radiation (β=0.052, $p_{corr}$=0.073) and corticospinal tract (β=0.050, $p_{corr}$=0.073) were

nominally significant. No association for FA was found for either g measures or tracts ($p_{corr}$>0.450).

### Associations between the measures for depressive symptoms and NODDI measures

Among all the NODDI measures, ISOVF showed similar results with MD. Detailed statistics of the results were shown in Appendix 2: Figure S4 and S5, Table S4, and supplementary results.

Figure 3. Associations between cross-sectional depressive symptoms and dMRI (heatmap) and the map for significant regions (brain map). FA=fractional anisotropy, MD=mean diffusivity. Depre=one-time assessment of depressive symptoms, Depre.mean=mean depressive level, Depre. variability=variability of depressive symptoms, and Depre.longitudinal=slope of growth curve model trajectory of depressive symptoms. Colour depth represents the standard effect size of a measure. As FA has negative direction with MD, here in this figure, the effect sizes for FA was reversed (×-1). The results were separated in two sections. The upper sections were the results for g measures and the lower sections showed the results of individual tracts. To aid comprehension, the lower part where results of tracts were shown, checks were divided into three categories by dashed lines as the tracts were in different subsets, i.e. association fibres, thalamic radiations and projection fibres (see Methods). Significant associations after FWE correction on 15 tracts/four g measures ($p_{corr}$<0.05) were marked with an asterisk. Significant associations in the g measures may not necessarily result in associations in individual tracts, as shown in the columns for Depre.longitudinal.

(see Figure 3 in the next page)

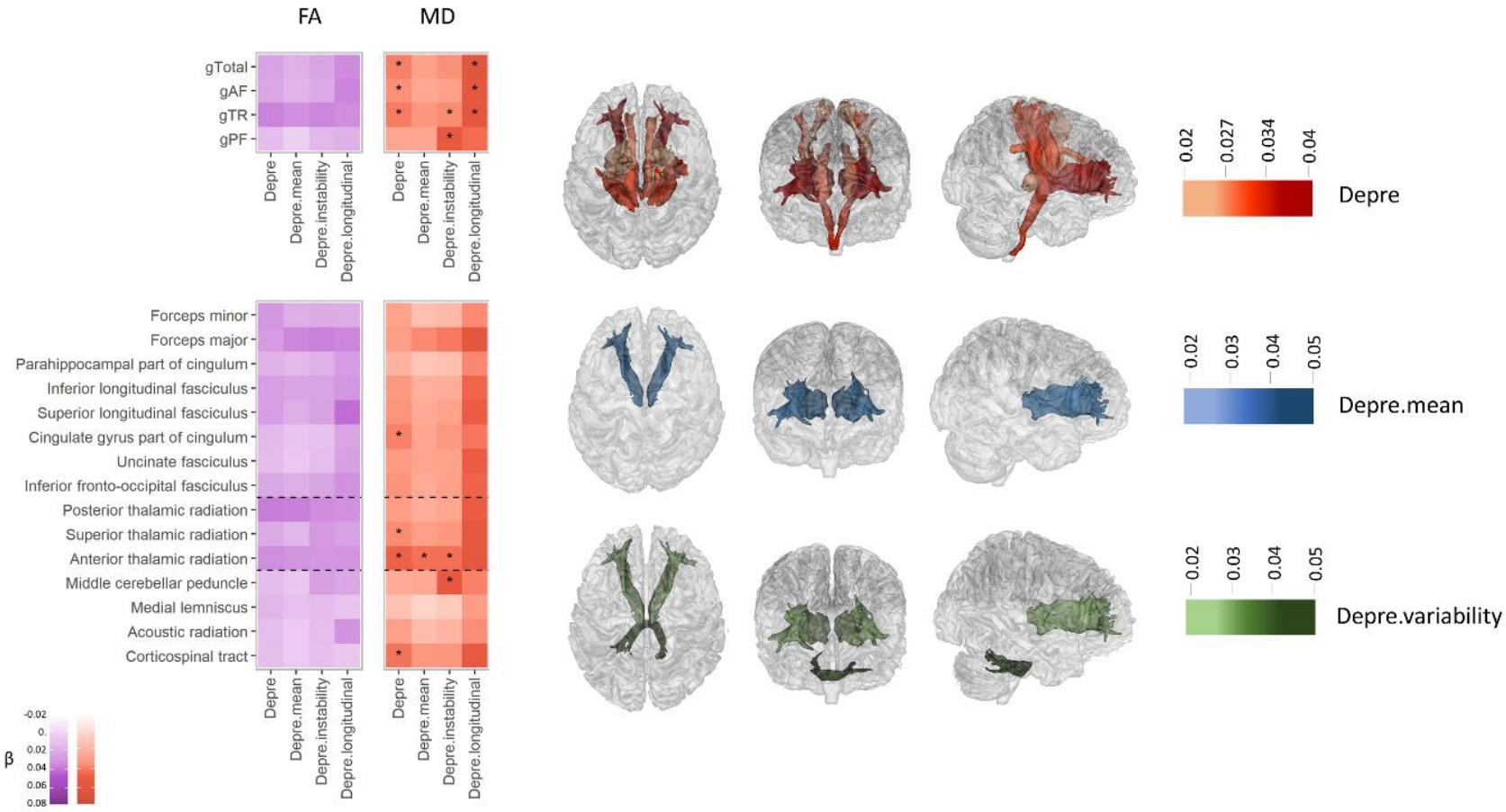
FA
MD
gTotal
gAF
gTR
gPF
Depre
Depre.mean
Depre.instability
Depre.longitudinal
Forceps minor
Forceps major
Parahippocampal part of cingulum
Inferior longitudinal fasciculus
Superior longitudinal fasciculus
Cingulate gyrus part of cingulum
Uncinate fasciculus
Inferior fronto-occipital fasciculus
Posterior thalamic radiation
Superior thalamic radiation
Anterior thalamic radiation
Middle cerebellar peduncle
Medial lemniscus
Acoustic radiation
Corticospinal tract
β
-0.02
0.
0.02
0.04
0.06
0.08
0.02
0.027
0.034
0.04
Depre
0.02
0.03
0.04
0.05
Depre.mean
0.02
0.03
0.04
0.05
Depre.variability

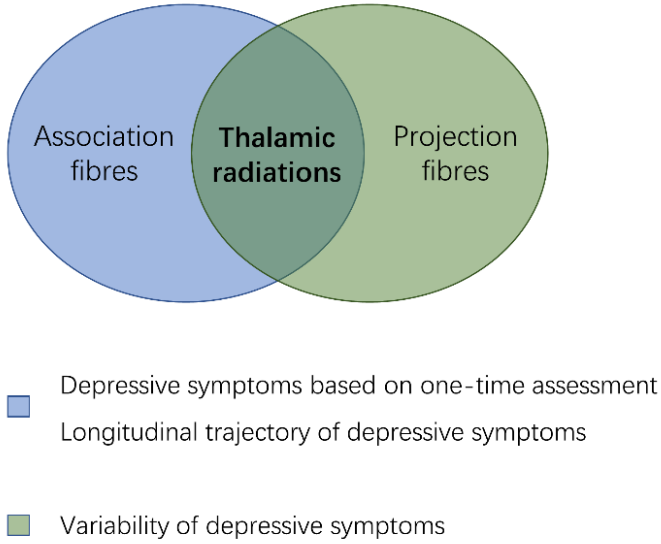


Figure 4. Venn graph for results of g measures for the distress measures that showed significant results in g measures. The overlapping association was shown in thalamic radiations (gTR) for all three distress measures. Dissociated effects were shown in association fibres (gAF) for depressive symptoms based on one-time assessment and slope of longitudinal trajectory, and projection fibres (gPF) was significant for variability of depressive symptoms.

## 2.5 Discussion

We found several novel associations between greater depressive symptom measures and ostensibly poorer WM microstructure as indexed by higher MD. Higher depressive symptoms at the time of the imaging assessment and a higher mean and variance of depressive symptoms over time were both associated with higher MD in the ATR. Higher general thalamic radiation (gTR) MD was also associated with higher depressive symptoms at the time of the assessment, higher variability in depressive symptoms over time, and with worsening depressive symptoms over time. Lower association fibre microstructure in MD was found in association with greater depressive symptoms at the time of the imaging assessment and with a longitudinal trajectory of worsening depressive symptoms over time. The association fibres subset includes tracts that localise to the prefrontal cortex and its connections. Higher MD in projection fibres, which locate in or connect to limbic areas, were also associated with high variability of depressive symptoms (Figure 4). The above results in MD were confirmed by ISOVF.

Lower microstructure of the anterior thalamic radiation has appeared repeatedly in association with the presence of several psychiatric illnesses, including depression (Coenen et al. 2012), psychosis (Sprooten et al. 2009) and schizophrenia (Young et al. 2000). The linkage built by ATR between prefrontal regions and thalamus is an important path of executive control and emotion regulation (Royall et al. 2002; Cheon et al. 2011). It is particularly interesting that ATR has been repeatedly found in patients in their adolescence or early adulthood (Lai and Wu 2014). Thalamic radiations as a tract category subset also showed significant effect of one-time measure, cross-sectional longitudinal variability and trajectory of depressive symptoms. Consistent associations of thalamic radiations with different distress measures may due to environmental impacts that had influenced neuronal maturation in early life (Voineskos et al. 2012), and thus the developmental gaps prolonged into adulthood. Alternatively,

those with early life psychiatric disorders may be subject to a different clinical mechanism which is influenced by gene structures (Frodl et al. 2012), and therefore lasts through-out the lifespan. These findings are also supported by a recent study that found thalamic radiations were associated with the polygenic risk profile derived from NETRIN-1 pathway, which was found in various genetic pathway studies for MDD (Barbu et al. 2018).

Deficit of microstructure in association fibres was associated with greater depressive symptoms at the time of the imaging assessment and with worsening depressive symptoms over time. The largest effect sizes were seen for a worsening longitudinal trajectory of depressive symptoms. Association fibres pathways are robustly associated executive cognition (Voineskos et al. 2012; Zheng et al. 2014; Cox, Ritchie, et al. 2016) and connections to the prefrontal cortex have been closely related to psychological resilience (Walsh et al. 2007). This could contribute to both temporary depressive status and longitudinal decline in mental well-being (Bachmann et al. 2005). Deficit in these pathways may reflect a declined capacity of psychological 'bounce-back', thus causes the accumulated deficit associated with longitudinal increase of depressive symptoms.

Variability of depressive symptoms showed a distinctive association with projection fibres. Projection fibres mainly locate in the limbic system or link limbic system with the cortex (Wakana et al. 2004). Previous fMRI studies found that depressive patients showed biased processing of emotional stimuli in both a negative emotional system including structures such as the amygdala and thalamus (Dalgleish 2004; Young et al. 2004), and the reward system located in the basal ganglia and mid-brain (Gradin et al. 2011). Variability of depressive symptoms can be the result of deficits in primary process for emotional input to the brain (Lammel et al. 2014; Polter and Kauer 2014). This may explain the treatment resistance for some MDD patients, as the conventional psychological treatment showed brain alterations mainly in prefrontal regions, which

may be less effective to those cases whose major concern was variability of depressive symptoms (Young et al. 2004). The distinct neurobiological associations between variability and mean depressive level indicate that dissociating psychological/biological treatment based on their different symptoms over time may help achieve better results.

Most of the results were presented in MD rather than FA. Despite the differences in the level of significance, MD and FA presented in the directions of effects and the scales were similar for the most robust findings, especially in thalamic radiations (Appendix 2: Table S3). Also, our findings in MD have shown similar patterns with a NODDI measure, ISOVF, which is related to neuronal loss (Kamagata et al. 2017). The discordance between MD and FA may be rooted in differential sensitivity of MD and FA to a variety of complex degenerative processes via a range of distinct neurobiological features. Changes in FA, which could result from increased transverse diffusion due to myelin and axonal disruption (Jones et al. 2013), may be masked by co-occurring processes such as fibre reorganisation and glial reactivity; in such instances where all three eigenvectors of the diffusion tensor experience proportional change, it is plausible that MD would offer greater sensitivity (Acosta-Cabronero et al. 2010). MD reportedly exhibits greater sensitivity to ageing than FA (Cox, Ritchie, et al. 2016) which notably included poorer microstructure in ATR (Cox, Ritchie, et al. 2016). Furthermore, higher MD in the absence of FA differences have been found in studies of cortisol reactivity to mild cognitive stress in older age (Cox, Bastin, et al. 2015; Cox, MacPherson, et al. 2015), and in ageing-associated disorders such as Alzheimer's disease and small vessel disease (Acosta-Cabronero et al. 2010; Maniega et al. 2015). Altogether, the current observations could therefore reflect an acceleration of normal or pathological ageing processes in the brain resulting from, or predisposing to, adverse effects of depressive symptoms on the brain.

In the present study, we used a very large single site imaging sample of over 8,000 people. Though the sample size of longitudinal change of depressive symptoms was

much lower (~2,000), it is still much larger than most neuroimaging studies, especially considering the data is longitudinal and covers up to ten years. All of this provides high statistical power to reliably detect modest associations (Smith and Nichols 2018). However, a limitation for the present study is that the time lag between adjacent assessments may vary from one year to six years. Though we did adjust the difference by controlling for the age of each time point and the growth curve models showed good fit (see supplementary methods), noise can be further reduced by controlling more finely on time lag for future experimental design or increasing time points. Another limitation is that the variability of depressive symptoms we derived would not be able to depict all types of variations for depressive symptoms and may be very different from variations in a short period (e.g. diurnal mood swing). These other measures of mood variability would have substantial biological meaning but potentially different neurobiological basis.

Our results provide evidence that deficit in WM microstructure is related to greater mean, variability and longitudinal deterioration of depressive symptoms. The longitudinal findings point towards associations between white matter integrity and depressive symptoms, and further causal conclusions will require examination using methods that are able to test for causal inferences in observational datasets.

## 3 Chapter conclusion

MD in thalamic radiations, especially in anterior thalamic radiation, was associated with variability and mean depressive level. Variability of depression exclusively showed association with MD in projection fibres. This study provided evidence that thalamic radiations are important not only for MDD case-control differences, as found in chapter 2, but also present as a common component associated with various longitudinal measures for depressive symptoms here in this chapter. The differences of associations between cross-sectional measures indicate that cross-sectional measures may provide information for heterogeneity of MDD.

# Chapter 4:

## Phenotype-wide association study of 212 behavioural and 1,532 neuroimaging phenotypes in UK Biobank using polygenic risk scores for depression

## 1 Chapter introduction

Several questions remain unanswered regarding neuroimaging features of polygenic risk for depression. First, whether white matter microstructure is associated with depression polygenic risk score is under-explored. Second, no study has been conducted that the author is aware of that had examined the association between resting-state connectivity and the polygenic risk scores for depression. Finally, whether brain phenotypes mediate the effect of depression polygenic risk on complex behavioural traits.

To answer these questions, a well-powered sample for finding associations with moderate effect sizes would be needed. Another important factor is to include a wide range of phenotypes, including behavioural and neuroimaging variables. This study used the UK Biobank imaging dataset release in May 2018, containing 14,506 people who attended imaging assessment. Polygenic risk scores of depression were derived using a meta-analysis combining data from UK Biobank, PGC (Psychiatric Genomics Consortium) and 23andme. A data-driven phenotype-wide association study was conducted to test the associations between the polygenic risk scores of depression and 212 behavioural plus 1,532 neuroimaging phenotypes.

The paper under preparation for submission. I independently conducted the analyses and completed the manuscript under supervision.

## 2 Paper

### 2.1 Abstract

Depression is a leading cause of disability worldwide but there is uncertainty regarding its genetic, neural and behavioural associations, hindering the discovery of its causes and mechanisms. Depression is highly heritable and polygenic, and the increasing availability of replicated genetic associations provides a timely opportunity to identify

traits that are genetically correlated with depression in UK Biobank, where there is a wide range of potentially relevant traits in a large number of consistently phenotyped individuals. We estimated polygenic risk scores for depression in 14,506 genotyped participants and examined their association with 212 behavioural and 1,532 neuroimaging phenotypes. Higher polygenic risk of depression (depression-PGRS) was associated with lower white matter microstructure (absolute standardised β: 0.027 to 0.036, p: $8.08\times10^{-5}$ to $1.57\times10^{-3}$), hyper-connectivity under resting-state in the default mode network, and weaker connectivity in the prefrontal cortex (absolute β: 0.031 to 0.046, p: $7.86\times10^{-6}$ to $1.64\times10^{-3}$). Other behavioural traits such as sleep, smoking, cardiovascular conditions and body mass were also found to be associated with depression-PGRS (absolute β: 0.031 to 0.017, p: $1.13\times10^{-37}$ to $1.64\times10^{-3}$). In order to address the direction of the associations between depression PRS, behaviour and brain, we then conducted mediation analyses of all the traits previously found to be associated with depression-PGRS. Sleep, smoking and general physical health mediated the association between polygenic risk and the presence of depression to the greatest extent (proportion of direct effect mediated > 6%, p: $8.55\times10^{-9}$ to $8.70\times10^{-4}$). We also found that white matter microstructure mediated the associations of depression-PGRS to subjective well-being, the number of major psychiatric illnesses diagnosed, and smoking behaviour (proportion of direct effect mediated>2.7%, p ranged from $4.51\times10^{-4}$ to 0.021). These findings suggest that sleep, smoking and poorer physical health may mediate the association between genetic risk and depression and that the effects of genetic risk on behaviour may be partly mediated through disrupted functional/structural brain connectivity.

## 2.2 Introduction

Major Depressive Disorder (MDD) is a major contributor to the overall global burden of disease, affecting 322 million people worldwide, and a leading cause of disability (World Health Organization 2017). MDD has a high heritability estimated around 37% based on twin studies(Sullivan et al. 2000), approximately 25% of the genetic contribution can be explained by single nucleotide polymorphisms (SNP) (Lee et al. 2013). This indicates that common genetic variants of small effect contribute a substantial proportion of the total genetic effect. For polygenic traits, polygenic risk profiling provides a way to investigate the additive common genetic risk (International and Consortium 2009; Wray et al. 2014). Uses allele effect weights estimated from an

independent genome-wide association study (GWAS), polygenic risk scores are generated for each individual in a second independent dataset from the product of allele dosages and effect sizes, summed across the genome (Howard, Adams, Shirali, et al. 2018; Wray et al. 2018).

Polygenic risk for MDD is associated with heritable behavioural traits, such as other major psychiatric disorders like bipolar disorder and schizophrenia, neuroticism, lower general cognitive function, lower educational attainment and socioeconomic status, and a higher risk of obesity (Clarke et al. 2015; Hagenaars et al. 2016). MDD is widely believed to result from perturbed brain function and is associated with many neuroimaging phenotypes such as white matter microstructure, regional brain volumes and functional connectivity (Disner et al. 2011; Russo and Nestler 2013; Shen et al. 2017). GWAS and heritability analyses conducted on brain phenotypes reveal significant heritability of up to 60% (Elliott et al. 2018), providing an opportunity to study the genetic overlap between neuroimaging phenotypes and other heritable traits with MDD (Glahn et al. 2007; Jahanshad et al. 2013; Kochunov et al. 2015; Centre et al. 2017), and test for directional causal relationships between these traits.

The associations between MDD polygenic risk and brain phenotypes have, so far, been poorly studied. Based on previous studies, small to moderate effect sizes are expected (Wray et al. 2014) and therefore most neuroimaging studies will be underpowered to investigate the genetic associations between depression and brain and behavioural phenotypes (Button et al. 2013). Higher sampling costs for MRI (magnetic resonance imaging) scanning, differences between functional imaging paradigms and inconsistencies in both quality control and statistical inferences across studies make meta-analysis challenging and suggest the need for single large samples and consistently applied methods of acquisition processing and analysis (Kaiser et al. 2015).

The latest neuroimaging data release from the UK Biobank imaging project (Miller et al. 2016) includes a maximum of 11,006 people, which is the largest cross-modality imaging dataset up to date. Summary statistics from the meta-analysis combining three big cohorts: PGC, UK Biobank and 23 and me, were used to produce depression polygenic risk scores (depression-PGRS). There are also a wide variety of other phenotypes available allowing for comparisons and mediation tests between traits, such as structural equational modelling for the associations of gene-behaviour-health

and gene-brain-behaviour relationships. In the current study, building upon UK Biobank's large sample size and detailed phenotyping, we conducted a phenotype-wide association test with depression-PGRS. The phenotypes available included contain ten categories ($N_p$ indicates number of phenotypes): early life factors ($N_p$=10), sociodemographic measure ($N_p$=4), lifestyle ($N_p$=69), physical measures ($N_p$=68), mental health ($N_p$=57), cognition ($N_p$=4), intracranial/subcortical volume ($N_p$=9), white matter microstructure ($N_p$=38) and resting-state functional connectivity ($N_p$=1485).

## 2.3 Methods

### Participants

A total of 14,506 people participated in the UKB Data release included in the current study. Data came from the latest release of the ongoing UK Biobank Imaging Project (released in May 2018, where age at the imaging assessment ranged from 44.58 to 80.25 years, mean age=62.69, standard deviation=7.48, and 47.91% were men). In total, 500,000 people were initially recruited for UK Biobank project. A subset was selected to attend a neuroimaging assessment following the initial visit. Behavioural and neuroimaging data acquisition were conducted under standard protocols (Sudlow et al. 2015; Miller et al. 2016). Written consents were acquired from all participants. Data acquisition and analyses in the present study were conducted under UK Biobank Application #4844.

### Depression-PGRS

Polygenic risk scores were calculated using the summary statistics from a meta-analysis of depression genome-wide association study (GWAS) from three cohorts, including 33 out of the 35 cohorts of the Psychiatric Genomics Consortium (PGC) analysis of major depression (Wray et al. 2018), the 23andMe discovery sample in the Hyde et al. analysis of self-reported clinical depression (Hyde et al. 2016), and a broad depression phenotype from UK Biobank non-imaging sample (Howard, Adams, Clarke, et al. 2018). This meta-analysis provided a total of 793,627 individuals (241,166 cases and 552,461 controls) with further details of this meta-analysis provided in a paper of meta-analysis (Howard *et al.*, 2018). The broad depression phenotype used in UK Biobank, though was self-declared and comparatively lenient, showed very strong

genetic correlation with clinically defined MDD with a high genetic correlation of 0.79(Howard, Adams, Shirali, et al. 2018). Training and testing datasets were ensured to have no overlap or relatedness (see methods in the meta-analysis in Howard *et al.,* 2018). In order to maximize replicable genetic variants derived from the training dataset, the summary statistics only included genetic variants that co-exist across all three cohorts, leaving 8,899,213 genetic variants left in the training sample.

We used PRSice 2.0 (incorporating PLINK 1.9) (Euesden et al. 2015) to calculate the depression-PGRS. Related or non-European-ancestry people and imaging subjects that were included in PGC, 23&me and UK Biobank MDD GWAS were removed from all following analysis. All sample sizes reported below will be the numbers after this data removal. Genotyping and quality control were conducted by UK Biobank as described in a protocol paper (Bycroft et al. 2017b). Eight p-value thresholds were applied to select genetic variants included in calculating polygenic risk scores, as $p<0.0005$, $p<0.001$, $p<0.005$, $p<0.01$, $p<0.05$, $p<0.1$, $p<0.5$ and $p<1$. Details of SNP quality control and imputation can be found elsewhere (Barbu et al. 2018).

**Behavioural phenotypes**

The behavioural phenotypes consisted of seven broad categories, containing 212 items in total, sample sizes included in brackets (see Table 1 for summary and Table S1 for full explanations): (1) Sociodemographic measures (N=8,318 to 10,260), (2) Early life factors (N=7,742 to 11,020), containing physical factors such as birth weight, and environmental variables like adoption and maternal smoking, (3) Life style (N=2,880 to 11,020), which include sleep, smoking, alcohol consumption and diet, (4) Physical health (N=2,227 to 11,020), consisting of self-declared medical conditions such as pain, cancer, operations, heart and artery disease and other major illnesses, and also machine assessed medical record for blood pressure, arterial stiffness and hand-grip strength, (5) Cognitive performance (N=5,247 to 6,075), which included four tests with acceptable biological reliability and a general measure derived based on these tests, (6) Mental health (N=3,788 to 8,340), including self-reported symptoms of major psychiatric conditions and diagnosis of major psychiatric illness under classifications of ICD-10 (10th revision of the International Statistical Classification of Diseases and Related Health Problems) based on systematic interview.

All of the behavioural phenotypes, with the exception of mental health items derived from online-follow up questionnaires and diagnosis from a systematic interview (see table 1), were acquired at the same time as the imaging assessment. For those who had absent behavioural data at the instance of imaging assessment but provided data at the initial visit, data from the initial visit was interpolated to fill the absent data at the imaging assessment where applicable. Sample sizes and descriptions for all the behavioural phenotypes used can be found in Appendix 3: Table S1.

Where summary data were available (e.g. neuroticism total score), the individual items used to derive the summary data were not included. Further, phenotypes with less than 2,000 people were excluded before the analyses.

**Neuroimaging phenotypes**

Neuroimaging data was consisted of: (1) intracranial/subcortical volume (N=11,006); (2) white matter microstructure, indexed by fractional anisotropy (FA, N=9,699) and mean diffusivity (MD, N=9,671); and finally, (3) resting-state connectivity (N=10,112). All four types of data consisted of the imaging-derived phenotypes (IDPs) provided by UK Biobank. Images were acquired, pre-processed and quality controlled by UK Biobank using FMRIB Software Library (FSL) packages by a standard protocol (URL: https://biobank.ctsu.ox.ac.uk/crystal/docs/brain_mri.pdf), which was also described in two protocol papers(Miller et al. 2016; Alfaro-Almagro et al. 2018). All pilot study data with inconsistent scanner settings and data that did not pass the initial quality assessment conducted by UK Biobank imaging team were not included in the analysis. All imaging data were collected using a 3T Siemens Skyra (software platform VD13) machine. For clarity, major steps of pre-processing were described below for each modality.

T1 data was processed to estimate intracranial and subcortical volumes. First, total volumes for white matter, grey matter and peripheral cerebrospinal fluid were calculated, and the sum of the three was the derived intracranial volume. Then volumes for thalamus, caudate, putamen, pallidum, hippocampus, amygdala, accumbens and brain stem (with $4^{th}$ ventricle) were estimated.

DTI data pre-processing included correction for eddy currents and head motion, outlier-slices correction and grand distortion correction. FA and MD maps were generated and

FA maps were used to generate tract masks, using probabilistic tractography analysis by AutoPtx package from FSL(Mori et al. 2002). 27 tracts were generated (12 bilateral and 3 unilateral tracts, see supplementary Figure S1 and Table S1)(Wakana et al. 2004). Weighted mean FA and MD were then calculated for each tract. To determine general variances in DTI measures and main subsets, as have validated in previous papers that weighted mean DTI measures for major white matter tracts are highly correlated, which makes generating general variances possible(Cox, Ritchie, et al. 2016; Shen et al. 2017), we performed principal component analyses on (1) FA/MD of all 27 tracts (gTotal), (2) FA/MD on association/commissural fibres (gAF), which connect the prefrontal cortex to other cortexes, (3) FA/MD on thalamic radiations (gTR), consisted of tracts that link the thalamus to the cortex, and (4) FA/MD on projection fibres (gPF), locating within brain stem or spinal cord or link them to the cortex. The scores for the first unrotated principal component were used as the indices for general variants of total variance and variances in three major subsets. In order to control for the effects driven by outliers, subjects with a total gFA/MD outside of +/-3 standard deviation from mean were excluded.

Resting-state data was pre-processed through FSL-style motion correction, grand-mean intensity normalisation, high-pass temporal filtering, EPI unwarping and grand-distortion-correction unwarping. A group-level independent component analysis was conducted on the first 4,100 people to reduce data dimension(Alfaro-Almagro et al. 2018). The brain was therefore parcellated into 100 independent components, and 55 of them were left for further analyses after 45 discarded as being identified manually as noise components. The timeseries data for nodes was then used to calculate functional connectivity between node pairs. It was achieved by estimating partial Pearson correlation with an L2 regularisation applied (rho set as 0.5 in FSLNets). All r-scores were then Fisher-transformed into z-scores. This resulted in a 55*55 correlation matrix of functional connectivity for each participant. In order to aid comprehension, all connectivity values were transformed into absolute strength by multiplying the sign of group-mean value for each of the connection (Shen et al. 2018) (see supplementary materials). Group-mean maps for each node can be found in a URL: http://www.fmrib.ox.ac.uk/datasets/ukbiobank/group_means/rfMRI_ICA_d100_good_nodes.html.

## Statistic models

The GLM function in R was used to test the PheWAS associations(Nelder and Baker 2004), and the LME function from nlme package in R(Pinheiro et al. 2007) was used to test bilateral brain structures where hemisphere as a within-subject variable needed to be controlled for. Depression-PGRS were set as factors, and behavioural and neuroimaging phenotypes were set as dependent variables. depression-PGRS at different p thresholds were tested independently. Overall, 1,744 phenotypes (212 behavioural phenotypes + 9 intracranial/subcortical volumes + 38 white matter microstructural measures + 1485 rsfMRI connectivity) * 8 depression-PGRS (under 8 p thresholds) = 13,952 tests across phenotypes and depression-PGRS p thresholds were corrected altogether by FDR-correction(Benjamini and Hochberg 2000) using p.adjust function in R ($q<0.05$).

Common covariates for all association tests included sex, age, age$^2$, the first 15 genetic principal components to control for population stratification and genotyping array (Howard, Adams, Shirali, et al. 2018). Scanner positions on x, y and z axis were also included in the models for all brain phenotypes to control for static-field heterogeneity(Smith and Nichols 2018). Mean motion was set as an additional covariate for the rsfMRI connectivity data (Bijsterbosch et al. 2017; Shen et al. 2018). Subcortical volumetric tests additionally controlled for intracranial volume (Schmaal et al. 2016; Shen et al. 2017). Hemisphere was controlled for where applicable in bilateral brain structural phenotypes(Shen et al. 2017). A list of covariates for each type of phenotype can be found in Table 1.

Table 1. Summary of phenotypes. 209 behavioural phenotypes (6 categories) and 1,586 neuroimaging variables (4 modalities) were included (see the next page).

| Category | General description | Number of traits | Range of sample sizes | Median sample size | UK Biobank data modality | Covariates for regression model |
|---|---|---|---|---|---|---|
| Early life factor | Self-declared early life factors. Mainly derived based on another study in ref X. Items include developmental factors such as birth weight and comparative weight and height at early ages. Parental factors such as early parental death were included too. | 10 | 7,742-11,020 | 10,880 | Touchscreen; Online follow-up | Sex, age, age$^2$, genetic PCs and genotyping array |
| Sociodemographic | Items include education, household income, ethnicity and immigration status | 4 | 8,318-10,260 | 9,152 | Touchscreen | Sex, age, age$^2$, genetic PCs and genotyping array |
| Life style | Self-declared life-style questions. Mainly include sleep patterns, smoking, alcohol consumption, electronic device usage, food and beverage intake, appearance, and social activities. | 69 | 2,880-11,020 | 11,020 | Touchscreen | Sex, age, age$^2$, genetic PCs and genotyping array |
| Physical | This category contains data from self-declared physical conditions from the 'touchscreen' data modality and measured physical data from the 'physical measures' modality. Self-declared items include overall physical health rate, limb pain which is related to suspicious claudication and peripheral artery disease, other types of pain, cardiovascular problems, general diabetes and cancer problems, and bone fractures. Measured physical data contains general and regional body mass/fat index, impedance and hand grip strength. | 68 | 2,227-11,020 | 10,880 | Touchscreen | Sex, age, age$^2$, genetic PCs and genotyping array |
| Cognition | Three tasks were selected for having acceptable reliability, which include trail making task, digit substitution, numeric memory. A variable of g score derived from the three tasks was added. | 4 | 5,247-6,075 | 5,740 | Touchscreen; Online follow-up | Sex, age, age$^2$, genetic PCs and genotyping array |
| Mental health | Mental health questionnaires from touchscreen's mental health section, questions from online follow-up and diagnostic results were included. Diagnostic results were based on systematic review was conducted based on ICD-10 (International Classification of Disease). Items include major psychiatric illness. | 57 | 3,788-8,340 | 8,340 | Touchscreen; Online follow-up | Sex, age, age$^2$, genetic PCs and genotyping array |
| Intracranial/subcortical volume | Measures were derived from T1 data. Seven subcortical regions were mapped and measured. Intracranial volume was derived by adding grey and white matter total volumes and ventricular cerebrospinal fluid. | 9 | 11,006 | -- | Brain imaging | Sex, age, age$^2$, genetic PCs, genotyping array, scanner position, intracranial volume (for subcortical volumes), and hemisphere (for bilateral measures) |
| White matter microstructure | Weighted-mean fractional anisotropy (FA) and mean diffusivity (MD) of major tracts were derived for 27 major tracts (12 bilateral and 3 unilateral). Tracts were mapped using probabilistic tractography. We used general measures derived from PCA and measures for individual tracts respectively. | 38 | FA: 9,699<br>MD: 9,671 | -- | Brain imaging | Sex, age, age$^2$, genetic PCs, genotyping array, scanner position and hemisphere (for bilateral measures) |
| Resting-state functional connectivity | Two-two paired, partial correlation matrix of 55 parcellated nodes generated by group-ICA was estimated and used as a measure for functional connectivity. | 1485 | 10,121 | -- | Brain imaging | Sex, age, age$^2$, genetic PCs, genotyping array, scanner position and mean motion |

Throughout the present study, we report standardised effect sizes (β) and uncorrected p values. All the reported p values were significant after FDR correction. When effect sizes of different signs were presented together, a range of absolute effect sizes was reported.

Following the PheWAS, investigations on endophenotypes were conducted using structural equational modelling with 'lavaan' package in R (Oberski 2014). Two types of mediation tests were conducted: (1) Mediation effect of traits that mediate the direct path between depression-PGRS and depression (x=depression-PGRS, m=other traits, and y=depression). Mediators were the phenotypes (imaging and behavioural) that were associated with depression-PGRS at minimum two thresholds. (2) Mediation effect of neuroimaging phenotypes that mediate the path between depression-PGRS and behavioural traits (x=depression-PGRS, m=neuroimaging phenotypes, and y=behavioural phenotypes). The mediators and outcome variables were associated with depression-PGRS at minimum two thresholds. Depression definitions were not included in the outcome variables for the second set of mediation tests. A full list of phenotypes included for these analyses can be found in Table S1 in Appendix 3.

Mediation models were conducted separately for each set of three traits (i.e. x=depression-PGRS, m=g.MD.Total and y=insomnia). Before multiple correction, tests that had low model fits (CFI<0.9/TLI<0.9/$p_{rmsea}$<0.05) or with the absent association between mediator and outcome (nominal p>0.05) were removed. This step was conducted to remove redundant tests and to exclude unreliable estimates. After this, p values were FDR-corrected.

In both types of mediation analyses, we used the traits that were significant in the PheWAS as mediators/outcomes and tested in independent models. Age, age$^2$ and sex were set as covariates for all phenotypes. In addition to these variables, depression-PGRS had genetic principal components and genotyping array controlled for as well. Covariates for neuroimaging phenotypes additionally included scanner position variables (position x, y and z), and where applicable, hemisphere, mean motion, and intracranial volume were corrected for.

## 2.4 Results

### PheWAS

We found that 91 (66 behavioural and 25 neuroimaging phenotypes) out of 1744 examined phenotypes (212 behavioural and 1532 neuroimaging) showed significant associations with depression-PGRS at a minimum of two p thresholds after correction for multiple comparisons (absolute β: 0.024 to 0.141, p: $9.63\times10^{-38}$ to $2.10\times10^{-3}$). Overall results for selected depression-PGRS of p thresholds at 1 and 0.01 are presented in Figure 1. Associations for significant phenotypes are shown in Figure 2.

Overall, the largest effect sizes were presented in mental health traits (Figure 3). Lifestyle and mental health showed the strongest agreements across depression-PGRS p thresholds. Other than neuroimaging phenotypes, all other traits showed an overall trend of having a larger effect when the depression-PGRS p threshold was higher. However, for neuroimaging phenotypes, optimal thresholds were at lower p thresholds, such as pT<0.01 for white matter microstructure, and pT<0.1 for resting-state amplitude and connectivity. Here in this section, we present the main results and the full list of significant results can be found in Figure 2.

### Depression-PGRS were associated with MDD definitions and symptomology, as well as other psychiatric disorders

Higher depression-PGRS were associated with the presence of depression based on four definitions, including depression-broad, which was a self-declared definition of whether had depression, though most lenient but had the largest statistic power (β: 0.074 to 0.141, p: $1.13\times10^{-37}$ to $1.89\times10^{-11}$), MDD-smith defined by Smith et al. (Smith et al. 2013), which was derived from self-declared symptoms of major depression and hospital admission history (β: 0.045 to 0.104, p: $2.24\times10^{-18}$ to $1.40\times10^{-4}$), MDD-ICD based on International Classification of Disease (ICD-10) using systematic review, with the smallest sample size (β: 0.055 to 0.073, p: $1.83\times10^{-6}$ to $2.89\times10^{-4}$), and MDD-CIDI based on self-answered questions from the structured Composite International Diagnostic Interview (β: 0.060 to 0.115, p: $3.55\times10^{-23}$ to $2.48\times10^{-7}$).

Other than MDD definitions, significant associations were found in MDD symptoms, assessed by PHQ-4 (Patient Health Questionnaire) and CIDI questionnaires, and other

self-reported traits including self-harm, subjective well-being, not worth living and neuroticism (absolute β: 0.083 to 0.122, p: $3.31\times10^{-27}$ to $2.09\times10^{-4}$).

Higher depression-PGRS were also associated with presence of other psychiatric illnesses based on results for diagnosis of major psychiatric illnesses such as psychosis (β: 0.035 to 0.066, p: $1.95\times10^{-9}$ to $1.64\times10^{-3}$), anxiety (β: 0.051 to 0.105, p: $3.51\times10^{-22}$ to $4.05\times10^{-6}$), bipolar disorder (β: 0.036 to 0.038, p: $7.21\times10^{-4}$ to $1.22\times10^{-3}$) and post-traumatic stress disorder (β: 0.036 to 0.104, p: $1.10\times10^{-21}$ to $1.25\times10^{-3}$).

Figure 1. Significance plot for all phenotypes at depression-PGRS p thresholds (pT) at pT<1 (top figure) and pT<0.01 (bottom figure). The x-axis represents phenotypes, and the y-axis shows the $-\log_{10}$ of uncorrected p values. Each dot represents one phenotype, and the colours indicate their according categories. The dashed lines indicate the threshold to survive FDR-correction. FDR-correction was applied over all the traits and all depression-PGRS (see Methods). From left to right on the x-axis, categories were shown by the sequence of: early life risk factors, sociodemographic measures, lifestyle measures, physical conditions, cognition, mental health measures, intracranial/subcortical volume, white matter microstructure and resting-state connectivity. Representative top findings are annotated in the figure. For those findings replicated in both left and right panels are only annotated in the left panel. (see the next page)

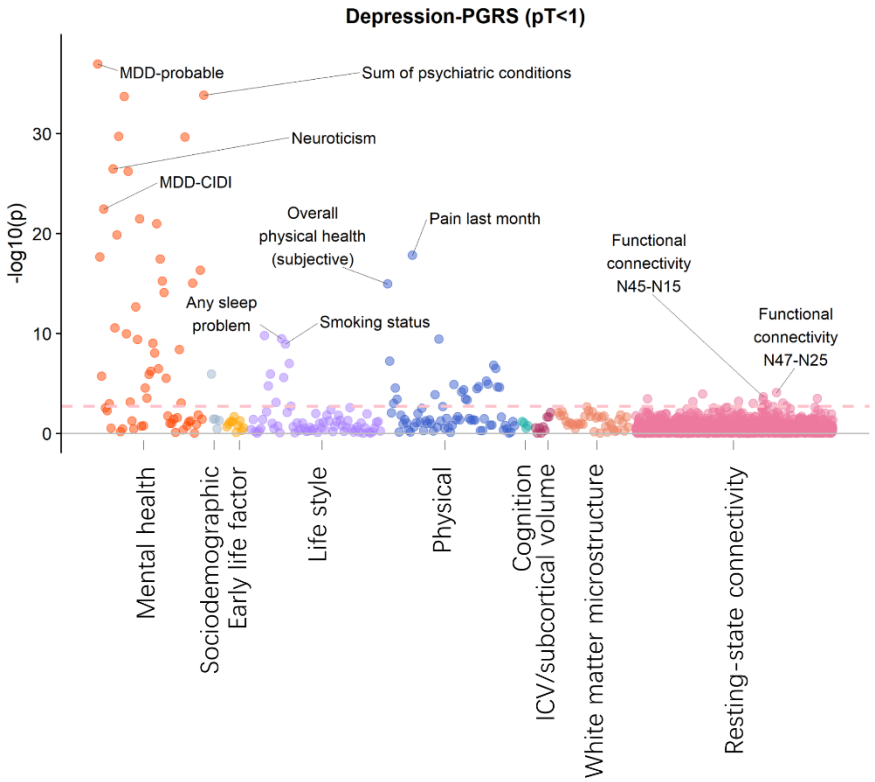
Depression-PGRS (pT<1)
-log10(p)
0
10
20
30
MDD-probable
Sum of psychiatric conditions
Neuroticism
MDD-CIDI
Overall physical health (subjective)
Pain last month
Any sleep problem
Smoking status
Functional connectivity N45-N15
Functional connectivity N47-N25
Mental health
Sociodemographic Early life factor
Life style
Physical
Cognition
ICV/subcortical volume
White matter microstructure
Resting-state connectivity

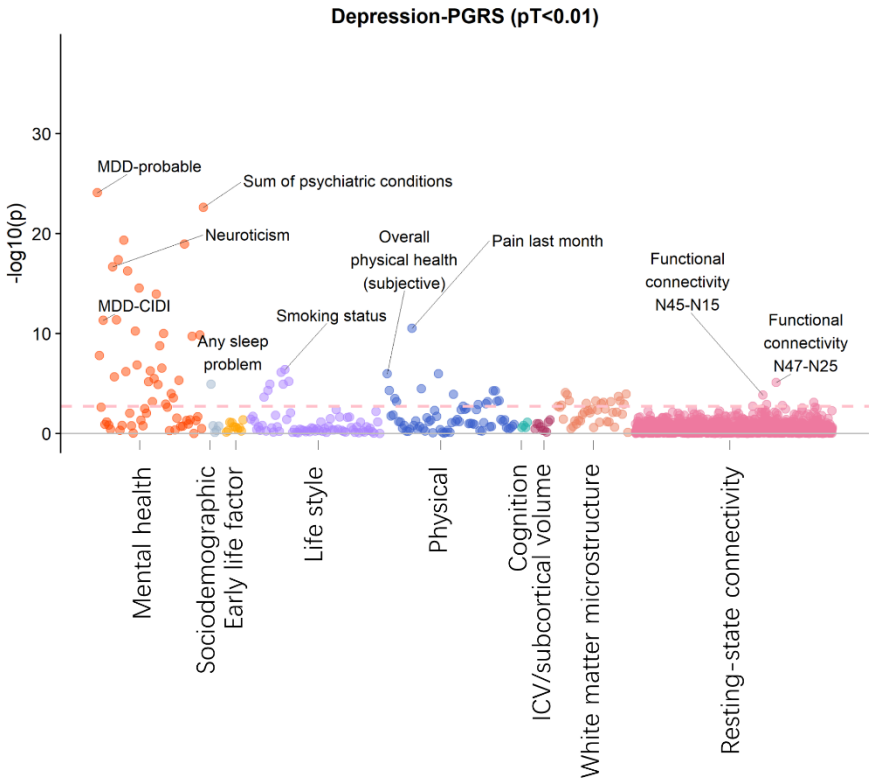
Depression-PGRS (pT<0.01)
-log10(p)
0
10
20
30
MDD-probable
Sum of psychiatric conditions
Neuroticism
MDD-CIDI
Overall physical health (subjective)
Pain last month
Any sleep problem
Smoking status
Functional connectivity N45-N15
Functional connectivity N47-N25
Mental health
Sociodemographic Early life factor
Life style
Physical
Cognition
ICV/subcortical volume
White matter microstructure
Resting-state connectivity

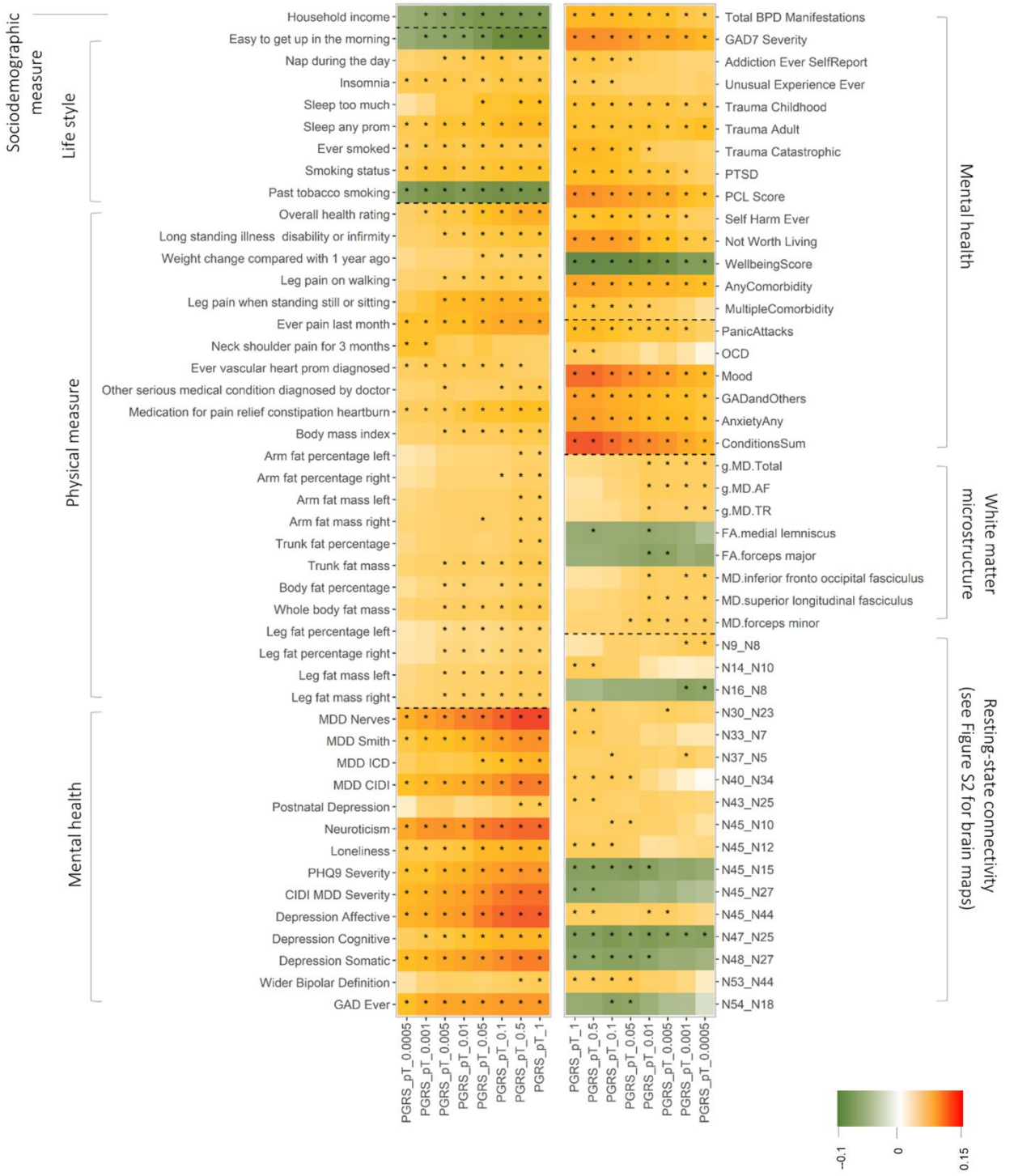


Figure 2. Heatmap for the traits that were significantly associated with depression-PGRS at minimum two p thresholds. Shades of cells indicate the standardised effect sizes (β). A larger effect size was indicated by a darker colour. Cells with an asterisk were significant after FDR-correction. Descriptions in detail can be found in Table 1 and Appendix 3: S1.

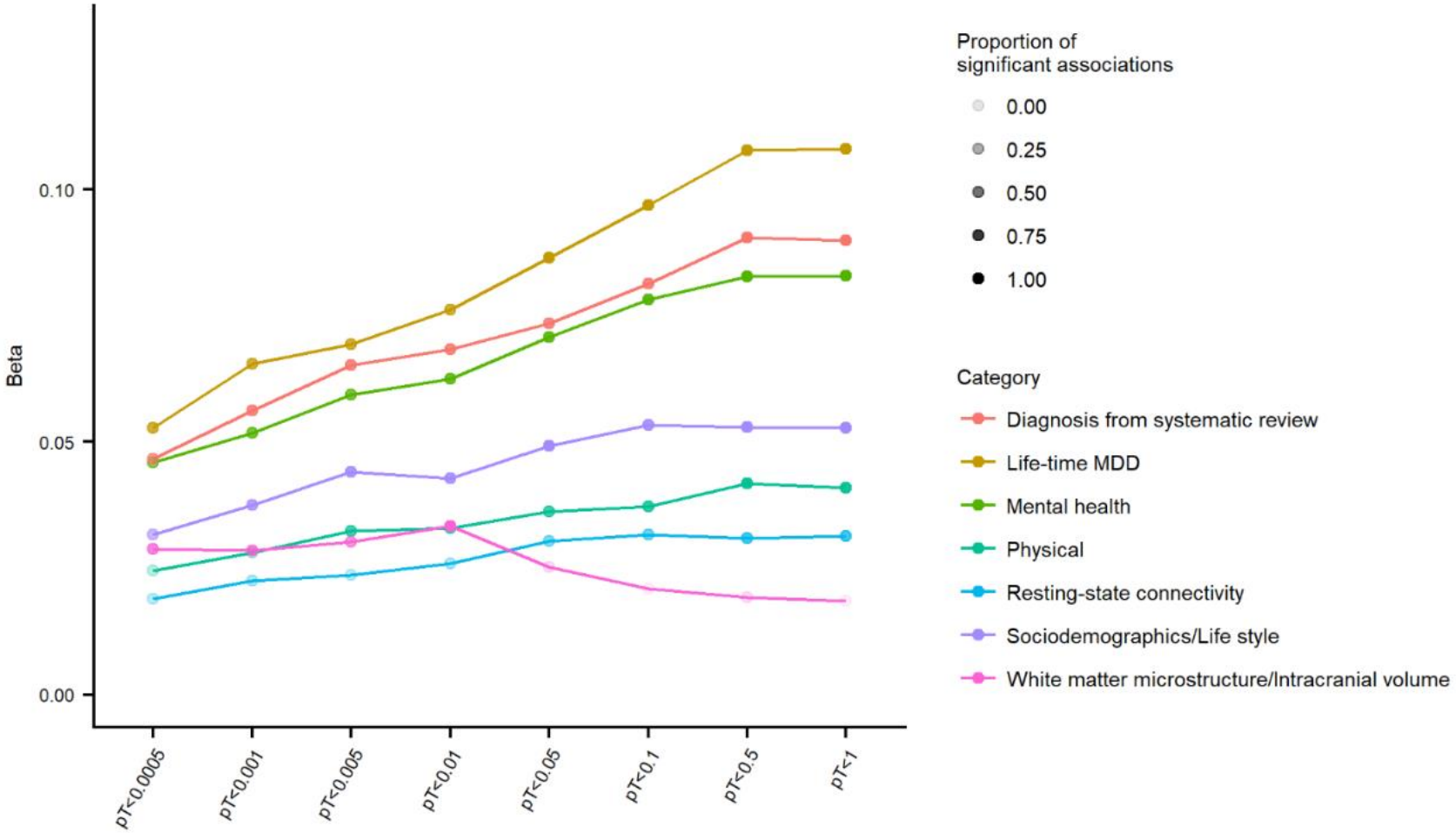


Figure 3. Mean effect sizes for each category. The figure shows the mean effect sizes across all eight depression-PGRS at different p thresholds. Phenotypes included were the ones that were significant at minimum one depression-PGRS. Other than effect sizes, transparency of the dots indicates the proportion of significant tests within their categories. A darker dot means that at this depression-PGRS, a higher proportion of traits/tests were significant under the category.

## Associations were found between depression-PGRS and white matter microstructure

Brain structural phenotypes in white matter microstructure were associated with depression-PGRS. General changes of higher global MD (β: 0.032 to 0.037, p: $8.08\times10^{-5}$ to $6.82\times10^{-4}$), higher MD in association fibres (β: 0.031 to 0.036, p: $1.35\times10^{-4}$ to $1.14\times10^{-3}$) and higher MD in thalamic radiations (β: 0.028 to 0.030, p: $5.24\times10^{-4}$ to $1.57\times10^{-3}$) were associated with higher depression-PGRS. For each tract in specific (Figure 4), significant associations with depression-PGRS was presented in FA in medial lemniscus (β: -0.028 to -0.027, p: $1.02\times10^{-3}$ to $1.38\times10^{-3}$) and forceps major (β: -0.034 to -0.033, p: $5.76\times10^{-4}$ to $8.92\times10^{-4}$), and MD in inferior fronto-occipital fasciculus (β: 0.031 to 0.032, p: $4.68\times10^{-4}$ to $6.59\times10^{-4}$), superior longitudinal fasciculus (β: 0.030 to 0.034, p: $1.99\times10^{-4}$ to $1.13\times10^{-3}$) and forceps minor (β: 0.030 to 0.036, p: $1.19\times10^{-4}$ to $1.34\times10^{-3}$).

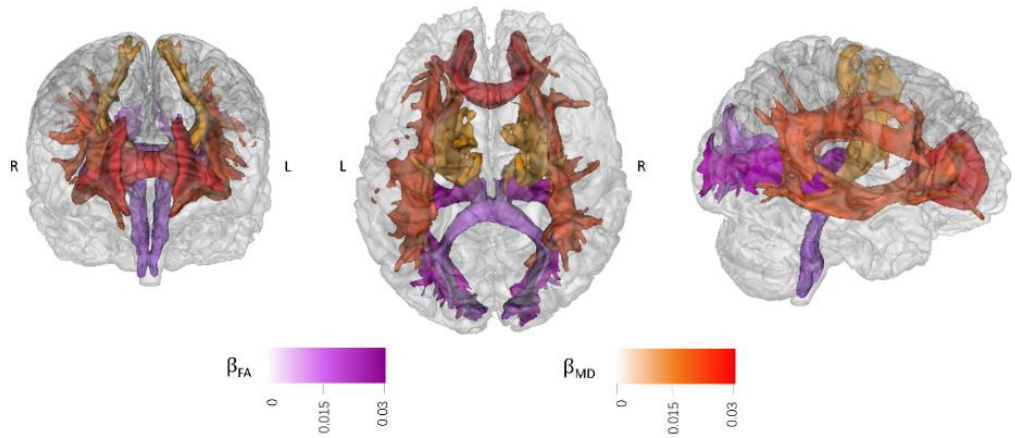


Figure 4. Brain maps for the significant associations between depression-PGRS and white matter microstructure in mean diffusivity (MD) and fractional anisotropy (FA) of major tracts. The shade of each tract represents the effect size (β). A darker shade indicates a greater β. From left to right are from anterior, superior and right view. For clarity purpose, among the tracts presented in Figure 2, the ones that showed consistent associations across at least two depression-PGRS p thresholds are presented. β for the selected tracts were the mean β across all depression-PGRS. Results for each depression-PGRS can be found in Appendix 3: Figure S2.

**Depression-PGRS were associated with resting-state functional connectivity**

Novel associations were found between depression-PGRS and resting-state functional connectivity (absolute β: 0.031 to 0.046, p: $7.86\times10^{-6}$ to $1.64\times10^{-3}$). High depression-PGRS were also correlated with hyper-connectivity in the 'default-mode network' areas such as clusters in bilateral posterior cingulate cortex (peak coordination: -10, -60, 18, cluster size=5,236, peak intensity=0.168) and right medial prefrontal cortex (peak coordination: 10, 48, -10, cluster size=22, peak intensity=0.063). Other regions involved in hyper-connectivity associated with higher depression-PGRS include: bilateral hippocampus (peak coordination: 24, -20, -16, cluster size=333, peak intensity=0.103), right mid-insula (peak coordination: 36, -6, 14, cluster size=130, peak intensity=0.010), bilateral mid-frontal gyrus (left: peak coordination: -22, 28, 40, cluster size=1,930, peak intensity=0.177; right: peak coordination: 26, 32, 34, cluster size=1,575, peak intensity=0.144). Weaker connectivity involved in orbito-superior frontal gyrus (peak coordination: 18, 64, -6, cluster size=13,359, peak intensity=-0.010), inferior parietal gyrus (peak coordination: -30, -46, 38, cluster size=1,207, peak intensity=-0.071) and right anterior insula (peak coordination: 32, 22, 10, cluster size=565, peak intensity=-0.089) (Figure 5). A full list of regions was reported in Appendix 3: Table S3 and S4.

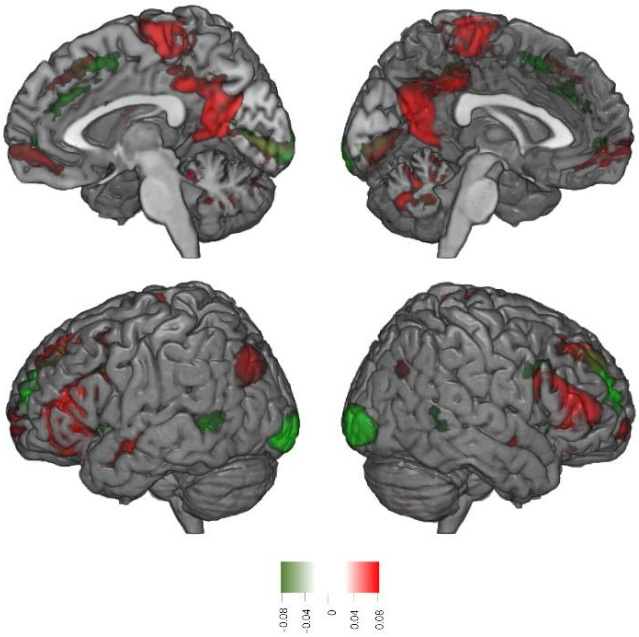

Figure 5. Brain maps for regions involved in significant associations between resting-state functional connectivity and depression-PGRS. In this figure, among the results presented in Figure 2, the ones that show consistent associations across at least two depression-PGRS p thresholds are presented. β for the selected tracts are the mean β across all depression-PGRS, regardless of whether the association was significant for each depression-PGRS.. Visualisation of results is achieved by calculating the mean of ICA maps, weighted by their mean β, respectively for positive and negative β. For clarity, the brain maps shown below have a threshold applied on, that values over 50% of highest intensity are shown. The shade of red/green represents the intensity. Maps in the top row had a cut-up at x=-1/1. The maps on the bottom are from left/right lateral view.

## Higher depression-PGRS were associated with sleep problems, smoking and poorer physical health

In terms lifestyle, sleep problems (absolute β: 0.035 to 0.068, p: $3.42\times10^{-10}$ to $1.66\times10^{-4}$) and smoking (absolute β: 0.033 to 0.062, p: $1.13\times10^{-9}$ to $8.63\times10^{-4}$) were found associated with depression-PGRS.

Physical health items associated with depression-PGRS can be summarised as the following four categories: (1) overall health level including self-reported general health condition (β: 0.037 to 0.077, p: $5.68\times10^{-16}$ to $1.06\times10^{-3}$) and condition of long-standing illnesses (β: 0.040 to 0.052, p: $2.60\times10^{-8}$ to $3.53\times10^{-5}$), (2) pain (β: 0.032 to 0.084, p: $1.41\times10^{-18}$ to $1.25\times10^{-3}$), (3) cardiovascular/heart problem (β: 0.031 to 0.040, p: $8.54\times10^{-4}$ to $3.43\times10^{-5}$), and (4) body mass and weight change (β: 0.017 to 0.041, p: $1.15\times10^{-7}$ to $1.61\times10^{-3}$).

## Mediation analysis: from depression-PGRS, via non-mental-health traits, to depression

We tested the mediation effects of 57 non-mental-health traits that were significant in the PheWAS at minimum one depression-PGRS p threshold. In order to cut down redundant tests, we chose two depression-PGRS at thresholds pT<1 and pT<0.01, and MDD-nerves as the major definition of depression.

There were 29 and 25 traits showed significant mediation effect for depression-PGRS, respectively at pT<1 and pT<0.01 (proportion of direct effect mediated (Δc): 1.11 to

7.57%, p: $4.08\times10^{-6}$ to $8.70\times10^{-4}$). Results for the two depression-PGRS pTs were similar, as in Figure 6. Therefore, we reported the statistics from depression-PGRS pT<1 below. Highest Δc were shown in overall self-declared physical health rating (Δc=7.57%, p=$1.11\times10^{-8}$) and whether there was any sleep problem (Δc=7.16%, p=$8.55\times10^{-9}$). Phenotypes related to sleep problems such as insomnia and sleep too much rank relatively high in terms of the proportion of direct effect mediated (Δc: 3.23 to 6.62%, p: $4.08\times10^{-6}$ to $8.70\times10^{-4}$). Mediation effect of smoking (Δc: 2.79 to 2.90%, p: $1.20\times10^{-4}$ to $1.67\times10^{-4}$) and physical variables including pain, long-standing illness and cardiovascular condition (Δc: 1.15 to 6.36%, p: $2.90\times10^{-9}$ to 0.029) ranked relatively middle and had high variance. Body mass variables explained the least proportion of direct effect between depression-PGRS and MDD compared to other significant traits (Δc: 1.20 to 1.86%, p: $1.27\times10^{-3}$ to 0.019).

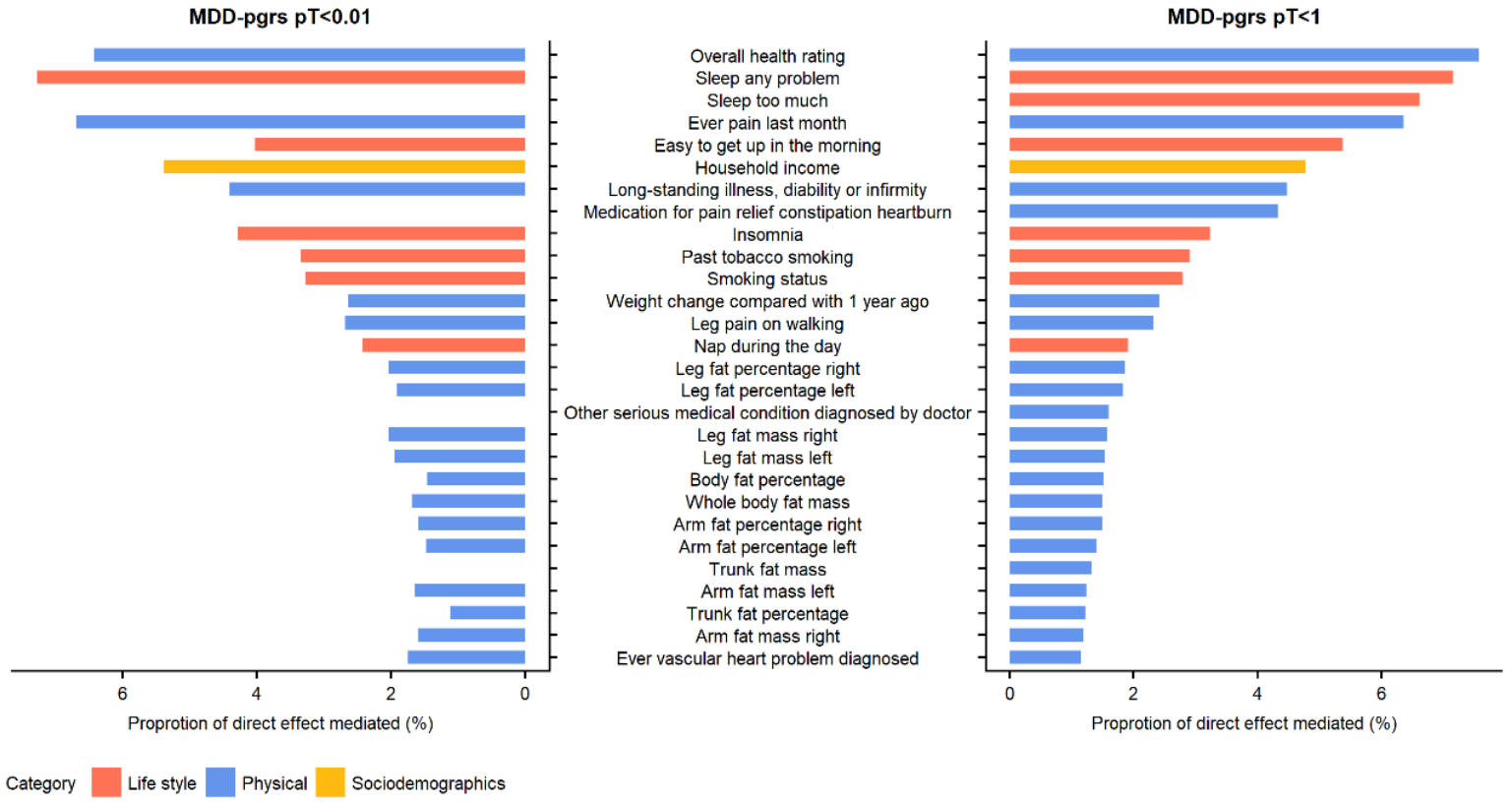


Figure 6. Proportion of direct association between depression-PGRS and MDD explained by mediators (x=depression-PGRS, y=MDD-nerve). The left side is the results for depression-PGRS at pT<0.01. The four absent bars are either having insignificant mediation effect or the mediation model has poor fits.

## Mediation analysis: from depression-PGRS, via neuroimaging phenotypes, to behavioural traits

Mainly in white matter microstructure showed a significant mediation effect between the direct path of depression-PGRS at pT<0.01 and behavioural traits (p: $4.51\times10^{-4}$ to 0.029). No significant mediation effect was found for the path between depression-PGRS at pT<1 and behavioural traits (minimum $p=4.74\times10^{-3}$, corrected p=0.264).

The effect between depression-PGRS and behavioural traits including subjective well-being score (Δc: 3.56 to 3.95%, p: $8.32\times10^{-3}$ to 0.021), overall number of psychiatric illnesses diagnosed (Δc: 1.40 to 1.50%, p: 0.016 to 0.018), smoking status (Δc: 2.70 to 4.58%, p: $2.14\times10^{-3}$ to 0.012), and ever had cardiovascular/heart problem (Δc: 7.00 to 10.20%, p: $4.51\times10^{-4}$ to $2.60\times10^{-3}$) were generally mediated by multiple white matter microstructural variables. Global MD and MD in association fibres negatively mediated the effect between depression-PGRS at pT<0.01 and body mass (p: $1.63\times10^{-3}$ to 0.010). This was due to an association that higher MD was associated with higher body mass. We further found that it was caused by the quadratic relationship between body mass and MD, indicating that worse white matter microstructure was associated with either being under- or over-weight. When the linear terms for body mass were replaced by quadratic terms, then the mediation effect became insignificant (see Table S7).

Table 2. Results for neuroimaging phenotypes mediating the direct association between depression-PGRS and behavioural phenotypes (x=depression-PGRS, m=neuroimaging phenotypes, and y=behavioural phenotypes). CFI=Comparative Fit Index, TLI= Tucker-Lewis Index, and $p_{rmsea}$ is the p statistic of whether RMSEA was significantly different from 0. All the results below are significant after FDR-correction (see the next page).

Table 2. Results for neuroimaging phenotypes mediating the direct association between depression-PGRS and behavioural phenotypes (x=depression-PGRS, m=neuroimaging phenotypes, and y=behavioural phenotypes). CFI=Comparative Fit Index, TLI= Tucker-Lewis Index, and $p_{rmsea}$ is the p statistic of whether RMSEA was significantly different from 0. All the results below are significant after FDR-correction.

| Predictor | Mediator | Outcome | Category | c' | standard error of c' | p | $p_{corr}$ | Proportion of effect mediated | CFI | TLI | RMSEA | $p_{rmsea}$ |
|---|---|---|---|---|---|---|---|---|---|---|---|---|
| depression-PGRS (pT<0.01) | g.MD.AF | Well-being score | Mental health | -0.002 | 0.001 | 0.012 | 0.029 | 0.034 | 1.000 | 1.000 | 0.001 | 1.000 |
| | | Past tobacco smoking | Life style | -0.001 | 0.001 | 0.013 | 0.029 | 0.029 | 0.977 | 0.960 | 0.010 | 1.000 |
| | | Smoking status | Life style | 0.001 | 0.001 | 0.012 | 0.029 | 0.026 | 0.970 | 0.948 | 0.011 | 1.000 |
| | | Ever vascular heart problem diagnosed | Physical | 0.002 | 0.001 | 0.001 | 0.020 | 0.068 | 0.959 | 0.929 | 0.015 | 1.000 |
| | | Arm fat mass left | Physical | -0.001 | 0.000 | 0.019 | 0.034 | -0.062 | 0.950 | 0.913 | 0.016 | 1.000 |
| | | Arm fat mass right | Physical | -0.001 | 0.000 | 0.015 | 0.032 | -0.065 | 0.951 | 0.915 | 0.016 | 1.000 |
| | | Arm fat percentage left | Physical | -0.001 | 0.000 | 0.006 | 0.022 | -0.077 | 0.983 | 0.970 | 0.019 | 1.000 |
| | | Arm fat percentage right | Physical | -0.001 | 0.000 | 0.005 | 0.022 | -0.071 | 0.983 | 0.971 | 0.019 | 1.000 |
| | | Body fat percentage | Physical | -0.001 | 0.000 | 0.002 | 0.020 | -0.084 | 0.983 | 0.970 | 0.019 | 1.000 |
| | | Leg fat mass left | Physical | -0.001 | 0.000 | 0.007 | 0.022 | -0.062 | 0.983 | 0.970 | 0.016 | 1.000 |
| | | Leg fat mass right | Physical | -0.001 | 0.000 | 0.008 | 0.024 | -0.060 | 0.982 | 0.969 | 0.016 | 1.000 |
| | | Leg fat percentage left | Physical | -0.001 | 0.000 | 0.001 | 0.020 | -0.072 | 0.990 | 0.983 | 0.021 | 1.000 |
| | | Leg fat percentage right | Physical | -0.001 | 0.000 | 0.002 | 0.020 | -0.069 | 0.989 | 0.981 | 0.021 | 1.000 |
| | | Trunk fat mass | Physical | -0.001 | 0.001 | 0.009 | 0.024 | -0.064 | 0.945 | 0.905 | 0.015 | 1.000 |
| | | Trunk fat percentage | Physical | -0.002 | 0.001 | 0.003 | 0.020 | -0.090 | 0.969 | 0.947 | 0.017 | 1.000 |
| | | Whole body fat mass | Physical | -0.001 | 0.001 | 0.009 | 0.024 | -0.059 | 0.955 | 0.922 | 0.016 | 1.000 |
| | g.MD.Total | Well-being score | Mental health | -0.002 | 0.001 | 0.007 | 0.023 | 0.038 | 1.000 | 1.005 | 0.000 | 1.000 |
| | | Overall ICD-10 psychiatric conditions | Mental health | 0.002 | 0.001 | 0.018 | 0.034 | 0.014 | 0.996 | 0.992 | 0.005 | 1.000 |
| | | Ever smoked | Life style | 0.001 | 0.001 | 0.015 | 0.031 | 0.030 | 0.972 | 0.951 | 0.012 | 1.000 |

| | | | | | | | | | | | |
|---|---|---|---|---|---|---|---|---|---|---|---|
| | Past tobacco smoking | Life style | -0.002 | 0.001 | 0.004 | 0.020 | 0.039 | 0.983 | 0.971 | 0.010 | 1.000 |
| | Smoking status | Life style | 0.002 | 0.001 | 0.003 | 0.020 | 0.037 | 0.978 | 0.962 | 0.011 | 1.000 |
| | Addiction.ever (Self-reported) | Life style | 0.001 | 0.001 | 0.027 | 0.041 | 0.038 | 0.988 | 0.980 | 0.008 | 1.000 |
| | Long standing illness, disability or infirmity | Physical | 0.001 | 0.001 | 0.021 | 0.036 | 0.032 | 0.996 | 0.993 | 0.005 | 1.000 |
| | Ever vascular heart problem diagnosed | Physical | 0.003 | 0.001 | 0.000 | 0.020 | 0.094 | 0.967 | 0.943 | 0.015 | 1.000 |
| | Overall health rating | Physical | 0.001 | 0.001 | 0.013 | 0.029 | 0.032 | 0.984 | 0.972 | 0.009 | 1.000 |
| | Arm fat percentage left | Physical | -0.001 | 0.000 | 0.018 | 0.034 | -0.059 | 0.983 | 0.971 | 0.019 | 1.000 |
| | Arm fat percentage right | Physical | -0.001 | 0.000 | 0.018 | 0.034 | -0.053 | 0.984 | 0.972 | 0.019 | 1.000 |
| | Body fat percentage | Physical | -0.001 | 0.000 | 0.006 | 0.022 | -0.067 | 0.983 | 0.971 | 0.019 | 1.000 |
| | Leg fat mass left | Physical | -0.001 | 0.000 | 0.021 | 0.036 | -0.047 | 0.984 | 0.972 | 0.016 | 1.000 |
| | Leg fat mass right | Physical | -0.001 | 0.000 | 0.025 | 0.039 | -0.045 | 0.983 | 0.971 | 0.016 | 1.000 |
| | Leg fat percentage left | Physical | -0.001 | 0.000 | 0.004 | 0.021 | -0.055 | 0.990 | 0.983 | 0.021 | 1.000 |
| | Leg fat percentage right | Physical | -0.001 | 0.000 | 0.006 | 0.022 | -0.052 | 0.989 | 0.981 | 0.021 | 1.000 |
| | Trunk fat mass | Physical | -0.001 | 0.001 | 0.023 | 0.038 | -0.053 | 0.955 | 0.922 | 0.015 | 1.000 |
| | Trunk fat percentage | Physical | -0.001 | 0.001 | 0.006 | 0.022 | -0.075 | 0.972 | 0.951 | 0.017 | 1.000 |
| | Whole body fat mass | Physical | -0.001 | 0.000 | 0.024 | 0.039 | -0.047 | 0.962 | 0.933 | 0.016 | 1.000 |
| g.MD.TR | Well-being score | Mental health | -0.002 | 0.001 | 0.009 | 0.024 | 0.036 | 1.000 | 1.004 | 0.000 | 1.000 |
| | Overall ICD-10 psychiatric conditions | Mental health | 0.002 | 0.001 | 0.016 | 0.033 | 0.015 | 0.998 | 0.996 | 0.005 | 1.000 |
| | Ever smoked | Life style | 0.002 | 0.001 | 0.006 | 0.022 | 0.036 | 0.982 | 0.968 | 0.013 | 1.000 |
| | Past tobacco smoking | Life style | -0.002 | 0.001 | 0.003 | 0.020 | 0.045 | 0.989 | 0.980 | 0.010 | 1.000 |
| | Smoking status | Life style | 0.002 | 0.001 | 0.002 | 0.020 | 0.046 | 0.986 | 0.976 | 0.011 | 1.000 |
| | Addiction.ever (Self-reported) | Life style | 0.001 | 0.001 | 0.029 | 0.043 | 0.035 | 0.993 | 0.987 | 0.008 | 1.000 |
| | Overall health rating | Physical | 0.002 | 0.001 | 0.004 | 0.020 | 0.043 | 0.991 | 0.984 | 0.009 | 1.000 |
| | Ever vascular heart problem diagnosed | Physical | 0.003 | 0.001 | 0.001 | 0.020 | 0.101 | 0.976 | 0.958 | 0.016 | 1.000 |
| | Long standing illness, disability or infirmity | Physical | 0.001 | 0.001 | 0.008 | 0.024 | 0.039 | 0.997 | 0.995 | 0.005 | 1.000 |

| | | | | | | | | | | | |
|---|---|---|---|---|---|---|---|---|---|---|---|
| | Other serious medical condition diagnosed by doctor | Physical | 0.001 | 0.000 | 0.024 | 0.039 | 0.054 | 0.995 | 0.992 | 0.006 | 1.000 |
| N30_N23 | Easy to get up in the morning | Life style | -0.001 | 0.001 | 0.015 | 0.031 | 0.041 | 0.951 | 0.915 | 0.011 | 1.000 |

## 2.5 Discussion

Associations between depression-PGRS, behavioural and neuroimaging phenotypes were found in the present study using the largest independent imaging cohort so far. Strongest associations were found between depression-PGRS and mental health. Novel associations were found that higher depression-PGRS correlated with lower white matter microstructure, hyper resting-state connectivity in default-mode network, weaker resting-state connectivity in the sensorimotor and dorsal lateral prefrontal cortex. Associations with MDD polygenic risk was also shown in worse sleep, smoking, presence of cardiovascular conditions and obesity. Sleep and general physical health mediated the largest proportion of the association between depression-PGRS and self-reported MDD, and white matter microstructural variation mediated the effect of depression-PGRS to smoking, subject well-being, an overall number of psychiatric illness diagnosed and ever had heart or cardiovascular problems.

Novel effects of depression-PGRS were found in both structural and functional connectivity in the brain. Recent GWAS suggest that MDD is a brain disorder based on gene expression results from the genome-wide significant hits (Howard, Adams, Shirali, et al. 2018), and our results further provided evidence for a robust association between the brain and subthreshold common polygenic variation (International and Consortium 2009). Especially, the associations involved in resting-state connectivity is, to our knowledge, the first to date. Findings from both DTI and resting-state data revealed the importance of prefrontal cortex, which is a hub for emotion regulation and executive control (Miller 2000; Etkin et al. 2015). Consistent with previous findings on MDD case-control differences (Kaiser et al. 2015; Shen et al. 2017), white matter anisotropic reduction and lack of functional strength involved in the prefrontal cortex were observed in our DTI and resting-state results respectively. The second main association was found in white matter alterations in thalamic radiations and FA

reduction in the brain stem, implying deficits in the limbic system for the processing of negative emotional stimuli and reward signals (Disner et al. 2011; Russo and Nestler 2013; Etkin et al. 2015). depression-PGRS were also associated with hyper-connectivity in the default-mode network areas (Raichle 2015), which was also found relevant to spontaneous rumination of negative thoughts and imbalanced goal-directed processing (Bartova et al. 2015; Kaiser et al. 2015; Posner et al. 2015). Compared to other phenotype categories, both white matter and resting-state data showed the largest effect sizes in lower p thresholds for MDD (for example $pT<0.01$ for white matter), along with the findings from GWAS that top-hits express in the brain (Howard, Adams, et al. 2017; Howard, Clarke, et al. 2017; Wray et al. 2018), these converging evidence indicate a heterogeneous genetic architecture for MDD, and that variation in the brain may be relevant to SNPs which have moderate to high effect sizes. In the present study, neuroimaging phenotypes generally showed smaller effect sizes compared to some behavioural traits such as sleep and smoking status. A major reason may be that self-reported lifestyle and physical conditions are likely to be directly associated with MDD diagnostic criteria. The importance of the associations found in neuroimaging phenotypes is supported by various facts. Firstly, findings in neuroimaging phenotypes associating with MDD is well replicated. Secondly, compared to behavioural patterns, neuroimaging phenotypes are much more directly related to currently available drugs and psychological interventions. Finally, brain structural and functional measures have a more certain role as endophenotypes, whereas it is much more difficult to define whether behavioural patterns such as self-reported patterns of sleep and smoking are the causes or outcomes of MDD.

Sleep, pain, smoking behaviour and whether there is any heart/cardiovascular condition mediated the association between depression-PGRS and self-reported MDD, and sleep specifically mediated by the largest proportions. Sleep disturbance is a major somatic symptom of MDD and an important reference of anti-depressant response

(Chen 1979; Winokur et al. 2003). Behavioural traits like sleeping pattern, smoking and pain have a significant impact or reciprocal association with activities in the hypothalamic-pituitary-adrenal axis (Pariante and Lightman 2008), which is responsible for stress response and possesses a regressive feedback system to maintain homeostasis (Gordon et al. 2015). Disruption of stasis in this system is a vulnerability factor for the onset of MDD (Pariante and Lightman 2008), and it is associated with brain development and synaptic formation (Maret et al. 2011; Stickgold et al. 2011). Mediator effect of white matter microstructure on the association between depression-PGRS, smoking and heart/cardiovascular condition then suggest that the relationship between depression-PGRS and phenotypic presence of MDD may have a multi-layered endophenotypic structure.

The findings from the mediation models provided insights for shared variances of depression-PGRS related phenotypes. These tests were partially hypothesis-driven, as neurobiological variability is in general believed to be less biologically distant to genetic effects, compared with complex traits on the behavioural level. However, our results and the method structural equational modelling itself would not rule out other possibilities for directionality. Though our results give limited information about causality, they narrowed down the spectrum of traits for future studies on causal inference using a longitudinal design or statistical methods like Mendelian Randomisation (Lawlor et al. 2008).

To conclude, the association tests revealed relationships between MDD polygenic risk and various behavioural and neuroimaging variables. These primary results were also accompanied by mediation analyses revealing shared variances of sleep, smoking, white matter microstructure and MDD polygenic risk. These findings altogether give insights of neurobiological and genetic mechanism of MDD, implying a multi-modality architecture for the biological inferences of its onset.

## 3 Chapter conclusion

This study provided a large scale of association tests, containing various behavioural and neuroimaging traits. Novel results were found that white matter microstructure and resting-state connectivity were associated with polygenic risk scores for depression. Mediation tests revealed that sleep, smoking behaviour, cardiovascular conditions and body mass mediated the effect of polygenic risk on the presence of depression. The study gave a broad presentation of major associations between behavioural, neuroimaging phenotypes and polygenic risk score.

# Chapter 5:

## Resting-state connectivity and its association with cognitive performance, educational attainment, and household income in UK Biobank (N = 3,950)

## 1 Chapter introduction

Cognition, educational attainment, and socioeconomic status have been found associated with polygenic risk of depression and the presence of various mood disorders. These variables are also important factors for phenotypic variances in the brain. Although task-relevant fMRI studies have been conducted broadly on these traits, resting-state connectivity and its association with the above variables has had limited investigations. The study in this chapter investigated resting-state connectivity and its associations with cognition, educational attainment, and household income. This paper was also one of first papers using UK Biobank imaging data testing the association between resting-state connectivity and behavioral patterns.

This study has been published as a journal paper entitled, “Resting-state connectivity and its association with cognitive performance, educational attainment, and household income in UK Biobank (N = 3,950)” (Shen et al. 2018). I conducted the analyses and drafted the manuscript with supervision, as the first author.

## 2 Paper

### 2.1 Abstract

**Background:** Cognitive ability is an important predictor of lifelong physical and mental well-being and impairments are associated with many psychiatric disorders. Higher cognitive ability is also associated with greater educational attainment and increased household income. Understanding neural mechanisms underlying cognitive ability is of crucial importance for determining the nature of these associations. In the current study, we examined the spontaneous activity of the brain at rest to investigate its relationships with not only cognitive ability, but also educational attainment and household income.

**Methods:** We used a large sample of resting-state neuroimaging data from UK Biobank (N=3,950).

**Results:** Firstly, analysis at the whole-brain level showed that connections involving the default mode network (DMN), frontoparietal network (FPN) and cingulo-opercular network (CON) were significantly positively associated with levels of cognitive performance assessed by a verbal-numerical reasoning test (standardized β ranged from 0.054 to 0.097, $p_{corrected}$<0.038). Connections associated with higher levels of cognitive performance were also significantly positively associated with educational attainment (r=0.48, N=4,160) and household income (r=0.38, N=3,793). Further, analysis on the coupling of functional networks showed that better cognitive performance was associated with more positive DMN-CON connections, decreased cross-hemisphere connections between the homotopic network in CON and FPN, and stronger CON-FPN connections (absolute β ranged from 0.034 to 0.063, $p_{corrected}$<0.045).

**Conclusion:** The present study finds that variation in brain resting state functional connectivity associated with individual differences in cognitive ability, largely involving DMN and lateral prefrontal networks. Additionally, we provide evidence of shared neural associations of cognitive ability, educational attainment, and household income.

## 2.2 Introduction

General cognitive ability is positively associated with higher educational attainment (Marioni et al. 2014), better workplace performance (Deary 2012), and with reduced risk of several mental and physical diseases (Deary 2012; Lencz et al. 2014; Calvin et al. 2017; Russ et al. 2017). Identifying the associated neural mechanisms will help better understand the causes of these associations.

Studies have been conducted to explore the relationship between resting-state network and cognitive ability (Dosenbach et al. 2007; Sheffield et al. 2015; Wen et al. 2018). Resting-state networks (RSN) involving lateral prefrontal cortex, such as executive control network and frontal-parietal network, have been previously reported to have positive associations attention and executive control (Deary et al. 2010). Newer evidence suggested that, other than prefrontal networks, the default mode network (DMN) is an important neurobiological marker for higher network efficiency as it is a metabolic and neural network hub for the whole brain (Broyd et al. 2009; Smith et al. 2015), and it is associated with a large number of positive sociodemographic variables

(Smith et al. 2015). However, prefrontal networks and DMN show distinctive metabolic activity (Raichle et al. 2001), and in certain tasks, they can be neuroanatomically antagonistic (Raichle 2015). The ambiguity of biomarkers for cognitive performance therefore limits the potential of using neural-network modeling for practical purposes like assisting clinical diagnoses and identifying the regional targets for neuronal interventions.

The variability of results in previous studies (Spreng et al. 2010; Cole et al. 2012; Smith et al. 2015) may be due to relatively small sample sizes, often limited to 100 participants or fewer. This limitation is difficult to overcome using meta-analysis, as methods of extracting functional networks may vary considerably between studies. Therefore, there is a need for large-scale studies using a single scanner and consistent methods of estimating the association of RSN activity with consistently-collected social and psychological phenotypes to determine the relationship between resting functional connectivity and cognitive ability.

In the current study, we examined resting-state data from the first release of the UK Biobank imaging project (Cox, Ritchie, et al. 2016; Miller et al. 2016). Participants from 40 to 75 years old were recruited widely across the United Kingdom (Matthews and Sudlow 2015; Hill, Davies, et al. 2016; Miller et al. 2016). For the resting-state fMRI (rs-fMRI) data used in the current study, 3,950 subjects underwent the cognitive assessment using a test of verbal-numerical reasoning (VNR; referred to in UK Biobank as a test of “fluid intelligence”). This measurement is genetically and phenotypically representative to the latent component of general cognitive performance (Davies et al. 2016; Hagenaars et al. 2016). This test had a test-retest reliability of 0.65 between the initial assessment visit in 2006-2010 and the first repeat assessment visit in 2012-2013 (Davies et al. 2016; Lyall et al. 2016). It also shows a significant genetic correlation with childhood general cognitive ability (r=0.81) (Hagenaars et al. 2016).

In addition to the utility of analyzing a large sample, the present study benefited from examining the neural associations between educational attainment and household income. The rs-fMRI data were available for educational attainment and household income on samples of 4,160 and 3,793 subjects, respectively. Both education and household income show phenotypic correlations and shared genetic architecture with cognitive ability (Davies et al. 2016; Hill, Hagenaars, et al. 2016); however, the

associations between cognitive ability and these two variables with respect to functional connectivity remain unclear.

In order to address the above issues, our analyses were conducted following the order: (1) We examined whole-brain resting-state connectivity using a very large sample, to identify functional networks associated with cognitive performance (2) We then tested which resting-state connections were associated with educational attainment and household income, as these two traits are highly relevant to cognitive performance. (3) to determine which regions are involved with the above three traits, pairwise correlation analyses were conducted between neural associations of cognitive performance, educational attainment and household income on all connections over the whole brain. For these three steps, we conducted the analysis on a correlation matrix derived from high-resolution brain parcellation. Finally, (4) we moved on to examine the coupling between bulk resting-state networks based on a low-resolution parcellation, focussing on networks identified by the previous two whole-brain analyses.

## 2.3 Methods

### Participants

The study was approved by the National Health Service (NHS) Research Ethics Service (reference: 11/NW/0382), and by the UK Biobank Access Committee (Project #4844). Written consent was obtained from all participants.

In total, 4,162 participants undertook a rs-fMRI assessment and passed the quality check undertaken by UK Biobank (http://www.fmrib.ox.ac.uk/ukbiobank/nnpaper/IDPinfo.txt) (Mean Age=62.20+/-7.56 years, Male=47.48%, 3576 (85.92%) White, 142 (3.41%) Asian, 31 (0.74%) Black and 142 (3.41%) mixed).

### Imaging data

We used the network matrices from the IDPs (imaging-derived phenotypes) which were processed by the UK Biobank imaging project team (Miller et al. 2016). The detailed methods of the UK Biobank imaging processing can be found in a previous protocol paper (Miller et al. 2016). For clarification, these processes are described briefly below.

All imaging data were obtained on a Siemens Skyra 3.0 T scanner (Siemens Medical Solutions, Germany, see http://biobank.ctsu.ox.ac.uk/crystal/refer.cgi?id=2367).

Data pre-processing, group-ICA parcellation and connectivity estimation were carried out using FSL packages (http://biobank.ctsu.ox.ac.uk/crystal/refer.cgi?id=1977) by UK Biobank. Briefly, pre-processing included motion correction, grand-mean intensity normalization, high-pass temporal filtering, EPI unwarping, gradient distortion correction unwarping and removal of structured artefacts (Miller et al. 2016).

Group-ICA were then performed on the preprocessed sample of 4,162 people, and two different ICAs were performed with the dimensionality (*D*) set as 100 and 25. The *D* determines the number of distinct ICA components. The dimensionality of *D*=100 infers a parcellation of high-resolution, whilst setting *D*=25 results in low-resolution parcellation, and larger functional networks that can be extracted as a single component(Smith et al. 2015; Miller et al. 2016). After the group-ICA, noise components were discarded; this resulted in 55 components in 100-*D* ICA and 21 components in 25-*D* ICA that remained for further analysis. The maps of both ICAs can be seen at: http://www.fmrib.ox.ac.uk/datasets/ukbiobank/index.html.

Finally, connections between pairs of ICA components for each subject were estimated. We used the partial correlation matrices calculated using the FSLNets toolbox: http://fsl.fmrib.ox.ac.uk/fsl/fslwiki/FSLNets. A partial correlation matrix was generated by controlling for the strength of other connections. The normalized estimation of partial correlation was conducted with an L2 regularization applied (rho=0.5 for Ridge Regression option in FSLnets). More details can be found in Miller et al.(2016) (Miller et al. 2016) and the URL: https://biobank.ctsu.ox.ac.uk/crystal/docs/brain_mri.pdf.

The final 55*55 and 21*21 partial correlation matrices were used as measurements of functional connections. The two matrices are different. A 100*100 matrix has a much higher spatial resolution, therefore gives better spatial details in terms of identifying what regions involve in significant connections. On the other hand, a 25*25 matrix has a low spatial resolution, but it allows us to estimate the temporal synchronization between bulk networks that are well-known, such as DMN. Hence, the functional networks that were found in the whole-brain analysis were selected from the 21*21 matrix as NOI, connections between the NOI were tested.

### Cognitive performance

A test of verbal-numerical reasoning (VNR) was carried out by UK Biobank according to the standard protocol (Parr et al. 2015; Davies et al. 2016; Keyes et al. 2016). Questions of the test can be found in the Touch-screen fluid intelligence test protocol document: http://biobank.ctsu.ox.ac.uk/crystal/refer.cgi?id=100231). The data used in the present study were collected at the time of imaging assessment (N=3,950, Age=62.07+/-7.54, Male=47.47%). Descriptive statistics is presented in supplementary results and Figure S1.

### Educational attainment and household income

Educational attainment and household income phenotypes were self-reported. The details are reported in the study website (http://biobank.ctsu.ox.ac.uk/crystal/refer.cgi?id=100471, http://biobank.ctsu.ox.ac.uk/crystal/refer.cgi?id=100256). Descriptive statistics of educational attainment and household income are presented in supplementary results and Figure S1.

For educational attainment, we used a proxy which was validated in previous studies(Davies et al. 2016; Hagenaars et al. 2016). We created a binary variable was created to indicate whether or not university/college level education was achieved. This proxy covered 4,160 participants (Age=62.20+/-7.56, Male=47.48%).

Household income was determined by the average total income before tax received by the participant's household in five levels (see supplementary methods). This measure had 3,793 non-empty responses (Age=61.98+/-7.57, Male=49.04%).

### Statistical methods

We used the partial correlation matrix as a measurement of functional connectivity. Values in the matrix are normalized correlation coefficients. A higher absolute value means stronger strength of connection, and the sign indicates whether the connection is positive/negative. To enable clearer interpretation of the results, the values of the connections were transformed into connection strength. This was achieved by multiplying the raw connection values with the signs of their mean value. This approach was used in a previous study by Smith *et al.*(2015) (Smith et al. 2015).

Analyses were performed in the following sequence: (1) A whole-brain analysis of the association between cognitive performance (VNR) and resting-state functional connectivity using the connectivity matrix derived from high-resolution parcellation. (2) Two separate whole-brain analyses on educational attainment and household income, respectively. (3) We then performed correlation analyses on the global functional connections predicted by the three phenotypic variables over all the connections in the 55*55 matrix over the whole brain, that is, testing whether the standardized effect sizes for the VNR score's link to functional connections were correlated with the corresponding effect sizes for educational attainment and household income. Two correlation analyses were then performed respectively on (a) the effect sizes of cognitive performance and educational attainment and (b) the effect sizes of cognitive performance and household income. (4) Network of interest. This method has been validated in various previous studies as well as in the protocol paper for UK Biobank imaging project (Reineberg et al. 2015; Miller et al. 2016).

The associations between brain connections and cognitive performance, educational attainment, and household income were tested by separate models using the linear GLM function in R (https://stat.ethz.ch/R-manual/R-devel/library/stats/html/glm.html). Each trait was set as the independent variable in their individual models, and the connectivity matrix (high/low-resolution matrices, 55*55 for whole-brain analysis and the selected networks in 21*21 matrix for network-of-interest analysis) was set as the dependent variable. All of the models were adjusted for age, age$^2$, and sex.

False Discovery Rate (FDR) (Benjamini et al. 1995) correction was applied over each set of test over the whole brain as a unit ($N_{test}$=1,485 for 55*55 matrix, $N_{test}$=16 for connections of bulk networks) using the p.adjust function in R setting $q<0.05$ for significance level (https://stat.ethz.ch/R-manual/R-devel/library/stats/html/p.adjust.html). All β-values reported in the results are standardized effect sizes.

## 2.4 Results

### Whole-brain test of the association of cognitive performance with functional connectivity

A group-ICA was applied to parcellate the whole brain into 55 components, and the pair-wise functional connectivity between the components was estimated using FSLnets (http://fsl.fmrib.ox.ac.uk/fsl/fslwiki/FSLNets). The 55*55 partial correlation matrix was used for whole-brain analysis. To enable clearer interpretation of the results, the values of the connections were transformed into connection strength(Smith et al. 2015).

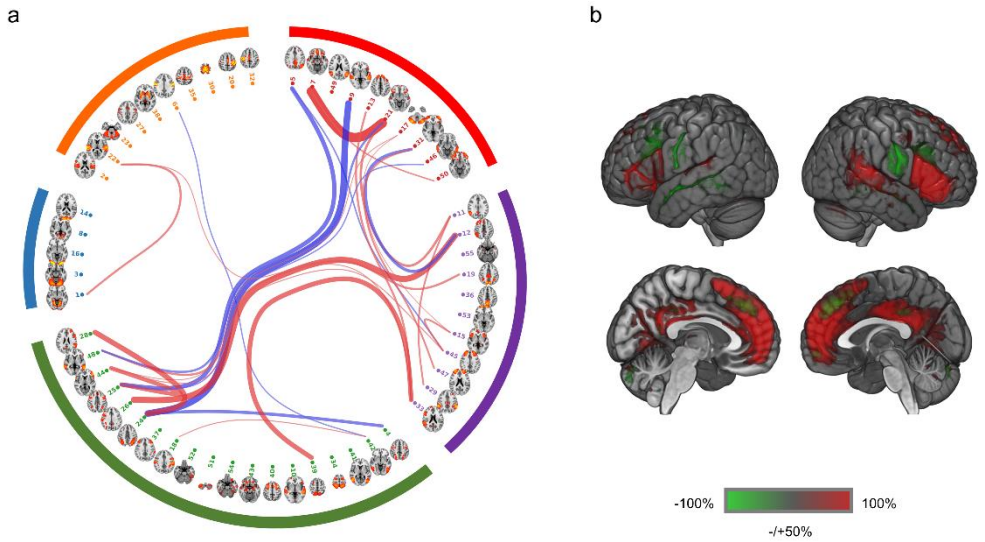


Figure 1. (A) Connections that showed significant associations with cognitive performance. The ICA components were clustered into five categories according to the group-mean full correlation matrix for better illustration and interpretation of the results. This clustering gives a data-driven, gross overview of the structure of the components, consistent with previous studies (ref 26 and 30). The clusters roughly represent the resting state networks (RSNs) of: default mode network (red), extended default mode network and cingulo-opercular network (purple), executive control and attention network (green), visual network (blue) and sensorimotor network (orange). Red lines are the connections where strength was positively associated with cognitive performance; blue lines denote negative associations with cognitive performance. The width of lines indicates the effect sizes of the associations between connection strength and cognitive performance (bigger width indicates a larger absolute effect size). The significant connections were mostly involved in the categories of default mode network, executive control/attention network and cingulo-opercular network. (B) The spatial map of regions involved with connections in (A). The spatial maps for the ICA nodes that involved in the significant connections were multiplied by their effect sizes, then the spatial map in (B) was generated by summing up the weighted maps. To better illustrate the regions involving in significant connections, a threshold of 50% of the highest intensity was applied, so the regions with intensity higher than the threshold would show

on the map.

Better performance in VNR was significantly associated with 26 connections (absolute β ranged from 0.054 to 0.097, all $p_{corrected}<0.05$, $p_{uncorrected}<6.73\times10^{-4}$, see Supplementary Table S1). These include 18 connections that showed higher strength with higher VNR, and 8 connections that had lower strength of connection in people with higher VNR (Supplementary Table S1). The 18 connections largely involved the DMN, which includes bilateral posterior cingulate cortex (PCC), bilateral medial prefrontal cortex (PFC) and right temporal-parietal junction (TPJ), see Figure 1. Additional areas of right inferior PFC, dorsal anterior cingulate cortex (ACC) bilateral anterior insula and visual cortex were also involved. The connections that were weaker with better cognitive performance included bilateral lateral postcentral gyrus and superior ACC (Figure 1).

We then conducted permutation test on an updated sample of unrelated people (N=7,749). Half-sized samples (N=3,572) were selected and tested the distributions of the p values for the significant connections found in our initial findings. After 1,000 times of randomly selecting half of our sample, conducting analyses on them, and then compared the distributions of p values for the significant connections with the p values for the rest of connections (see supplementary materials). Two connections' p values were higher ($t>6.95$, $p<6.62\times10^{-12}$), and all others' were lower, which takes up 92.3% of the connections that were significant in the initial findings (all t ranged from -1076.88 to -2.21, all $p<0.028$, see in Appendix 4: Figure S7).

**Whole-brain tests on the association of educational attainment and household income with functional connectivity**

There were 33 connections that showed significant associations with educational attainment (absolute β ranged from 0.103 to 0.161, all $p_{corrected}<0.05$, $p_{uncorrected}<8.53\times10^{-4}$ see Supplementary Table S2). Of these, the strength of 21 connections was stronger with higher educational attainment, whereas 12 were weaker. The regions involved in connections that were stronger with better educational attainment included regions in DMN and dlPFC. A large area of ACC was also involved. Connections that were weaker with higher educational attainment were located in the Inferior part of PCC and lingual gyrus (Figure 2).

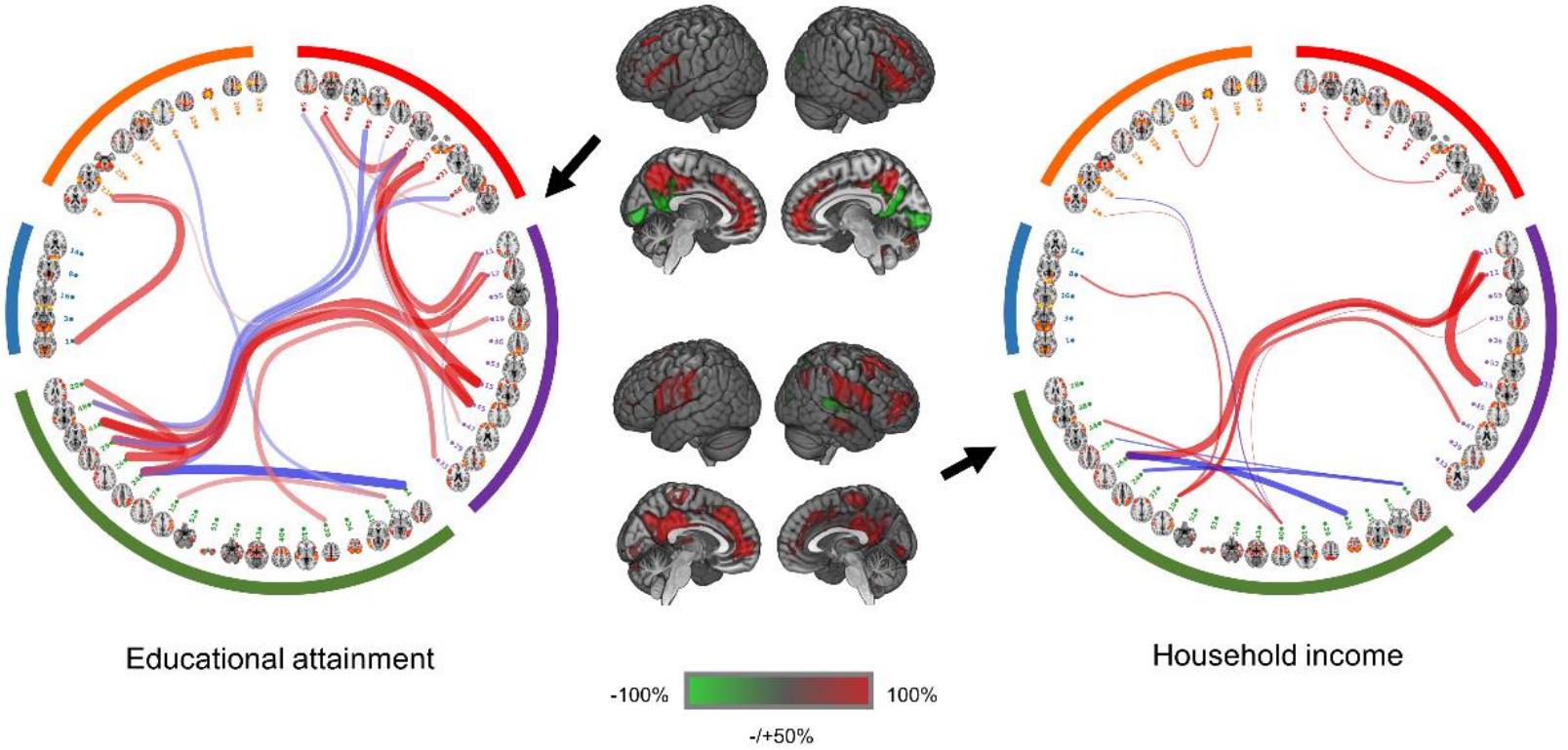


Figure 2. The connections that showed significant associations with educational attainment and household income. Red lines are the connections of which the strength was positively associated with cognitive performance, and the blue lines are the ones having negative associations. The width of lines indicates the effect sizes of the strength of the connections, see the legend of Figure 1. The categorisation of components of brain regions in the circular brain network illustration is identical with Figure 1. Again like Figure 1, A threshold of 50% of the highest value was applied for better illustration of the projection of brain regions on MNI template.

For household income, 15 connections were significant, 11 of which were stronger with higher household income and 4 showed weaker connections (absolute β ranged from 0.060 to 0.082, all $p_{corrected}<0.05$, $p_{uncorrected}<4.27\times10^{-4}$ Appendix 4: Table S3). The regions of the connections that were stronger for higher household income again fell in similar regions as in tests of educational attainment and cognitive performance, which included PCC, medial PFC, ventral lateral PFC and dorsal lateral PFC (Figure 2). The areas that showed weaker connections for higher household income were smaller, which mainly included superior temporal lobe. Full lists of regions for the above results are presented in Table S4.

The spatial maps for the results of cognitive performance in VNR, educational attainment, and household income overlapped substantially (Figures 2 and 3). By performing correlation analysis at the standardized effect sizes of the whole brain (see Methods, Statistical methods), we found a correlation of r=0.47 (df=1,483, $p<2X10^{-16}$) between the global effect sizes for cognitive performance and educational attainment. The correlation between the effect sizes of cognitive performance and household income was r=0.38 (df=1,483, $p<2X10^{-16}$) (Figure 3).

Similar to the permutation test performed on VNR, the distributions of p values for 93.3% of the significant connections found in for educational attainment were lower than the mean p value for the rest of connections (all t ranged from -1429.77 to 11.54, all $p<4.22\times10^{-4}$, Figure S8) and all for household income were lower (all t ranged from -704.07 to -5.49, all $p<4.97\times10^{-8}$, see Appendix 4: Figure S9).

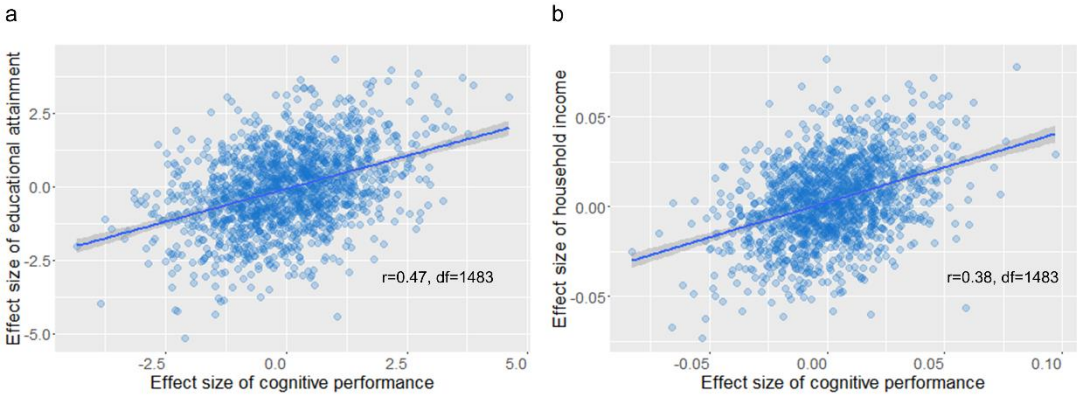


Figure 3. Correlations of the effect sizes of (A) cognitive performance and educational attainment and (B) cognitive performance and household income on whole-brain connections using 55*55 partial correlation matrix as the proxy. Regression line with 95% confident intervals (shaded) are shown.

### Network-of-interest (NOI) test on VNR, educational attainment, and household income

The whole-brain tests showed that the connections associated with cognitive performance in VNR, educational attainment and household income were predominantly located within the DMN (covering medial PFC, PCC and TPJ), cingulo-opecular network (CON, covering ventral lateral PFC, and dorsal ACC) and frontoparietal network (FPN, covering dorsal lateral PFC and posterior parietal cortex). Therefore, DMN, CON, and FPN were selected as NOI from another group-ICA of lower resolution so these networks could be fully extracted (see Methods). The pairwise between-network coupling of these five networks (DMN was unilateral, and CON and FPN were separately extracted on each hemisphere) were tested to determine their association with cognitive performance, educational attainment, and/or household income. The above components can be viewed in Figure S2. The valence and values for the coupling of the above NOI were shown in Table 1. Similar with the analyses at whole-brain connectivity, the values of the connections were transformed into coupling strength before they were fed into the model.

There were 8 coupling between functional networks significantly associated with VNR performance out of 10 connections tested (all $p_{corrected}<0.05$, $p_{uncorrected}<0.035$. βreported below). For educational attainment, 3 connections were significant, and none was found significantly associated with household income.

For the coupling between DMN and networks involving with lateral PFC, better VNR performance was associated with stronger positive connections between DMN and bilateral CON (stronger positive connection between DMN and left CON: β=0.061, $p_{corrected}=6.7X10^{-3}$; weaker negative connection of DMN with right CON: β=-0.045, $p_{corrected}=0.011$).

On the other hand, greater strength of coupling within the networks involving with lateral PFC was significantly associated with better cognitive performance. Stronger positive CON-FPN connection was also associated with higher VNR score. In the same hemisphere, people with better cognitive performance showed stronger positive CON-FPN connections (left CON-left FPN: β=0.044, $p_{corrected}=0.011$; right CON-right FPN: β=0.051, $p_{corrected}=0.005$), whilst across hemispheres, stronger negative CON-FPN connections were higher (left CON-right FPN: β=0.034, $p_{corrected}=0.044$; right CON-left FPN: β=0.043, $p_{corrected}=0.011$). Finally, higher VNR scores were associated with weaker cross-hemisphere connections between the homotopic network components (left-right FPN: β=-0.040, $p_{corrected}=0.018$. left-right CON: β=-0.063, $p_{corrected}=6.7X10^{-4}$). The above results are presented in Table 1 and Appendix 4: Figure S3.

Educational attainment and household income had generally smaller associations with network coupling, and fewer significant connections were found. People with higher educational attainment showed a stronger positive connection between DMN and right FPN (β=0.104, $p_{corrected}=0.004$) and lower positive connection between DMN and right CON (β=-0.149, $p_{corrected}=1.99X10^{-5}$). A stronger positive connection between right FPN and CON was associated with better educational attainment (β=0.086, $p_{corrected}=6.24X10^{-3}$). No significant association between household income and the coupling of networks was found (all $p_{corrected}>0.124$).

For the connections that were significant for both cognitive performance and educational attainment, we performed mediation analysis using Lavaan in R to test whether the effect between educational attainment and bulk network connections were mediated by cognitive performance (Appendix 4: Figure S6). Network connectivity was set as the predictor, and cognitive performance as the dependent variable. Educational

attainment was specified as the mediator. We found that the association between rFPN-rCON and rCON-DMN connectivity and educational attainment was mediated by cognitive performance (18.4% and 76.2% of direct path mediated by indirect path respectively for each model, CFI = TLI = 1, see Appendix 4: Figure S6).

Table 1. The significant associations between the connections of networks of interest and cognitive performance (verbal-numerical reasoning) and educational attainment. The values of connections were transformed into strength before conducting the analyses, by multiplying the connection values with the signs of their means. This approach was consistent with ref 28. Mean values and their 95% confident intervals of connections reported here are the values before being transformed into strength.

**Verbal-Numerical Reasoning**

| Type | Connections | Beta | Standard error | t.value | p | pcorrected | Mean value of connection | 95% confident interval of value of connection | |
|---|---|---|---|---|---|---|---|---|---|
| inter-hemisphere | left FPN - right FPN | -0.040 | 0.016 | -2.493 | 1.27E-02 | 0.018 | 1.156 | 1.127 | 1.185 |
| | right CON - left CON | -0.063 | 0.016 | -3.923 | 8.89E-05 | 6.67E-04 | 0.379 | 0.356 | 0.402 |
| CON - FPN | left CON - right FPN | 0.034 | 0.016 | -2.106 | 3.52E-02 | 0.044 | -1.359 | -1.387 | -1.330 |
| | right CON - left FPN | 0.043 | 0.016 | -2.714 | 6.68E-03 | 0.011 | -2.088 | -2.122 | -2.054 |
| | left CON - left FPN | 0.044 | 0.016 | 2.732 | 6.33E-03 | 0.011 | 1.043 | 1.018 | 1.067 |
| | right CON - right FPN | 0.051 | 0.016 | 3.200 | 1.38E-03 | 0.005 | 0.648 | 0.620 | 0.676 |
| DMN-related | left CON - DMN | 0.061 | 0.016 | 3.824 | 1.33E-04 | 6.67E-04 | 0.675 | 0.652 | 0.698 |
| | right CON - DMN | -0.045 | 0.016 | 2.797 | 5.18E-03 | 0.011 | -0.275 | -0.300 | -0.250 |

**Educational attainment**

| Type | Connections | Beta | Standard error | t.value | p | pcorrected | Mean value of connection | 95% CI of value of connection | |
|---|---|---|---|---|---|---|---|---|---|
| CON - FPN | right CON - right FPN | 0.086 | 0.031 | 2.736 | 6.24E-03 | 0.021 | 0.648 | 0.620 | 0.676 |
| DMN-related | right FPN - DMN | 0.104 | 0.031 | -3.335 | 8.59E-04 | 0.004 | -0.710 | -0.738 | -0.682 |
| | right CON - DMN | -0.149 | 0.031 | 4.761 | 1.99E-06 | 1.99E-05 | -0.275 | -0.300 | -0.250 |

## 2.5 Discussion

In the present study, we utilized a large population-based sample of ~4,000 participants and found that strength of connections involved with DMN regions, anterior insula, dorsal lateral prefrontal cortex in FPN and inferior frontal gyrus in CON were positively associated with performance in a verbal-numerical reasoning test. The brain regions associated with cognitive performance also overlapped with those related to educational attainment and household income. These above results were validated in a bigger updated sample of N>7,000 people. For cognitive performance in particular, better cognitive functioning was marked by a more strongly positive DMN-CON connection, weaker cross-hemisphere connections of the left-right CON and left-right FPN, and stronger CON-FPN connections.

We used a large sample and provided evidence that, in addition to the broadly suggested idea of lateral PFC, which involves dorsal lateral prefrontal cortex in FPN and inferior frontal gyrus in CON, playing a crucial role in cognitive processing, DMN was also associated with cognitive performance (β of connections positively associated with cognitive ability ranged from 0.054 to 0.097) (Bunge et al. 2005; Kievit et al. 2014; Parr et al. 2015). Previous studies showed that DMN serves as a hub for the whole brain (Raichle 2015). In comparison with other functional networks, DMN showed a higher metabolic rate in resting-state (Raichle et al. 2001), stronger connections with the rest of the whole brain in both task-free and task-engaging situations (Buckner et al. 2009), and a key role in maintaining basic levels of wakefulness/alertness in the brain (Sämann et al. 2011). Higher efficiency within the DMN was reported to be associated with various cognitive functions, including memory (Shapira-Lichter et al. 2013), theory of mind (Spreng and Grady 2010), working memory (Sambataro et al. 2010), and performance in general intelligence tests (van den Heuvel et al. 2009). The high-level cognitive abilities mentioned above often involve the activity of multiple, spatially distant brain regions (Corbetta et al. 2008; Shapira-Lichter et al. 2013).

Therefore the DMN, as a communicative hub, contributes to functional efficiency over the whole brain (van den Heuvel et al. 2009), potentially producing better integration and cooperation in core regions that are important for cognitive tasks.

Additionally, the present study tested the coupling between networks of interest. Stronger positive DMN-CON coupling was associated with better cognitive ability (absolute $\beta>0.045$). In addition to the well-recognised task-positive lateral prefrontal cortex (therefore anti-correlated with the DMN), our findings in this large single-scanner sample lend substantial credence to increasing evidence that the CON itself (Fox et al. 2006; Vossel et al. 2014), and its positive coupling with the DMN in both resting-state (Anticevic et al. 2012) and event-related studies (Bluhm et al. 2011)) is highly pertinent for important aspects of cognitive performance. The role of the CON was related to maintaining task-engaging status (Fox et al. 2006; Petersen and Posner 2012) and flexibly switching between the DMN and central executive network based on experimental context (Cocchi et al. 2013; Goulden et al. 2014). The experimental context in which CON and DMN were found to be simultaneously activated was often about goal-directed cognition (Cocchi et al. 2013), which involves self-driven retrieval of memory or learned experience and self-regulatory planning (Spreng et al. 2010). As the DMN is associated with self-referential processing (Raichle 2015) and self-driven cognition like retrieval of personal experience (Kamourieh et al. 2015) and planning (Spreng et al. 2010; Gerlach et al. 2011), positive coupling of the CON and DMN may indicate recruitment of self-referential and goal-oriented activity. Therefore successful DMN-CON coupling may be useful in maintaining internal mechanisms that support cognitive processing and long-term learning (Cocchi et al. 2013).

The connections between networks involving lateral PFC showed that better cognitive performance was associated with stronger CON-FPN connections (absolute $\beta>0.034$). This result is consistent with previous structural and functional findings that support the key role of prefrontal areas on cognitive performance (Higgins et al. 2007; Kievit et al.

2014). We also found that better cognitive performance was related to between-hemisphere dissociation within networks (absolute β>0.040). Whereas this is the first time to our knowledge that this has been examined in a study of a large sample, such reduced structural connection between the left and right lateral PFC has been observed in schizophrenic patients with impaired cognitive performance(Wheeler et al. 2014). More lateralization of the brain is associated with better cognitive performance (Toga and Thompson 2003; Gotts et al. 2013), whereas, less lateralization, especially in prefrontal cortex, is related with reduced specialization of brain functions across hemispheres, therefore the advantageous anti-correlated connection we report here potentially denotes increased brain efficiency (Toga and Thompson 2003; Hyodo et al. 2016).

The whole-brain connection map for cognitive performance overlaps substantially with those from educational attainment and household income. Further analyses showed that there were global correlations of cognitive ability with educational attainment (r=0.47) and with household income (r=0.38). GWAS studies found that cognitive performance and educational attainment share a similar genetic architecture (r=0.906) (Marioni et al. 2014; Hagenaars et al. 2016). There was, in particular, an overlapping finding for educational attainment and cognitive performance in rFPN-rCON connection, and rCON-DMN connection. We found that cognitive performance significant mediated the association between NOI connectivity and educational attainment (Figure S6). The right-hemisphere connection for the two prefrontal networks (FPN and CON) may therefore reveal the association between education and executive control abilities, which was shows consistently associated with right lateral prefrontal cortex (Mohr et al. 2016). Early life intelligence (relatively stable across the life-course (Deary et al. 2012; Deary 2014)) and educational attainment show partially overlapping associations with some structural brain measures in older age (Cox, Dickie, et al. 2016). Taken together, one interpretation of these data is that the functional hallmarks of a more ‘intelligent’ and better-educated brain are related to

income by virtue of these temporally preceding factors. It could equally be the case that income confers additional lifestyle benefits that also influence these cerebral characteristics; the causal direction that gives rise to the highly overlapping functional connectivity reported here would be more adequately addressed with longitudinal multi-modal data.

A limitation for the current study is that the verbal-numerical reasoning test, as a brief measure, may not confer the same level of reflection on general cognitive ability as other longer, in depth general cognitive measures. The test-retest reliability was moderate, mainly because rather than the usual short time period between test and retest, this was performed in UK Biobank between 2-5 years which may contribute to the relatively low value. However, as previous studies found that verbal-numerical reasoning shared significant genetic and phenotypic correlation with the latent component of general cognitive performance (Davies et al. 2016; Hagenaars et al. 2016), it therefore confers adequate representativeness of general cognitive ability. Another limitation is that the sample covers an older age range, and there is potential bias to healthy, better-educated people. A notable strength of the present study is that we used a large sample, providing compelling evidence that both dorsal prefrontal areas and DMN were associated with cognitive ability, educational attainment and household income. To disentangle how multiple networks involved in the cognitive ability, we examined functional connectivity by estimating connections between brain components derived in two different resolutions, giving us another strength of studying both the connections over the whole brain and the connections of bulk intrinsic functional networks within a single dataset. Finally, in addition to visual checking of overlapping regions of the significant connections, we statistically compared the functional connectivity associated with cognitive ability, educational attainment and household income over the whole brain, giving a magnitude of neural associations among them.

### 2.6 Conclusion

The present study used a large, population-based sample, who provided multi-dimensional rs-fMRI data, and found substantial evidence for functional neural associations cognitive ability (verbal-numerical reasoning) both in whole-brain dynamics and the coupling for intrinsic functional networks. The findings also characterized the degree of rs-fMRI overlap between cognitive ability and educational and socioeconomic level, providing evidence of the overlapping biological associations on the neurological level.

## 3 Chapter conclusion

The main finding of the study is the huge neurobiological overlap across cognition, educational attainment, and household income. The big sample also allowed further permutation tests validated the results in the updated data that contained a different set of 4,000 people. The results showed the importance of both the central executive system and the default mode network.

# Chapter 6: Discussion

The present thesis investigated the relationship between neurobiological traits and MDD in four aspects: MDD case-control differences, neurobiological associations with longitudinal depressive symptoms, with polygenic risk for depression (in association with other wider traits), and with depression related traits (such as cognition). Very large samples from the on-going UK Biobank imaging project were used (initially n= 5,000, then 12,000 people with further releases of data).

## 1 Summary of main findings in the present thesis

### 1.1 white matter microstructure in thalamic radiations is a key marker for MDD

One of the main findings in this thesis was the repeated implication of thalamic connections in association with MDD. The thesis found lower general FA in thalamic radiations in a large sample of MDD cases compared with controls in chapter 2. Higher general MD in thalamic radiations was associated with greater variability of depressive symptoms, a steeper slope of worsening trajectory of depressive conditions in chapter 3, and higher polygenic risk of depression in chapter 4. There was a significant mediation effect of general MD in thalamic radiations between depression polygenic risk and subjective well-being, and the number of psychiatric conditions diagnosed.

The thalamus is directly associated with negative emotional processing and decision making in goal-directed context and is an important part of the wider limbic system. Compared with other subcortical regions, the thalamus has its special role, because it is highly associated with various behavioural patterns that show robust relations to depression. For example, the thalamus is a key region that is sensitive to sleep and causally mediates the effect of sleep deprivation to the activity in anatomically downstream regions like the brainstem (Krause et al. 2017), and the firing activities of

the region is correlated with the transition of sleep phases (Gent et al. 2018). It is also highly associated with wakefulness and consciousness (Krause et al. 2017). It is a main amplifier of pain (Fischer and Waxman 2010) and highly associated with various of addictions (Sullivan et al. 2003; Almeida et al. 2008; James and Dayas 2013).

One reason why it is so broadly associated with various complex traits relevant to depression originates back to its anatomic position as a hub. Thalamus is located at the top of the brainstem, with axons generating from dorsal thalamus to amygdala, striatum and hippocampus, and a rich amount of fibres projecting from thalamus to the anterior, superior and posterior cerebral cortex (Sullivan et al. 2003). The special location of the thalamus makes it a hub of the limbic system and the bridge from the limbic system to the cortex, especially to prefrontal cortex where emotion regulation is involved. Depression is a complex trait, with additive effects contributed by abnormal brain cognitive and emotional processes, disrupted HPA-axis activity, genetic risks, and various interacting effects from the environment such as traumas, parenting styles and lack of education and social support. The impacts of these wide ranges of complex and possibly antagonistic factors being associated with thalamus and thalamocortical connection, the so-called ‘grand incoming station’ which bears the additive effects from the global interactions in the brain, is therefore not completely unexpected. The absence of associations of depression with other brain regions/connections may due to the counterbalancing effect of various factors that contribute to depression, or even subtypes of depression of which the neurobiological associations may possibly show opposite effects (Kohler et al. 2010). The important role of thalamic radiations being found is largely due to the generous sample sizes, which not only allow for heterogeneity, as a big sample is able to cover a large range of population-based cases, and the heterogeneity can be overcome by statistic power, and therefore the most consistent neurobiological associations with depression can be found.

### 1.2 White matter microstructural alterations were associated with not just current symptoms, but also cross-sectional symptomology such as variability, mean depressive level and longitudinal trajectory, as well as polygenic risk

Various traits have been tested, including case-control difference, variability and longitudinal progression of depression, as well as polygenic risk. Although these traits are self-correlated, they differ in which white matter tracts are associated with. Here the insights of neurobiological heterogeneity of different depression-related traits are summarised.

First, the largest amount of significant findings were found in the associations between white matter microstructure, measured by mean diffusivity (MD), and depressive symptoms at the imaging assessment, rather than cross-sectional and lifetime traits. Many studies have found white matter microstructural changes related to current depressive symptoms, however, comparing cross-sectional and longitudinal measures is rare. The reason why we found the largest scale of associations in MD may due to that this measure is sensitive to myelination. This notion was supported by NODDI findings in chapter 3, where ICVF showed a similarly large scale of associations with current depressive symptoms. ICVF is a measure of neurite density, highly correlated with myelin development. These indicate that (1) current symptom is an unneglectable contributor to white matter microstructural variation, and (2) it is important to consider variations of depressive symptoms assessed at different occasions, which can potentially contribute to heterogeneity or different levels of severity.

Second, white matter microstructure in MD can be associated with lifetime and cross-sectional measures of depression or depressive symptoms. Although current symptoms of depression showed the association with white matter structure in the largest number of tracts, white matter microstructure did not associate with temporal

depressive status only. Along with the findings from a recent GWAS study on UK Biobank imaging phenotypes, revealing that white matter probabilistic tractography has a high heritability of around 20-60% (Bycroft et al. 2017a), these together indicate that there is a potential of looking for genetic overlap between psychiatric traits and brain imaging phenotypes.

### 1.3 Novel associations found between polygenic risk of depression and resting-state connectivity

Resting-state connectivity has been believed to be a more transient measure of the brain's network. However, recent findings suggest that some resting-state connectivity and slow-frequency amplitude of the blood-oxygen-level dependent (BOLD) signal can have significant heritability, comparable to that of structural measures like white matter microstructure and subcortical volumes (Bycroft et al. 2017a). The unexpectedly high heritability is likely due to the discrepancy between the former understanding of the flexibility of BOLD signal and what temporal correlations of the BOLD signal in resting state actually mean in terms of its neurobiological basis. Studies suggest that functional connectivity, especially in important networks such as the default mode, salience and executive control networks, is formed by joint efforts from white matter linkage and a shared metabolic mechanism (Greicius et al. 2009; Bero et al. 2011). For instance, Bero et al. found that a protein called amyloid β may be the by-product of the metabolic activities in the default mode network, as the activity of the network showed a causal impact on its concentration (Bero et al. 2011). Another study by Hahn et al. showed that serotonin-1A receptors explained a significant amount of individual variability of the synchronised activity in the default mode network (Hahn et al. 2012). These indicate that resting-state connectivity is not merely an external outcome of white matter structures, but rather a different set of measures, of which the biological mechanism is yet to be disentangled.

The difference between white matter microstructure and resting-state connectivity is also shown in our results. Decreased white matter microstructural integrity was in general associated with higher polygenic risk of depression. However, there are several regions where hyperconnectivity on resting state is associated with higher polygenic risk. One important finding is that the hyper-connectivity in default mode network was found associated with higher polygenic risk for depression. This is consistent with previous studies that found depressive patients showed hyperactivity or stronger connectivity within the default mode network. The connectivity in the default mode network has a potentially non-linear relationship with cognitive performance and mental health. Lack of activity in the work has been found associated with reduced wakefulness and global connectivity (Greicius et al. 2008; Krause et al. 2017), whereas extensive strength or duration of the activity in the default mode network may cause a higher concentration of interstitial fluid amyloid-β which is associated with atrophy (Bero et al. 2011). More studies on the causes of individual differences in resting-state network are needed for a clearer conclusion.

### 1.4 Depression is likely to be mainly a "connectome-driven" disorder

Schmaal et al. using ENIGMA data found that the largest difference between MDD cases versus controls was shown in the volume of hippocampus (Schmaal et al. 2016). However, in our findings, associations for subcortical volumes were absent for all depression-related measures, including current symptoms and cross-sectional depressive symptoms. This may due to a relatively older age range (age ranged from 40 to 75 years). In other studies that recruited middle-aged participants, they also found that subcortical volumetric differences were null (see Discussion in Chapter 2). Despite that the results are different in subcortical differences between ENIGMA and UK Biobank, structural and functional connectivity showed much larger effect sizes compared to subcortical volumes. Associations presented in white matter microstructure and resting-state connectivity for various depression-related traits in

UK Biobank have Cohen's d at around 0.23, and standardised regression coefficients were around 0.025 to 0.036. The Cohen's d found for subcortical volumes in the ENIGMA sample was 0.15 for the only significant MDD case-control difference shown in the hippocampus (Schmaal et al. 2016). An alternative explanation for the different effect sizes could be that ENIGMA in generally still has larger samples compared to UK Biobank imaging project, therefore the effect sizes derived from UK Biobank imaging data may be comparatively inflated. However, according to our findings employing from the first release of around 5,000 people to the latest release of around 12,000 people, the regression coefficients for significant linear associations stably remained around 0.025 to 0.03, regardless of the changes of the sample structure and changes in the standard deviations. If the effect sizes estimated by UK Biobank imaging project was inflated, it is more likely to observe large variations between sample releases, which is contradictory with what we found. Hence, there could be a truly larger association of depression with functional/structural connectivity than with subcortical volumes. However, a more definite conclusion should be drawn based on a replication study when UK Biobank collected similar-sized sample to ENIGMA, or that ENIGMA or other large cohorts reveal similar advantageous correlation of depression with structural connectivity.

Another contribution from the studies in the present thesis is that they give a robust estimation of effect sizes for the associations between functional/structural connectivity and depressive symptoms in a population-based sample. Large variance explained can be achieved due to sample bias, chance, or a combination of both (Wray et al. 2013). The effect sizes estimated in the present thesis using very large cohort data therefore to provide tools for power estimation of new studies for which the sample size needs to be pre-defined.

## 2 Limitations and indications of future work

One limitation for most of the phenotypic studies conducted in the present thesis is the depth of phenotyping. MDD definitions and depressive symptoms were assessed mainly based on self-reported questionnaires, which are in general shorter than other studies (e.g. PHQ-4 instead of PHQ-9 used for self-assessment of depression in the National Health Service of the UK, and broad definition of depression was acquired based on a simple self-declaration of whether had depression or not). Cognitive performance in verbal-numeric reasoning was assessed using a brief questionnaire consisting of 12 questions. The rationale is that the depth of phenotyping and the scale of phenotypes/sample sizes are two counterbalancing factors. A reasonable balance between the two should be able to allow for a large sample to be collected, therefore to overcome the noise introduced by the coarseness of phenotypes, as long as the phenotypes show acceptable agreement with traditional assessments. Acceptably rough phenotyping, though the depth was compromised to some extent, allows for more space to fit in more assessments so that data-driven association tests as in the PheWAS in chapter 4 can be conducted. It means that it is possible to have a large scale of people assessed, especially for longitudinal assessments, which is important for heterogeneous conditions such as depression. Thus, the main concern for the UK Biobank-style phenotypes is whether they deliver a good estimation of traits of interest, in comparison with traditional phenotypes collected in small-sample studies. The answer to this question is affirmative. Genetic correlation between self-declared depression and clinically defined MDD showed a very high correlation with a $r_g$=0.79 (Howard, Adams, Shirali, et al. 2018), and the brief assessment of depressive symptoms from PHQ-4 showed very high correlation with the full questionnaire PHQ-9 with an AUC (area under the curve) at 0.8 (Khubchandani et al. 2016).

Sample selection in UK Biobank has been recently discussed and identified as a limitation. The age range did not cover adolescence and early adulthood since the study was conceived to investigate neurodegenerative disorders. UK Biobank participants typically have higher household income and are relatively better educated compared to the overall UK population. The selection bias is a limitation that needs to be acknowledged and taken into account when interpretations are made. This bias could also be part of the reason for observing the non-conventional prevalence of depression in our sample. Although big data is a cutting-edge trend in the recent academic world, some carefully balanced studies with very specific hypothesis would be extremely helpful for confirming the findings that came from big samples. Having acknowledged this, the opinion of this thesis is that UK Biobank imaging project, as one of the largest neuroimaging projects so far, and is still on-going, has the advantages of very large sample size which still deserves to be appreciated over the potential impact of sample biases.

Another limitation is that larger sample sizes are still needed for studies regarding genetic overlaps between psychiatric illness and neuroimaging phenotypes. Even though over ten thousand people with both in-depth genotyping and neuroimaging phenotyping was un-thinkable within a decade ago, now the hope is given by very large cohorts like UK Biobank, ENIGMA, Human Connectome Project and some new cohorts like the Adolescent Brain Cognitive Development Study. Though it is encouraging to have these large samples, an increase of sample size is still needed for other analyses such as GWAS and Mendelian Randomisation. Especially for Mendelian Randomisation, which is an important tool for making causative inferences, having reliable genetic associations utilising well-powered samples is the primary requirement for conducting such analyses. Enlarging sample sizes by including independent cohorts may also allow us to conduct replication studies, of which the importance has been much more acknowledged in genetic fields, but yet to be more

appreciated in the cross-discipline field that looks at the associations between genetics, neuroimaging and psychiatry.

In the present thesis, medication information has been used to rule out medication effects on the brain. However, medication usage in UK Biobank largely relies on self-reported information. Future possibilities of data linkage between UK Biobank participants and health care services may be able to provide in-depth information that aid analyses of drug effect on the brain and drug efficiency in MDD population.

The fifth limitation is that the neuroimaging phenotypes used in the thesis are bulk illustrations, and more detailed phenotypes such as voxel-wise measures and graph-theory measures may be able to reveal some other biologically meaningful results, and they may potentially have a much higher spatial resolution. However, this does not necessarily mean that the bulk measures used in the thesis are inferior compared to voxel-wise measures. The latter may include more noise introduced by pre-processing steps and may likely to survive at a higher chance.

The findings from the thesis demonstrate the benefits of large sample sizes, particularly for such a heterogeneous condition like MDD. These studies are beginning to suggest reliable deficits associated with MDD condition in thalamocortical connections and resting-state connectivity in the disorder. Taking these findings further, in terms of future work, the current studies could be used to guide further focussed studies on younger individuals. For example, large cohorts such as the Adolescent Brain Cognitive Development study could provide the opportunity to determine whether the neuroimaging differences associated with adult MDD are apparent earlier in life and whether there are any mechanisms that could lead to discoveries of potential early interventions and preventions.

One important future direction may be using the biomarkers found in the present studies, combining machine learning methods to predict MDD status and classify

MDD cases. So far, in the present thesis, key biomarkers have been primarily identified as whole-genome polygenic risk, white matter microstructure in thalamic radiations and superior longitudinal fasciculus, resting-state connectivity in the default-mode network and behavioural patterns that associate with HPA-axis activity. The relationships between these biomarkers – whether they share a common latent component that drives the MDD case-control differences, whether they each provide an additive risk of having MDD, and whether these factors have significant interactions within themselves – remain largely unknown. After more empirical evidence has been provided based on large samples that help disentangle the MDD-related phenotypes, future studies should use these biomarkers to identify subtypes of MDD and related drug response of the identified subgroups. Successful attempts may largely benefit prediction of clinical outcomes, therefore lead to more efficient diagnoses and treatments.

Finally, several questions relating to the biological mechanism of individual differences of brain structure and functions have been raised from the findings from the present thesis. Firstly, how much genetic effect of common genetic variants may have on brain phenotypes, especially the ones that are associated with MDD, is an imminent question that should be soon investigated. The recently released genetic and neuroimaging data from ENIGMA and UK Biobank may allow for genetic association studies to be conducted on brain phenotypes. Studies using these up-to-date datasets have shown that some brain phenotypes have very high SNP heritability up to 80% (Elliott et al. 2018). However, the earliest attempts were mainly made to investigate at a general level about which brain phenotypes are heritable. More sophisticated studies on the heritable features of brain phenotypes should be conducted to find out the localised genetic effects, especially for the disease-related ones. Secondly, the genetic studies on brain phenotypes are restricted to bulk phenotypes, genetic

association studies on high spatial resolution data and graph-theory features in functional and structural MRI data may possess large potentials in future studies.

## 3 General conclusions

MDD poses a major challenge in both genetic and neuroimaging fields, due to its clinical and causal heterogeneity, its complex genetic architecture and interactions of environmental associations. The small effect sizes reported for both imaging and genetic studies suggest a need for better diagnosis and stratification of the disorder. However, before any clear stratifying variable is identified, there is a necessity of using big samples to give robust findings in relation to the liability of the trait. The findings in the present thesis provided evidence of robust neurobiological associations with the presence of depression, depressive symptoms and polygenic risk of depression in white matter microstructure and resting-state connectivity, indicating a shared genetic aetiology of MDD and brain structural/functional connectome. Our findings also indicate that neurobiological alterations may be able to explain variances of behaviour influenced by the genetic risk, which allow more in-depth inferences compared with previous studies finding mere associations. Based on the findings presented in the thesis, finding the causal relationship between the brain's neural networks, genetic risk and environmental factors should be explored in future studies.

# Appendix 1:

# Supplementary Materials of Chapter 2: Subcortical volume and white matter integrity in Major Depressive Disorder (MDD): findings from UK Biobank imaging data

## Method

### MRI acquisition

MRI data were acquired using a Siemens Skyra 3T scanner running VD13A SP4, with a Siemens 32-channel RF receive head coil (https://www.healthcare.siemens.com/magnetic-resonance-imaging). The sequence for the T1-weighted data was a standard 3D MPRAGE scan (Resolution = 1×1×1 mm, FoV = 208×256×256 matrix, TR = 2000ms, TE = 2.01ms, Orientation = sagittal, in-plane acceleration = 2, Filter = prescan-normalise). The overall duration of T1-weighted scanning was 5 minutes. For the DTI data, the diffusion preparation was a standard ("monopolar") Stejskal-Tanner pulse sequence (Resolution = 2×2×2 mm, FoV = 104×104×72 matrix, TR = 3600ms, TE = 92.00ms, SE-EPI with x3 multislice acceleration, in-plane acceleration = off, fat saturation = on). Ten baseline volumes were collected (b = 0 s/mm$^2$), with 50 b=1000 s/mm$^2$ and 50 b=2000s/mm$^2$. The overall duration was 7 minutes.

### MRI preprocessing

The MRI preprocessing of both T1-weighted and DTI data were run by UK Biobank (https://ww5.aievolution.com/hbm1601/index.cfm?do=abs.viewAbs&abs=3664). Images were preprocessed and analysed with the FMRIB Software Library (FSL) (http://www.fmrib.ox.ac.uk/fsl). The IDPs from UK Biobank was released in September, 2016, which covered more than 8000 participants.

To prepare the T1-weighted volumes for standard pre-processing procedures, the face area was removed to maintain anonymity. Following this, gradient distortion

correction was applied for the whole image using BET (Brain Extraction Tool) (Smith 2002) and FLIRT (FMRIB's Linear Image Registration Tool) (Jenkinson and Smith 2001; Jenkinson et al. 2002). The brain was non-linearly warped to the MNI152 "nonlinear 6th generation" standard-space T1-weighted volume template, and the brain area of the images was then extracted using FNIRT (FMRIB's Nonlinear Image Registration Tool) (Andersson et al. 2007a) for segmentation. Segmentation of brain was conducted in two steps: firstly, a tissue-type segmentation using FAST (FMRIB's Automated Segmentation Tool) (Zhang et al. 2001) was applied to extract cerebrospinal fluid, grey matter and white matter; then subcortical structures are extracted using FIRST (FMRIB's Integrated Registration and Segmentation Tool) (Patenaude et al. 2011). The volumes of ICV, thalamus, putamen, pallidum, hippocampus, caudate, brain stem, amygdala and accumbens were calculated for further analysis.

DTI data was initially corrected by the Eddy tool for eddy currents, head motion and outlier-slices (Andersson and Sotiropoulos 2015b), and the following gradient distortion correction was applied in the same way as it is applied on T1-weighted volumes. The corrected b=1000 s/mm$^2$ shell was then used for modeling whole brain water diffusivity biomarkers using DTIFIT, thereby creating the FA (fractional anisotropy) maps.

The DTI data we used was processed by UK biobank using a probabilistic tractography based method. FA maps were initially warped to standard space, and then the BEDPOSTx tool (Bayesian Estimation of Diffusion Parameters Obtained using Sampling Techniques) was used to generate the fibres derived from major anatomical seeds (http://fsl.fmrib.ox.ac.uk/fsl/fslwiki/FDT/UserGuide). This maps 27 major tracts (12 bilateral tracts in both hemispheres and 3 tracts that went across brain) by utilizing the standard-space start/stop ROI masks defined by AutoPtx (De Groot et al. 2013).

## Statistical methods

We used lme function in nlme package of R (Bliese 2016) to conduct repeated-effect linear model on the structures with bilateral measures, as hemisphere was a within-subject variable, whereas all other covariates and the variable of interest are between-subject variables. The general linear model of unilateral structures was conducted using the default glm function of R. Choices of covariates were based on the recent meta-analytic studies on big samples of psychiatric illnesses (Schmaal et al. 2016; van Erp et al. 2016).

## Participants

The acquisition and preprocessing were conducted by UK biobank. 5724 participants finished T1 image acquisition and the scans were preprocessed, while 4941 participants' DTI images were acquired and preprocessed. After the outliers were excluded, there were 5403 with T1 images and 4594 with DTI images. Outlier exclusion was conducted within the overall sample with according imaging data available, therefore this step of exclusion is unbiased against the final samples which were consisted of only MDD cases and healthy controls. For transparency, the results of the main models that tested the effect of MDD definitions, with or without excluding outliers, were both presented in the tables below (Table S4, S5, S7, S8). Then the participants that had a diagnosis of Parkinson's disease, bipolar disorder, multiple personality disorder, schizophrenia, autism or intellectual disability were also excluded.

After the applying the filters described above, cases and controls for MDD definitions were chosen according to their self-reported depressive symptoms and hospital admission history (see below in Method, MDD definitions). Details of the sample and exclusions were listed in Table S3.

## MDD definitions

The putative MDD category summarized by Smith et al. was based on depressive symptoms and hospital admission history reported by participants. Self-report symptoms included whether they had ever been depressed or had anhedonia, whether they experienced a depressive period of over two weeks, and how many depressive episodes they had. Hospital admission history was also self-reported by answering whether they have seen a GP or psychiatrist for nerves, anxiety, tension or depression. As described in Figure S4, people were categorized into four groups: single episode major depression, recurrent major depression (moderate), recurrent major depression (severe) and absent of depression. These MDD categories were tested over phenotypes of lifestyle, demographics, social states, overall health condition and emotion disorder related personality. The results showed similar patterns with clinical ascertained samples (Smith et al. 2013). The tests were conducted in the sample of 172,751 participants of UK Biobank. Though participants who had imaging assessments were recruited within this pretested sample, we compared neuroticism level between cases and controls in the current, smaller sample to validate the MDD definitions we used as below.

In addition to their MDD categories, we added another category as unspecified group. They reported depressive symptoms or relative hospital admission history, but did not meet the criteria to be categorized as MDD. They either reported of having had at least two weeks duration of low mood or anhedonia, and at least 2 episodes of depression, but had not seen a GP/psychiatrist; or reported of having had seen a GP/psychiatrist and had at least two weeks duration of low mood or anhedonia, but didn't know episodes or duration.

For the principal definition of MDD, cases included recurrent and single-episode MDD, and controls included only those who were identified of being depression absent. For the definition of recurrent MDD, cases were only recurrent MDD, whilst the controls included the rest of the categories, which included single-episode MDD, depression

absent participants and participants who weren't identified as MDD but self-reported of having had depressive symptoms or had hospital admission history of seeing a GP or a psychiatrist for nerves, anxiety, depression. See Figure S4. The participants who did not respond to any of the questions used as criteria for categorization were excluded.

In the sample with T1-weighted data, MDD cases have significantly higher neuroticism level in both principal and recurrent MDD definition, $\beta = 0.678$, $p < 2e\text{-}16$; $\beta = 0.555$, $p = 2e\text{-}16$ respectively. The differences remained the same if age, age$^2$, sex were set as covariates, $\beta = 0.600$, $p < 2e\text{-}16$; $\beta = 0.480$, $p = 2.84e\text{-}13$. Comparisons were again conducted within the sample with DTI data. They similarly showed that cases were more neurotic than controls in both definitions, with or without controlling sex and age, $\beta$s = 0.550~0.717, ps < 7.36e-16. The above neuroticism scores were calculated using the same method in the prevalence study by Smith et al (Smith et al. 2013).

We tested separately in both MDD definitions on group differences of gender, age and level of education between cases and controls. Level of education was coded as below: A levels/AS levels = 6, O levels/GCSEs = 5, CSEs = 4, NVQ or HND or HNC = 3, Other qualifications =2, No respond/refuse to answer = 1. Gender differences were significant in both definitions ($\chi^2_{probable} = 35.43$, df = 1, $p_{probable} = 2.64e\text{-}9$; $\chi^2_{recurrent} = 4.74$, df = 1, $p_{recurrent} = 0.030$ respectively for probable and recurrent definition for T1-weighted sample. $\chi^2_{probable} = 30.90$, df = 1, $p_{probable} = 2.72e\text{-}8$; $\chi^2_{recurrent} = 12.90$, df = 1, $p_{recurrent} = 3.29e\text{-}4$ for DTI sample). Age differences were also significant (T1-weighted sample: $\beta_{probable} = -0.296$, $p_{probable} = 1.57e\text{-}6$; $\beta_{recurrent} = -0.242$, $p_{recurrent} = 2.57e\text{-}4$; DTI sample: $\beta_{probable} = -0.302$, $p_{probable} = 3.20e\text{-}6$; $\beta_{recurrent} = -0.278$, $p_{recurrent} = 6.81e\text{-}5$). Difference of education level was not significant (T1-weighted sample: $\beta_{probable} = 0.001$, $p_{probable} = 0.984$; $\beta_{recurrent} = 0.061$, $p_{recurrent} = 0.387$; DTI sample: $\beta_{probable} = 0.012$, $p_{probable} = 0.861$; $\beta_{recurrent} = 0.063$, $p_{recurrent} =$

0.387), and the differences were even lower when age and sex were set as covariates (ps > 0.369). Many previous meta-analyses included only age and sex as covariates, and the recent protocol paper of UKB brain imaging phenotypes stated that sex and age could largely influence tests. The above descriptive statistics also reassured that the differences of age and sex between cases and controls were significant, while education differences were not robustly large. Therefore, we set sex, age, age$^2$ and assessment centre as covariates in all the models, whereas additional model to test the effect of MDD definitions on FA values included education level and number of release as covariates was tested, and the results remained the same (Table S10).

For the findings on the PCA scores on FA, association/commissural fibres, thalamic radiations and projection fibres, we similarly checked the effect of self-declare depression. Among the DTI-data sample, there were 239 self-declare depression cases and 4349 controls. We found that self-declare depression cases showed decreased gFA (β=-0.14, p=0.026), gAF (β=-0.14, p=0.032) and gTR (β=-0.17, p=0.009). This self-declare status was collected based on a general report of non-cancer illnesses on data field 20002 of UK Biobank touchscreen-assessment data (http://biobank.ctsu.ox.ac.uk/crystal/field.cgi?id=20002). This question was a general question to which participants were to recall all non-cancer illnesses that they had, and no hospital admission record was considered. Therefore was only used in validation tests on the findings of PCA components.

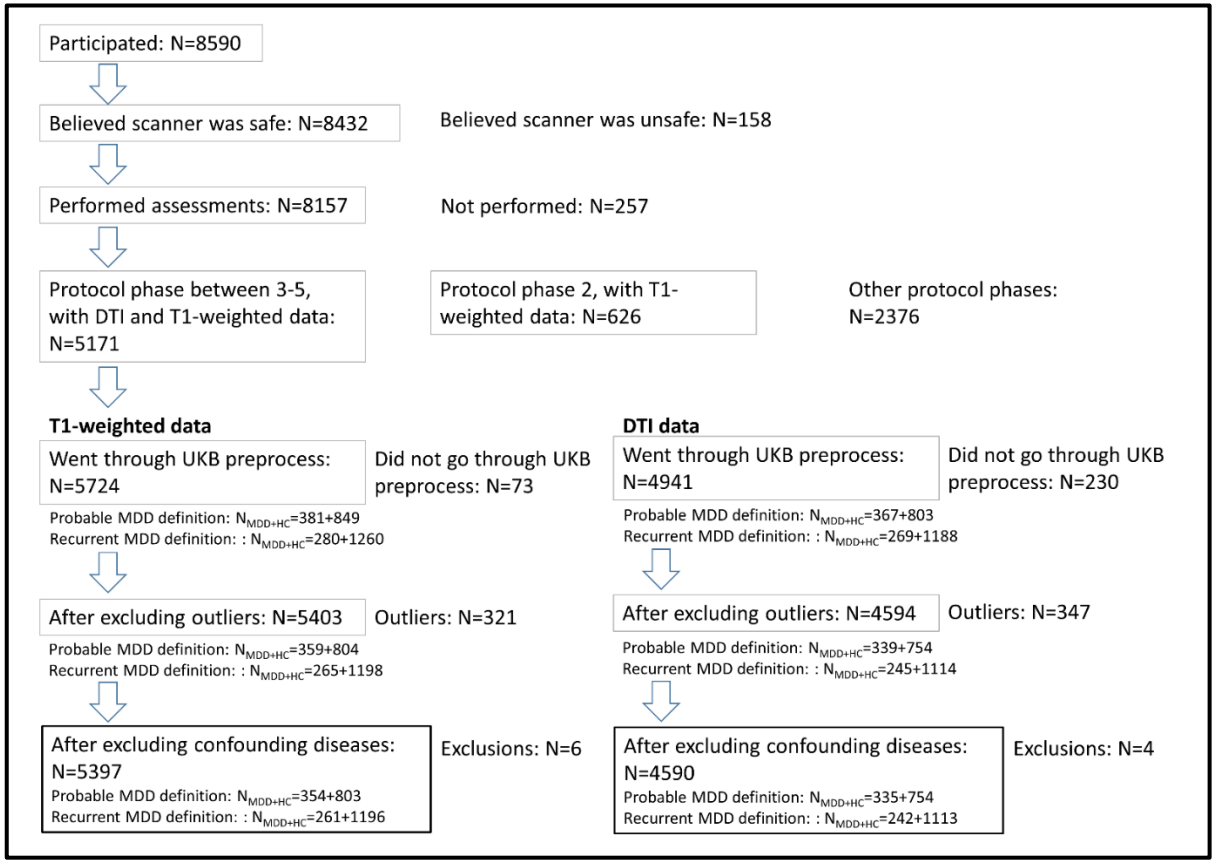


Figure S1. Sample size change after each step of exclusion. The boxes with grey outline were kept for the next step. For the steps “went through UKB preprocess” and “After excluding outliers” , number of participants with imaging data and the numbers of subjects included as a case or control in both definitions were stated separately.

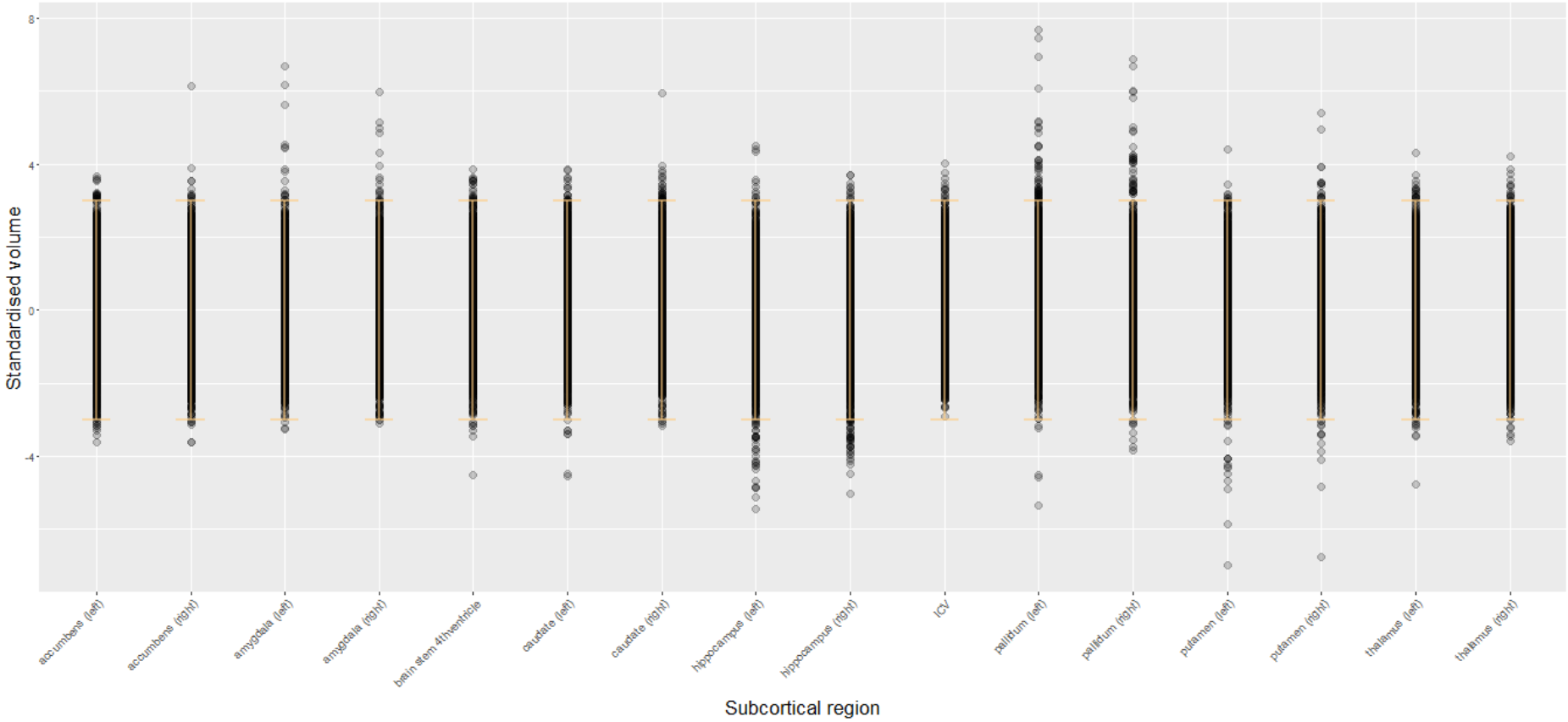


Figure S2. Standardised data of subcortical volumes. Each data point represents one person/region. The number of participants excluded as outliers was state in Figure S1. The error bars represent +/-3 standard deviation.

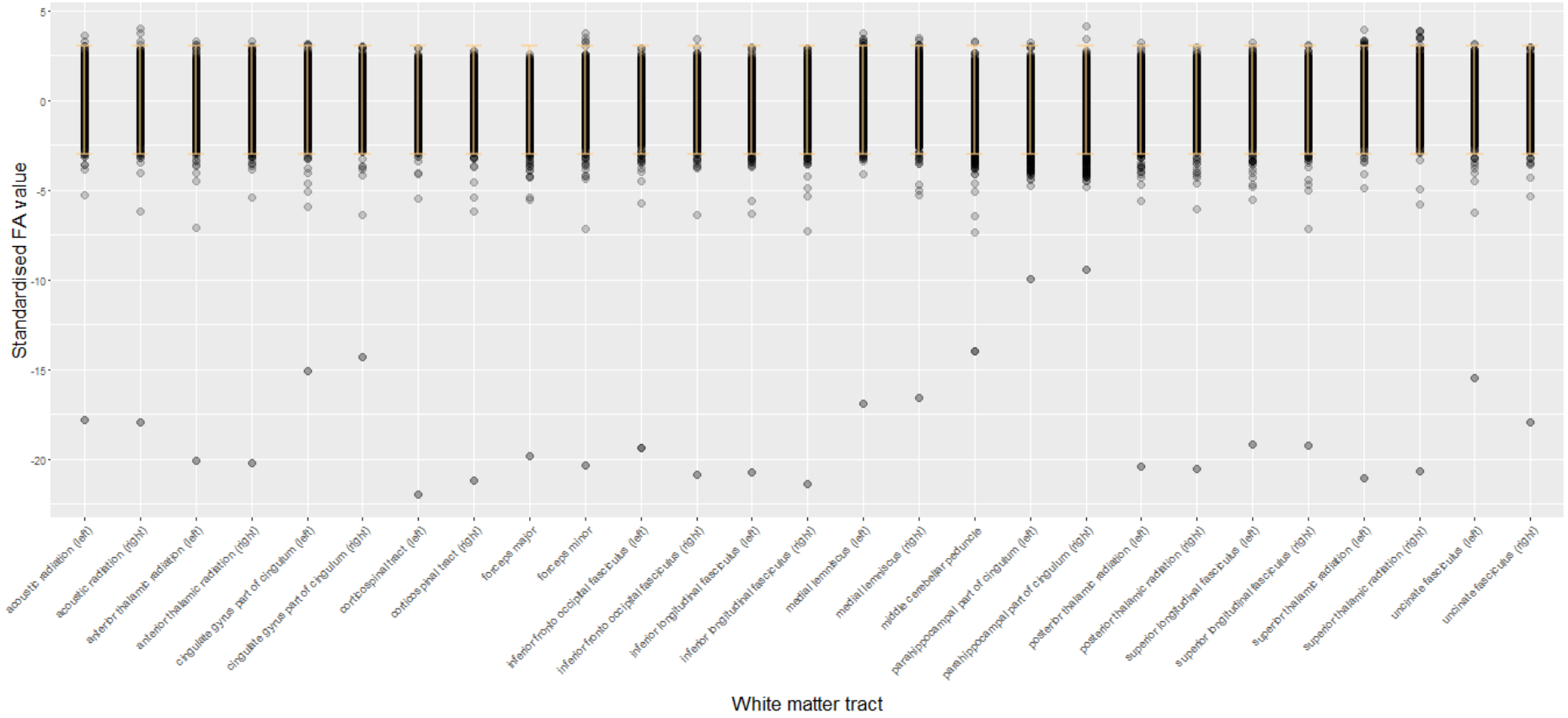


Figure S3. Standardised data of white matter integrity. Each data point represents one person/region. The number of participants excluded as outliers was state in Figure S1. The error bars represent +/-3 standard deviation.

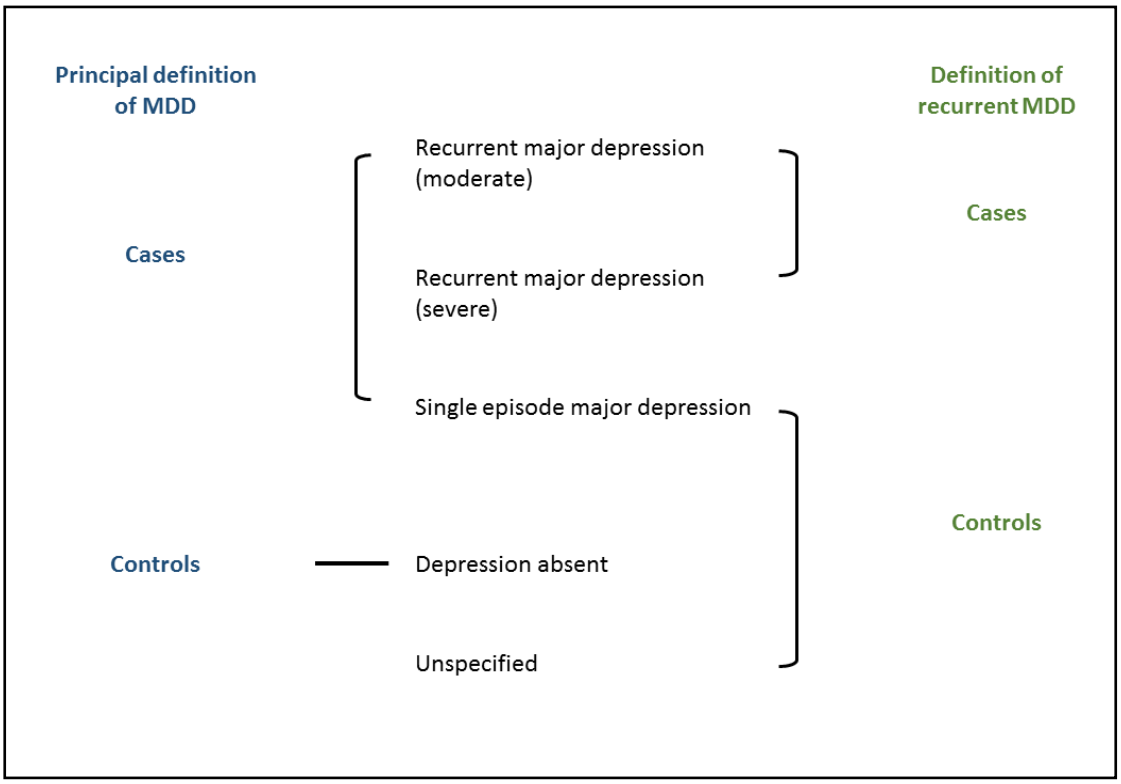


Figure S4. Principal definition of MDD and the definition of recurrent MDD. The categorization of moderate and severe recurrent major depression, single episode major depression and depression absent were summarized by Smith *et al.* (2013). An additional group of participants who self-reported of having had depressive symptoms or hospital admission history of nerves, anxiety or depression were categorized as 'unspecified'. The principal definition of MDD compared all MDD cases with those who were depression absent, and the definition of recurrent MDD compared recurrent MDD verses single-episode MDD, participants who were depression absent and the unspecified group.

Table S1. Descriptive statistics of imaging phenotypes. The statistics were concluded from the samples with imaging data regardless of MDD definitions (see Figure S1). Briefly, the raw T1-weighted data included 5724 people, and there were 5403 remained after the QC. Raw DTI data included 4941 people, and 4594 remained after the QC.

T1-weighted data:

| Tract | Raw data | | Data after QC | |
|---|---|---|---|---|
| | Mean | SD | Mean | SD |
| thalamus (left) | 7799.39 | 752.42 | 7781.45 | 709.95 |
| thalamus (right) | 7603.63 | 728.01 | 7586.65 | 689.60 |
| caudate (left) | 3396.74 | 421.10 | 3382.02 | 399.54 |
| caudate (right) | 3573.61 | 440.54 | 3555.72 | 416.01 |
| putamen (left) | 4815.74 | 604.28 | 4808.70 | 567.80 |
| putamen (right) | 4859.38 | 586.82 | 4848.13 | 552.87 |
| pallidum (left) | 1763.60 | 243.70 | 1751.53 | 217.47 |
| pallidum (right) | 1809.15 | 244.23 | 1798.13 | 218.11 |
| hippocampus (left) | 3813.23 | 474.68 | 3817.03 | 438.50 |
| hippocampus (right) | 3925.20 | 485.96 | 3926.84 | 450.72 |
| amygdala (left) | 1277.81 | 248.99 | 1273.88 | 237.74 |
| amygdala (right) | 1246.91 | 276.44 | 1243.24 | 266.44 |
| accumbens (left) | 507.55 | 120.42 | 506.79 | 115.44 |
| accumbens (right) | 402.64 | 111.31 | 402.37 | 107.82 |
| brain stem | 22857.44 | 2764.28 | 22772.54 | 2635.68 |
| ICV | 1203924.85 | 115196.69 | 1199108.04 | 110698.23 |

DTI data:

| Tract | Raw data | | Data after QC | |
|---|---|---|---|---|
| | Mean | SD | Mean | SD |
| acoustic radiation (left) | 0.423 | 0.024 | 0.424 | 0.022 |
| acoustic radiation (right) | 0.414 | 0.023 | 0.415 | 0.021 |
| anterior thalamic radiation (left) | 0.401 | 0.020 | 0.401 | 0.017 |
| anterior thalamic radiation (right) | 0.393 | 0.019 | 0.394 | 0.017 |
| cingulate gyrus part of cingulum (left) | 0.537 | 0.036 | 0.538 | 0.033 |
| cingulate gyrus part of cingulum (right) | 0.498 | 0.035 | 0.499 | 0.033 |
| parahippocampal part of cingulum (left) | 0.312 | 0.031 | 0.315 | 0.027 |
| parahippocampal part of cingulum (right) | 0.311 | 0.033 | 0.314 | 0.028 |
| corticospinal tract (left) | 0.547 | 0.025 | 0.548 | 0.022 |
| corticospinal tract (right) | 0.541 | 0.026 | 0.542 | 0.022 |
| forceps major | 0.582 | 0.029 | 0.583 | 0.026 |
| forceps minor | 0.466 | 0.023 | 0.467 | 0.020 |
| inferior fronto occipital fasciculus (left) | 0.476 | 0.025 | 0.477 | 0.020 |
| inferior fronto occipital fasciculus (right) | 0.466 | 0.022 | 0.467 | 0.019 |
| inferior longitudinal fasciculus (left) | 0.461 | 0.022 | 0.462 | 0.019 |

| | | | | |
|---|---|---|---|---|
| inferior longitudinal fasciculus (right) | 0.452 | 0.021 | 0.453 | 0.018 |
| middle cerebellar peduncle | 0.477 | 0.034 | 0.479 | 0.030 |
| medial lemniscus (left) | 0.418 | 0.025 | 0.419 | 0.023 |
| medial lemniscus (right) | 0.421 | 0.025 | 0.422 | 0.024 |
| posterior thalamic radiation (left) | 0.458 | 0.022 | 0.459 | 0.020 |
| posterior thalamic radiation (right) | 0.454 | 0.022 | 0.456 | 0.019 |
| superior longitudinal fasciculus (left) | 0.442 | 0.023 | 0.443 | 0.020 |
| superior longitudinal fasciculus (right) | 0.425 | 0.022 | 0.426 | 0.019 |
| superior thalamic radiation (left) | 0.423 | 0.020 | 0.424 | 0.018 |
| superior thalamic radiation (right) | 0.422 | 0.020 | 0.423 | 0.018 |
| uncinate fasciculus (left) | 0.391 | 0.025 | 0.392 | 0.023 |
| uncinate fasciculus (right) | 0.391 | 0.022 | 0.392 | 0.020 |

Table S2. Major depressive disorder criteria summarized by Smith et al. (2013)

| **Category** | Criteria |
|---|---|
| **Single probable episode of major depression** | Ever depressed/down for a whole week, plus at least two weeks duration, plus only one episode, plus ever seen a GP or a psychiatrist for nerves, anxiety, depression.<br>OR<br>Ever anhedonia (unenthusiasm/uninterest) for a whole week, plus at least two weeks, plus only one episode, plus ever seen a GP or a psychiatrist for nerves, anxiety, depression |
| **Probable recurrent major depression (moderate)** | Ever depressed/down for a whole week, plus at least two weeks duration, plus at least two episodes, plus ever seen a GP (but not a psychiatrist) for nerves, anxiety, depression<br>OR<br>Ever anhedonia (unenthusiasm/uninterest) for a whole week, plus at least two weeks, plus at least two episodes, plus ever seen a GP (but not a psychiatrist) for nerves, anxiety, depression |
| **Probable recurrent major depression (severe)** | Ever depressed/down for a whole week, plus at least two weeks duration, plus at least two episodes, plus ever seen a psychiatrist for nerves, anxiety, depression<br>OR<br>Ever anhedonia (unenthusiasm/uninterest) for a whole week, plus at least two weeks, plus at least two episodes, plus ever seen a psychiatrist for nerves, anxiety, depression |
| **Depression absent** | 1. Mood question answered 'no'<br>2. Reported symptoms but duration was too short.<br>3. Reported symptoms but period was below threshold.<br>4. Had not seen GP or psychiatrist and did not self-report depression |

Note: Participants needed to meet all four criterion to be categorized as depression absent.

Table S3. Demographic features of samples with T1-weighted and DTI data. The descriptive statistics below are summarised based on the samples that were analysed in the present study (see the final sample size in Figure S1).

Subjects with T1-weighted data:

| | Principal MDD definition | | | Recurrent MDD definition | | |
|---|---|---|---|---|---|---|
| | Case | Control | N | Case | Control | N |
| Sample size | 354 | 803 | -- | 261 | 1196 | -- |
| Age (Mean±SD) | 54.97±7.38 | 57.19±7.14 | 1157 | 54.99±7.33 | 56.80±7.21 | 1457 |
| Number of Male | 123 | 433 | 1157 | 97 | 593 | 1457 |
| Proportion of Male (%) | 34.75 | 53.92 | | 37.16 | 49.58 | |
| Average Education level | 4.74 | 4.74 | 1157 | 4.78 | 4.69 | 1157 |
| College or University degree (%) | 45.48 | 40.72 | -- | 46.36 | 39.38 | -- |
| A levels/AS levels (%) | 13.28 | 15.82 | -- | 14.94 | 15.05 | -- |
| O levels/GCSEs (%) | 18.36 | 21.30 | -- | 16.09 | 21.57 | -- |
| CSEs (%) | 5.93 | 4.23 | -- | 6.13 | 4.68 | -- |
| NVQ or HND or HNC (%) | 5.65 | 5.48 | -- | 5.75 | 5.77 | -- |
| Other qualifications (%) | 5.65 | 4.61 | -- | 5.36 | 4.85 | -- |
| No respond/refuse to answer (%) | 5.65 | 7.85 | -- | 5.36 | 8.70 | -- |

Subjects with DTI data:

| | Principal MDD definition | | | Recurrent MDD definition | | |
|---|---|---|---|---|---|---|
| | Case | Control | N | Case | Control | N |
| Sample size | 335 | 754 | -- | 242 | 1113 | -- |
| Age (Mean±SD) | 54.83±7.40 | 57.07±7.24 | 1089 | 54.63±7.34 | 56.69±7.24 | 1355 |
| Number of Male | 119 | 408 | 1089 | 91 | 563 | 1355 |
| Proportion of Male (%) | 35.52 | 54.11 | | 37.60 | 50.58 | |
| Average Education level | 4.74 | 4.72 | 1089 | 4.78 | 4.69 | 1355 |
| College or University degree () | 46.27 | 39.66 | -- | 47.93 | 38.90 | -- |
| A levels/AS levels () | 12.84 | 16.71 | -- | 14.05 | 15.45 | -- |
| O levels/GCSEs () | 19.10 | 21.22 | -- | 16.94 | 21.56 | -- |
| CSEs () | 5.97 | 3.98 | -- | 6.20 | 4.58 | -- |
| NVQ or HND or HNC () | 5.37 | 5.44 | -- | 5.37 | 5.84 | -- |
| Other qualifications () | 5.97 | 4.91 | -- | 5.79 | 4.67 | -- |
| No respond/refuse to answer () | 4.48 | 8.09 | -- | 3.72 | 8.98 | -- |

Table S4. The effect of MDD definition on the volumes of subcortical regions and brain matters (without excluding outliers). The same model was conducted with age, age$^2$, sex and assessment centre set as covariates. Hemisphere was also set as a covariate when appropriate. Sample sizes were $N_{case}$=381, $N_{control}$=849 and $N_{case}$=280, $N_{control}$=1260 for principal and recurrent definitions respectively.

| Subcortical regions | Principal definition | | | | | Recurrent definition | | | | |
|---|---|---|---|---|---|---|---|---|---|---|
| | Effect size | Standard deviation | t value | p value | $p_{corrected}$ | Effect size | Standard deviation | t value | p value | $p_{corrected}$ |
| **Accumbens** | 0.013 | 0.048 | 0.277 | 0.782 | 0.879 | -0.012 | 0.051 | -0.247 | 0.805 | 0.913 |
| **Amygdala** | -0.032 | 0.049 | -0.658 | 0.511 | 0.879 | 0.026 | 0.052 | 0.497 | 0.620 | 0.913 |
| **Caudate** | 0.047 | 0.050 | 0.923 | 0.356 | 0.879 | 0.017 | 0.053 | 0.329 | 0.742 | 0.913 |
| **Hippocampus** | -0.036 | 0.049 | -0.724 | 0.469 | 0.879 | -0.056 | 0.051 | -1.089 | 0.276 | 0.829 |
| **Pallidum** | 0.014 | 0.051 | 0.277 | 0.782 | 0.879 | 0.006 | 0.054 | 0.110 | 0.913 | 0.913 |
| **Putamen** | 0.020 | 0.046 | 0.429 | 0.668 | 0.879 | -0.006 | 0.047 | -0.119 | 0.905 | 0.913 |
| **Thalamus** | -0.058 | 0.038 | -1.543 | 0.123 | 0.879 | -0.067 | 0.040 | -1.695 | 0.090 | 0.813 |
| **Brain stem** | -0.007 | 0.051 | -0.134 | 0.893 | 0.893 | 0.043 | 0.054 | 0.797 | 0.425 | 0.913 |
| **ICV** | -0.058 | 0.045 | -1.287 | 0.198 | 0.879 | -0.062 | 0.048 | -1.295 | 0.196 | 0.829 |

Table S5. The interaction between MDD definition and hemisphere on the volumes of subcortical regions and brain matters. In this model, again age, age$^2$, sex and assessment centre were set as covariates. MDD definition, hemisphere and the interaction between MDD definition and hemisphere were also included in the model. As brain stem and ICV were unilateral structure/measure, therefore these two measure were not tested in this model.

| Subcortical regions | **Principal definition** | | | | | **Recurrent definition** | | | | |
|---|---|---|---|---|---|---|---|---|---|---|
| | Effect size | Standard deviation | t value | p value | $p_{corrected}$ | Effect size | Standard deviation | t value | p value | $p_{corrected}$ |
| **Accumbens** | -0.014 | 0.056 | -0.250 | 0.803 | 0.907 | -0.064 | 0.059 | -1.088 | 0.277 | 0.879 |
| **Amygdala** | 0.066 | 0.070 | 0.936 | 0.349 | 0.907 | -0.011 | 0.074 | -0.143 | 0.886 | 0.945 |
| **Caudate** | 0.011 | 0.028 | 0.388 | 0.698 | 0.907 | -0.008 | 0.030 | -0.280 | 0.779 | 0.945 |
| **Hippocampus** | 0.034 | 0.054 | 0.633 | 0.527 | 0.907 | 0.004 | 0.059 | 0.070 | 0.945 | 0.945 |
| **Pallidum** | -0.006 | 0.048 | -0.117 | 0.907 | 0.907 | -0.015 | 0.051 | -0.290 | 0.772 | 0.945 |
| **Putamen** | -0.047 | 0.034 | -1.383 | 0.167 | 0.907 | -0.047 | 0.036 | -1.312 | 0.190 | 0.879 |
| **Thalamus** | 0.015 | 0.023 | 0.671 | 0.502 | 0.907 | 0.022 | 0.024 | 0.884 | 0.377 | 0.879 |

Table S6. The effect of MDD definition on FA values of DTI tracts (gFA included as a convariate). In order to test whether the significant effect of MDD definitions remains significant when general FA change was controlled, this model included gFA score as a covariate. The method to extract gFA score was stated in the main text (Methods-Statistical methods-White matter integrity).

| DTI tracts | **Principal definition** | | | | | **Recurrent definition** | | | | |
|---|---|---|---|---|---|---|---|---|---|---|
| | Effect size | Standard deviation | t value | p value | $p_{corrected}$ | Effect size | Standard deviation | t value | p value | $p_{corrected}$ |
| **Acoustic radiation** | 0.030 | 0.043 | 0.707 | 4.80E-001 | 0.849 | 0.006 | 0.046 | 0.136 | 8.92E-001 | 0.946 |
| **Anterior thalamic radiation** | 0.062 | 0.039 | 1.572 | 1.16E-001 | 0.372 | 0.056 | 0.042 | 1.349 | 1.78E-001 | 0.568 |
| **Cingulate gyrus part of cingulum** | -0.026 | 0.046 | -0.563 | 5.74E-001 | 0.849 | -0.008 | 0.049 | -0.173 | 8.63E-001 | 0.946 |
| **Corticospinal tract** | 0.003 | 0.051 | 0.053 | 9.58E-001 | 0.958 | 0.023 | 0.055 | 0.415 | 6.78E-001 | 0.946 |
| **Inferior fronto-occipital fasciculus** | 0.029 | 0.031 | 0.928 | 3.53E-001 | 0.808 | 0.007 | 0.032 | 0.221 | 8.25E-001 | 0.946 |
| **Inferior longitudinal fasciculus** | 0.017 | 0.032 | 0.548 | 5.84E-001 | 0.849 | -0.010 | 0.032 | -0.316 | 7.52E-001 | 0.946 |
| **Medial lemniscus** | 0.007 | 0.056 | 0.117 | 9.07E-001 | 0.958 | 0.018 | 0.058 | 0.312 | 7.55E-001 | 0.946 |
| **Parahippocampal part of cingulum** | -0.012 | 0.054 | -0.218 | 8.27E-001 | 0.958 | 0.010 | 0.057 | 0.171 | 8.64E-001 | 0.946 |
| **Posterior thalamic radiation** | 0.037 | 0.045 | 0.808 | 4.19E-001 | 0.839 | 0.013 | 0.047 | 0.265 | 7.91E-001 | 0.946 |
| **Superior longitudinal fasciculus (bilateral)** | 0.006 | 0.035 | 0.174 | 8.62E-001 | 0.958 | -0.021 | 0.038 | -0.566 | 5.72E-001 | 0.946 |
| **Superior longitudinal fasciculus (left)** | -0.194 | 0.066 | -2.951 | 3.23E-003 | 0.038 | -0.221 | 0.070 | -3.165 | 1.59E-003 | 0.025 |
| **Superior thalamic radiation** | -0.110 | 0.051 | -2.168 | 3.03E-002 | 0.162 | -0.077 | 0.053 | -1.442 | 1.50E-001 | 0.568 |
| **Uncinate fasciculus** | 0.013 | 0.040 | 0.330 | 7.42E-001 | 0.958 | -0.003 | 0.043 | -0.068 | 9.46E-001 | 0.946 |
| **Forceps major** | -0.193 | 0.068 | -2.834 | 4.69E-003 | 0.038 | -0.133 | 0.072 | -1.842 | 6.57E-002 | 0.350 |
| **Forceps minor** | -0.112 | 0.065 | -1.723 | 8.52E-002 | 0.341 | -0.159 | 0.070 | -2.266 | 2.36E-002 | 0.189 |
| **Middle cerebellar peduncle** | -0.066 | 0.064 | -1.024 | 3.06E-001 | 0.808 | 0.039 | 0.068 | 0.576 | 5.65E-001 | 0.946 |

Table S7. The effect of MDD definition on FA values of DTI tracts (Without excluding outliers). The same model for Table 2 was conducted, with age, age$^2$, sex and assessment centre controlled and hemisphere also controlled when appropriate. Sample sizes were $N_{case}$=367, $N_{control}$=803 and $N_{case}$=269, $N_{control}$=1188 for principal and recurrent definitions respectively. The standard effect sizes of significant tracts found within the sample that outliers were excluded remained in similar trend. Significant tracts included left superior longitudinal fasciculus, forceps major and superior thalamic radiation.

| DTI tracts | Principal definition | | | | | Recurrent definition | | | | |
|---|---|---|---|---|---|---|---|---|---|---|
| | Effect size | Standard deviation | t value | p value | $p_{corrected}$ | Effect size | Standard deviation | t value | p value | $p_{corrected}$ |
| **Acoustic radiation** | -0.055 | 0.052 | -1.053 | 2.92E-001 | 0.425 | -0.032 | 0.065 | -0.488 | 6.26E-001 | 0.807 |
| **Anterior thalamic radiation** | -0.042 | 0.055 | -0.759 | 4.48E-001 | 0.506 | -0.002 | 0.069 | -0.024 | 9.81E-001 | 0.981 |
| **Cingulate gyrus part of cingulum** | -0.072 | 0.054 | -1.348 | 1.78E-001 | 0.376 | -0.021 | 0.064 | -0.322 | 7.48E-001 | 0.854 |
| **Corticospinal tract** | -0.091 | 0.056 | -1.626 | 1.04E-001 | 0.376 | -0.071 | 0.061 | -1.151 | 2.50E-001 | 0.807 |
| **Inferior fronto-occipital fasciculus** | -0.038 | 0.053 | -0.715 | 4.75E-001 | 0.506 | 0.013 | 0.068 | 0.192 | 8.47E-001 | 0.904 |
| **Inferior longitudinal fasciculus** | -0.049 | 0.056 | -0.866 | 3.87E-001 | 0.490 | -0.033 | 0.069 | -0.472 | 6.37E-001 | 0.807 |
| **Medial lemniscus** | -0.083 | 0.054 | -1.537 | 1.24E-001 | 0.376 | -0.063 | 0.068 | -0.922 | 3.57E-001 | 0.807 |
| **Parahippocampal part of cingulum** | 0.014 | 0.053 | 0.258 | 7.96E-001 | 0.796 | 0.047 | 0.062 | 0.767 | 4.43E-001 | 0.807 |
| **Posterior thalamic radiation** | -0.046 | 0.054 | -0.845 | 3.98E-001 | 0.490 | -0.044 | 0.067 | -0.648 | 5.17E-001 | 0.807 |
| **Superior longitudinal fasciculus (bilateral)** | -0.066 | 0.056 | -1.188 | 2.35E-001 | 0.376 | -0.039 | 0.069 | -0.569 | 5.69E-001 | 0.807 |
| **Superior longitudinal fasciculus (left)** | -0.107 | 0.058 | -1.836 | 6.66E-002 | 0.355 | -0.092 | 0.071 | -1.302 | 1.93E-001 | 0.807 |
| **Superior thalamic radiation** | -0.148 | 0.056 | -2.656 | 8.01E-003 | 0.089 | -0.079 | 0.070 | -1.122 | 2.62E-001 | 0.807 |
| **Uncinate fasciculus** | -0.064 | 0.053 | -1.195 | 2.32E-001 | 0.376 | -0.029 | 0.064 | -0.447 | 6.55E-001 | 0.807 |
| **Forceps major** | -0.151 | 0.059 | -2.544 | 1.11E-002 | 0.089 | -0.086 | 0.072 | -1.197 | 2.31E-001 | 0.807 |
| **Forceps minor** | -0.070 | 0.057 | -1.226 | 2.21E-001 | 0.376 | -0.066 | 0.072 | -0.922 | 3.57E-001 | 0.807 |
| **Middle cerebellar peduncle** | -0.079 | 0.058 | -1.364 | 1.73E-001 | 0.376 | 0.034 | 0.067 | 0.501 | 6.16E-001 | 0.807 |

Table S8. The interaction between MDD definition and hemisphere on FA values of DTI tracts. The results below were for follow-up model to test whether there was a lateralised effect of MDD definition (see main text, section Methods-Statistical methods-White matter integrity). Forceps major and minor and middle cerebellar peduncle were not included in this analysis as they were unilateral tracts. A significant effect of the interaction between recurrent definition and hemisphere was found in superior longitudinal fasciculus, therefore individual tests on the FA values on each hemisphere of superior longitudinal fasciculus was conducted. As the effect of MDD definitions were significant on left superior longitudinal fasciculus, the results were added in Table 1, S6 and S7.

| DTI tracts | **Principal definition** | | | | | **Recurrent definition** | | | | |
|---|---|---|---|---|---|---|---|---|---|---|
| | Effect size | Standard deviation | t value | p value | $p_{corrected}$ | Effect size | Standard deviation | t value | p value | $p_{corrected}$ |
| **Acoustic radiation** | -0.108 | 0.063 | -1.712 | 8.72E-002 | 0.348 | -0.069 | 0.067 | -1.034 | 3.01E-001 | 0.932 |
| **Anterior thalamic radiation** | -0.061 | 0.038 | -1.631 | 1.03E-001 | 0.348 | -0.026 | 0.041 | -0.631 | 5.28E-001 | 0.932 |
| **Cingulate gyrus part of cingulum** | -0.026 | 0.063 | -0.411 | 6.81E-001 | 0.894 | -0.002 | 0.067 | -0.036 | 9.71E-001 | 0.971 |
| **Corticospinal tract** | -0.088 | 0.060 | -1.459 | 1.45E-001 | 0.348 | -0.033 | 0.066 | -0.494 | 6.21E-001 | 0.932 |
| **Inferior fronto-occipital fasciculus** | 0.005 | 0.047 | 0.110 | 9.12E-001 | 0.933 | 0.038 | 0.050 | 0.753 | 4.51E-001 | 0.932 |
| **Inferior longitudinal fasciculus** | 0.012 | 0.038 | 0.325 | 7.45E-001 | 0.894 | 0.024 | 0.041 | 0.582 | 5.61E-001 | 0.932 |
| **Medial lemniscus** | 0.021 | 0.036 | 0.579 | 5.63E-001 | 0.894 | 0.031 | 0.039 | 0.801 | 4.23E-001 | 0.932 |
| **Parahippocampal part of cingulum** | -0.044 | 0.071 | -0.628 | 5.30E-001 | 0.894 | -0.008 | 0.075 | -0.111 | 9.12E-001 | 0.971 |
| **Posterior thalamic radiation** | -0.071 | 0.047 | -1.517 | 1.30E-001 | 0.348 | -0.008 | 0.050 | -0.151 | 8.80E-001 | 0.971 |
| **Superior longitudinal fasciculus** | 0.069 | 0.036 | 1.939 | 5.27E-002 | 0.348 | 0.117 | 0.038 | 3.076 | 2.14E-003 | 0.026 |
| **Superior thalamic radiation** | -0.003 | 0.036 | -0.085 | 9.33E-001 | 0.933 | 0.023 | 0.038 | 0.596 | 5.51E-001 | 0.932 |
| **Uncinate fasciculus** | 0.021 | 0.057 | 0.369 | 7.12E-001 | 0.894 | -0.005 | 0.062 | -0.075 | 9.40E-001 | 0.971 |

Table S9. The effect of MDD definition on FA values of DTI tracts (education level and release included as covariates). There was no significant effect of education level and number of release on the definitions of MDD (see supplementary materials, Methods-MDD definitions). However, in order to double check whether the results would remain the same when these factors were included, a validation test was conducted. The regions that were found significant in the section of results in the main text remained significant (left superior longitudinal fasciculus, forceps major and superior thalamic radiation).

| DTI tracts | Principal definition | | | | | Recurrent definition | | | | |
|---|---|---|---|---|---|---|---|---|---|---|
| | Effect size | Standard deviation | t value | p value | $p_{corrected}$ | Effect size | Standard deviation | t value | p value | $p_{corrected}$ |
| **Acoustic radiation** | -0.080 | 0.058 | -1.371 | 1.71E-001 | 0.227 | -0.089 | 0.062 | -1.428 | 1.53E-001 | 0.239 |
| **Anterior thalamic radiation** | -0.075 | 0.063 | -1.195 | 2.32E-001 | 0.266 | -0.062 | 0.067 | -0.926 | 3.55E-001 | 0.464 |
| **Cingulate gyrus part of cingulum** | -0.130 | 0.059 | -2.198 | 2.82E-002 | 0.090 | -0.100 | 0.063 | -1.575 | 1.15E-001 | 0.205 |
| **Corticospinal tract** | -0.079 | 0.058 | -1.351 | 1.77E-001 | 0.227 | -0.052 | 0.062 | -0.832 | 4.06E-001 | 0.464 |
| **Inferior fronto-occipital fasciculus** | -0.088 | 0.060 | -1.457 | 1.45E-001 | 0.227 | -0.055 | 0.065 | -0.847 | 3.97E-001 | 0.464 |
| **Inferior longitudinal fasciculus** | -0.120 | 0.062 | -1.959 | 5.04E-002 | 0.115 | -0.121 | 0.065 | -1.849 | 6.47E-002 | 0.171 |
| **Medial lemniscus** | -0.131 | 0.062 | -2.127 | 3.36E-002 | 0.090 | -0.138 | 0.065 | -2.119 | 3.43E-002 | 0.110 |
| **Parahippocampal part of cingulum** | -0.040 | 0.058 | -0.696 | 4.87E-001 | 0.487 | -0.019 | 0.060 | -0.315 | 7.53E-001 | 0.753 |
| **Posterior thalamic radiation** | -0.081 | 0.061 | -1.327 | 1.85E-001 | 0.227 | -0.090 | 0.065 | -1.392 | 1.64E-001 | 0.239 |
| **Superior longitudinal fasciculus (bilateral)** | -0.140 | 0.063 | -2.220 | 2.66E-002 | 0.090 | -0.147 | 0.067 | -2.185 | 2.91E-002 | 0.110 |
| **Superior longitudinal fasciculus (left)** | -0.192 | 0.066 | -2.927 | 3.49E-003 | 0.027 | -0.217 | 0.069 | -3.127 | 1.80E-003 | 0.029 |
| **Superior thalamic radiation** | -0.225 | 0.065 | -3.464 | 5.53E-004 | 0.009 | -0.178 | 0.069 | -2.571 | 1.02E-002 | 0.082 |
| **Uncinate fasciculus** | -0.104 | 0.058 | -1.787 | 7.43E-002 | 0.149 | -0.104 | 0.062 | -1.679 | 9.33E-002 | 0.187 |
| **Forceps major** | -0.188 | 0.067 | -2.809 | 5.06E-003 | 0.027 | -0.127 | 0.071 | -1.784 | 7.47E-002 | 0.171 |
| **Forceps minor** | -0.111 | 0.065 | -1.702 | 8.91E-002 | 0.158 | -0.156 | 0.070 | -2.233 | 2.57E-002 | 0.110 |
| **Middle cerebellar peduncle** | -0.070 | 0.064 | -1.093 | 2.75E-001 | 0.293 | 0.035 | 0.068 | 0.518 | 6.05E-001 | 0.645 |

Table S10. Loadings of first latent factor of PCA on global FA, association/commissural fibres, thalamic radiations and projection fibres. The individual tracts included for these four PCA were stated in the main text (Methods-Statistical methods-White matter integrity). All the PCA were performed on the overall sample after outliers were excluded to maximize the accuracy of the models in the largest sample possible (N=4594).

| Tracts | PCA analyses | | | |
|---|---|---|---|---|
| | Global FA | Association/ Commissural fibres | Thalamic radiations | Projection fibres |
| Cingulate gyrus part of cingulum (left) | 0.583 | 0.663 | -- | -- |
| Cingulate gyrus part of cingulum (right) | 0.544 | 0.629 | -- | -- |
| Inferior fronto-occipital fasciculus (left) | 0.817 | 0.820 | -- | -- |
| Inferior fronto-occipital fasciculus (right) | 0.836 | 0.824 | -- | -- |
| Inferior longitudinal fasciculus (left) | 0.808 | 0.798 | -- | -- |
| Inferior longitudinal fasciculus (right) | 0.839 | 0.815 | -- | -- |
| Parahippocampal part of cingulum (left) | 0.408 | 0.415 | -- | -- |
| Parahippocampal part of cingulum (right) | 0.356 | 0.356 | -- | -- |
| Superior longitudinal fasciculus (left) | 0.798 | 0.788 | -- | -- |
| Superior longitudinal fasciculus (right) | 0.820 | 0.796 | -- | -- |
| Uncinate fasciculus (left) | 0.657 | 0.678 | -- | -- |
| Uncinate fasciculus (right) | 0.673 | 0.687 | -- | -- |
| Forceps major | 0.539 | 0.551 | -- | -- |
| Forceps minor | 0.784 | 0.782 | -- | -- |
| Anterior thalamic radiation (left) | 0.762 | -- | 0.784 | -- |
| Anterior thalamic radiation (right) | 0.759 | -- | 0.809 | -- |
| Posterior thalamic radiation (left) | 0.645 | -- | 0.761 | -- |
| Posterior thalamic radiation (right) | 0.641 | -- | 0.794 | -- |
| Superior thalamic radiation (left) | 0.636 | -- | 0.744 | -- |
| Superior thalamic radiation (right) | 0.610 | -- | 0.744 | -- |
| Acoustic radiation (left) | 0.607 | -- | -- | 0.536 |
| Acoustic radiation (right) | 0.626 | -- | -- | 0.610 |
| Corticospinal tract (left) | 0.554 | -- | -- | 0.782 |
| Corticospinal tract (right) | 0.552 | -- | -- | 0.800 |
| Medial lemniscus (left) | 0.237 | -- | -- | 0.475 |
| Medial lemniscus (right) | 0.232 | -- | -- | 0.490 |
| Middle cerebellar peduncle | 0.325 | -- | -- | 0.571 |

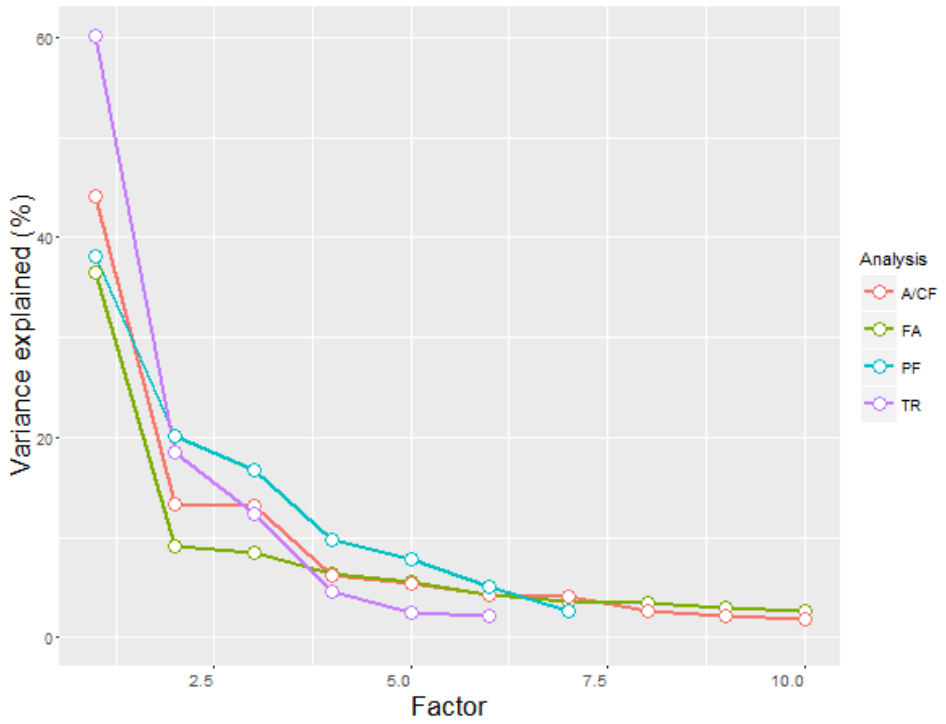


Figure S5. Scree plot of the four PCA analyses on global FA (FA), association/commissural fibres (A/CF), thalamic radiations (TR) and projection fibres (PF). Variance explained were stated in the results of the main text.

# Appendix 2:

# Supplementary materials of Chapter 3: White matter microstructure is related to the mean and within-subject variance of depressive symptoms

## Supplementary methods

### PHQ-4 questionnaire

PHQ4 questions include: “Frequency of depressed mood in last 2 weeks”, “Frequency of unenthusiasm/disinterest in last 2 weeks”, “Frequency of tenseness/restlessness in last 2 weeks” and “Frequency of tiredness / lethargy in last 2 weeks”. This questionnaire assesses depression-related symptoms within a 2-week timeframe. The sum of the score was calculated to indicate depressive symptoms.

The mean time lag between the first and second occasion was 4.25 years with a standard deviation of 0.93 years. Between the second and third occasion, mean time lag was 2.59 years with a standard deviation of 0.64 years. Between the third and the final occasion, mean time lag was 0.95 years with a standard deviation of 0.60 years.

For each measure of depressive symptoms derived from cross-sectional assessments, mean time lag of mean level of depressive symptoms was 7.91 years (sd=0.97 years), variability of depressive symptoms was 7.91 years (sd=0.97 years), and slope of longitudinal trajectory was 7.92 years (sd=0.97 years). No significant difference was found for the time lags between cross-sectional assessments ($p>0.05$). Also the correlations between cross-sectional measures and time lag was

very small and therefore this variable was not included in the main model (r ranged from 0.012 to 0.032).

**dMRI measures**

The processed tracts included 12 bilateral tracts that has a value for each brain hemisphere (acoustic radiation, anterior thalamic radiation, cingulate gyrus part of cingulum, corticospinal tract, inferior fronto-occipital fasciculus, inferior longitudinal fasciculus, medial lemniscus, parahippocampal part of cingulum, posterior thalamic radiation, superior longitudinal fasciculus, superior thalamic radiation and uncinate fasciculus) and 3 unilateral tracts (forceps major, forceps minor and middle cerebellar peduncle).

**Depressive symptoms**

For the growth curve model, we used the 'growth' function from lavaan package (http://lavaan.ugent.be/tutorial/growth.html) in R (Rosseel 2012). Scaled age at each assessment was controlled for. The growth curve model showed good fit to the data (CFI = 0.989, TLI = 0.986, RMSEA = 0.031, SRMR = 0.023, Chi-square (17) = 99.419 with a $p<0.001$). Longitudinal change within the whole population was in a negative direction but did not reach to significance ($\beta = -0.110$, $p = 0.220$). Both the intercept ($\beta= -0.029$, $p = 0.007$) and variance ($\beta=0.053$, $p < 0.001$) of the mean slope of growth curve model was significant. Each individual's slope of longitudinal trajectory was estimated for further analysis.

**Depression-related phenotypes**

These include 'MDD self' (self-reported history of whether has seen a doctor/psychiatrist for nerves, anxiety, tension or depression , see in: http://biobank.ctsu.ox.ac.uk/crystal/field.cgi?id=2010), 'MDD status' definition according to Smith et al (based on self-reported depressed symptoms and hospital

admission history, http://biobank.ctsu.ox.ac.uk/crystal/field.cgi?id=20126) and CIDI - based MDD (derived from Composite International Diagnostic Interview results, UK Biobank used the questions but the results were self-reported, http://biobank.ctsu.ox.ac.uk/crystal/label.cgi?id=138). CIDI MDD is the most clinical definition, whilst MDD broad is the most lenient and has the biggest sample size. Other phenotypes include MDD severity assessed by CIDI and length of depression (years from first to last episode). Other phenotypes include onset age for the first episode (http://biobank.ctsu.ox.ac.uk/crystal/field.cgi?id=20433) and whether had self-harm behaviour (http://biobank.ctsu.ox.ac.uk/crystal/field.cgi?id=20480). Coefficients for MDD phenotypes are odds ratios, and for other phenotypes are standardised effect sizes of glm models, and age, age$^2$ and gender were set as covariates for mean depressive level and temporal change. Only gender was controlled for slope of longitudinal trajectory because the measure was derived controlling for age in the growth curve model. All MDD definitions and self-harm behaviour were binary variables, and other phenotypes were continuous.

**Covariates**

In addition to age, age$^2$ and gender, we also included scanner positions for all three axis, alcohol consumption, smoking status and stressful life events. The covariates except for age and gender will be explained in detail below. All the covariates described here were acquired with the imaging assessments. See also Table S1, S5 and S6.

The scanner position was used for controlling for systematic change in the static magnetic field (the last four fields in: http://biobank.ctsu.ox.ac.uk/crystal/label.cgi?id=110). These proxies for scanner position showed minimal correlation with our white matter phenotypes, but in order to achieve a better estimated model, we chose to include them in our models.

Alcohol consumption was self-reported weekly consumption which was used in a published paper on the overall UK Biobank sample of about 500k people (Clarke et al. 2017). We used a slightly different approach to exclude impossible numbers. In the referenced study, they excluded values over 5 standard deviations from mean, and we employed their values as upper and low thresholds instead of calculating our own standard deviations and mean in the sub sample with imaging data, because we have much smaller sample, which may introduce more noise and exclude excessive amount of people.

For smoking status, we used the self-reported smoking status information (http://biobank.ctsu.ox.ac.uk/crystal/field.cgi?id=20116). Participants could chose from one of the four options: (a) current smoker, (b) previous smoker, (c) non-smoker and (d) prefer not to answer. There were NAs for those did not answer. As the number of people who chose 'prefer not to answer' was very small, we did not transfer this into NA so to maximize our sample size. We treated this covariate as a categorical variable in our model. For the sensitivity analysis shown in Table S1, S4 and S5, in order to make it easier for demonstration, we transferred it into a numeric variable (current smoker = 2, previous smoker =1, non-smoker = 0, prefer not to answer = NA). This still represent the effects of smoking to depressive symptoms and white matter microstructure, as it is generally believed that there should be a gradient effect from current smoker to non-smoker.

Stressful life events described the number of events happened within 2 years before scanning session (http://biobank.ctsu.ox.ac.uk/crystal/field.cgi?id=6145). Items include: serious illness, injury or assault to oneself, death of a close relative, death of a spouse or partner, marital separation/divorce and financial difficulties.

## Supplementary results

### Associations between measures of depressive symptoms and NODDI measures

#### One-time assessment of depressive symptoms

No general variation for NODDI measures was found associated with one-time assessment of depressive symptoms (absolute β ranged from 0.002 to 0.022, all $p_{corr} > 0.159$). No tract association was found either for ICVF or OD (absolute β ranged from 0.003 to 0.019, all $p_{corr} > 0.191$). However, ISOVF in anterior thalamic radiation was significantly associated with depressive symptoms (β =0.043, $p_{corr} = 2.49\times10^{-4}$), as was the cingulate gyrus part of cingulum (β =0.028, $p_{corr} = 0.022$).

#### The mean and variability of depressive symptoms derived from multiple assessments

No associations were found between ISOVF, ICVF or OD (all $p_{corr} > 0.143$) and mean of depressive symptoms. ISOVF was associated with greater variability in depressive symptoms in total variance (β = 0.031, $p_{corr} = 0.013$), thalamic radiations (β = 0.024, $p_{corr} = 0.030$), and projection fibres (β = 0.047, $p_{corr} = 5.11\times10^{-4}$). No other measures were associated with variability of depressive symptoms (all $p_{corr} > 0.875$).

Tract-wise analysis showed that ISOVF of anterior thalamic radiations (β = 0.055, $p_{corr} = 8.07\times10^{-7}$), cingulate gyrus part of cingulum (β = 0.032, $p_{corr} = 0.007$) and uncinate fasciculus (β = 0.029, $p_{corr} = 0.020$) were associated with higher mean depressive symptoms. ISOVF of anterior thalamic radiation (β = 0.053, $p_{corr} = 1.45\times10^{-5}$), cingulate gyrus part of cingulum (β = 0.036, $p_{corr} = 0.002$), superior thalamic radiation (β = 0.032, $p_{corr} = 0.003$), forceps major (β = 0.031, $p_{corr} = 0.003$)

and middle cerebellar peduncle (β = 0.048, $p_{corr}$ =5.29×$10^{-4}$) were both associated with variability.

**Longitudinal trajectory of depressive symptoms**

No general variances found associated with slope of longitudinal growth curve for all measures (all $p_{corr}$ > 0.087). Tract-wise, superior thalamic radiation in ISOVF (β = 0.068, $p_{corr}$ = 0.004) was associated with worsening depressive symptoms over time.

**Additional analysis comparing temporal change and longitudinal change**

General variations of association fibres (gAF) was associated with both one-time assessment of depressive symptoms and longitudinal trajectory (see results, Figure 3 in the main text). One-time depressive level should be contributed by (1) mean level and (2) temporal deviation at the time of assessment. Therefore we derived a proxy for temporal deviation by calculating the residuals of one-time depressive level from mean level. This proxy has a N of 8,309.

We then conducted GLM using temporal change of depressive level as a factor on the g measures. On the other hand, longitudinal change showed association with gAF, gTR and gTotal in both MD and ISOVF (see Figure S3, S4 and Table S7).

We then further conducted analysis of structural equational modelling to test how much variance was mediated by NODDI measures. NODDI measures include ICVF (intercellular volume fraction, describing neurite density), ISOVF (isotropic of free water volume fraction, i.e. extracellular water proportion describing the proportion of water outside of cellular space) and OD (orientation dispersion index, describes morphology of tract organisation) (Zhang et al. 2012). There are increasing interests on the use of NODDI measures as complementary dMRI measures in addition to FA and MD since these measures depict additional sources of FA and MD variations which conventional DTI measures cannot distinguish (Beaulieu 2002). These

NODDI measures are relatively new but are encouragingly robust (Zhang et al. 2012) , and importantly have been shown to demonstrate distinct sensitivity to aging (Cox, Ritchie, et al. 2016) and within clinical samples (Rae et al. 2017).

NODDI measures were set as mediators, g of white matter microstructure was the outcomes, and finally temporal and longitudinal changes of depressive symptoms were the predictors. Results were shown in Figure S6.

Though both temporal and longitudinal change showed associations with gAF, gTR and gTotal, temporal change had associations with ICVF for these g measures, whereas the associations for longitudinal change was shown in ISOVF. Although both one-time measure and longitudinal trajectory had association with gAF in MD, they showed distinct effects in NODDI measures. We conducted an additional analysis for temporal change at the one-time assessments in relation to mean level across time (supplementary methods) to compare the differences between temporal and longitudinal changes in NODDI measures. We found that neurite density (ICVF) were more associated with temporal change, and reduced isotropic water proportion (ISOVF) was associate with longitudinal change (Figure S9). Neurite density is closely related to changeable brain structural features like myelination(Rae et al. 2017), whereas reduced ISOVF may reflect a more severe level of the dispersed structure in neuronal tissue. It therefore indicate that temporal deviation at the one-time assessment and longitudinal change may have distinct neurobiological reversibility and severity(Kamagata et al. 2017).

## Measures of depressive symptoms and their associations with MDD phenotypes

### Association with age and gender

Depressive symptoms at the imaging assessment, as well as the mean and variability over time, all showed a negative association with age (β ranged from -

0.212 to -0.143, $p<1X10^{-6}$). Each measure was higher in females (Cohen's d ranged from -0.197 to -0.150, $p<2.35X10^{-12}$, male=1, female=0), except for longitudinal slope of depressive symptoms (Cohen's d=-0.048, p=0.296). Its association with age was not tested because for better estimation of growth curve, age was controlled for in each time point of assessment.

Association with MDD phenotypes

We then tested the associations between the four measures of depressive symptoms and phenotypes for life-time MDD (MDD-self, MDD-status and MDD-CIDI), (see legend of Table S8 and supplementary methods). All four measures for depressive symptoms were positively associated with all MDD phenotypes (odds ratios for a standard deviation change in each measure ranged from 1.153 to 3.414, $p<6.15\times10^{-16}$). Among the three measures, mean depressive symptoms level showed the largest effect sizes for association with major depression, and longitudinal slope showed the smallest (Table S8). Correlations between them were shown in Table S2.

**Effect of partial-volume contamination to FA and MD**

We observed differences of results for FA and MD. To control for possible effects of partial-volume contamination related to structural atrophy, we have included age and $age^2$ as covariates(Smith and Nichols 2018). We also conducted an additional analysis including brain size as one of the covariates and the results remained significant for MD except for one association turned null (Figure S8).

Figure S1. Description of sample sizes and changes due to each step of data merging or outlier removal. Depre = depressive level at the imaging assessment, depre.mean = mean level of depressive symptoms based on multiple assessments for at least two times, depre.instability = standard deviation of depressive level of multiple assessments for at least three times, and depre.longitudinal = slope of longitudinal changes over all four times of assessments.

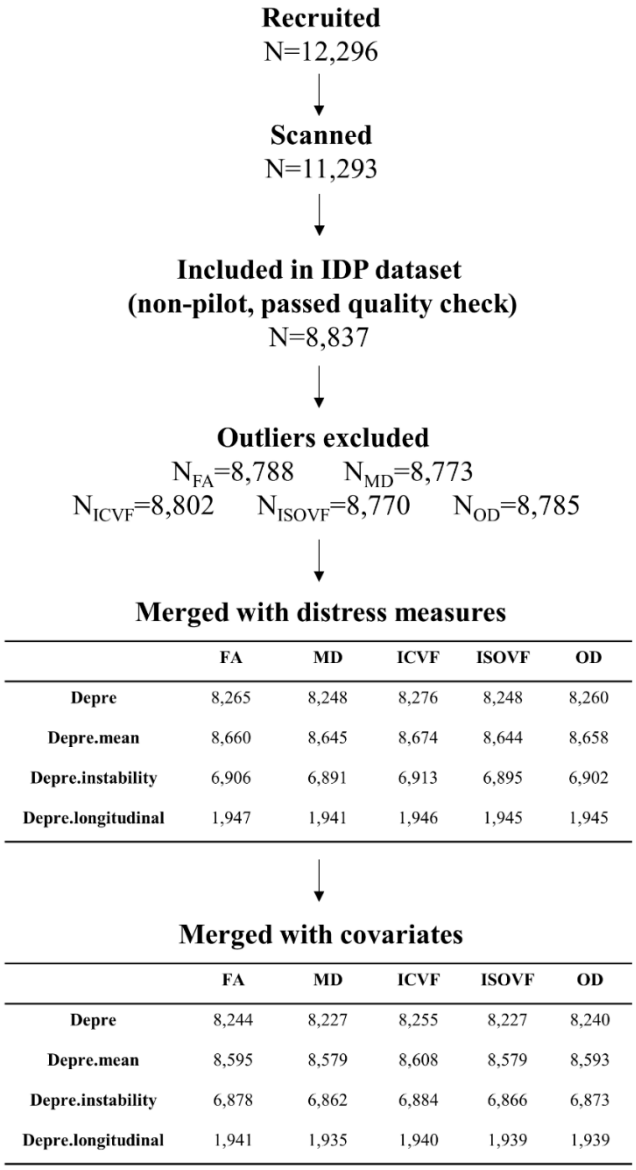


| | FA | MD | ICVF | ISOVF | OD |
|---|---|---|---|---|---|
| **Depre** | 8,265 | 8,248 | 8,276 | 8,248 | 8,260 |
| **Depre.mean** | 8,660 | 8,645 | 8,674 | 8,644 | 8,658 |
| **Depre.instability** | 6,906 | 6,891 | 6,913 | 6,895 | 6,902 |
| **Depre.longitudinal** | 1,947 | 1,941 | 1,946 | 1,945 | 1,945 |



**Merged with covariates**

| | FA | MD | ICVF | ISOVF | OD |
|---|---|---|---|---|---|
| **Depre** | 8,244 | 8,227 | 8,255 | 8,227 | 8,240 |
| **Depre.mean** | 8,595 | 8,579 | 8,608 | 8,579 | 8,593 |
| **Depre.instability** | 6,878 | 6,862 | 6,884 | 6,866 | 6,873 |
| **Depre.longitudinal** | 1,941 | 1,935 | 1,940 | 1,939 | 1,939 |

Figure S2. Distributions PHQ-4 and derived measures for depressive symptoms. (a) Density map for all four time points of assessments for PHQ-4. Instance 2 was for imaging assessment, and the depressive level acquired from this instance was used as a baseline, one-time measure for depressive symptoms. The mean depressive level over a minimum of two time points of assessment was also presented in this sub-figure (Depre.mean). (b) Density map for instability of depressive symptoms (Depre.instability). (c) Density map for the distribution of slope for longitudinal trajectory of depressive level over four instances (Depre.longitudinal).

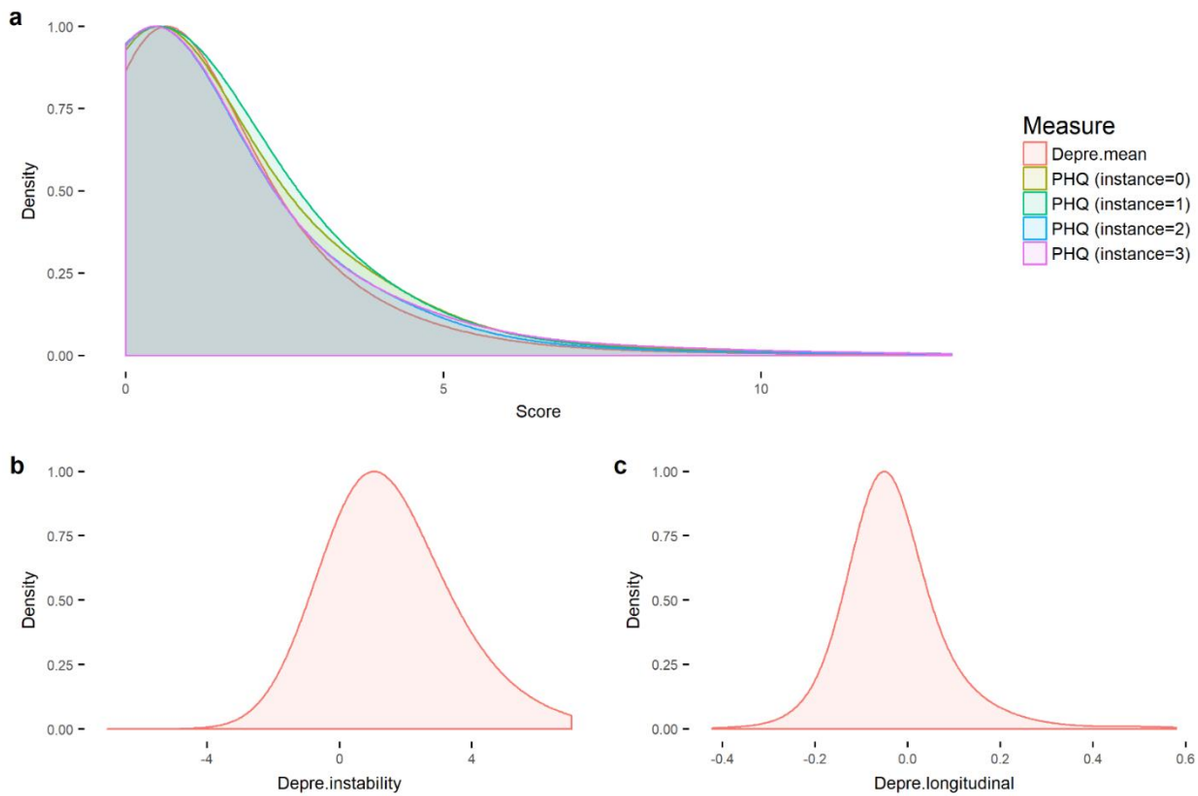

Figure S3. Results for the main model, including results for NODDI measures. More descriptive statistics were shown in Table S2 and S3, results in the main text and supplementary results. In the heatmaps, each colour theme represents one dMRI measure. For the measures of depressive symptoms: depre = depressive level at the imaging assessment, depre.mean = mean level of depressive symptoms based on multiple assessments for at least two times, depre.instability = standard deviation of depressive level of multiple assessments for at least three times, and depre.longitudinal = slope of longitudinal changes over all four times of assessments. As the measures of FA, ICVF and OD have negative direction with MD and ISOVF, here in this figure, the effect sizes for FA, ICVF and OD were reversed (×-1). Significant associations after FWE correction on 15 tracts/four g measures ($p_{corr}$<0.05) were marked with a single asterisk.

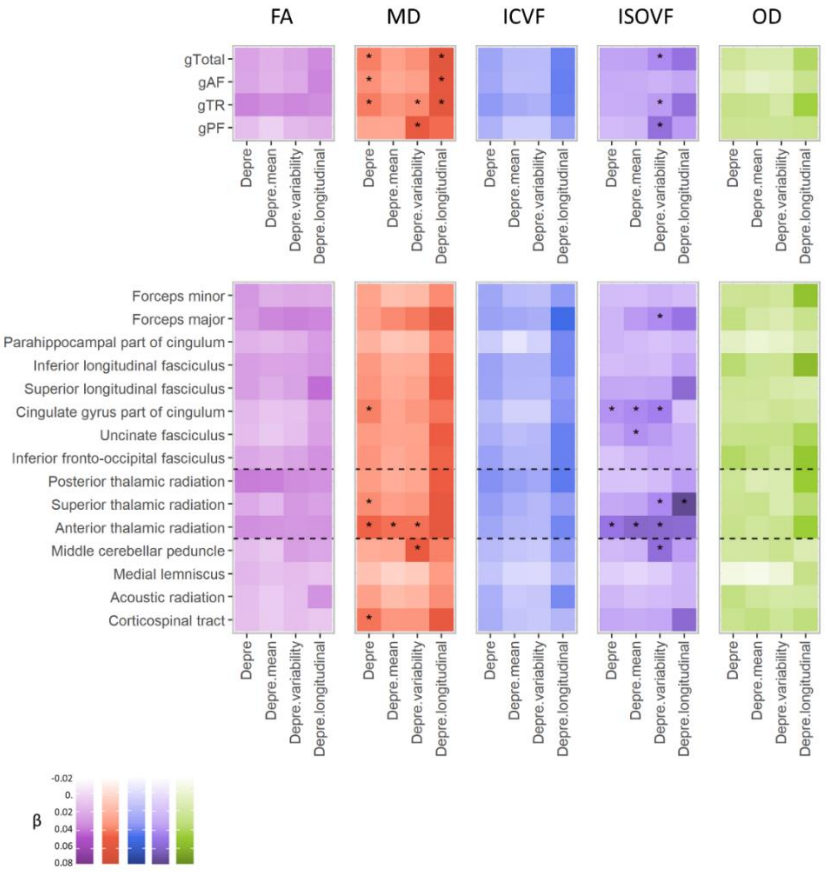

Figure S4. Results for the main model using two different multiple correction methods. More descriptive statistics were shown in Table S2 and S3, results in the main text and supplementary results. In the heatmaps, each colour theme represents one dMRI measure. For the measures of depressive symptoms: depre = depressive level at the imaging assessment, depre.mean = mean level of depressive symptoms based on multiple assessments for at least two times, depre.instability = standard deviation of depressive level of multiple assessments for at least three times, and depre.longitudinal = slope of longitudinal changes over all four times of assessments. As the measures of FA, ICVF and OD have negative direction with MD and ISOVF, here in this figure, the effect sizes for FA, ICVF and OD were reversed (×-1). Significant associations after FWE correction on 15 tracts/four g measures ($p_{corr}$<0.05) were marked with a single asterisk, and significant associations after FDR-correcting on all the tests within a dMRI measure (15 tracts * 4 measures for depressive symptoms=60 tests) were marked by a double asterisk.

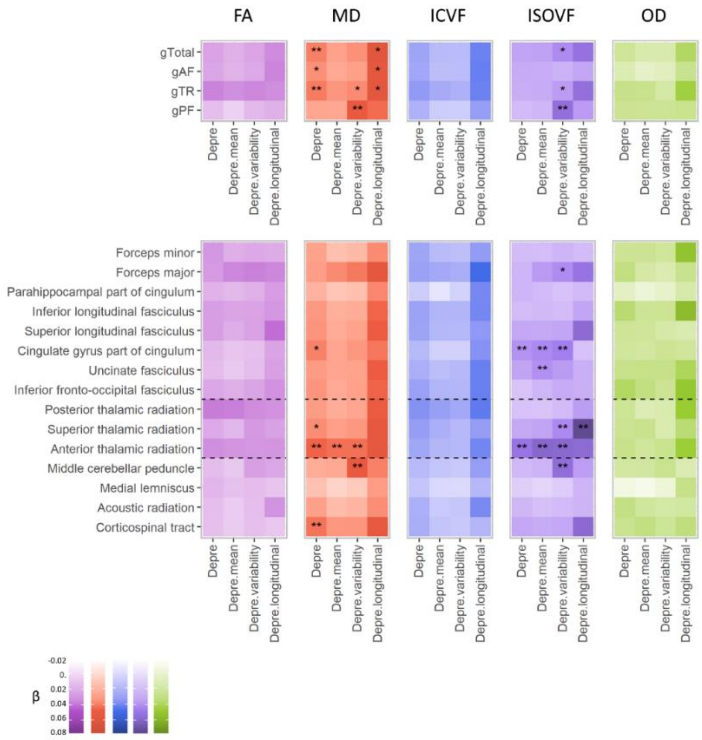

Figure S5. Results for including outliers in the sample. Outlier exclusion procedures were shown in methods in the main text. Significant associations appeared in this sample including outliers but did not in the main results described in the main text were marked with blue squares. No association was exclusively in the main results from which the sample excluded outliers. For the abbreviations and multiple correction methods, see the legend of Figure S2.

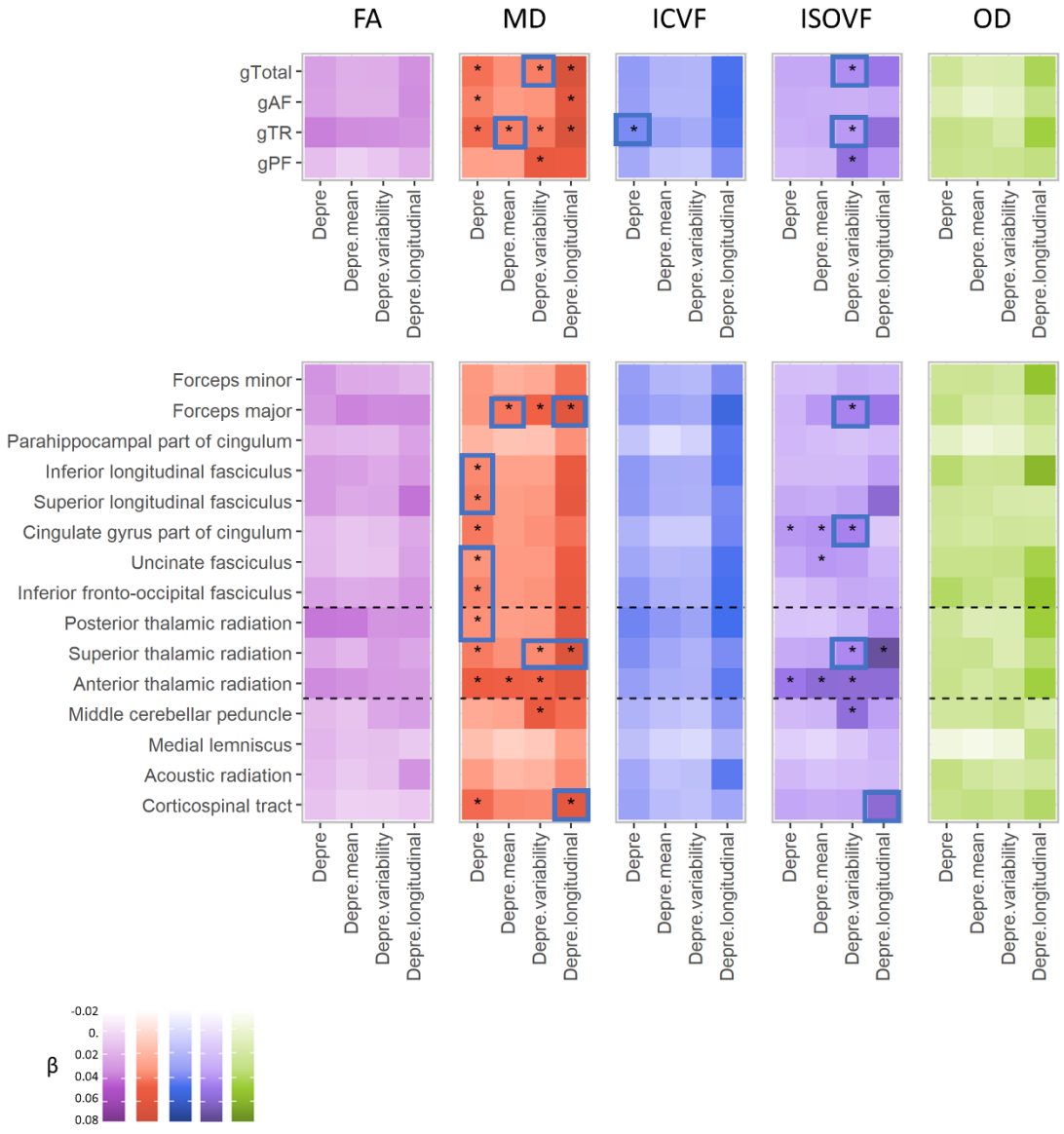

Figure S6. Variance explained by the principal components of PCA on total and subsets of white matter tracts.

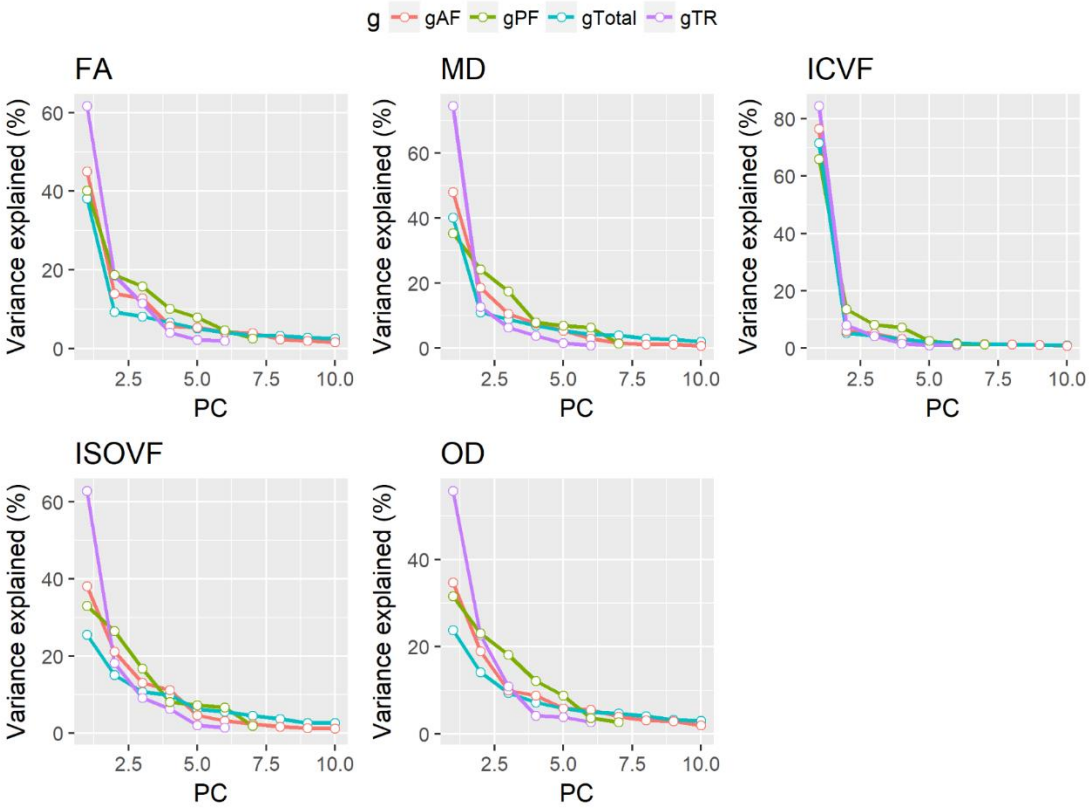

Figure S7. Results for the secondary model without controlling for stressful life events, smoking status or alcohol consumption. Significant associations appeared in this secondary model but did not in the main model were marked with blue squares. Yellow squares are the significant associations exclusively appeared in the main model. The results may indicate that controlling for the four covariates helped to remove confounding/mediating factors rather than creating bias (more blue squares than yellow ones). More descriptive statistics were shown in Table S1,4 and 5. For the abbreviations and multiple correction methods, see the legend of Figure S2.

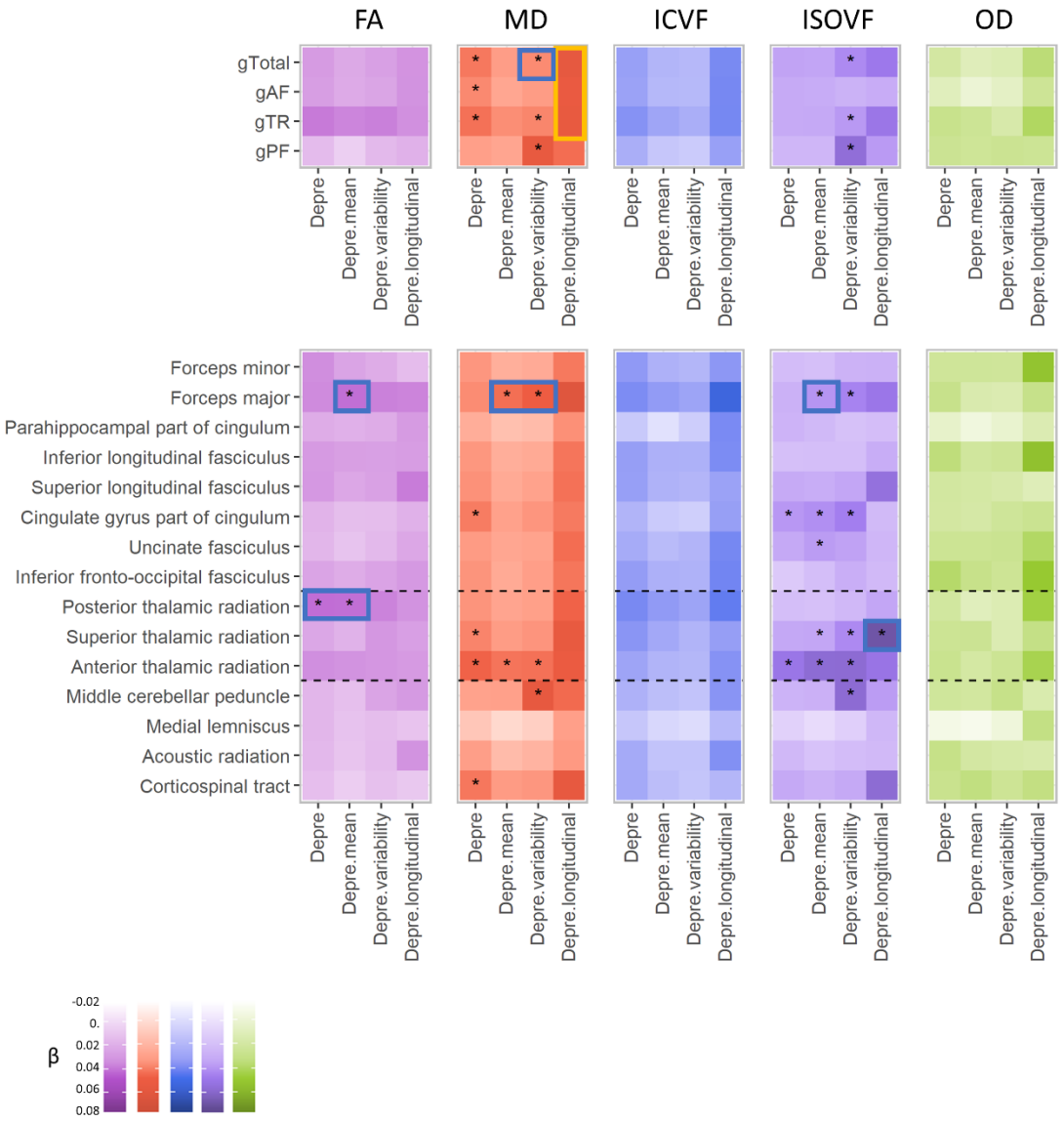


Figure S8. Results for adding brain size as a covariate. The yellow square indicates the significant associations exclusively appeared in the main model. No other associations turned null after controlling for brain size.

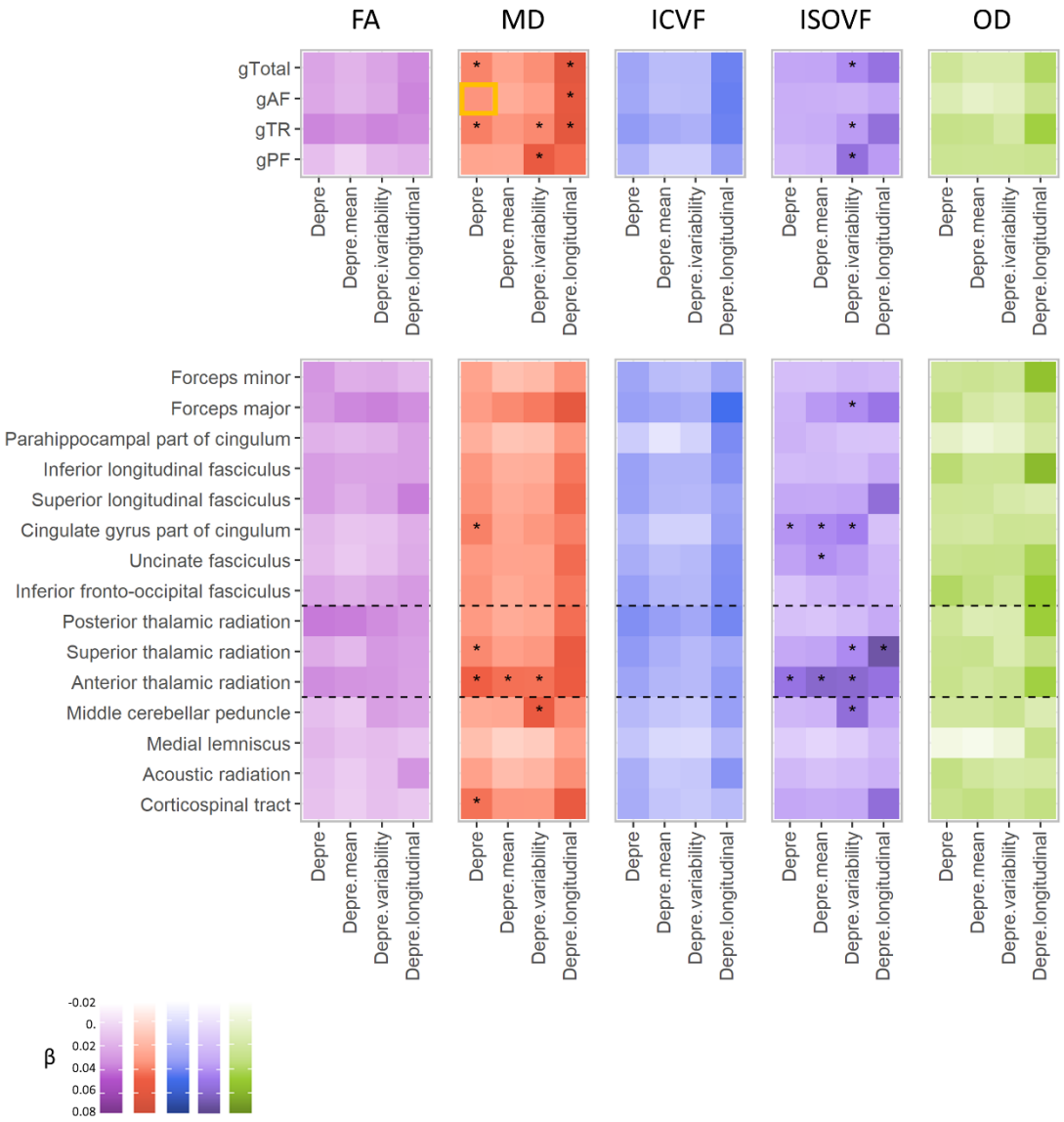
FA
MD
ICVF
ISOVF
OD
gTotal
gAF
gTR
gPF
Depre
Depre.mean
Depre.ivariability
Depre.longitudinal
Forceps minor
Forceps major
Parahippocampal part of cingulum
Inferior longitudinal fasciculus
Superior longitudinal fasciculus
Cingulate gyrus part of cingulum
Uncinate fasciculus
Inferior fronto-occipital fasciculus
Posterior thalamic radiation
Superior thalamic radiation
Anterior thalamic radiation
Middle cerebellar peduncle
Medial lemniscus
Acoustic radiation
Corticospinal tract
Depre.variability
β
-0.02
0.
0.02
0.04
0.06
0.08

Figure S9. Mediation analysis for temporal and longitudinal change of depressive symptoms. Details for the analysis were stated in supplementary methods. (a) the path for mediation analysis. (b) mediation effect for ICVF. TC = temporal change, and LC = longitudinal change. (c) mediation effect for ISOVF. Bars marked by asterixis showed significant indirect effect through mediation.

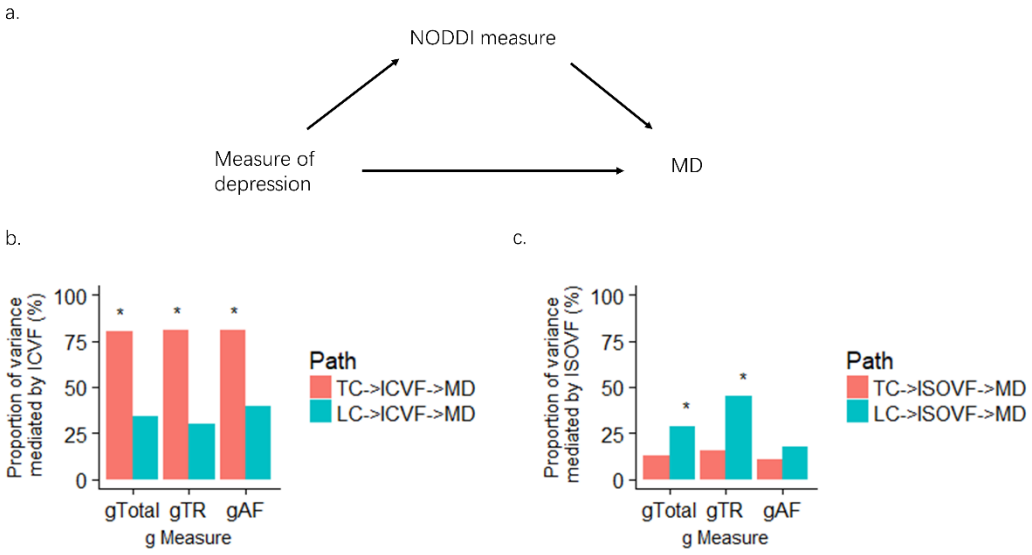


Table S1. Correlation matrix for all measures for depressive symptoms, smoking status, alcohol consumption, stressful life events, neuroticism and age range (time lag) for the multiple assessments used for generating mean level of depressive symptoms. For the measures of depressive symptoms: depre = depressive level at the imaging assessment, depre.mean = mean level of depressive symptoms based on multiple assessments for at least two times, depre.instability = standard deviation of depressive level of multiple assessments for at least three times, and depre.longitudinal = slope of longitudinal changes over all four times of assessments. All r>0.3 were highlighted in bold. Measures for depressive symptoms were correlated with one another. None of the covariates or age range was correlated with measures for depressive symptoms apart from neuroticism. This justifies that controlling for smoking status, alcohol consumption, stressful life events (SLE) would

serve for adjusting the effects rather than creating bias (Figure S3). For neuroticism, we did not find any significant association with any of the dMRI measures in the overall IDP sample after outliers were removed (N~=8,200, sample size varies according to the dMRI measure, see Table S4,5).

| | Distress | Distress.instability | Distress.mean | Distress.longitudinal | Smoking | Alcohol | SLE | N of occasions | Time lag |
|---|---|---|---|---|---|---|---|---|---|
| Distress | 1 | **0.804** | **0.528** | **0.566** | 0.038 | -0.015 | 0.164 | -- | -- |
| Distress.instability | **0.804** | 1 | **0.732** | **0.447** | 0.056 | -0.027 | 0.19 | -0.027 | 0.032 |
| Distress.mean | **0.528** | **0.732** | 1 | **0.305** | 0.034 | -0.034 | 0.119 | -0.064 | 0.012 |
| Distress.longitudinal | **0.566** | **0.447** | **0.305** | 1 | 0.01 | -0.008 | 0.102 | -- | 0.022 |
| Smoking | 0.038 | 0.056 | 0.034 | 0.01 | 1 | 0.196 | -0.01 | 0.012 | 0.024 |
| Alcohol | -0.015 | -0.027 | -0.034 | -0.008 | 0.196 | 1 | -0.057 | 0.017 | 0.022 |
| SLE | 0.164 | 0.19 | 0.119 | 0.102 | -0.01 | -0.057 | 1 | 0.001 | 0.033 |
| N of occassions | -- | -0.027 | -0.064 | -- | 0.012 | 0.017 | 0.001 | 1 | -0.029 |
| Time lag | -- | 0.032 | 0.012 | 0.022 | 0.024 | 0.022 | 0.033 | -0.029 | 1 |

Table S2. Correlation loadings of each tract of PCA. For each dMRI measure, PCA on all tracts, association fibres, thalamic radiations and projection fibres were performed respectively. The loadings were reported as correlation loadings.

| Tract | FA | | | | MD | | | | ICVF | | | | ISOVF | | | | OD | | | |
|---|---|---|---|---|---|---|---|---|---|---|---|---|---|---|---|---|---|---|---|---|
| | gTotal | gAF | gTR | gPF | gTotal | gAF | gTR | gPF | gTotal | gAF | gTR | gPF | gTotal | gAF | gTR | gPF | gTotal | gAF | gTR | gPF |
| Parahippocampal part of cingulum | 0.363 | 0.363 | -- | -- | 0.47 | 0.575 | -- | -- | 0.619 | 0.627 | -- | -- | 0.577 | 0.821 | -- | -- | 0.724 | 0.864 | -- | -- |
| Parahippocampal part of cingulum | 0.412 | 0.423 | -- | -- | 0.444 | 0.55 | -- | -- | 0.637 | 0.648 | -- | -- | 0.584 | 0.832 | -- | -- | 0.669 | 0.831 | -- | -- |
| Forceps major | 0.544 | 0.557 | -- | -- | 0.502 | 0.562 | -- | -- | 0.796 | 0.795 | -- | -- | 0.272 | 0.267 | -- | -- | 0.185 | 0.1 | -- | -- |
| Cingulate gyrus part of cingulum | 0.558 | 0.634 | -- | -- | 0.653 | 0.611 | -- | -- | 0.792 | 0.806 | -- | -- | 0.419 | 0.248 | -- | -- | 0.251 | 0.183 | -- | -- |
| Cingulate gyrus part of cingulum | 0.585 | 0.662 | -- | -- | 0.657 | 0.626 | -- | -- | 0.795 | 0.81 | -- | -- | 0.396 | 0.261 | -- | -- | 0.251 | 0.178 | -- | -- |
| Uncinate fasciculus | 0.654 | 0.675 | -- | -- | 0.675 | 0.727 | -- | -- | 0.801 | 0.818 | -- | -- | 0.47 | 0.404 | -- | -- | 0.48 | 0.445 | -- | -- |
| Uncinate fasciculus | 0.694 | 0.709 | -- | -- | 0.762 | 0.791 | -- | -- | 0.845 | 0.862 | -- | -- | 0.531 | 0.427 | -- | -- | 0.519 | 0.491 | -- | -- |
| Forceps minor | 0.805 | 0.806 | -- | -- | 0.731 | 0.678 | -- | -- | 0.912 | 0.928 | -- | -- | 0.473 | 0.215 | -- | -- | 0.384 | 0.255 | -- | -- |
| Superior longitudinal fasciculus | 0.822 | 0.813 | -- | -- | 0.866 | 0.813 | -- | -- | 0.933 | 0.935 | -- | -- | 0.672 | 0.373 | -- | -- | 0.431 | 0.193 | -- | -- |
| Superior longitudinal fasciculus | 0.836 | 0.818 | -- | -- | 0.849 | 0.789 | -- | -- | 0.93 | 0.93 | -- | -- | 0.682 | 0.378 | -- | -- | 0.449 | 0.197 | -- | -- |
| Inferior longitudinal fasciculus | 0.827 | 0.821 | -- | -- | 0.872 | 0.872 | -- | -- | 0.939 | 0.942 | -- | -- | 0.696 | 0.453 | -- | -- | 0.511 | 0.407 | -- | -- |
| Inferior fronto-occipital fasciculus | 0.817 | 0.824 | -- | -- | 0.865 | 0.854 | -- | -- | 0.942 | 0.948 | -- | -- | 0.68 | 0.439 | -- | -- | 0.477 | 0.379 | -- | -- |

| | | | | | | | | | | | | | | | | | | | | |
|---|---|---|---|---|---|---|---|---|---|---|---|---|---|---|---|---|---|---|---|---|
| Inferior longitudinal fasciculus | 0.852 | 0.833 | -- | -- | 0.91 | 0.892 | -- | -- | 0.946 | 0.944 | -- | -- | 0.753 | 0.48 | -- | -- | 0.561 | 0.458 | -- | -- |
| Inferior fronto-occipital fasciculus | 0.853 | 0.843 | -- | -- | 0.912 | 0.884 | -- | -- | 0.953 | 0.956 | -- | -- | 0.708 | 0.45 | -- | -- | 0.516 | 0.401 | -- | -- |
| Superior thalamic radiation | 0.661 | -- | 0.75 | -- | 0.778 | -- | 0.853 | -- | 0.881 | -- | 0.923 | -- | 0.626 | -- | 0.708 | -- | 0.512 | -- | 0.902 | -- |
| Superior thalamic radiation | 0.645 | -- | 0.752 | -- | 0.74 | -- | 0.829 | -- | 0.87 | -- | 0.918 | -- | 0.598 | -- | 0.698 | -- | 0.52 | -- | 0.911 | -- |
| Posterior thalamic radiation | 0.681 | -- | 0.778 | -- | 0.762 | -- | 0.86 | -- | 0.877 | -- | 0.9 | -- | 0.64 | -- | 0.867 | -- | 0.41 | -- | 0.287 | -- |
| Posterior thalamic radiation | 0.683 | -- | 0.805 | -- | 0.778 | -- | 0.882 | -- | 0.879 | -- | 0.905 | -- | 0.675 | -- | 0.888 | -- | 0.429 | -- | 0.349 | -- |
| Anterior thalamic radiation | 0.78 | -- | 0.806 | -- | 0.841 | -- | 0.864 | -- | 0.906 | -- | 0.936 | -- | 0.624 | -- | 0.618 | -- | 0.536 | -- | 0.587 | -- |
| Anterior thalamic radiation | 0.775 | -- | 0.818 | -- | 0.833 | -- | 0.87 | -- | 0.898 | -- | 0.931 | -- | 0.629 | -- | 0.651 | -- | 0.557 | -- | 0.669 | -- |
| Medial lemniscus | 0.267 | -- | -- | 0.501 | 0.209 | -- | -- | 0.169 | 0.49 | -- | -- | 0.721 | 0.349 | -- | -- | 0.262 | 0.223 | -- | -- | 0.288 |
| Medial lemniscus | 0.287 | -- | -- | 0.534 | 0.183 | -- | -- | 0.137 | 0.481 | -- | -- | 0.719 | 0.36 | -- | -- | 0.258 | 0.292 | -- | -- | 0.328 |
| Middle cerebellar peduncle | 0.359 | -- | -- | 0.545 | 0.305 | -- | -- | 0.975 | 0.53 | -- | -- | 0.738 | 0.331 | -- | -- | 0.972 | 0.345 | -- | -- | 0.781 |
| Acoustic radiation | 0.623 | -- | -- | 0.553 | 0.512 | -- | -- | 0.241 | 0.876 | -- | -- | 0.867 | 0.317 | -- | -- | 0.039 | 0.324 | -- | -- | 0.355 |
| Acoustic radiation | 0.646 | -- | -- | 0.619 | 0.546 | -- | -- | 0.199 | 0.873 | -- | -- | 0.874 | 0.366 | -- | -- | -0.007 | 0.37 | -- | -- | 0.361 |
| Corticospinal tract | 0.566 | -- | -- | 0.809 | 0.59 | -- | -- | 0.237 | 0.787 | -- | -- | 0.852 | 0.351 | -- | -- | 0.039 | 0.425 | -- | -- | 0.629 |
| Corticospinal tract | 0.574 | -- | -- | 0.828 | 0.593 | -- | -- | 0.237 | 0.771 | -- | -- | 0.843 | 0.412 | -- | -- | 0.075 | 0.454 | -- | -- | 0.654 |

Table S3. Main results for DTI measures (FA and MD). Betas were standardised effect sizes. P values were un-corrected p values. All $p_{corrected}<0.05$ were marked by asterixis. FDR correction was applied on subsets of brain measures within a unit of a whole brain (n=15 for tract analysis, and n=4 for g analysis). For the measures of depressive symptoms: depre = depressive level at the imaging assessment, depre.mean = mean level of depressive symptoms based on multiple assessments for at least two times, depre.instability = standard deviation of depressive level of multiple assessments for at least three times, and depre.longitudinal = slope of longitudinal changes over all four times of assessments.

| | | **Depre** | | **Depre.mean** | | **Depre.instability** | | **Depre.longitudinal** | |
|---|---|---|---|---|---|---|---|---|---|
| **Tract name** | **Measure** | **Beta** | **p** | **Beta** | **p** | **Beta** | **p** | **Beta** | **p** |
| g.Total | FA | -0.011 (0.011) | 0.315 | -0.004 (0.011) | 0.735 | -0.01 (0.012) | 0.394 | -0.022 (0.023) | 0.341 |
| | MD | 0.028 (0.01) | 0.008* | 0.015 (0.011) | 0.146 | 0.022 (0.011) | 0.046 | 0.056 (0.023) | 0.014* |
| g.AF | FA | -0.009 (0.011) | 0.393 | -0.003 (0.011) | 0.8 | -0.007 (0.012) | 0.531 | -0.024 (0.023) | 0.302 |
| | MD | 0.023 (0.011) | 0.032* | 0.011 (0.011) | 0.323 | 0.016 (0.011) | 0.172 | 0.05 (0.023) | 0.026* |
| g.TR | FA | -0.024 (0.011) | 0.029 | -0.02 (0.011) | 0.072 | -0.023 (0.012) | 0.052 | -0.021 (0.023) | 0.361 |
| | MD | 0.029 (0.01) | 0.003* | 0.021 (0.01) | 0.031 | 0.024 (0.01) | 0.022* | 0.053 (0.022) | 0.016* |
| g.PF | FA | 0.003 (0.011) | 0.802 | 0.012 (0.011) | 0.262 | -1.41e-04 (0.012) | 0.99 | -0.004 (0.022) | 0.873 |
| | MD | 0.013 (0.011) | 0.259 | 0.012 (0.011) | 0.3 | 0.045 (0.012) | 2.05e-04* | 0.034 (0.022) | 0.122 |
| | | | | | | | | | |
| Acoustic radiation | FA | 0.003 (0.01) | 0.784 | 0.009 (0.01) | 0.333 | 0.003 (0.01) | 0.783 | -0.019 (0.019) | 0.336 |

| | | | | | | | | | |
|---|---|---|---|---|---|---|---|---|---|
| | MD | 0.016 (0.01) | 0.102 | 6.63e-04 (0.01) | 0.945 | 0.005 (0.01) | 0.646 | 0.023 (0.019) | 0.225 |
| Anterior thalamic radiation | FA | -0.021 (0.01) | 0.05 | -0.018 (0.011) | 0.091 | -0.017 (0.011) | 0.145 | -0.018 (0.022) | 0.413 |
| | MD | 0.036 (0.01) | 1.48e-04* | 0.032 (0.01) | 8.90e-04* | 0.032 (0.01) | 0.002* | 0.05 (0.022) | 0.024 |
| Cingulate gyrus part of cingulum | FA | 4.43e-04 (0.01) | 0.964 | 0.006 (0.01) | 0.546 | 0.004 (0.011) | 0.702 | -0.01 (0.02) | 0.614 |
| | MD | 0.027 (0.01) | 0.005* | 0.013 (0.01) | 0.193 | 0.02 (0.011) | 0.057 | 0.03 (0.02) | 0.13 |
| Parahippocampal part of cingulum | FA | -0.003 (0.01) | 0.749 | -4.52e-04 (0.01) | 0.964 | -0.004 (0.011) | 0.741 | -0.014 (0.02) | 0.476 |
| | MD | 0.006 (0.01) | 0.541 | -0.004 (0.01) | 0.676 | -0.001 (0.011) | 0.919 | 0.025 (0.02) | 0.195 |
| Corticospinal tract | FA | 0.003 (0.01) | 0.759 | 0.01 (0.01) | 0.343 | 0.003 (0.011) | 0.758 | 0.007 (0.021) | 0.735 |
| | MD | 0.031 (0.01) | 0.003* | 0.02 (0.011) | 0.055 | 0.021 (0.012) | 0.075 | 0.049 (0.02) | 0.016 |
| Inferior fronto occipital fasciculus | FA | -0.009 (0.011) | 0.405 | -0.004 (0.011) | 0.683 | -0.01 (0.011) | 0.387 | -0.019 (0.022) | 0.384 |
| | MD | 0.021 (0.01) | 0.037 | 0.01 (0.01) | 0.319 | 0.015 (0.011) | 0.171 | 0.036 (0.021) | 0.094 |
| Inferior longitudinal fasciculus | FA | -0.013 (0.01) | 0.212 | -0.01 (0.011) | 0.332 | -0.011 (0.011) | 0.343 | -0.017 (0.022) | 0.455 |
| | MD | 0.019 (0.01) | 0.056 | 0.007 (0.01) | 0.473 | 0.009 (0.011) | 0.414 | 0.036 (0.021) | 0.097 |
| Medial lemniscus | FA | -0.001 (0.009) | 0.897 | 0.004 (0.01) | 0.656 | 0.002 (0.01) | 0.852 | 0.006 (0.019) | 0.76 |
| | MD | -0.002 (0.01) | 0.841 | -0.011 (0.01) | 0.255 | -0.007 (0.011) | 0.493 | 0.018 (0.019) | 0.356 |
| Posterior thalamic radiation | FA | -0.026 (0.01) | 0.01 | -0.026 (0.01) | 0.013 | -0.021 (0.011) | 0.054 | -0.019 (0.021) | 0.365 |
| | MD | 0.017 (0.01) | 0.07 | 0.009 (0.01) | 0.344 | 0.013 (0.01) | 0.218 | 0.04 (0.021) | 0.055 |

| | | | | | | | | | |
|---|---|---|---|---|---|---|---|---|---|
| Superior longitudinal fasciculus | FA | -0.013 (0.011) | 0.217 | -0.005 (0.011) | 0.61 | -0.011 (0.011) | 0.332 | -0.031 (0.022) | 0.162 |
| | MD | 0.022 (0.01) | 0.036 | 0.01 (0.01) | 0.342 | 0.014 (0.011) | 0.209 | 0.039 (0.022) | 0.08 |
| Superior thalamic radiation | FA | -0.007 (0.011) | 0.488 | -6.68e-04 (0.011) | 0.951 | -0.016 (0.012) | 0.183 | -0.011 (0.022) | 0.609 |
| | MD | 0.024 (0.009) | 0.008* | 0.016 (0.009) | 0.081 | 0.02 (0.01) | 0.041 | 0.051 (0.02) | 0.013 |
| Uncinate fasciculus | FA | 0.002 (0.01) | 0.859 | 0.008 (0.01) | 0.41 | 0.003 (0.011) | 0.8 | -0.012 (0.021) | 0.572 |
| | MD | 0.018 (0.009) | 0.053 | 0.013 (0.01) | 0.159 | 0.014 (0.01) | 0.165 | 0.04 (0.02) | 0.047 |
| Forceps major | FA | -0.014 (0.011) | 0.189 | -0.023 (0.011) | 0.04 | -0.025 (0.012) | 0.035 | -0.023 (0.022) | 0.298 |
| | MD | 0.017 (0.011) | 0.128 | 0.025 (0.011) | 0.027 | 0.03 (0.012) | 0.012 | 0.052 (0.022) | 0.018 |
| Forceps minor | FA | -0.017 (0.011) | 0.132 | -0.005 (0.011) | 0.655 | -0.007 (0.012) | 0.557 | -0.006 (0.023) | 0.801 |
| | MD | 0.014 (0.011) | 0.183 | -0.001 (0.011) | 0.897 | 0.002 (0.011) | 0.831 | 0.024 (0.022) | 0.263 |
| Middle cerebellar peduncle | FA | 0.002 (0.011) | 0.841 | 0.008 (0.011) | 0.505 | -0.013 (0.012) | 0.301 | -0.009 (0.023) | 0.702 |
| | MD | 0.009 (0.011) | 0.412 | 0.012 (0.011) | 0.305 | 0.045 (0.012) | 2.05e-04* | 0.028 (0.022) | 0.207 |

Table S4. Main results for NODDI measures (ICVF, ISOVF, and OD). Betas were standardised effect sizes. P values were un-corrected p values. All $p_{corrected}$<0.05 were marked by asterixis. FDR correction was applied on subsets of brain measures within a unit of a whole brain (n=15 for tract analysis, and n=4 for g analysis). For the abbreviations of measures for depressive symptoms, see the legend of Table S2.

| | | Depre | | Depre.mean | | Depre.instability | | Depre.longitudinal | |
|---|---|---|---|---|---|---|---|---|---|
| Tract name | Measure | Beta | p | Beta | p | Beta | p | Beta | p |
| g.Total | ICVF | -0.016 (0.011) | 0.157 | -0.003 (0.011) | 0.8 | -0.002 (0.012) | 0.858 | -0.031 (0.023) | 0.19 |
| | ISOVF | 0.021 (0.01) | 0.04 | 0.022 (0.011) | 0.036 | 0.031 (0.011) | 0.006* | 0.045 (0.022) | 0.044 |
| | OD | -0.009 (0.011) | 0.406 | -2.83e-04 (0.011) | 0.979 | -4.74e-04 (0.012) | 0.967 | -0.028 (0.021) | 0.2 |
| g.AF | ICVF | -0.014 (0.011) | 0.2 | -0.001 (0.011) | 0.909 | -0.002 (0.012) | 0.875 | -0.032 (0.023) | 0.175 |
| | ISOVF | 0.017 (0.011) | 0.119 | 0.016 (0.011) | 0.144 | 0.012 (0.012) | 0.302 | 0.02 (0.023) | 0.376 |
| | OD | 0.002 (0.011) | 0.825 | 0.012 (0.011) | 0.278 | 0.007 (0.012) | 0.552 | -0.013 (0.022) | 0.533 |
| g.TR | ICVF | -0.022 (0.011) | 0.044 | -0.012 (0.011) | 0.259 | -0.008 (0.012) | 0.48 | -0.03 (0.023) | 0.188 |
| | ISOVF | 0.015 (0.01) | 0.117 | 0.017 (0.01) | 0.078 | 0.024 (0.011) | 0.022* | 0.047 (0.021) | 0.025 |
| | OD | -0.016 (0.01) | 0.124 | -0.014 (0.01) | 0.176 | -0.003 (0.011) | 0.754 | -0.035 (0.021) | 0.097 |
| g.PF | ICVF | -0.008 (0.011) | 0.484 | 0.007 (0.011) | 0.506 | 0.008 (0.012) | 0.502 | -0.019 (0.023) | 0.387 |
| | ISOVF | 0.007 (0.011) | 0.516 | 0.01 (0.011) | 0.39 | 0.047 (0.012) | 1.28e-04* | 0.025 (0.023) | 0.27 |

| | | | | | | | | | |
|---|---|---|---|---|---|---|---|---|---|
| | OD | -0.012 (0.011) | 0.275 | -0.011 (0.011) | 0.319 | -0.011 (0.012) | 0.356 | -0.013 (0.022) | 0.541 |
| | | | | | | | | | |
| Acoustic radiation | ICVF | -0.009 (0.011) | 0.39 | 0.006 (0.011) | 0.587 | 0.004 (0.012) | 0.746 | -0.028 (0.022) | 0.213 |
| | ISOVF | 0.01 (0.009) | 0.302 | 0.004 (0.01) | 0.662 | 0.007 (0.01) | 0.497 | 0.012 (0.019) | 0.539 |
| | OD | -0.018 (0.009) | 0.051 | -0.008 (0.009) | 0.41 | -0.003 (0.01) | 0.756 | -0.006 (0.018) | 0.756 |
| Anterior thalamic radiation | ICVF | -0.015 (0.01) | 0.157 | -0.005 (0.01) | 0.612 | -0.004 (0.011) | 0.706 | -0.029 (0.023) | 0.204 |
| | ISOVF | 0.043 (0.01) | 1.66e-05* | 0.055 (0.01) | 5.38e-08* | 0.053 (0.011) | 9.65e-07* | 0.051 (0.021) | 0.016 |
| | OD | -0.015 (0.01) | 0.151 | -0.007 (0.01) | 0.475 | -0.012 (0.011) | 0.262 | -0.037 (0.021) | 0.078 |
| Cingulate gyrus part of cingulum | ICVF | -0.004 (0.01) | 0.733 | 0.01 (0.01) | 0.351 | 0.01 (0.011) | 0.398 | -0.024 (0.022) | 0.268 |
| | ISOVF | 0.028 (0.009) | 0.003* | 0.032 (0.01) | 9.93e-04* | 0.036 (0.01) | 4.60e-04* | 0.003 (0.019) | 0.895 |
| | OD | -0.008 (0.009) | 0.398 | -0.005 (0.009) | 0.552 | -0.011 (0.01) | 0.26 | -0.007 (0.018) | 0.681 |
| Parahippocampal part of cingulum | ICVF | 0.007 (0.01) | 0.474 | 0.021 (0.01) | 0.043 | 0.01 (0.011) | 0.362 | -0.028 (0.021) | 0.174 |
| | ISOVF | 0.011 (0.01) | 0.261 | 0.007 (0.01) | 0.452 | 0.002 (0.01) | 0.815 | 0.008 (0.019) | 0.686 |
| | OD | 0.009 (0.009) | 0.302 | 0.018 (0.009) | 0.058 | 0.012 (0.01) | 0.221 | -0.001 (0.019) | 0.954 |
| Corticospinal tract | ICVF | -0.01 (0.011) | 0.351 | 0.003 (0.011) | 0.819 | 0.005 (0.012) | 0.678 | -0.005 (0.021) | 0.799 |
| | ISOVF | 0.02 (0.01) | 0.053 | 0.017 (0.01) | 0.092 | 0.019 (0.011) | 0.081 | 0.052 (0.021) | 0.011 |
| | OD | -0.013 (0.01) | 0.195 | -0.019 (0.01) | 0.059 | -0.01 (0.011) | 0.36 | -0.021 (0.02) | 0.286 |

| | | | | | | | | | |
|---|---|---|---|---|---|---|---|---|---|
| Inferior fronto occipital fasciculus | ICVF | -0.018 (0.011) | 0.095 | -0.006 (0.011) | 0.572 | -0.005 (0.012) | 0.643 | -0.031 (0.023) | 0.166 |
| | ISOVF | 0.002 (0.01) | 0.88 | 0.01 (0.01) | 0.339 | 0.017 (0.011) | 0.13 | 0.015 (0.021) | 0.484 |
| | OD | -0.027 (0.01) | 0.007 | -0.019 (0.01) | 0.064 | -0.01 (0.011) | 0.354 | -0.042 (0.02) | 0.039 |
| Inferior longitudinal fasciculus | ICVF | -0.017 (0.011) | 0.117 | -0.006 (0.011) | 0.585 | -0.006 (0.012) | 0.596 | -0.029 (0.023) | 0.207 |
| | ISOVF | 0.007 (0.01) | 0.529 | 0.009 (0.011) | 0.416 | 0.006 (0.011) | 0.582 | 0.021 (0.022) | 0.337 |
| | OD | -0.024 (0.01) | 0.018 | -0.011 (0.01) | 0.286 | -0.011 (0.011) | 0.313 | -0.051 (0.02) | 0.013 |
| Medial lemniscus | ICVF | 0.003 (0.009) | 0.735 | 0.014 (0.01) | 0.139 | 0.015 (0.01) | 0.142 | -0.004 (0.019) | 0.824 |
| | ISOVF | -0.004 (0.01) | 0.645 | -0.01 (0.01) | 0.332 | -0.004 (0.011) | 0.718 | 0.011 (0.02) | 0.581 |
| | OD | 0.023 (0.01) | 0.023 | 0.027 (0.01) | 0.01 | 0.019 (0.011) | 0.093 | -0.016 (0.02) | 0.43 |
| Posterior thalamic radiation | ICVF | -0.025 (0.011) | 0.021 | -0.019 (0.011) | 0.085 | -0.014 (0.012) | 0.239 | -0.033 (0.022) | 0.136 |
| | ISOVF | 0.002 (0.01) | 0.8 | 0.001 (0.01) | 0.904 | 0.007 (0.011) | 0.51 | 0.024 (0.02) | 0.232 |
| | OD | -0.01 (0.01) | 0.303 | 0.003 (0.01) | 0.777 | 9.53e-04 (0.01) | 0.927 | -0.038 (0.02) | 0.053 |
| Superior longitudinal fasciculus | ICVF | -0.016 (0.011) | 0.136 | -0.005 (0.011) | 0.648 | -0.005 (0.012) | 0.702 | -0.022 (0.023) | 0.342 |
| | ISOVF | 0.019 (0.01) | 0.051 | 0.019 (0.01) | 0.065 | 0.021 (0.011) | 0.056 | 0.052 (0.02) | 0.012 |
| | OD | -0.009 (0.009) | 0.31 | -0.009 (0.009) | 0.344 | -0.002 (0.01) | 0.817 | 5.94e-04 (0.019) | 0.974 |
| Superior thalamic radiation | ICVF | -0.02 (0.01) | 0.055 | -0.01 (0.011) | 0.369 | -0.004 (0.011) | 0.711 | -0.02 (0.023) | 0.375 |
| | ISOVF | 0.019 (0.009) | 0.03 | 0.022 (0.009) | 0.014 | 0.032 (0.009) | 7.43e-04* | 0.068 (0.019) | 2.66e-04* |

| | | | | | | | | | |
|---|---|---|---|---|---|---|---|---|---|
| | OD | -0.012 (0.01) | 0.241 | -0.014 (0.01) | 0.169 | 4.93e-04 (0.011) | 0.964 | -0.023 (0.02) | 0.255 |
| Uncinate fasciculus | ICVF | -0.009 (0.01) | 0.36 | -9.03e-04 (0.01) | 0.931 | -0.004 (0.011) | 0.699 | -0.031 (0.022) | 0.147 |
| | ISOVF | 0.022 (0.01) | 0.028 | 0.029 (0.01) | 0.004* | 0.025 (0.011) | 0.022 | 0.015 (0.019) | 0.444 |
| | OD | -0.015 (0.009) | 0.12 | -0.016 (0.01) | 0.092 | -0.016 (0.01) | 0.121 | -0.03 (0.019) | 0.119 |
| Forceps major | ICVF | -0.018 (0.011) | 0.119 | -0.013 (0.011) | 0.245 | -0.01 (0.012) | 0.406 | -0.041 (0.024) | 0.079 |
| | ISOVF | 0.011 (0.011) | 0.313 | 0.025 (0.011) | 0.021 | 0.031 (0.012) | 0.009* | 0.044 (0.022) | 0.045 |
| | OD | -0.019 (0.011) | 0.077 | -0.004 (0.011) | 0.728 | 0.002 (0.012) | 0.876 | -0.014 (0.021) | 0.501 |
| Forceps minor | ICVF | -0.015 (0.011) | 0.172 | -0.002 (0.011) | 0.843 | -3.67e-04 (0.012) | 0.975 | -0.02 (0.023) | 0.379 |
| | ISOVF | 0.006 (0.01) | 0.559 | 0.006 (0.01) | 0.597 | 0.011 (0.011) | 0.339 | 0.006 (0.021) | 0.76 |
| | OD | -0.01 (0.011) | 0.342 | -0.012 (0.011) | 0.278 | -0.008 (0.012) | 0.483 | -0.045 (0.022) | 0.04 |
| Middle cerebellar peduncle | ICVF | -0.003 (0.011) | 0.75 | 0.003 (0.011) | 0.782 | 0.006 (0.011) | 0.624 | -0.02 (0.02) | 0.332 |
| | ISOVF | 0.008 (0.011) | 0.455 | 0.012 (0.011) | 0.299 | 0.048 (0.012) | 7.06e-05* | 0.024 (0.023) | 0.292 |
| | OD | -0.006 (0.011) | 0.568 | -0.007 (0.011) | 0.553 | -0.013 (0.012) | 0.296 | 0.002 (0.023) | 0.942 |

Table S5. The effects of stressful life events (SLE), neuroticism, smoking status and alcohol consumption as covariates for DTI measures. The test was conducted on the full sample of IDP from UK Biobank imaging team, without outlier exclusion or phenotypic data merging (N~=8,200). Betas were standardised effect sizes. P values were un-corrected p values. All $p_{corrected}$<0.05 were marked by asterixis. FDR correction was applied on subsets of brain measures within a unit of a whole brain (n=15 for tract analysis, and n=4 for g analysis).

| | | **SLE** | | **Smoking** | | **Alcohol** | |
|---|---|---|---|---|---|---|---|
| **Tract name** | **Measure** | **Beta** | **p** | **Beta** | **p** | **Beta** | **p** |
| g.Total | FA | -0.015 (0.015) | 0.318 | -0.025 (0.019) | 0.18 | -3.03e-04 (7.61e-04) | 0.691 |
| | MD | 0.01 (0.015) | 0.514 | 0.034 (0.018) | 0.057 | 0.004 (7.26e-04) | 1.01e-06* |
| g.AF | FA | -0.02 (0.015) | 0.187 | -0.028 (0.019) | 0.139 | -7.39e-04 (7.58e-04) | 0.329 |
| | MD | 0.013 (0.015) | 0.401 | 0.023 (0.018) | 0.207 | 0.003 (7.40e-04) | 4.76e-04* |
| g.TR | FA | -0.002 (0.016) | 0.921 | -0.04 (0.019) | 0.034 | -0.001 (7.69e-04) | 0.058 |
| | MD | 0.009 (0.014) | 0.525 | 0.053 (0.017) | 0.001* | 0.004 (6.74e-04) | 2.70e-11* |
| g.PF | FA | -0.003 (0.015) | 0.867 | 6.36e-04 (0.019) | 0.973 | 0.002 (7.56e-04) | 0.001* |
| | MD | -0.003 (0.016) | 0.859 | 0.078 (0.019) | 4.63e-05* | 0.004 (7.79e-04) | 7.85e-07* |
| | | | | | | | |
| Acoustic radiation | FA | -0.028 (0.014) | 0.042 | 0.015 (0.017) | 0.359 | 9.89e-04 (6.72e-04) | 0.141 |

| | | | | | | | |
|---|---|---|---|---|---|---|---|
| | MD | 0.011 (0.013) | 0.417 | -0.028 (0.017) | 0.092 | 3.57e-04 (6.67e-04) | 0.592 |
| Anterior thalamic radiation | FA | -0.006 (0.015) | 0.689 | 0.009 (0.018) | 0.636 | -0.002 (7.28e-04) | 0.008* |
| | MD | 0.001 (0.013) | 0.919 | 0.012 (0.016) | 0.476 | 0.003 (6.63e-04) | 6.98e-07* |
| Cingulate gyrus part of cingulum | FA | -0.015 (0.014) | 0.287 | -0.036 (0.017) | 0.033 | -8.71e-04 (6.78e-04) | 0.199 |
| | MD | 0.003 (0.014) | 0.829 | 0.016 (0.017) | 0.333 | 5.62e-04 (6.76e-04) | 0.406 |
| Parahippocampal part of cingulum | FA | -0.014 (0.014) | 0.308 | -0.025 (0.017) | 0.146 | 0.001 (6.82e-04) | 0.081 |
| | MD | 0.016 (0.014) | 0.24 | 0.022 (0.017) | 0.19 | 4.79e-05 (6.70e-04) | 0.943 |
| Corticospinal tract | FA | 0.007 (0.015) | 0.614 | -0.02 (0.018) | 0.267 | 0.002 (7.22e-04) | 5.90e-04* |
| | MD | -0.004 (0.015) | 0.79 | 6.30e-04 (0.018) | 0.972 | 0.002 (7.27e-04) | 0.022* |
| Inferior fronto occipital fasciculus | FA | -0.002 (0.015) | 0.895 | -0.023 (0.018) | 0.214 | -1.61e-04 (7.32e-04) | 0.825 |
| | MD | 0.002 (0.014) | 0.871 | 0.022 (0.018) | 0.205 | 0.003 (7.07e-04) | 2.35e-05* |
| Inferior longitudinal fasciculus | FA | -0.009 (0.015) | 0.544 | -0.029 (0.018) | 0.113 | -3.95e-04 (7.28e-04) | 0.588 |
| | MD | 0.008 (0.014) | 0.584 | 0.013 (0.018) | 0.454 | 0.003 (7.07e-04) | 4.01e-06* |
| Medial lemniscus | FA | 0.006 (0.013) | 0.646 | -0.002 (0.016) | 0.887 | 5.77e-04 (6.61e-04) | 0.383 |
| | MD | -0.032 (0.014) | 0.018 | 0.001 (0.017) | 0.933 | 6.84e-04 (6.79e-04) | 0.314 |
| Posterior thalamic radiation | FA | -0.01 (0.014) | 0.481 | -0.073 (0.018) | 3.65e-05* | -0.001 (7.09e-04) | 0.037 |
| | MD | 0.017 (0.014) | 0.222 | 0.069 (0.017) | 3.17e-05* | 0.004 (6.71e-04) | 3.82e-11* |

| | | | | | | | |
|---|---|---|---|---|---|---|---|
| Superior longitudinal fasciculus | FA | -0.027 (0.015) | 0.071 | -0.011 (0.018) | 0.559 | -2.87e-04 (7.35e-04) | 0.696 |
| | MD | 0.006 (0.014) | 0.662 | 0.012 (0.018) | 0.497 | 0.002 (7.16e-04) | 0.001* |
| Superior thalamic radiation | FA | 0.005 (0.015) | 0.748 | -0.036 (0.019) | 0.053 | 5.97e-04 (7.53e-04) | 0.428 |
| | MD | 0.005 (0.013) | 0.71 | 0.045 (0.016) | 0.004* | 0.003 (6.31e-04) | 1.17e-05* |
| Uncinate fasciculus | FA | -0.024 (0.014) | 0.089 | 2.29e-04 (0.017) | 0.989 | -8.46e-04 (6.87e-04) | 0.218 |
| | MD | 0.002 (0.013) | 0.859 | -0.008 (0.016) | 0.623 | 0.002 (6.58e-04) | 4.13e-04* |
| Forceps major | FA | -0.041 (0.015) | 0.009 | -0.014 (0.019) | 0.456 | 4.88e-05 (7.65e-04) | 0.949 |
| | MD | 0.026 (0.015) | 0.094 | 0.015 (0.019) | 0.43 | 0.002 (7.62e-04) | 0.034* |
| Forceps minor | FA | -3.77e-04 (0.015) | 0.981 | -0.016 (0.019) | 0.41 | -0.002 (7.66e-04) | 0.049 |
| | MD | -0.002 (0.015) | 0.882 | 0.031 (0.018) | 0.09 | 0.002 (7.36e-04) | 0.005* |
| Middle cerebellar peduncle | FA | -0.007 (0.016) | 0.676 | 0.006 (0.019) | 0.776 | 0.002 (7.79e-04) | 0.007* |
| | MD | -0.001 (0.016) | 0.935 | 0.084 (0.019) | 1.38e-05* | 0.004 (7.81e-04) | 1.91e-06* |

Table S6. The effects of stressful life events (SLE), neuroticism, smoking status and alcohol consumption as covariates for NODDI measures. The test was conducted on the full sample of IDP from UK Biobank imaging team, without outlier exclusion or phenotypic data merging (N~=8,200). Betas were standardised effect sizes. P values were un-corrected p values. All $p_{corrected}$<0.05 were marked by asterixis. FDR correction was applied on subsets of brain measures within a unit of a whole brain (n=15 for tract analysis, and n=4 for g analysis).

| | | **SLE** | | **Smoking** | | **Alcohol** | |
|---|---|---|---|---|---|---|---|
| **Tract name** | **Measure** | **Beta** | **p** | **Beta** | **p** | **Beta** | **p** |
| g.Total | ICVF | -0.014 (0.015) | 0.368 | -0.027 (0.019) | 0.16 | -0.002 (7.62e-04) | 0.002* |
| | ISOVF | 7.46e-04 (0.015) | 0.959 | 0.016 (0.018) | 0.385 | 0.003 (7.27e-04) | 3.76e-05* |
| | OD | 0.015 (0.015) | 0.334 | 0.028 (0.018) | 0.133 | -0.003 (7.46e-04) | 4.04e-06* |
| g.AF | ICVF | -0.015 (0.015) | 0.329 | -0.024 (0.019) | 0.203 | -0.002 (7.63e-04) | 0.002* |
| | ISOVF | 0.008 (0.015) | 0.586 | 3.25e-04 (0.019) | 0.986 | 3.19e-04 (7.64e-04) | 0.676 |
| | OD | 0.015 (0.015) | 0.327 | 0.038 (0.018) | 0.038 | -0.002 (7.42e-04) | 0.001* |
| g.TR | ICVF | -0.011 (0.015) | 0.466 | -0.03 (0.018) | 0.105 | -0.003 (7.45e-04) | 2.78e-04* |
| | ISOVF | 0.008 (0.014) | 0.553 | 0.043 (0.017) | 0.01* | 0.004 (6.82e-04) | 5.39e-11* |
| | OD | -0.003 (0.014) | 0.823 | 0.02 (0.018) | 0.25 | -0.002 (7.12e-04) | 7.06e-04* |
| g.PF | ICVF | -0.009 (0.015) | 0.571 | -0.025 (0.019) | 0.185 | -6.51e-04 (7.61e-04) | 0.392 |

| | | | | | | | |
|---|---|---|---|---|---|---|---|
| | ISOVF | -0.007 (0.016) | 0.638 | 0.08 (0.019) | 3.60e-05* | 0.004 (7.79e-04) | 1.75e-06* |
| | OD | 0.002 (0.015) | 0.913 | -0.023 (0.019) | 0.211 | -0.004 (7.57e-04) | 2.71e-07* |
| | | | | | | | |
| Acoustic radiation | ICVF | -0.018 (0.015) | 0.217 | -0.019 (0.018) | 0.304 | -0.001 (7.40e-04) | 0.073 |
| | ISOVF | 0.003 (0.013) | 0.85 | -0.043 (0.016) | 0.009* | -1.76e-04 (6.59e-04) | 0.789 |
| | OD | 0.022 (0.013) | 0.084 | -0.034 (0.016) | 0.031 | -0.002 (6.38e-04) | 0.012* |
| Anterior thalamic radiation | ICVF | -0.011 (0.014) | 0.46 | -0.002 (0.018) | 0.89 | -0.002 (7.15e-04) | 0.002* |
| | ISOVF | -0.012 (0.014) | 0.388 | 0.017 (0.017) | 0.334 | 0.003 (6.90e-04) | 1.35e-05* |
| | OD | 0.007 (0.014) | 0.638 | -3.21e-04 (0.018) | 0.985 | 1.74e-04 (7.11e-04) | 0.807 |
| Cingulate gyrus part of cingulum | ICVF | -0.017 (0.015) | 0.238 | -0.024 (0.018) | 0.175 | -0.001 (7.20e-04) | 0.156 |
| | ISOVF | -0.017 (0.013) | 0.21 | -0.001 (0.016) | 0.951 | 1.10e-04 (6.56e-04) | 0.866 |
| | OD | 0.01 (0.013) | 0.442 | 0.027 (0.016) | 0.084 | 1.44e-04 (6.31e-04) | 0.819 |
| Parahippocampal part of cingulum | ICVF | -0.01 (0.014) | 0.507 | -0.018 (0.018) | 0.301 | -8.63e-04 (7.10e-04) | 0.224 |
| | ISOVF | 0.012 (0.013) | 0.379 | 0.016 (0.016) | 0.34 | -3.81e-04 (6.65e-04) | 0.567 |
| | OD | 0.009 (0.013) | 0.472 | 0.025 (0.016) | 0.112 | -0.002 (6.41e-04) | 0.01* |
| Corticospinal tract | ICVF | -0.012 (0.015) | 0.423 | -0.037 (0.019) | 0.051 | -5.42e-04 (7.62e-04) | 0.477 |
| | ISOVF | -0.008 (0.014) | 0.567 | -0.015 (0.017) | 0.389 | 0.001 (7.03e-04) | 0.051 |
| | OD | -0.02 (0.014) | 0.155 | 0.01 (0.017) | 0.544 | -0.004 (6.97e-04) | 2.59e-07* |

| | | | | | | | |
|---|---|---|---|---|---|---|---|
| Inferior fronto occipital fasciculus | ICVF | -0.011 (0.015) | 0.46 | -0.028 (0.019) | 0.133 | -0.002 (7.48e-04) | 0.002* |
| | ISOVF | -0.011 (0.015) | 0.462 | -0.013 (0.018) | 0.482 | 0.002 (7.18e-04) | 0.002* |
| | OD | -0.003 (0.014) | 0.831 | 4.89e-04 (0.017) | 0.978 | -0.003 (7.01e-04) | 4.13e-05* |
| Inferior longitudinal fasciculus | ICVF | -0.011 (0.015) | 0.461 | -0.026 (0.019) | 0.158 | -0.002 (7.54e-04) | 0.003* |
| | ISOVF | -0.001 (0.015) | 0.931 | -0.015 (0.018) | 0.411 | 0.002 (7.21e-04) | 5.48e-04* |
| | OD | 0.002 (0.014) | 0.882 | 0.015 (0.017) | 0.402 | -0.003 (7.05e-04) | 6.46e-06* |
| Medial lemniscus | ICVF | 0.016 (0.013) | 0.228 | -0.006 (0.016) | 0.72 | 0.002 (6.52e-04) | 0.012* |
| | ISOVF | -0.022 (0.014) | 0.106 | 0.002 (0.017) | 0.897 | 0.001 (6.79e-04) | 0.053 |
| | OD | -0.002 (0.014) | 0.912 | 0.026 (0.018) | 0.135 | 7.01e-04 (7.12e-04) | 0.325 |
| Posterior thalamic radiation | ICVF | -0.007 (0.015) | 0.636 | -0.047 (0.018) | 0.011 | -0.002 (7.44e-04) | 0.002* |
| | ISOVF | 0.017 (0.014) | 0.213 | 0.052 (0.017) | 0.002* | 0.004 (6.70e-04) | 1.07e-09* |
| | OD | 0.005 (0.013) | 0.712 | 0.027 (0.017) | 0.103 | -0.002 (6.68e-04) | 0.011* |
| Superior longitudinal fasciculus | ICVF | -0.014 (0.015) | 0.352 | -0.019 (0.019) | 0.312 | -0.002 (7.56e-04) | 0.009* |
| | ISOVF | -0.006 (0.014) | 0.677 | -0.006 (0.017) | 0.724 | 0.002 (6.95e-04) | 0.015* |
| | OD | 0.029 (0.013) | 0.029 | -0.006 (0.016) | 0.722 | -0.003 (6.47e-04) | 1.46e-05* |
| Superior thalamic radiation | ICVF | -0.014 (0.015) | 0.351 | -0.039 (0.018) | 0.032 | -0.002 (7.29e-04) | 0.002* |
| | ISOVF | -0.007 (0.012) | 0.587 | 0.027 (0.015) | 0.069 | 0.002 (6.07e-04) | 9.54e-04* |

| | | | | | | | |
|---|---|---|---|---|---|---|---|
| | OD | -0.008 (0.014) | 0.558 | 0.016 (0.017) | 0.342 | -0.003 (6.94e-04) | 2.39e-04* |
| Uncinate fasciculus | ICVF | -0.015 (0.014) | 0.283 | -0.014 (0.018) | 0.43 | -0.003 (7.13e-04) | 4.18e-04* |
| | ISOVF | -0.014 (0.014) | 0.316 | -0.023 (0.017) | 0.186 | 6.85e-04 (6.87e-04) | 0.319 |
| | OD | 0.016 (0.013) | 0.221 | 0.005 (0.016) | 0.739 | -8.15e-04 (6.61e-04) | 0.217 |
| Forceps major | ICVF | -0.026 (0.016) | 0.099 | -0.029 (0.019) | 0.131 | -0.002 (7.82e-04) | 0.005* |
| | ISOVF | 0.021 (0.015) | 0.171 | 5.21e-04 (0.019) | 0.978 | 5.53e-04 (7.60e-04) | 0.467 |
| | OD | 0.044 (0.015) | 0.004 | -0.022 (0.019) | 0.245 | -0.002 (7.50e-04) | 0.003* |
| Forceps minor | ICVF | -0.007 (0.015) | 0.662 | -0.013 (0.019) | 0.497 | -0.002 (7.60e-04) | 0.003* |
| | ISOVF | -0.008 (0.015) | 0.561 | 0.016 (0.018) | 0.382 | 9.63e-04 (7.21e-04) | 0.182 |
| | OD | 0.005 (0.015) | 0.721 | 0.004 (0.019) | 0.841 | -0.001 (7.59e-04) | 0.188 |
| Middle cerebellar peduncle | ICVF | -5.21e-05 (0.015) | 0.997 | -0.014 (0.019) | 0.439 | -5.33e-04 (7.48e-04) | 0.476 |
| | ISOVF | -0.003 (0.016) | 0.834 | 0.081 (0.019) | 2.92e-05* | 0.004 (7.80e-04) | 6.90e-06* |
| | OD | 0.004 (0.016) | 0.784 | -0.037 (0.019) | 0.055 | -0.003 (7.74e-04) | 8.81e-04* |

Table S7. The associations between temporal change of depressive level at the imaging assessment compared with mean level and g measures in MD, ISOVF and ICVF. P values were uncorrected. Significant p value after FDR correction were marked by asterixis.

| g measure | MD | | | ISOVF | | | ICVF | | |
|---|---|---|---|---|---|---|---|---|---|
| | **Beta** | **std** | **p** | **Beta** | **std** | **p** | **Beta** | **std** | **p** |
| g.Total | 0.027 | 0.010 | 0.007* | 0.005 | 0.010 | 0.598 | -0.025 | 0.011 | 0.017* |
| g.AF | 0.025 | 0.010 | 0.015* | 0.006 | 0.011 | 0.586 | -0.025 | 0.011 | 0.019* |
| g.TR | 0.022 | 0.009 | 0.019* | 0.002 | 0.009 | 0.832 | -0.023 | 0.010 | 0.029* |
| g.PF | 0.006 | 0.011 | 0.558 | -0.001 | 0.011 | 0.923 | -0.026 | 0.011 | 0.013* |

Table S8. Measures for depressive symptoms and MDD-related phenotypes. MDD phenotypes include three definitions of life-time MDD status (Howard, Adams, et al. 2017). These include MDD self (self-reported status of ever had depression or not), smith's MDD definition (based on self-reported depressed symptoms and hospital admission history) and CIDI MDD (derived from Composite International Diagnostic Interview results). CIDI MDD is the most clinical definition, whilst MDD self is the most lenient and has the biggest sample size. Other phenotypes include MDD severity assessed by CIDI, whether had self-harm behaviour ever in the life time and length of depression (years from first to last episode). Coefficients for MDD phenotypes and gender are odds ratios, and for other phenotypes are standardised effect sizes of glm models, and age, age$^2$ and gender were set as covariates for depre, depre.mean and depre.instability. Only gender was controlled for depre.longitudinal because the measure was derived controlling for age in the growth curve model. All MDD definitions and self-harm behaviour were binary variables, and other phenotypes were continuous.

| | **Depre** | | | **Depre.mean** | | | **Depre.instability** | | | **Depre.longitudinal** | | |
|---|---|---|---|---|---|---|---|---|---|---|---|---|
| **Dependent variable** | **Coefficient** | **std** | **p** | **Coefficient** | **std** | **p** | **Coefficient** | **std** | **p** | **Coefficient** | **std** | **p** |
| MDD self | 1.867 | 0.029 | <1.00E-16 | 2.239 | 0.03 | <1.00E-16 | 1.797 | 0.026 | <1.00E-16 | 1.27 | 0.049 | 4.64E-07 |
| MDD smith | 1.59 | 0.027 | <1.00E-16 | 1.824 | 0.029 | <1.00E-16 | 1.654 | 0.026 | <1.00E-16 | 1.148 | 0.053 | 6.87E-03 |
| MDD CIDI | 2.514 | 0.042 | <1.00E-16 | 4.096 | 0.052 | <1.00E-16 | 2.363 | 0.037 | <1.00E-16 | 1.808 | 0.068 | <1.00E-16 |
| Self harm | 1.581 | 0.041 | <1.00E-16 | 1.714 | 0.041 | <1.00E-16 | 1.507 | 0.039 | <1.00E-16 | 1.325 | 0.089 | 1.56E-03 |
| Age of onset | -0.102 | 0.015 | 2.10E-11 | -0.128 | 0.015 | <1.00E-16 | -0.057 | 0.015 | 1.97E-04 | -0.029 | 0.026 | 0.266 |

| | **Depre** | | | **Depre.mean** | | | **Depre.instability** | | | **Depre.longitudinal** | | |
|---|---|---|---|---|---|---|---|---|---|---|---|---|
| **Factor** | **Coefficient** | **std** | **p** | **Coefficient** | **std** | **p** | **Coefficient** | **std** | **p** | **Coefficient** | **std** | **p** |
| Age | -0.173 | 0.011 | <1.00E-16 | -0.212 | 0.011 | <1.00E-16 | -0.152 | 0.011 | <1.00E-16 | -- | -- | -- |
| Gender | -0.155 | 0.022 | 1.59E-12 | -0.197 | 0.021 | <1.00E-16 | -0.142 | 0.021 | 3.67E-09 | -0.048 | 0.045 | 0.285 |

# Appendix 3:

# Supplementary materials of Chapter 4: Phenotype-wide association study of 212 behavioural and 1,532 neuroimaging phenotypes in UK Biobank using polygenic risk scores for depression

Figure S1. Scree plots for PCA on white matter microstructure

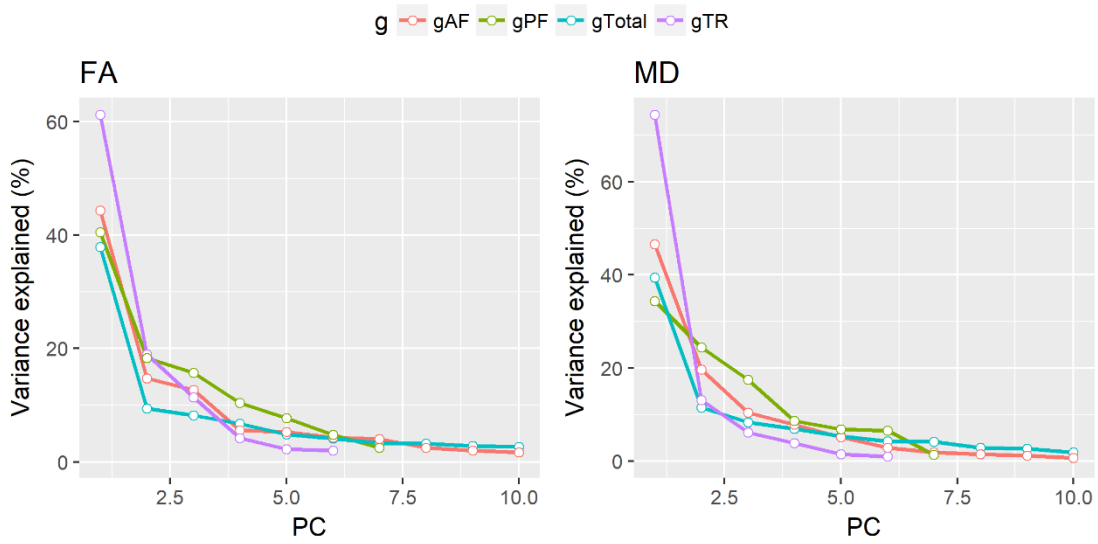

Figure S2. Manhatan-like plot for PheWas results at all eight MDD-pgrs.

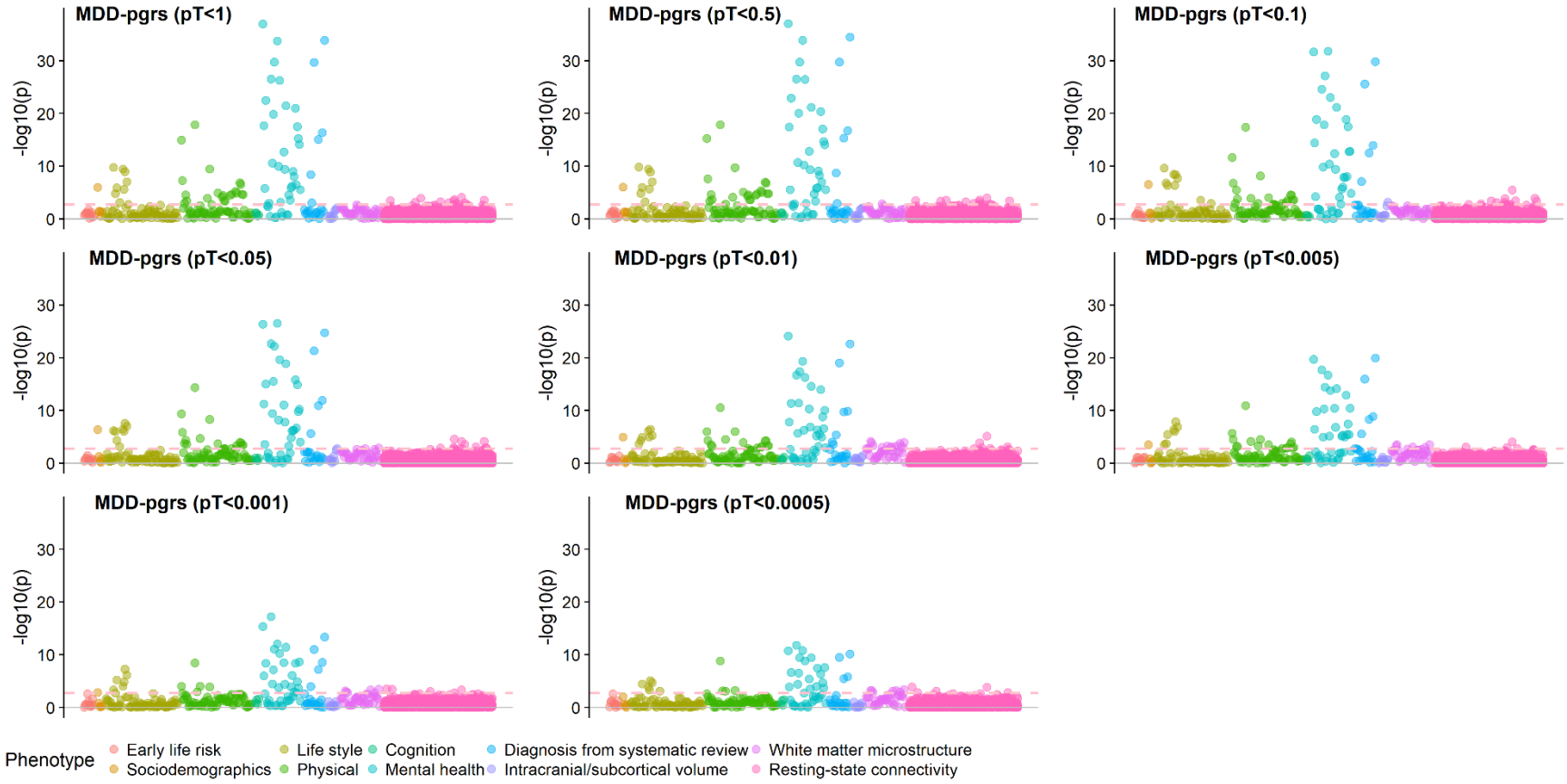

Figure S3. Quantile-quantile plot of PheWAS

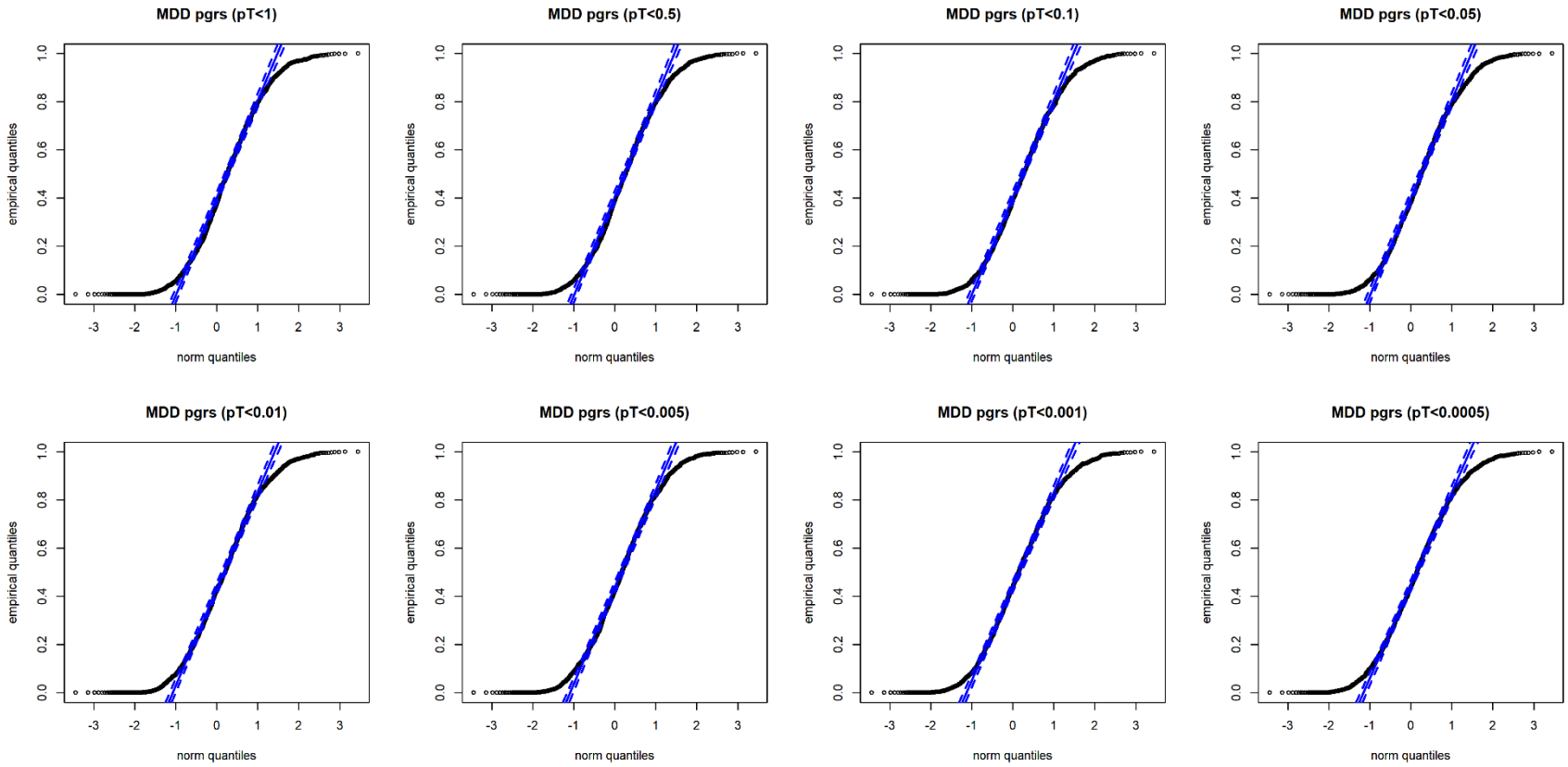

Figure S4. Manhatan-like plot for MDD-pgrs*MDD interaction

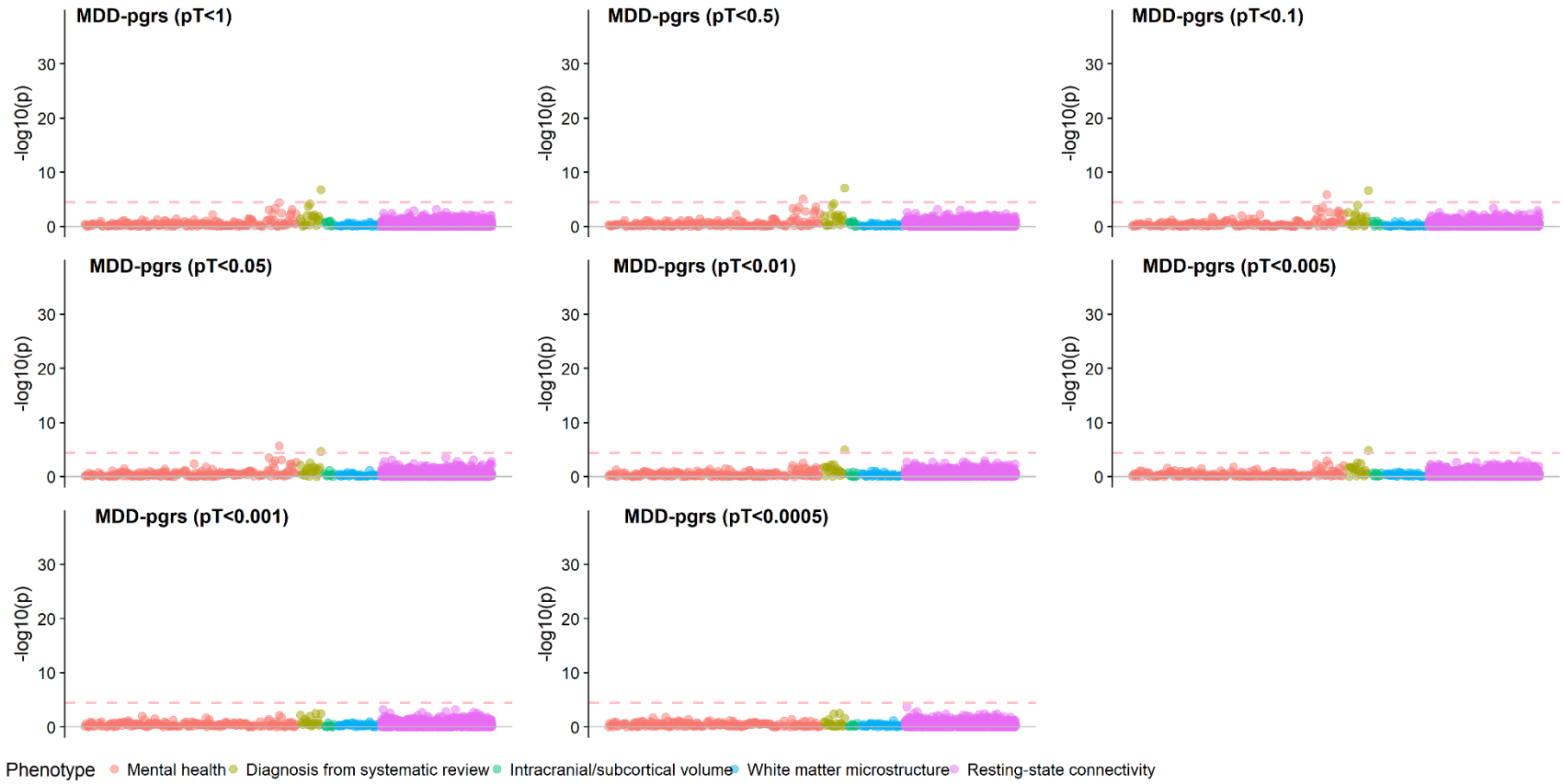

Table S1. All phenotypes used in the study.

| Category | Phenotype | Modality | Field ID | N | Note |
|---|---|---|---|---|---|
| Early life factor | Breast fed | Touchscreen | 1677 | 8173 | |
| Early life factor | Bodysize at age=10 | Touchscreen | 1687 | 10878 | |
| Early life factor | Height at age=10 | Touchscreen | 1697 | 10902 | |
| Early life factor | Adopted | Touchscreen | 1767 | 11006 | |
| Early life factor | Maternal smoking | Touchscreen | 1787 | 9633 | |
| Early life factor | Multiple birth | Touchscreen | 1777 | 10872 | Question asked: Are you a twin, triplet or other multiple birth? |
| Early life factor | Age father death | Touchscreen | 1807 | 9180 | if age<40 then coded as 1, age<=40 then coded as 0 |
| Early life factor | Age mother death | Touchscreen | 3526 | 7742 | if age<40 then coded as 1, age<=40 then coded as 0 |
| Early life factor | Birth weight | Interview | 20022 | 11017 | |
| Early life factor | Cancer early | Interview | 20007 | 11017 | if age<30 then coded as 1, age<=30 then coded as 0 |
| Sociodemographic | Household income | Touchscreen | 738 | 9964 | |
| Sociodemographic | Education | Touchscreen | 6138 | 10258 | |
| Sociodemographic | Ethnicity | Touchscreen | 21000 | 8318 | Dimensions were reduced down to: White, Black, Asian, Chinese, Mixed and others |
| Sociodemographic | Migrant status | Touchscreen | 1647 | 8339 | |
| Sociodemographic | Townsend Deprivation Index tertiles | Touchscreen | 189 | 8333 | |
| Life style | Length of mobile phone use | Touchscreen | 1110 | 11014 | |

| | | | | | |
|---|---|---|---|---|---|
| Life style | Weekly usage of mobile phone in last 3 months | Touchscreen | 1120 | 10350 | |
| Life style | Hands free device speakerphone use with mobile phone in last 3 month | Touchscreen | 1130 | 10360 | |
| Life style | Difference in mobile phone use compared to two years previously | Touchscreen | 1140 | 10358 | |
| Life style | Usual side of head for mobile phone use | Touchscreen | 1150 | 10344 | |
| Life style | Plays computer games | Touchscreen | 2237 | 11017 | |
| Life style | Sleep duration | Touchscreen | 1160 | 11017 | |
| Life style | Easy to get up in the morning | Touchscreen | 1170 | 11017 | |
| Life style | Morning or evening person | Touchscreen | 1180 | 10586 | |
| Life style | Nap during the day | Touchscreen | 1190 | 11017 | |
| Life style | Insomnia | Touchscreen | 1200 | 11017 | |
| Life style | Snoring | Touchscreen | 1210 | 10814 | |
| Life style | Daytime dozing sleeping | Touchscreen | 1220 | 11017 | |
| Life style | Sleep too much | Touchscreen | 20534 | 3231 | |
| Life style | Sleep trouble start | Touchscreen | 20533 | 3231 | |
| Life style | Sleep trouble end | Touchscreen | 20535 | 3231 | |
| Life style | Sleep any problem | Touchscreen | 20517 | 8327 | |
| Life style | Ever smoked | Touchscreen | 20160 | 11017 | |
| Life style | Smoking status | Touchscreen | 20116 | 11017 | |

| | | | | | |
|---|---|---|---|---|---|
| Life style | Current tobacco smoking | Touchscreen | 1239 | 11017 | |
| Life style | Past tobacco smoking | Touchscreen | 1249 | 10778 | |
| Life style | Light smokers at least 100 smokes in lifetime | Touchscreen | 2644 | 4057 | |
| Life style | Age started smoking in former smokers | Touchscreen | 2867 | 2995 | |
| Life style | Type of tobacco previously smoked | Touchscreen | 2877 | 2995 | |
| Life style | Number of cigarettes previously smoked daily | Touchscreen | 2887 | 2880 | |
| Life style | Age stopped smoking | Touchscreen | 2897 | 2995 | |
| Life style | Ever stopped smoking for 6 months | Touchscreen | 2907 | 2963 | |
| Life style | Number of unsuccessful stop smoking attempts | Touchscreen | 2926 | 2993 | |
| Life style | Likelihood of resuming smoking | Touchscreen | 2936 | 2971 | |
| Life style | Smoking smokers in household | Touchscreen | 1259 | 10775 | |
| Life style | Exposure to tobacco smoke at home | Touchscreen | 1269 | 10782 | |
| Life style | Exposure to tobacco smoke outside home | Touchscreen | 1279 | 10782 | |
| Life style | Cooked vegetable intake | Touchscreen | 1289 | 11017 | |
| Life style | Salad raw vegetable intake | Touchscreen | 1299 | 11017 | |

| | | | | | |
|---|---|---|---|---|---|
| Life style | Fresh fruit intake | Touchscreen | 1309 | 11017 | |
| Life style | Dried fruit intake | Touchscreen | 1319 | 11017 | |
| Life style | Oily fish intake | Touchscreen | 1329 | 11016 | |
| Life style | Non oily fish intake | Touchscreen | 1339 | 11016 | |
| Life style | Processed meat intake | Touchscreen | 1349 | 11017 | |
| Life style | Poultry intake | Touchscreen | 1359 | 11017 | |
| Life style | Beef intake | Touchscreen | 1369 | 11016 | |
| Life style | Lamb mutton intake | Touchscreen | 1379 | 11017 | |
| Life style | Pork intake | Touchscreen | 1389 | 11013 | |
| Life style | Never eat eggs dairy wheat sugar | Touchscreen | 6144 | 11017 | |
| Life style | Cheese intake | Touchscreen | 1408 | 10954 | |
| Life style | Bread intake | Touchscreen | 1438 | 11017 | |
| Life style | Cereal intake | Touchscreen | 1458 | 11017 | |
| Life style | Salt added to food | Touchscreen | 1478 | 11017 | |
| Life style | Tea intake | Touchscreen | 1488 | 11017 | |
| Life style | Coffee intake | Touchscreen | 1498 | 11017 | |
| Life style | Hot drink temperature | Touchscreen | 1518 | 11017 | |
| Life style | Water intake | Touchscreen | 1528 | 11017 | |
| Life style | Major dietary changes in the last 5 years | Touchscreen | 1538 | 11017 | |
| Life style | Variation in diet | Touchscreen | 1548 | 11016 | |
| Life style | Time spend outdoors in summer | Touchscreen | 1050 | 11017 | |
| Life style | Time spent outdoors in winter | Touchscreen | 1060 | 11017 | |

| | | | | | |
|---|---|---|---|---|---|
| Life style | Skin colour | Touchscreen | 1717 | 10987 | |
| Life style | Ease of skin tanning | Touchscreen | 1727 | 10951 | |
| Life style | Childhood sunburn occasions | Touchscreen | 1737 | 11017 | |
| Life style | Hair colour | Touchscreen | 1747 | 11015 | |
| Life style | Facial ageing | Touchscreen | 1757 | 10708 | |
| Life style | Use of sun protection | Touchscreen | 2267 | 11017 | |
| Life style | Frequency of solarium sunlamp use | Touchscreen | 2277 | 11017 | |
| Life style | Frequency of friend family visits | Touchscreen | 1031 | 11016 | |
| Life style | Leisure activities | Touchscreen | 6160 | 11016 | |
| Life style | Able to confide | Touchscreen | 2110 | 10970 | |
| Life style | Vitamin and mineral supplements | Touchscreen | 6155 | 11016 | |
| Life style | Mineral and other dietary supplements | Touchscreen | 6179 | 11017 | |
| Life style | Alcohol weekly unit | Touchscreen | 1568, 1578, 1588, 1598, 5364, 1608, 4407, 4418, 4429, 4440, 4451, 4462 | 11017 | Derived based on multiple fields. Ref: Clarke et al. (2017) Mol Psychiatry (22),1376–1384 |
| Physical measure | Overall health rating | Touchscreen | 2178 | 11016 | |
| Physical measure | Long standing illness, disability or infirmity | Touchscreen | 2188 | 10996 | |
| Physical measure | Falls in the last year | Touchscreen | 2296 | 11017 | |

| | | | | | |
|---|---|---|---|---|---|
| Physical measure | Weight change compared with 1 year ago | Touchscreen | 2306 | 11003 | |
| Physical measure | Leg pain on walking | Touchscreen | 4728 | 10964 | |
| Physical measure | Leg pain when standing still or sitting | Touchscreen | 5452 | 2455 | |
| Physical measure | Leg pain in calf/calves | Touchscreen | 5463 | 2491 | |
| Physical measure | Leg pain when walking uphill or hurrying | Touchscreen | 5474 | 2436 | |
| Physical measure | Leg pain when walking normally | Touchscreen | 5485 | 2473 | |
| Physical measure | Leg pain on walking action taken | Touchscreen | 5507 | 2491 | |
| Physical measure | Leg pain on walking effect of standing still | Touchscreen | 5518 | 2227 | |
| Physical measure | Surgery on leg arteries other than for varicose veins | Touchscreen | 5529 | 2513 | |
| Physical measure | Surgery amputation of toe or leg | Touchscreen | 5540 | 2507 | |
| Physical measure | Ever pain last month | Touchscreen | 6159 | 11017 | |
| Physical measure | Headaches for 3 months | Touchscreen | 3799 | 2865 | |
| Physical measure | Neck shoulder pain for 3 months | Touchscreen | 3404 | 3507 | |
| Physical measure | Back pain for 3 months | Touchscreen | 3571 | 3803 | |
| Physical measure | Knee pain for 3 months | Touchscreen | 3773 | 3401 | |

| | | | | | |
|---|---|---|---|---|---|
| Physical measure | Ever vascular heart problem diagnosed | Touchscreen | 6150 | 11014 | |
| Physical measure | Age high blood pressure diagnosed | Touchscreen | 2966 | 3201 | |
| Physical measure | Blood clot problem diagnosed | Touchscreen | 6152 | 11017 | |
| Physical measure | Age hay fever, rhinitis or eczema diagnosed | Touchscreen | 3761 | 3406 | |
| Physical measure | Diabetes diagnosed by doctor | Touchscreen | 2443 | 11016 | |
| Physical measure | Cancer diagnosed by doctor | Touchscreen | 2453 | 11016 | |
| Physical measure | Fractured broken bones in last 5 years | Touchscreen | 2463 | 11011 | |
| Physical measure | Other serious medical condition diagnosed by doctor | Touchscreen | 2473 | 11000 | |
| Physical measure | Medication for cholesterol, blood pressure, diabetes or take exogenous hormones | Touchscreen | 6153 | 5700 | |
| Physical measure | Medication for pain relief, constipation or heartburn | Touchscreen | 6154 | 11015 | |
| Physical measure | Diastolic blood pressure (automated reading) | Physical measure | 4079 | 10983 | |

| | | | | | |
|---|---|---|---|---|---|
| Physical measure | Pulse rate (automated reading) | Physical measure | 94 | 10983 | |
| Physical measure | Systolic blood pressure (automated reading) | Physical measure | 95 | 10983 | |
| Physical measure | Pulse rate | Physical measure | 4194 | 10951 | |
| Physical measure | Pulse wave Arterial Stiffness Index | Physical measure | 21021 | 10932 | |
| Physical measure | Pulse wave peak to peak time | Physical measure | 4196 | 10946 | |
| Physical measure | Pulse wave Reflection Index | Physical measure | 4195 | 10951 | |
| Physical measure | Body Mass Index | Physical measure | 23104 | 10883 | |
| Physical measure | Leg fat free mass (right) | Physical measure | 23113 | 10883 | |
| Physical measure | Leg predicted mass (left) | Physical measure | 23118 | 10883 | |
| Physical measure | Leg predicted mass (right) | Physical measure | 23114 | 10883 | |
| Physical measure | Arm fat percentage (left) | Physical measure | 23123 | 10882 | |
| Physical measure | Arm fat percentage (right) | Physical measure | 23119 | 10883 | |
| Physical measure | Arm fat mass (left) | Physical measure | 23124 | 10881 | |
| Physical measure | Arm fat mass (right) | Physical measure | 23120 | 10881 | |
| Physical measure | Arm fat free mass (right) | Physical measure | 23121 | 10882 | |
| Physical measure | Arm fat free mass (left) | Physical measure | 23125 | 10880 | |
| Physical measure | Arm predicted mass (left) | Physical measure | 23126 | 10879 | |
| Physical measure | Arm predicted mass (right) | Physical measure | 23122 | 10882 | |
| Physical measure | Trunk fat percentage | Physical measure | 23127 | 10877 | |
| Physical measure | Trunk fat mass | Physical measure | 23128 | 10875 | |
| Physical measure | Trunk fat free mass | Physical measure | 23129 | 10870 | |

| | | | | | |
|---|---|---|---|---|---|
| Physical measure | Trunk predicted mass | Physical measure | 23130 | 10869 | |
| Physical measure | Basal metabolic rate | Physical measure | 23105 | 10883 | |
| Physical measure | Body fat percentage | Physical measure | 23099 | 10876 | |
| Physical measure | Whole body fat mass | Physical measure | 23100 | 10868 | |
| Physical measure | Whole body fat free mass | Physical measure | 23101 | 10883 | |
| Physical measure | Whole body water mass | Physical measure | 23102 | 10883 | |
| Physical measure | Leg fat percentage (left) | Physical measure | 23115 | 10883 | |
| Physical measure | Leg fat percentage (right) | Physical measure | 23111 | 10883 | |
| Physical measure | Leg fat mass (left) | Physical measure | 23116 | 10883 | |
| Physical measure | Leg fat mass (right) | Physical measure | 23112 | 10883 | |
| Physical measure | Leg fat free mass (left) | Physical measure | 23117 | 10883 | |
| Physical measure | Impedance of whole body | Physical measure | 23106 | 10882 | |
| Physical measure | Impedance of arm (left) | Physical measure | 23110 | 10883 | |
| Physical measure | Impedance of arm (right) | Physical measure | 23109 | 10883 | |
| Physical measure | Impedance of leg (left) | Physical measure | 23108 | 10883 | |
| Physical measure | Impedance of leg (right) | Physical measure | 23107 | 10883 | |
| Physical measure | Hand grip strength (left) | Physical measure | 46 | 11016 | |
| Physical measure | Hand grip strength (right) | Physical measure | 47 | 11017 | |
| Cognition | Trail making | Touchscreen | 6348, 6350 | 5699 | Derived by substuding Trail#1 by Trail#2 |
| Cognition | Digit substitute | Touchscreen | 23324 | 6075 | |
| Cognition | Numeric memory | Touchscreen | 100029 | 5781 | |
| Cognition | gCog | NA | NA | 5247 | Derived by conducting PCA on all cognition results. The scores of the first un-rotated principal component were extracted as the g measure. |
| Mental health | MDD-Nerves | Touchscreen | 2090 | 8164 | |

| | | | | | |
|---|---|---|---|---|---|
| Mental health | MDD-Smith | Touchscreen | 20126 | 7137 | |
| Mental health | MDD-ICD | Interview | 135 | 4430 | |
| Mental health | MDD-CIDI | Online follow-up | 20446, 20441, 20449, 20536, 20532, 20435, 20450, 20437 | 7201 | Over four items met then coded as 1, otherwise 0 |
| Mental health | Recurrent depression | Online follow-up | 20442 | 3788 | MDD-CIDI=1, plus episodes reported > 1 |
| Mental health | Single depression | Online follow-up | 20442 | 3788 | MDD-CIDI=1, plus episodes reported = 1 |
| Mental health | Postnatal depression | Online follow-up | 20445 | 7201 | MDD-CIDI=1, plus postnatal reasons reported = 1 |
| Mental health | Single depression Following Trauma | Online follow-up | 20447 | 3788 | Single depression=1, plus trauma reported |
| Mental health | Neuroticism | Touchscreen | 20127 | 7085 | |
| Mental health | Loneliness | Online follow-up | 2020 | 8257 | |
| Mental health | PHQ9 Severity | Online follow-up | 20514, 20507, 20510, 20508, 20517, 20518, 20519, 20511, 20513 | 8340 | Add up score |
| Mental health | CIDI MDD Severity | Online follow-up | 20446, 20441, 20449, 20536, 20532, 20435, 20450, 20437 | 8340 | Add up score |
| Mental health | Depression age onset | Online follow-up | 20433 | 4702 | |
| Mental health | Depression age last episode | Online follow-up | 20434 | 4702 | |

| | | | | | |
|---|---|---|---|---|---|
| Mental health | Depression affective symptoms | Online follow-up | 20446, 20441, 20450, 20437, 20514, 20507, 20510, 20513 | 8340 | |
| Mental health | Depression cognitive symptoms | Online follow-up | 20435, 20508 | 8340 | |
| Mental health | Depression somatic symptoms | Online follow-up | 20449, 20536, 20532, 20517, 20518, 20519, 20511 | 8340 | |
| Mental health | Wider Bipolar definition | Online follow-up | 20548 | 8269 | Total manifestations >=3 items |
| Mental health | Bipolar disorder (type I) | Online follow-up | 20493 | 8269 | MDD-CIDI=1, plus schizophrenic symptoms reported |
| Mental health | Bipolar disorder (type II) | Online follow-up | 20493 | 8269 | MDD-CIDI=1, plus schizophrenic symptoms absent |
| Mental health | General anxiety disorder ever | Online follow-up | 20506, 20509, 20520, 20515, 20516, 20505, 20512 | 5816 | Total manifestations >=5 items |
| Mental health | Total bipolar disorder manifestations | Online follow-up | 20548 | 8340 | |
| Mental health | General anxiety disorder Severity | Online follow-up | 20506, 20509, 20520, 20515, 20516, 20505, 20512 | 8340 | |

| | | | | | |
|---|---|---|---|---|---|
| Mental health | AUDIT Score | Online follow-up | 20403, 20416, 20409, 20408, 20411, 20405, 20413, 20407, 20412 | 8340 | |
| Mental health | Cannabis ever | Online follow-up | 20453 | 8327 | |
| Mental health | Addiction ever (self-reported) | Online follow-up | 20543, 20454, 20401 | 8263 | Reported cannabis use or AUDIT score >=16 |
| Mental health | Unusual experience ever | Online follow-up | 20471, 20463, 20474, 20468 | 8329 | |
| Mental health | Trauma (childhood) | Online follow-up | 20488, 20487, 20490, 20491, 20489 | 8167 | |
| Mental health | Trauma (adult) | Online follow-up | 20523, 20521, 20524, 20522, 20525 | 8059 | |
| Mental health | Trauma (catastrophic) | Online follow-up | 20527, 20526, 20528, 20529, 20531, 20530 | 8339 | |
| Mental health | Post-traumatic stress disorder (PTSD) | Online follow-up | 20497, 20498, 20495, 20496, 20494, 20508 | 8317 | PCL (PTSD check list) score > 13 |
| Mental health | PTSD check list score | Online follow-up | 20497, 20498, 20495, 20496, 20494, 20508 | 8340 | |
| Mental health | Self harm ever | Online follow-up | 20480 | 8317 | |

| | | | | | |
|---|---|---|---|---|---|
| Mental health | Not worth living | Online follow-up | 20479 | 8340 | |
| Mental health | Subjective well-being | Online follow-up | 20458, 20459, 20460 | 8139 | |
| Mental health | Any comorbidity | Online follow-up | NA | 8340 | Summary of whether is case in wider bipolar definition, GAD ever, addiction ever, and unusual experience ever. If is case in any of the conditions then coded as 1, otherwise 0. |
| Mental health | Multiple comorbidity | Online follow-up | NA | 8340 | Summary of total conditions in wider bipolar definition, GAD ever, addiction ever, and unusual experience ever |
| Mental health | Social phobia | Interview | 20499, 20544 | 8340 | |
| Mental health | Schizophrenia | Interview | | 8340 | |
| Mental health | Psychosis (other than social phobia and Schizophrenia) | Interview | | 8340 | |
| Mental health | Any phychosis | Interview | | 8340 | |
| Mental health | Personality disorder | Interview | | 8340 | |
| Mental health | Uncategorised phobia | Interview | | 8340 | |
| Mental health | Panic attacks | Interview | | 8340 | |
| Mental health | Obsessive-compulsive disorder | Interview | | 8340 | |
| Mental health | Mania bipolar | Interview | | 8340 | |
| Mental health | Mood disorder | Interview | | 8340 | |
| Mental health | Bulimia nervosa | Interview | | 8340 | |
| Mental health | Binge eating | Interview | | 8340 | |
| Mental health | Autism spectrum disorder | Interview | | 8340 | |

| | | | | | |
|---|---|---|---|---|---|
| Mental health | General anxiety disorder and others | Interview | | 8340 | |
| Mental health | Anorexia nervosa | Interview | | 8340 | |
| Mental health | Any eating disorder | Interview | | 8340 | |
| Mental health | Agoraphobia | Interview | | 8340 | |
| Mental health | Any anxiety disorder | Interview | | 8340 | |
| Mental health | Attention deficit hyperactivity disorder | Interview | | 8340 | |
| Mental health | Sum of all ICD-10 psychiatric diagnoses | Interview | | 8340 | |
| Intracranial/subcortical volume | Thalamus | Imaging | 25011, 25012 | 9750 | |
| Intracranial/subcortical volume | Caudate | Imaging | 25013, 25014 | | |
| Intracranial/subcortical volume | Putamen | Imaging | 25015, 25016 | | |
| Intracranial/subcortical volume | Pallidum | Imaging | 25017, 25018 | | |
| Intracranial/subcortical volume | Hippocampus | Imaging | 25019, 25020 | | |
| Intracranial/subcortical volume | Amygdala | Imaging | 25021, 25022 | | |
| Intracranial/subcortical volume | Accumbens | Imaging | 25023, 25024 | | |
| Intracranial/subcortical volume | Brain stem and the 4th ventricle | Imaging | 25025 | | |

| | | | | | |
|---|---|---|---|---|---|
| Intracranial/subcortical volume | Intracranial volume | Imaging | 25088, 25006, 25004 | | Add-up of grey matter, white matter and ventricular cerebrospinal fluid was generated as a measure of intracranial volume. |
| White matter microstructure | g.FA.Total | Imaging | NA | 9,699 | PCA on sub-group of tracts. See methods for more information |
| White matter microstructure | g.FA.Association fibres | Imaging | NA | | |
| White matter microstructure | g.FA.Thalamic radiations | Imaging | NA | | |
| White matter microstructure | g.FA.Projection fibres | Imaging | NA | | |
| White matter microstructure | g.MD.Total | Imaging | NA | 9,671 | |
| White matter microstructure | g.MD.Association fibres | Imaging | NA | | |
| White matter microstructure | g.MD.Thalamic radiations | Imaging | NA | | |
| White matter microstructure | g.MD.Projection fibres | Imaging | NA | | |
| White matter microstructure | FA.Acoustic radiation | Imaging | 25488, 25489 | 9699 | Bilateral tracts. Hemisphere was controlled for. |
| White matter microstructure | FA.Anterior thalamic radiation | Imaging | 25490. 25491 | | |
| White matter microstructure | FA.Cingulate gyrus part of cingulum | Imaging | 25492, 25493 | | |

| | | | | | |
|---|---|---|---|---|---|
| White matter microstructure | FA.Parahippocampal part of cingulum | Imaging | 25494, 25495 | | |
| White matter microstructure | FA.Corticospinal tract | Imaging | 25496, 25497 | | |
| White matter microstructure | FA.Inferior fronto-occipital fasciculus | Imaging | 25500, 25501 | | |
| White matter microstructure | FA.Inferior longitudinal fasciculus | Imaging | 25502, 25503 | | |
| White matter microstructure | FA.Medial lemniscus | Imaging | 25505, 25506 | | |
| White matter microstructure | FA.Posterior thalamic radiation | Imaging | 25507, 25508 | | |
| White matter microstructure | FA.Superior longitudinal fasciculus | Imaging | 25509, 25510 | | |
| White matter microstructure | FA.Superior thalamic radiation | Imaging | 25511, 25512 | | |
| White matter microstructure | FA.Uncinate fasciculus | Imaging | 25513, 25514 | | |
| White matter microstructure | FA.Forceps major | Imaging | 25498 | | |
| White matter microstructure | FA.Forceps minor | Imaging | 25499 | | |
| White matter microstructure | FA.Middle cerebellar peduncle | Imaging | 25504 | | |
| White matter microstructure | MD.Acoustic radiation | Imaging | 25516, 25517 | 9671 | Bilateral tracts. Hemisphere was controlled for. |

| | | | | | |
|---|---|---|---|---|---|
| White matter microstructure | MD.Anterior thalamic radiation | Imaging | 25517, 25518 | | |
| White matter microstructure | MD.Cingulate gyrus part of cingulum | Imaging | 25519, 25520 | | |
| White matter microstructure | MD.Parahippocampal part of cingulum | Imaging | 25523, 25524 | | |
| White matter microstructure | MD.Corticospinal tract | Imaging | 25523, 25524 | | |
| White matter microstructure | MD.Inferior fronto-occipital fasciculus | Imaging | 25527, 25528 | | |
| White matter microstructure | MD.Inferior longitudinal fasciculus | Imaging | 25529, 25530 | | |
| White matter microstructure | MD.Medial lemniscus | Imaging | 25532, 25533 | | |
| White matter microstructure | MD.Posterior thalamic radiation | Imaging | 25534, 25535 | | |
| White matter microstructure | MD.Superior longitudinal fasciculus | Imaging | 25536, 25537 | | |
| White matter microstructure | MD.Superior thalamic radiation | Imaging | 25538, 25539 | | |
| White matter microstructure | MD.Uncinate fasciculus | Imaging | 25540, 25541 | | |
| White matter microstructure | MD.Forceps major | Imaging | 25525 | | |
| White matter microstructure | MD.Forceps minor | Imaging | 25526 | | |

| | | | | | |
|---|---|---|---|---|---|
| White matter microstructure | MD.Middle cerebellar peduncle | Imaging | 25531 | | |
| Resting-state connectivity | 1548 connections between 55 nodes | Imaging | 25753 | 10121 | |

Table S2. Loadings of each tract on gTotal, gAF, gTR and gPF in FA and MD.

| Tract | FA | | | | MD | | | |
|---|---|---|---|---|---|---|---|---|
| | g.Total | gAF | gTR | gPF | g.Total | gAF | gTR | gPF |
| Parahippocampal part of cingulum | 0.353 | 0.361 | -- | -- | 0.461 | 0.575 | -- | -- |
| Parahippocampal part of cingulum | 0.397 | 0.413 | -- | -- | 0.433 | 0.544 | -- | -- |
| Forceps major | 0.546 | 0.557 | -- | -- | 0.489 | 0.54 | -- | -- |
| Cingulate gyrus part of cingulum | 0.563 | 0.639 | -- | -- | 0.633 | 0.598 | -- | -- |
| Cingulate gyrus part of cingulum | 0.586 | 0.662 | -- | -- | 0.638 | 0.614 | -- | -- |
| Uncinate fasciculus | 0.647 | 0.665 | -- | -- | 0.665 | 0.716 | -- | -- |
| Uncinate fasciculus | 0.684 | 0.698 | -- | -- | 0.749 | 0.777 | -- | -- |
| Superior longitudinal fasciculus | 0.823 | 0.801 | -- | -- | 0.85 | 0.788 | -- | -- |
| Superior longitudinal fasciculus | 0.814 | 0.802 | -- | -- | 0.865 | 0.809 | -- | -- |
| Forceps minor | 0.804 | 0.804 | -- | -- | 0.725 | 0.668 | -- | -- |
| Inferior longitudinal fasciculus | 0.824 | 0.818 | -- | -- | 0.855 | 0.856 | -- | -- |
| Inferior longitudinal fasciculus | 0.844 | 0.824 | -- | -- | 0.902 | 0.878 | -- | -- |
| Inferior fronto-occipital fasciculus | 0.822 | 0.828 | -- | -- | 0.859 | 0.848 | -- | -- |
| Inferior fronto-occipital fasciculus | 0.852 | 0.842 | -- | -- | 0.892 | 0.868 | -- | -- |
| Superior thalamic radiation | 0.651 | -- | 0.739 | -- | 0.778 | -- | 0.853 | -- |
| Superior thalamic radiation | 0.641 | -- | 0.744 | -- | 0.746 | -- | 0.83 | -- |
| Posterior thalamic radiation | 0.672 | -- | 0.779 | -- | 0.756 | -- | 0.86 | -- |
| Posterior thalamic radiation | 0.677 | -- | 0.804 | -- | 0.775 | -- | 0.884 | -- |
| Anterior thalamic radiation | 0.775 | -- | 0.806 | -- | 0.837 | -- | 0.863 | -- |
| Anterior thalamic radiation | 0.769 | -- | 0.818 | -- | 0.83 | -- | 0.863 | -- |
| Medial lemniscus | 0.273 | -- | -- | 0.505 | 0.22 | -- | -- | 0.231 |
| Middle cerebellar peduncle | 0.364 | -- | -- | 0.525 | 0.325 | -- | -- | 0.956 |
| Medial lemniscus | 0.286 | -- | -- | 0.53 | 0.197 | -- | -- | 0.2 |
| Acoustic radiation | 0.621 | -- | -- | 0.57 | 0.492 | -- | -- | 0.289 |
| Acoustic radiation | 0.635 | -- | -- | 0.627 | 0.524 | -- | -- | 0.245 |
| Corticospinal tract | 0.579 | -- | -- | 0.817 | 0.585 | -- | -- | 0.268 |
| Corticospinal tract | 0.586 | -- | -- | 0.834 | 0.585 | -- | -- | 0.274 |

Table S3. List of regions for the functional connectivity that positively associate with higher Depression-PGRS. The report was generated using the 'report' function in SPM 12.

| Coordination of the voxel with the highest intensity in the cluster | AAL regions | Number of voxels | Highest intensity |
|---|---|---|---|
| -10, -60, 18 | Precuneus_L (aal) | 5236 | 0.16795 |
| -34, 36, -10 | Frontal_Inf_Orb_L (aal) | 2807 | 0.14045 |
| -22, 28, 40 | Frontal_Mid_L (aal) | 1930 | 0.17721 |
| 26, 32, 34 | Frontal_Mid_R (aal) | 1575 | 0.14386 |
| 58, -8, -10 | Temporal_Mid_L (aal) | 933 | 0.096372 |
| 14, -78, -32 | Cerebelum_Crus1_R (aal) | 897 | 0.092922 |
| -52, -12, 32 | Postcentral_L (aal) | 886 | 0.17333 |
| -20, 58, , 0 | Frontal_Sup_L (aal) | 851 | 0.10166 |
| -40, -70, 34 | Occipital_Mid_L (aal) | 545 | 0.074744 |
| 50, -12, -12 | Temporal_Mid_R (aal) | 540 | 0.078985 |
| -32, -40, -12 | Fusiform_L (aal) | 462 | 0.11144 |
| 22, 60, -2 | Frontal_Sup_Orb_R (aal) | 372 | 0.097698 |
| -12, 48, 14 | Frontal_Sup_Medial_L (aal) | 243 | 0.082818 |
| 16, -60, -24 | Cerebelum_6_L (aal) | 224 | 0.086436 |
| 0, -60, -24 | Vermis_6 (aal) | 203 | 0.076384 |
| 24, -20, -16 | Hippocampus_R (aal) | 192 | 0.090945 |
| 24, -38, -12 | Fusiform_R (aal) | 174 | 0.085587 |
| 24, -20, -16 | Hippocampus_L (aal) | 141 | 0.10302 |
| 16, -62, -18 | Cerebelum_6_R (aal) | 137 | 0.075099 |
| 36, -6, 14 | Insula_R (aal) | 130 | 0.09974 |
| -36, -8, 14 | Rolandic_Oper_L (aal) | 91 | 0.086849 |
| 46, -52, -10 | Temporal_Inf_L (aal) | 84 | 0.061853 |
| -10, -78, -32 | Cerebelum_Crus2_L (aal) | 56 | 0.05745 |
| -10, -2, 14 | Caudate_L (aal) | 54 | 0.077763 |
| 48, -66, 36 | Angular_R (aal) | 42 | 0.047485 |
| 10, -68, -50 | Cerebelum_8_L (aal) | 40 | 0.061126 |
| 2, -52, -18 | Vermis_4_5 (aal) | 33 | 0.060399 |
| 42, -16, -24 | Fusiform_R (aal) | 27 | 0.071946 |
| 40, -4, -44 | Temporal_Inf_R (aal) | 22 | 0.066757 |
| 10, 48, -10 | Frontal_Med_Orb_R (aal) | 22 | 0.062801 |
| -34, -52, -32 | Cerebelum_6_L (aal) | 22 | 0.059631 |

Table S4. List of regions for the functional connectivity that negatively associate with higher Depression-PGRS. The report was generated using the 'report' function in SPM 12.

| Coordination of the voxel with the highest intensity in the cluster | AAL regions | Number of voxels | Lowest intensity |
|---|---|---|---|
| 18, 64, -6 | Frontal_Sup_Orb_R, (aal) | 13358 | -0.10955 |
| 26, -96, -4 | Occipital_Inf_R, (aal) | 3818 | -0.16348 |
| -52, -48,, 4 | Temporal_Mid_L, (aal) | 1244 | -0.06084 |
| -30, -46, 38 | Parietal_Inf_L, (aal) | 1207 | -0.07073 |
| 44, 12, 32 | Frontal_Inf_Oper_R, (aal) | 977 | -0.06305 |
| 32, 22, 10 | Insula_R, (aal) | 565 | -0.08861 |
| -10, -66, 32 | Precuneus_L, (aal) | 514 | -0.09174 |
| 14, -64, 34 | Precuneus_R, (aal) | 376 | -0.08152 |
| 30, -6, 52 | Precentral_R, (aal) | 374 | -0.06178 |
| 44, -24, 38 | Postcentral_R, (aal) | 300 | -0.0564 |
| 60, -22, -6 | Temporal_Sup_R, (aal) | 245 | -0.04927 |
| 38, -54, -42 | Cerebelum_Crus1_L, (aal) | 180 | -0.05439 |
| 44, -52, -12 | Temporal_Inf_L, (aal) | 150 | -0.05388 |
| 64, -50, , 6 | Temporal_Mid_R, (aal) | 65 | -0.03867 |
| 22, -68, -50 | Cerebelum_8_L, (aal) | 64 | -0.04105 |
| 22, -38, -44 | Cerebelum_10_R, (aal) | 50 | -0.0544 |
| 16, -42, -44 | Cerebelum_9_L, (aal) | 50 | -0.05161 |
| -28, -70, 26 | Occipital_Mid_L, (aal) | 50 | -0.04033 |
| -10, -2, 14 | Caudate_L, (aal) | 33 | -0.06296 |
| -38, -4, 16 | Insula_L, (aal) | 33 | -0.06194 |
| 22, 28, -16 | Frontal_Sup_Orb_R, (aal) | 26 | -0.0404 |
| 44, -8, 54 | Precentral_R, (aal) | 26 | -0.03745 |
| 20, -28, -6 | Hippocampus_L, (aal) | 25 | -0.06612 |
| 38, -2, 16 | Insula_R, (aal) | 24 | -0.05134 |
| 24, -56, -50 | Cerebelum_8_L, (aal) | 23 | -0.04057 |
| 0, -50, -20 | Vermis_4_5, (aal) | 22 | -0.04336 |

# Appendix 4:

# Supplementary materials of Chapter 5: Resting-State Connectivity and Its Association With Cognitive Performance, Educational Attainment, and Household Income in UK Biobank

## Supplementary Methods

### Participants

The UK Biobank covers an age range from 40 to 70 at the initial visit, and by the time of the imaging assessment, the age range was from 45 to 75, because the imaging assessment took place after the initial visit. The imaging sample was selected within the overall sample for predominantly healthy participants to achieve a selection of population-based sample. The UK Biobank sample chose mainly white people with European ancestry. The education level was comparatively high, with a proportion of 53.15% received college or university level degree.

### Clustering of 55*55 matrix

The clustering for the whole-brain analyses on 55*55 connectivity matrix was for better illustration, using hierarchical clustering approach described in: http://journals.plos.org/plosone/article?id=10.1371/journal.pone.0076315. The number of cluster was user-defined as n=5.

### Educational attainment and household income

For educational attainment, participants could choose at least one of the following options: College or university degree, A levels/AS levels or equivalent, O levels/GCSEs or equivalent, CSEs or equivalent, NVQ or HND or HNC or equivalent, other professional qualifications, none of the above, and prefer not to answer.

For household income, available choices were: <£18,000, £18,000 to £30,999, £31,000 to £51,999, £52,000 to £100,000, >£100,000, do not know and prefer not to answer. An ordinal variable from 1 to 5 was created to determine the level of household income (<£18,000 as 1, >£100,000 as 5).

### PCA analysis for cognitive performance, educational attainment and household

**income**

As the results in the main text showed that the regions involved in the three traits were highly overlapping, we have conducted a PCA analysis to extract the first unrotated latent component of the three traits, and used the scores for the factor to test the resting-state-network associations with the common variance of all three traits.

PCA was conducted using princomp in R (https://stat.ethz.ch/R-manual/R-devel/library/stats/html/princomp.html). Results are shown in supplementary results and Figure S5.

**Permutation test**

As we now have an updated sample of 7,144 people (from the latest data release), we have now additionally conducted two further sets of analyses to validate our results.

First we performed permutation test on half-sized sample (N=3,572) and tested the distributions of the p values for the significant connections found in 55*55 matrix described in our initial findings. After 1,000 times of randomly selecting half of our sample, conducting analyses on them, we found that the distributions of p values for over 90% of the significant connections found in our initial results were lower, compared with the mean p value for the rest of connections (Figure S7-S9).

Second, another permutation test was performed to test whether the results found in a training subsample can predict the results in a separate testing sample. We cut the sample in halves, and used the first half as a training dataset and the second half as a testing dataset. We extracted the effect sizes for the 55*55 connectivity matrix acquired from the training sample and applied them on the testing dataset to calculate a neural connectivity score for the trait. And then we used the neural connectivity score to predict the variances for the traits in the testing sample. For instance, we used the effect sizes of cognitive performance in the training sample ($\beta_{training}$), and calculated the sum of $\beta training * Connectivity_{testing}$ as the neural-network score of cognitive performance in the testing sample. We then used this score to predict the cognitive performance, educational attainment and household income in the testing sample. Age, $age^2$, gender, scanner positions and mean motion were controlled. Likewise permutation tests were conducted to use the neural associations of educational attainment or household income to predict other traits in the testing

sample. Results are shown in Figure S10.

## Supplementary Results

### Phenotypic associations

The mean test performance score for the VNR was 6.92 (SD = 2.15). Age and sex both showed significant associations with VNR score (age: β=-0.07, p=3.50X10-5, sex: β=0.19, p=3.18X10-9; Male=1, Female=0).

In total, 1,801 participants reported having obtained a college/university-level degree (43.29% of the overall sample). The mean age of people with a college/university-level degree was 61.62 (SD=7.49), which was significantly lower than the group without (Mean age=62.65, SD=7.58, t=4.37, p=1.27X10-5). Men reported a significantly higher proportion of college degrees (48.80%) than women (39.73%), χ2=34.8, df=1, p=3.65X10-9. Educational attainment showed positive association with cognitive performance, with age, age2 and sex controlled (β=0.457, p<2X10-16).

The proportion of people who reported having household income at each level is shown in Figure S1. The income band of £31,000 to £51,999 contained the highest proportion (29.98%) of individuals, and the band >£100,000 contained the lowest proportion (6.06%). Both age and sex showed significant associations with household income (age: β=-0.29, p<2X10-16; sex: β=0.20, p=1.04X10-9). Higher household income was associated with better cognitive performance (β=0.167, p<2X10-16), with age, age2, and sex controlled in the model.

### PCA analysis of cognitive performance, educational attainment and household income

The first latent component (g) of the three traits explains a major portion of total variance (75.6%), it was heavily loaded on cognitive performance (correlation loadings: cognitive performance: 0.998, educational attainment: 0.261, household income: 0.220).

We have conducted an additional analysis using the first latent component as a predictor and tested the shared component of cognitive performance, educational attainment and household income on the resting-state networks (see supplementary methods). Results are shown in Figure S7. As expected, the regions involved with

stronger connections with latent g of the three traits were mainly located in default mode network areas and lateral prefrontal cortex.

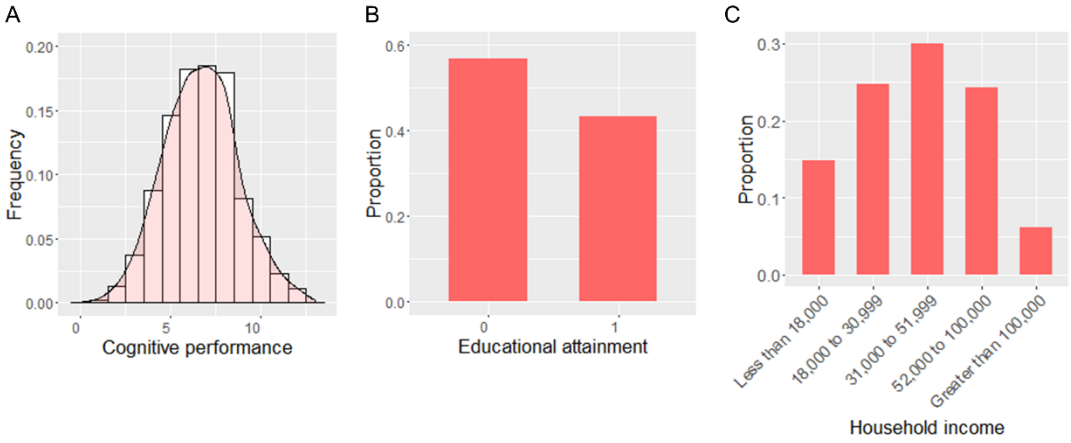


Figure S1. Descriptive statistics of (a) cognitive performance on the verbal-numerical reasoning test; (b) educational attainment (those with [0] and without [1] a college degree; and (c) household income (GBP per annum).

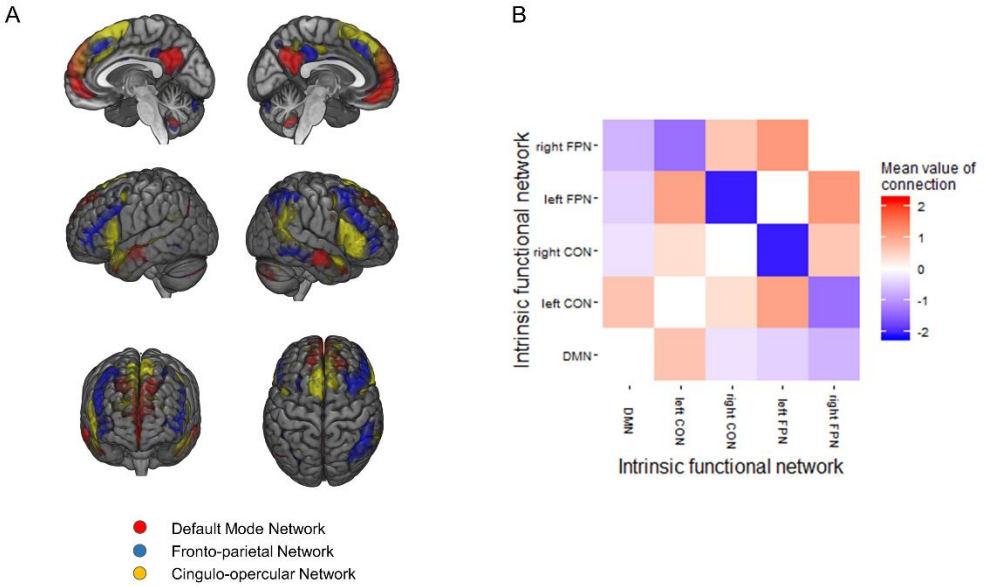


Figure S2. (A) Five intrinsic functional networks selected from the 21 components generated by low-dimension ICA (see Methods, Imaging data). Component 1 was identified as the default mode network (DMN, red). Component 13 and 21 were left and right cingulo-opercular network (CON) respectively (yellow). And finally, component 5 and 6 were identified as right and left fronto-parietal network (FPN, blue). (B) The mean values of couplings of networks of interest. The values are standardised temporal correlation coefficient between networks of interest. A higher absolute value indicates a higher strength, and the sign indicates the directionality of the connection. A negative value means an anti-correlated connection, whilst a positive value indicates a positive connection. Mean values and 95% confident intervals of the connections can be viewed in Table 1.

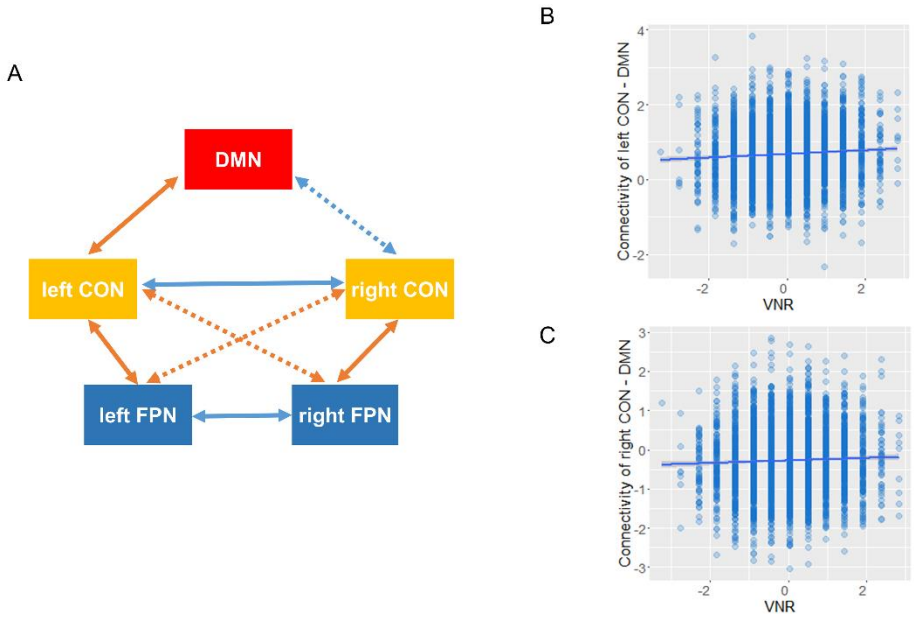


Figure S3. (A) Significant network couplings associated with cognitive performance in verbal-numerical reasoning (absolute β ranged from 0.034 to 0.063, all effect sizes of the significant connections are reported in Table 1). An orange arrow means positive association between cognitive ability with the absolute strength of a connection, whilst a blue arrow indicates decreased absolute strength of a connection with better cognitive performance. Solid arrows are positive connections and dashed ones are negative. An orange arrow reflects positive associations between cognitive ability with the absolute strength of a connection, whilst a blue arrow indicates decreased absolute strength of a connection with better cognitive performance. (B) and (C) represent the association of cognitive performance in verbal-numerical reasoning and the connection between left/right CON (β=0.061 and -0.045 respectively for left/right CON) and DMN (β=-0.045). Y-axis represent the normalised correlation coefficient between temporal modulations of networks. Better cognitive performance was associated with more positive connections between DMN and bilateral CON. The spatial maps of the functional networks can be found in Figure S2.

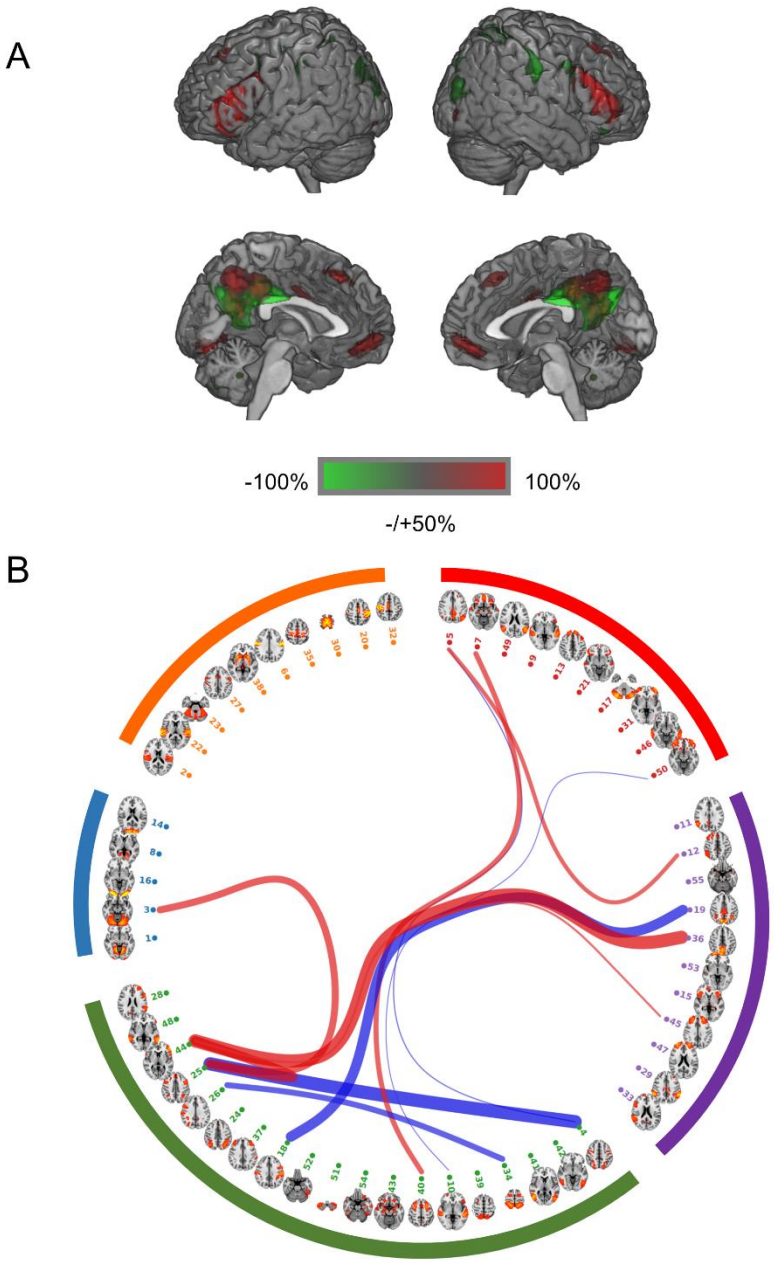


Figure S4. Results for whole-brain analysis of non-binary proxy for educational attainment. Three levels were set, which included: college or university level, A or AS level, and all other levels.

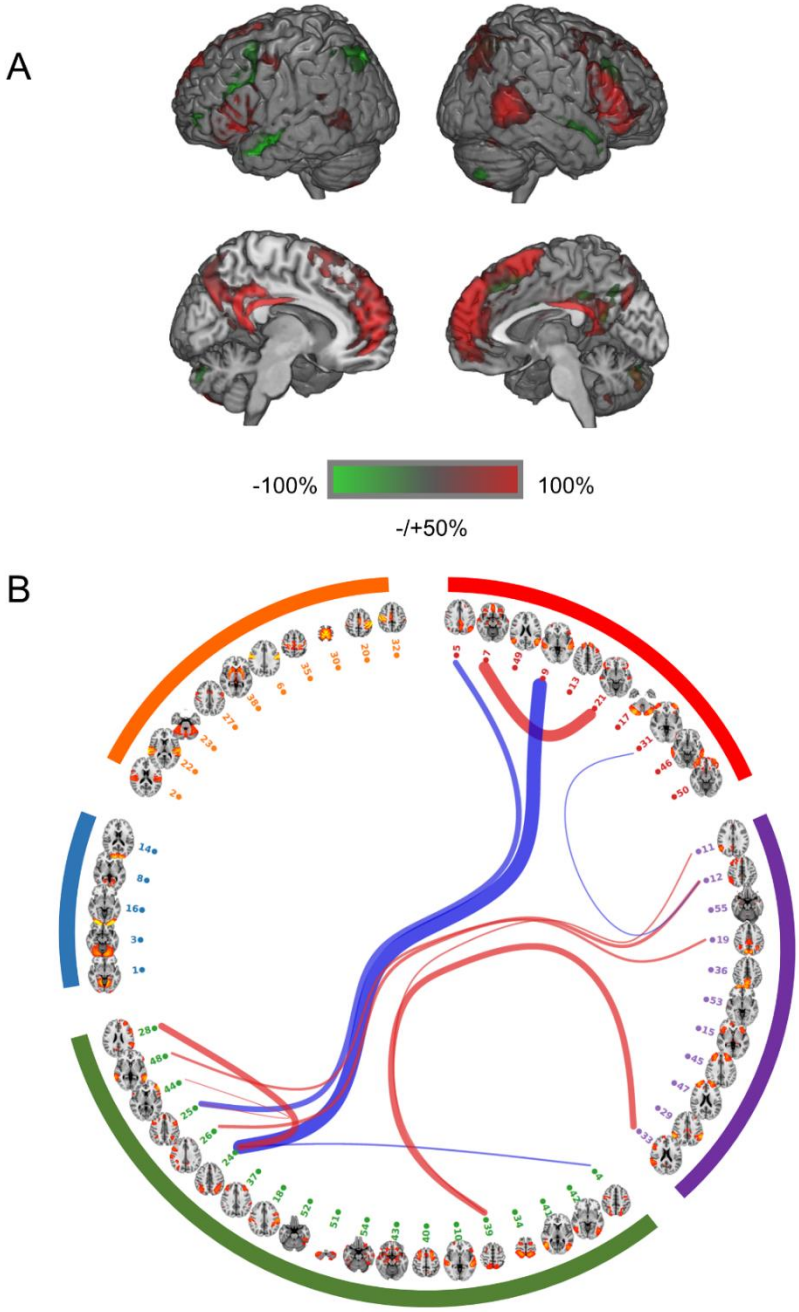


Figure S5. Results for whole brain analysis of the first latent component of cognitive performance (VNR), educational attainment and household income. The first latent component was extracted from unrotated PCA by using princomp in R (https://stat.ethz.ch/R-manual/R-devel/library/stats/html/princomp.html). This component explains 75.6% of total variance. Correlation loadings for the factor are: cognitive performance: 0.998, educational attainment: 0.261, household income: 0.220.

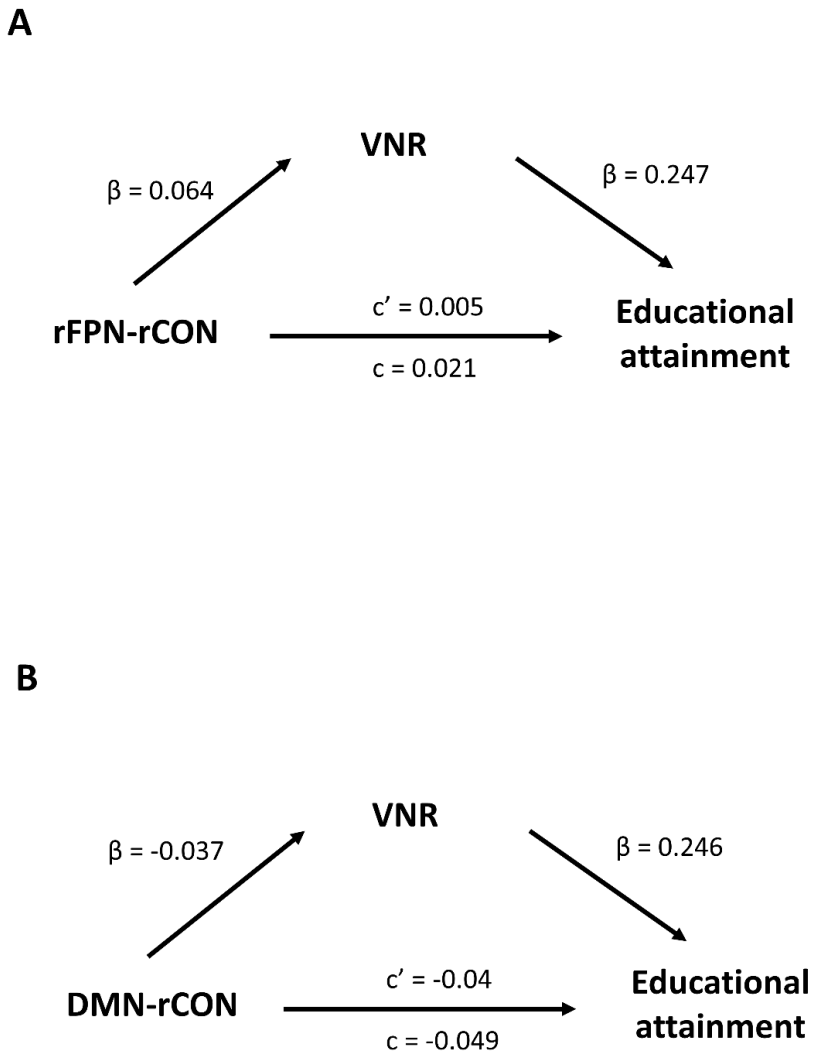


Figure S6. Mediation analysis for NOI results. Network connectivity was set as the predictor, and educational attainment as the dependent variable. Mediator was set as cognitive performance. We tested on two network connections that were significant for both educational attainment and cognitive performance. The association between rFPN-rCON and rCON-DMN connectivity and educational attainment was mediated by cognitive performance (18.4% and 76.2% of direct path mediated by indirect path respectively for each model, CFI = TLI = 1).

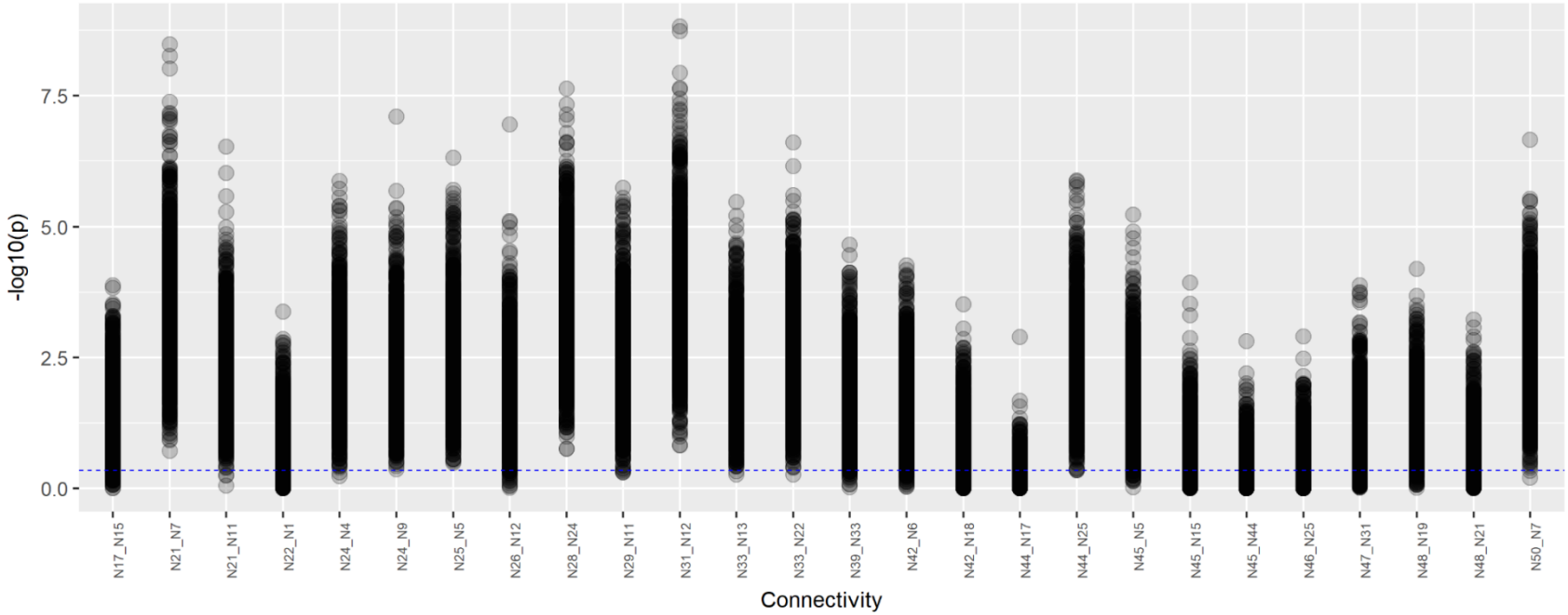


Figure S7. Permutation test on cognitive performance (VNR). X axis shows the connections, and y axis shows the uncorrected p value transformed by -log10 function. T-test was performed on the p-value distributions for each connection that was found associated with VNR to test whether these tested connections have significantly lower p values compared to the non-significant connections in the initial finding. The dashed blue line is the mean uncorrected p value of all other connections. Two connections' p values were not significantly lower than the mean p value of all other connections (N44-N17: t(999)=18.25, p<1E-16, and N45-N44: t(999)=6.95, p=6.50E-12). All other connections have lower p values compared to the non-significant ones, which takes up 92.3% of all 26 connections (t-test p<1E-16).

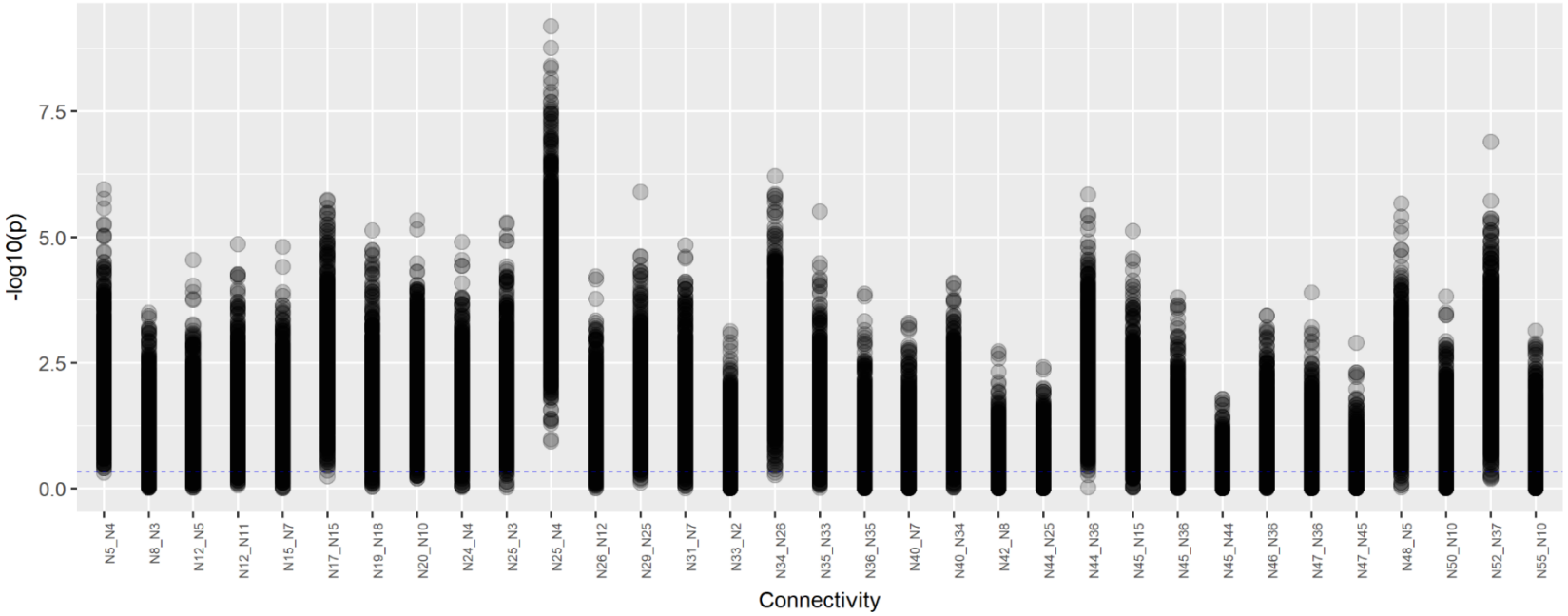


Figure S8. Permutation test on educational attainment. X axis shows the connections, and y axis shows the uncorrected p value transformed by -log10 function. T-test was performed on the p-value distributions for each connection that was found associated with educational attainment to test whether these tested connections have significantly lower p values compared to the non-significant connections in the initial finding. The dashed blue line is the mean uncorrected p value of all other connections. Three connections' p values were not significantly lower than the mean p value of all other connections (N44-N25: t(999)=1.22, p=0.22, N45-N44: t(999)=11.55, p<1E-16, and N47-N45: t(999)=4.98, p=7.34E-7). All other connections have lower p values compared to the non-significant ones, which takes up 90.0% of all 33 connections (t-test p<1E-16).

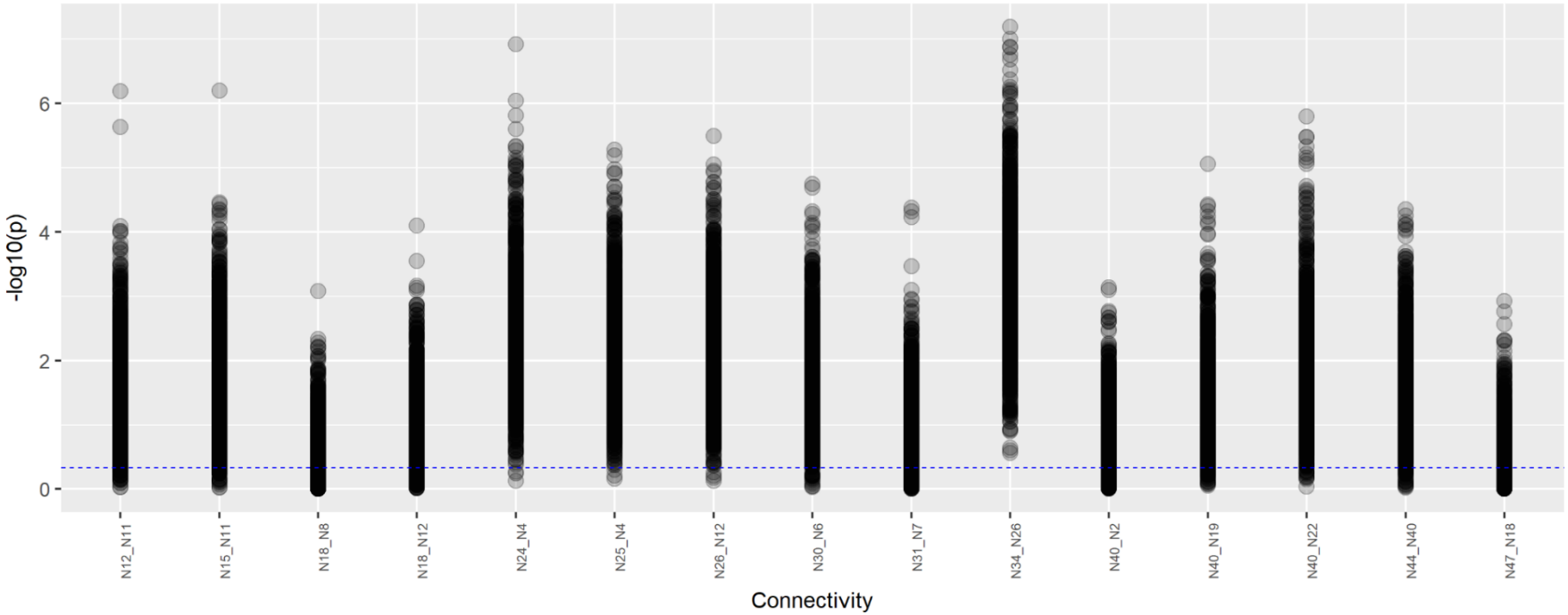


Figure S9. Permutation test on household income. X axis shows the connections, and y axis shows the uncorrected p value transformed by -log10 function. T-test was performed on the p-value distributions for each connection that was found associated with household income to test whether these tested connections have significantly lower p values compared to the non-significant connections in the initial finding. The dashed blue line is the mean uncorrected p value of all other connections. All the connections have lower p values compared to the non-significant ones (t-test p<4.91E-8).

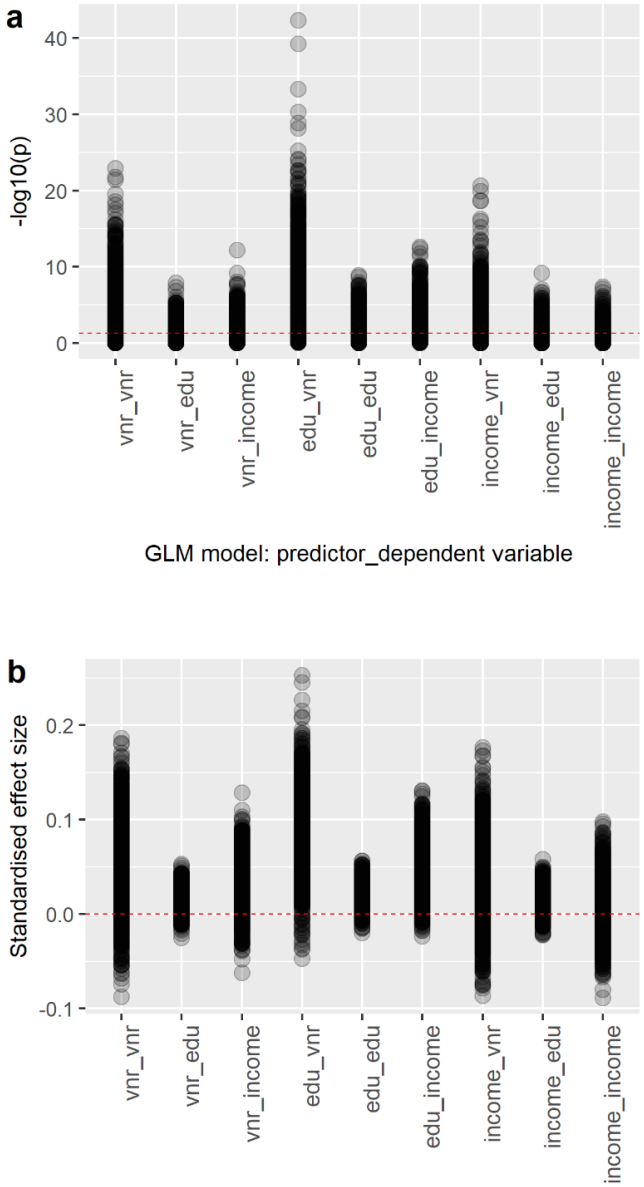


Figure S10. Using the model built by the training sample to predict the traits in the testing sample. The x axis is the models of using predictors derived from training sample to predict the trait as the dependent variable in the testing sample. In panel a, the y axis is the uncorrected p value transformed by -log10. In panel a, the red dashed line is the p=0.05 significance line, as there is no baseline mean p value to compare with like in Figure S6-8. In Figure b, the y axis is the standardised effect size. We also conducted t-test to compare the effect sizes with 0, and all models showed significant difference from 0 (income_income: $p = 0.009$, for all other models: $p < 1 \times 10^{-16}$).

Table S1. Connections that showed significant association with cognitive performance in VNR on 55*55 partial correlation matrix. All reported betas are standardised effect sizes. The regression model was applied to test the association between VNR and absolute strength of connections, which was achieved by multiplying values of connections with the sign of their mean value (see Methods). The spatial maps of the nodes in the table indicated by numbers can be found in Figure 2.

| | Beta | Standard error | t.value | p | p.corrected | Valence of connection | 95% CI of value of connection | |
|---|---|---|---|---|---|---|---|---|
| **N17_N15** | 0.054 | 0.016 | -3.403 | 6.73E-04 | 0.038 | + | 1.215 | 1.275 |
| **N21_N11** | 0.062 | 0.016 | 3.901 | 9.72E-05 | 0.014 | - | -1.939 | -1.881 |
| **N21_N7** | 0.097 | 0.016 | 6.140 | 9.09E-10 | 0.000 | + | 3.746 | 3.829 |
| **N22_N1** | 0.061 | 0.016 | -3.789 | 1.53E-04 | 0.018 | - | -0.561 | -0.510 |
| **N24_N4** | -0.066 | 0.016 | -4.092 | 4.37E-05 | 0.007 | - | -1.136 | -1.075 |
| **N24_N9** | -0.083 | 0.016 | 5.196 | 2.14E-07 | <0.001 | + | 0.319 | 0.363 |
| **N25_N5** | -0.072 | 0.016 | 4.488 | 7.39E-06 | 0.002 | - | -0.639 | -0.579 |
| **N26_N12** | 0.081 | 0.016 | 5.036 | 4.96E-07 | 0.000 | + | 3.746 | 3.829 |
| **N28_N24** | 0.076 | 0.016 | 4.737 | 2.25E-06 | 0.001 | + | 0.151 | 0.206 |
| **N29_N11** | 0.059 | 0.016 | 3.671 | 2.45E-04 | 0.021 | + | 0.762 | 0.830 |
| **N31_N12** | -0.066 | 0.016 | -4.109 | 4.06E-05 | 0.007 | + | 1.234 | 1.300 |
| **N33_N13** | 0.060 | 0.016 | -3.751 | 1.78E-04 | 0.018 | - | -0.702 | -0.649 |
| **N33_N22** | 0.055 | 0.016 | 3.412 | 6.52E-04 | 0.038 | + | 0.649 | 0.701 |
| **N39_N33** | 0.074 | 0.016 | -4.580 | 4.80E-06 | 0.001 | - | -0.561 | -0.510 |
| **N42_N18** | 0.055 | 0.016 | 3.445 | 5.77E-04 | 0.037 | + | 1.671 | 1.737 |
| **N42_N6** | -0.056 | 0.016 | 3.516 | 4.43E-04 | 0.031 | - | -0.594 | -0.548 |
| **N44_N17** | 0.054 | 0.016 | 3.425 | 6.21E-04 | 0.038 | + | 0.276 | 0.314 |
| **N44_N25** | 0.071 | 0.016 | 4.477 | 7.78E-06 | 0.002 | + | 2.321 | 2.383 |
| **N45_N15** | 0.059 | 0.016 | 3.682 | 2.34E-04 | 0.021 | + | 1.233 | 1.291 |
| **N45_N44** | 0.055 | 0.016 | -3.494 | 4.81E-04 | 0.032 | - | -1.264 | -1.217 |

| | Beta | Standard error | t.value | p | p.corrected | Valence of connection | 95% CI of value of connection | |
|---|---|---|---|---|---|---|---|---|
| **N45_N5** | -0.058 | 0.016 | -3.625 | 2.93E-04 | 0.024 | + | 0.026 | 0.095 |
| **N46_N25** | -0.057 | 0.016 | -3.543 | 4.00E-04 | 0.030 | + | 0.002 | 0.046 |
| **N47_N31** | 0.059 | 0.016 | 3.766 | 1.68E-04 | 0.018 | + | 1.096 | 1.159 |
| **N48_N19** | 0.061 | 0.016 | -3.780 | 1.59E-04 | 0.018 | - | -0.679 | -0.627 |
| **N48_N21** | -0.061 | 0.016 | -3.804 | 1.44E-04 | 0.018 | + | 0.005 | 0.053 |
| **N50_N7** | 0.057 | 0.016 | -3.591 | 3.33E-04 | 0.026 | - | -0.251 | -0.213 |

Table S2. Connections that showed significant association between their absolute strength with educational attainment on the whole brain proxied by 55*55 partial correlation matrix. The spatial maps of the nodes in the table indicated by numbers can be found in Figure 2.

| | Beta | Standard error | t.value | p | p.corrected | Valence of connection | 95% CI of value of connection | |
|---|---|---|---|---|---|---|---|---|
| **N5-N4** | -0.103 | 0.031 | 3.290 | 1.01E-03 | 0.045 | - | -0.720 | -0.660 |
| **N8-N3** | -0.119 | 0.031 | -3.809 | 1.42E-04 | 0.018 | + | 0.903 | 0.994 |
| **N12-N5** | 0.132 | 0.031 | -4.201 | 2.71E-05 | 0.007 | - | -2.111 | -2.036 |
| **N12-N11** | 0.106 | 0.031 | 3.394 | 6.94E-04 | 0.040 | + | 6.507 | 6.608 |
| **N15-N7** | 0.122 | 0.031 | 3.949 | 7.96E-05 | 0.015 | + | 0.875 | 0.929 |
| **N17-N15** | 0.121 | 0.031 | -3.905 | 9.59E-05 | 0.015 | - | -0.825 | -0.784 |
| **N19-N18** | -0.136 | 0.031 | 4.338 | 1.47E-05 | 0.005 | - | -0.747 | -0.689 |
| **N20-N10** | -0.109 | 0.031 | 3.488 | 4.91E-04 | 0.038 | - | -0.443 | -0.399 |
| **N24-N4** | -0.108 | 0.031 | -3.428 | 6.15E-04 | 0.038 | + | 0.588 | 0.651 |
| **N25-N3** | 0.137 | 0.031 | -4.355 | 1.36E-05 | 0.005 | - | -0.264 | -0.223 |
| **N25-N4** | -0.161 | 0.031 | -5.150 | 2.73E-07 | <0.001 | + | 0.995 | 1.059 |
| **N26-N12** | 0.108 | 0.031 | 3.457 | 5.51E-04 | 0.038 | + | 3.746 | 3.829 |
| **N29-N25** | 0.108 | 0.031 | -3.440 | 5.88E-04 | 0.038 | + | 0.180 | 0.241 |
| **N31-N7** | 0.125 | 0.031 | -3.995 | 6.57E-05 | 0.014 | - | -1.939 | -1.881 |
| **N33-N2** | -0.103 | 0.031 | -3.294 | 9.96E-04 | 0.045 | + | 0.257 | 0.310 |
| **N34-N26** | -0.133 | 0.031 | -4.254 | 2.14E-05 | 0.006 | + | 0.320 | 0.378 |
| **N35-N33** | 0.108 | 0.031 | -3.452 | 5.63E-04 | 0.038 | - | -0.075 | -0.035 |
| **N36-N35** | 0.105 | 0.031 | -3.363 | 7.79E-04 | 0.041 | - | -0.636 | -0.596 |
| **N40-N7** | 0.118 | 0.031 | -3.761 | 1.72E-04 | 0.020 | - | -0.694 | -0.648 |
| **N40-N34** | 0.122 | 0.031 | -3.888 | 1.03E-04 | 0.015 | - | -0.479 | -0.429 |
| **N42-N8** | -0.108 | 0.031 | 3.439 | 5.89E-04 | 0.038 | - | -0.756 | -0.699 |
| **N44-N25** | 0.112 | 0.031 | 3.589 | 3.35E-04 | 0.029 | + | 2.321 | 2.383 |
| **N44-N36** | 0.139 | 0.031 | -4.431 | 9.61E-06 | 0.005 | - | -1.469 | -1.424 |

| | Beta | Standard error | t.value | p | p.corrected | Valence of connection | 95% CI of value of connection | |
|---|---|---|---|---|---|---|---|---|
| **N45-N15** | 0.117 | 0.031 | 3.717 | 2.05E-04 | 0.022 | + | 1.233 | 1.291 |
| **N45-N36** | 0.105 | 0.031 | 3.348 | 8.20E-04 | 0.041 | + | 0.617 | 0.662 |
| **N45-N44** | 0.105 | 0.031 | -3.403 | 6.74E-04 | 0.040 | - | -1.264 | -1.217 |
| **N46-N36** | 0.110 | 0.031 | -3.509 | 4.54E-04 | 0.037 | - | -0.935 | -0.890 |
| **N47-N36** | 0.105 | 0.031 | 3.358 | 7.93E-04 | 0.041 | + | 0.721 | 0.766 |
| **N47-N45** | 0.110 | 0.031 | 3.590 | 3.35E-04 | 0.029 | + | 2.071 | 2.130 |
| **N48-N5** | -0.114 | 0.031 | 3.641 | 2.75E-04 | 0.027 | - | -0.123 | -0.055 |
| **N50-N10** | -0.121 | 0.031 | 3.861 | 1.15E-04 | 0.015 | - | -0.606 | -0.569 |
| **N52-N37** | 0.104 | 0.031 | 3.343 | 8.37E-04 | 0.041 | + | 0.303 | 0.344 |
| **N55-N10** | -0.105 | 0.031 | 3.337 | 8.53E-04 | 0.041 | - | -0.063 | -0.034 |

Table S3. Connections that showed significant association between their absolute strength with household income on the whole brain proxied by 55*55 partial correlation matrix. The significant connections presented in the table is identical with those connections shown in Figure 2.

| | Beta | Standard error | t.value | p | p.corrected | Valence of connection | 95% CI of value of connection | |
|---|---|---|---|---|---|---|---|---|
| **N12_N11** | 0.072 | 0.017 | 4.208 | 2.64E-05 | 0.010 | + | 6.507 | 6.608 |
| **N15_N11** | 0.082 | 0.017 | -4.806 | 1.60E-06 | 0.002 | - | -1.246 | -1.185 |
| **N18_N8** | 0.064 | 0.017 | 3.720 | 2.02E-04 | 0.033 | + | 0.216 | 0.267 |
| **N18_N12** | 0.067 | 0.017 | -3.909 | 9.42E-05 | 0.020 | - | -2.099 | -2.035 |
| **N24_N4** | -0.067 | 0.017 | -3.908 | 9.49E-05 | 0.020 | + | 0.588 | 0.651 |
| **N25_N4** | -0.062 | 0.017 | -3.629 | 2.88E-04 | 0.039 | + | 0.995 | 1.059 |
| **N26_N12** | 0.078 | 0.017 | 4.531 | 6.04E-06 | 0.004 | + | 3.746 | 3.829 |
| **N30_N6** | 0.062 | 0.017 | 3.634 | 2.83E-04 | 0.039 | + | 0.350 | 0.411 |
| **N31_N7** | 0.062 | 0.017 | -3.603 | 3.19E-04 | 0.039 | - | -1.939 | -1.881 |
| **N34_N26** | -0.073 | 0.017 | -4.269 | 2.01E-05 | 0.010 | + | 0.320 | 0.378 |
| **N40_N2** | 0.060 | 0.017 | -3.526 | 4.27E-04 | 0.042 | - | -1.806 | -1.752 |
| **N40_N19** | 0.060 | 0.017 | -3.539 | 4.06E-04 | 0.042 | - | -1.136 | -1.075 |
| **N40_N22** | -0.061 | 0.017 | 3.554 | 3.84E-04 | 0.042 | - | -0.548 | -0.506 |
| **N44_N40** | 0.065 | 0.017 | -3.812 | 1.40E-04 | 0.026 | - | -0.509 | -0.460 |
| **N47_N18** | 0.068 | 0.017 | -3.967 | 7.42E-05 | 0.020 | - | -0.724 | -0.679 |

Table S4. Regions involved in the significant connections of VNR. The regions were extracted using the "result" function of SPM (http://www.fil.ion.ucl.ac.uk/spm/). Clusters that were above 50% of the highest global intensity and cluster size above 20 are reported in the following tables. The coordinates and AAL labels indicate the peak of the reported cluster.

**Positive connections**

| No | Coordinate of peak region | AAL label | Number of voxels | Intensity of peak region |
|---|---|---|---|---|
| 1 | -22, -74, -26 | Cerebelum_Crus1_L | 2804 | 6.4319 |
| 2 | 36, -72, -40 | Cerebelum_Crus2_R | 2661 | 4.765 |
| 3 | -12, -48, -42 | Cerebelum_9_L | 159 | 3.0327 |
| 4 | 50, 4, -38 | Temporal_Inf_R | 157 | 3.0399 |
| 5 | 2, -68, -32 | Vermis_8 | 36 | 2.5446 |
| 6 | 56, 34, 0 | Frontal_Inf_Tri_R | 35023 | 6.9587 |
| 7 | -48, -54, -12 | Temporal_Inf_L | 313 | 2.8549 |
| 8 | 26, -20, -14 | Hippocampus_R | 58 | 3.2229 |
| 9 | 10, 0, 14 | Caudate_R | 78 | 3.1414 |
| 10 | -10, -4, 16 | Caudate_L | 35 | 2.8065 |
| 11 | 4, -20, 8 | Thalamus_R | 29 | 2.6283 |
| 12 | -40, -46, 40 | Parietal_Inf_L | 713 | 3.1276 |
| 13 | -24, -10, 50 | Frontal_Sup_L | 147 | 2.5947 |
| 14 | 34, -2, 60 | Frontal_Mid_R | 54 | 2.053 |

**Negative connections**

| No | Coordinate of peak region | AAL label | Number of voxels | Intensity of peak region |
|---|---|---|---|---|
| 1 | 32, -70, -48 | Cerebelum_7b_R | 351 | -3.5296 |
| 2 | 8, -74, -24 | Cerebelum_Crus1_R | 1982 | -3.4538 |
| 3 | -2, -52, -34 | Cerebelum_9_L | 225 | -2.4617 |
| 4 | -22, -34, -42 | Cerebelum_10_L | 56 | -2.3538 |
| 5 | 48, -60, -8 | Temporal_Inf_R | 2456 | -3.9686 |
| 6 | -28, -74, 22 | Occipital_Mid_L | 8857 | -8.2862 |
| 7 | 30, -64, -28 | Cerebelum_6_R | 147 | -2.8812 |
| 8 | -46, 14, -14 | Temporal_Pole_Sup_L | 26 | -1.8379 |
| 9 | -8, 38, -12 | Frontal_Med_Orb_L | 275 | -2.3001 |
| 10 | -30, 26, -2 | Insula_L | 988 | -3.4967 |
| 11 | 34, 38, -8 | Frontal_Inf_Orb_R | 144 | -3.0886 |
| 12 | 32, 26, -2 | Insula_R | 260 | -3.2563 |
| 16 | -50, -12, 30 | Postcentral_L | 6311 | -4.4245 |
| 17 | 26, 52, -2 | Frontal_Mid_R | 338 | -2.4291 |
| 19 | 32, -72, 22 | Occipital_Mid_R | 3881 | -7.9954 |

| No | Coordinate of peak region | AAL label | Number of voxels | Intensity of peak region |
|---|---|---|---|---|
| 22 | -10, -40, 34 | Cingulum_Mid_L | 1340 | -3.8093 |
| 23 | -8, 0, 12 | Caudate_L | 51 | -2.1585 |
| 24 | -34, -32, 20 | Insula_L | 20 | -1.757 |
| 25 | 36, -30, 18 | Insula_R | 23 | -1.7716 |
| 26 | 6, 4, 56 | Supp_Motor_Area_R | 71 | -2.3897 |
| 27 | -4, 6, 54 | Supp_Motor_Area_L | 31 | -1.6887 |
| 28 | 12, -32, 66 | Paracentral_Lobule_R | 32 | -1.8698 |

Table S5. Regions involved in the significant connections of educational attainment. The coordinates and AAL labels indicate the peak of the reported cluster.

**Positive connections**

| No | Coordinate of peak region | AAL label | Number of voxels | Intensity of peak region |
|---|---|---|---|---|
| 1 | 12, -46, -44 | Cerebelum_9_R | 311 | 8.8438 |
| 2 | -38, -66, -42 | Cerebelum_Crus2_L | 3413 | 11.1 |
| 3 | -2, -68, -34 | Vermis_8 | 29 | 4.7242 |
| 4 | 2, -58, -24 | Vermis_6 | 22 | 5.1606 |
| 5 | 58, -6, -14 | Temporal_Mid_R | 402 | 8.8827 |
| 6 | -26, -36, -16 | Fusiform_L | 75 | 6.8778 |
| 7 | -24, -20, -16 | Hippocampus_L | 55 | 7.7283 |
| 8 | 0, -58, 44 | Precuneus_L | 13050 | 15.5606 |
| 9 | 22, 28, 46 | Frontal_Sup_R | 8148 | 14.3976 |
| 10 | -20, 30, 38 | Frontal_Mid_L | 6549 | 14.9328 |
| 11 | -32, 36, -10 | Frontal_Inf_Orb_L | 421 | 10.9456 |
| 12 | -60, -12, -10 | Temporal_Mid_L | 212 | 7.2928 |
| 13 | -54, -46, -12 | Temporal_Inf_L | 55 | 6.1464 |
| 14 | -20, -84, -10 | Fusiform_L | 739 | 6.1887 |
| 15 | 56, -40, -10 | Temporal_Mid_R | 40 | 4.8633 |
| 16 | 24, -76, -6 | Lingual_R | 187 | 6.9006 |
| 17 | -8, 4, 6 | Caudate_L | 40 | 7.5075 |
| 18 | 8, 6, 4 | Caudate_R | 73 | 7.6276 |
| 19 | -48, -24, 6 | Temporal_Sup_L | 56 | 5.9954 |
| 20 | 36, -84, 10 | Occipital_Mid_R | 25 | 4.1809 |
| 21 | -46, -48, 12 | Temporal_Mid_L | 26 | 4.5143 |
| 22 | 50, -44, 26 | SupraMarginal_R | 1413 | 6.1332 |
| 23 | 34, -26, 18 | Insula_R | 37 | 5.3353 |
| 24 | 30, -74, 20 | Occipital_Mid_R | 26 | 4.8628 |
| 25 | 38, -14, 20 | Insula_R | 20 | 5.6089 |
| 26 | -34, -18, 42 | Postcentral_L | 189 | 7.0578 |
| 27 | -50, -40, 46 | Parietal_Inf_L | 343 | 5.4355 |
| 28 | -16, -4, 68 | Frontal_Sup_L | 40 | 5.1036 |

**Negative connections**

| No | Coordinate of peak region | AAL label | Number of voxels | Intensity of peak region |
|---|---|---|---|---|
| 1 | -10, -72, -26 | Cerebelum_Crus1_L | 453 | -5.7127 |
| 2 | 34, -70, -48 | Cerebelum_7b_R | 77 | -5.1072 |
| 3 | -16, -42, -46 | Cerebelum_9_L | 109 | -6.2768 |
| 4 | 18, -42, -46 | Cerebelum_9_R | 114 | -7.2587 |
| 5 | 10, -84, -38 | Cerebelum_Crus2_R | 60 | -4.8257 |
| 6 | -2, -52, -34 | Cerebelum_9_L | 78 | -6.9646 |
| 7 | 10, -74, -24 | Cerebelum_6_R | 27 | -4.779 |
| 8 | -16, -58, 16 | Precuneus_L | 15001 | -15.7718 |
| 9 | 24, -20, -16 | Hippocampus_R | 43 | -4.5335 |
| 10 | -22, -22, -16 | Hippocampus_L | 25 | -4.972 |
| 11 | 56, -4, -18 | Temporal_Mid_R | 110 | -5.2959 |
| 12 | -34, 36, -12 | Frontal_Inf_Orb_L | 111 | -5.2593 |
| 13 | 32, 38, -8 | Frontal_Inf_Orb_R | 851 | -6.4684 |
| 14 | 50, -58, -6 | Temporal_Inf_R | 366 | -6.3365 |
| 15 | -40, -66, -6 | Occipital_Inf_L | 689 | -6.7649 |
| 16 | 8, 52, -10 | Frontal_Med_Orb_R | 35 | -4.3472 |
| 17 | -10, 46, -6 | Frontal_Med_Orb_L | 30 | -4.1374 |
| 18 | 40, -18, 0 | Insula_R | 22 | -4.7318 |
| 19 | 38, 0, 14 | Insula_R | 35 | -5.385 |
| 20 | -46, -22, 20 | Rolandic_Oper_L | 111 | -5.0322 |
| 21 | -38, -4, 16 | Insula_L | 38 | -7.1293 |
| 22 | 60, -26, 32 | SupraMarginal_R | 106 | -4.2938 |
| 23 | 50, 4, 34 | Precentral_R | 151 | -4.4223 |
| 24 | -20, 28, 38 | Frontal_Sup_L | 144 | -5.3051 |
| 25 | -38, -24, 60 | Precentral_L | 373 | -7.4667 |
| 26 | -26, -8, 48 | Precentral_L | 89 | -4.6457 |

Table S6. Regions involved in the significant connections of household income. The coordinates and AAL labels indicate the peak of the reported cluster.

**Positive connections**

| No | Coordinate of peak region | AAL label | Number of voxels | Intensity of peak region |
|---|---|---|---|---|
| 1 | 24, 26, 50 | Frontal_Sup_R | 21182 | 5.4614 |
| 2 | 12, -72, -48 | Cerebelum_8_R | 394 | 2.7072 |
| 3 | 64, -16, -16 | Temporal_Mid_R | 1409 | 3.2367 |
| 4 | 42, 18, -36 | Temporal_Pole_Mid_R | 41 | 1.8175 |
| 5 | 54, 10, -32 | Temporal_Pole_Mid_R | 21 | 2.0982 |
| 6 | 28, -70, -24 | Cerebelum_6_R | 182 | 2.1569 |
| 7 | -16, -62, -22 | Cerebelum_6_L | 56 | 2.2845 |
| 8 | 10, 44, -20 | Rectus_R | 35 | 2.7192 |
| 9 | 40, -2, 16 | Insula_R | 7530 | 5.667 |
| 10 | -38, -4, 16 | Insula_L | 6699 | 6.2029 |
| 11 | -42, -44, -14 | Temporal_Inf_L | 38 | 1.8629 |
| 12 | -24, 42, -14 | Frontal_Sup_Orb_L | 116 | 2.5622 |
| 13 | -38, 48, 2 | Frontal_Mid_L | 1066 | 2.6366 |
| 14 | -46, -68, 8 | Temporal_Mid_L | 381 | 2.5717 |
| 15 | -10, -16, 10 | Thalamus_L | 121 | 2.7542 |

**Negative connections**

| No | Coordinate of peak region | AAL label | Number of voxels | Intensity of peak region |
|---|---|---|---|---|
| 1 | -28, -70, -50 | Cerebelum_8_L | 89 | -1.7068 |
| 2 | -14, -52, -48 | Cerebelum_9_L | 20 | -1.5 |
| 3 | -6, -74, -40 | Cerebelum_7b_L | 147 | -1.8434 |
| 4 | 22, -38, -44 | Cerebelum_10_R | 34 | -1.7134 |
| 5 | -20, -36, -44 | Cerebelum_10_L | 31 | -1.6446 |
| 6 | 6, -76, -34 | Cerebelum_Crus2_R | 42 | -1.6713 |
| 7 | -2, -52, -34 | Cerebelum_9_L | 33 | -1.7678 |
| 8 | -40, -72, -28 | Cerebelum_Crus1_L | 29 | -1.5027 |
| 9 | -28, -62, -30 | Cerebelum_6_L | 52 | -1.994 |
| 10 | 30, -64, -28 | Cerebelum_6_R | 21 | -1.5615 |
| 11 | 32, -46, -8 | Fusiform_R | 227 | -2.5744 |
| 12 | 52, -16, 6 | Temporal_Sup_R | 1372 | -2.9145 |
| 13 | 44, -56, -6 | Temporal_Inf_R | 270 | -2.3303 |
| 14 | -40, -32, 10 | Temporal_Sup_L | 922 | -3.1724 |
| 15 | 34, 36, -10 | Frontal_Inf_Orb_R | 43 | -1.6368 |
| 16 | -28, -60, -8 | Fusiform_L | 165 | -2.5173 |

| No | Coordinate of peak region | AAL label | Number of voxels | Intensity of peak region |
|---|---|---|---|---|
| 17 | -40, -66, -6 | Occipital_Inf_L | 319 | -2.3311 |
| 18 | 32, 28, 0 | Insula_R | 39 | -1.5766 |
| 19 | -28, -74, 22 | Occipital_Mid_L | 3066 | -5.032 |
| 20 | 32, -70, 24 | Occipital_Mid_R | 4320 | -5.2122 |
| 21 | 46, 6, 24 | Frontal_Inf_Oper_R | 793 | -2.1462 |
| 22 | -34, 8, 28 | Frontal_Inf_Oper_L | 413 | -1.8625 |
| 23 | 8, 16, 50 | Supp_Motor_Area_R | 58 | -1.5919 |
| 24 | -24, -4, 50 | Frontal_Mid_L | 707 | -2.2576 |
| 25 | -14, -42, 48 | Cingulum_Mid_L | 20 | -1.436 |
| 26 | 16, -40, 48 | Paracentral_Lobule_R | 33 | -1.5304 |
| 27 | -6, 16, 48 | Supp_Motor_Area_L | 29 | -1.5881 |

Table S7. Network-of-interest (NOI) results for cognitive performance (VNR) and educational attainment. The significant between-network connections were shown in the results below.

| VNR | | | | | | | | | |
|---|---|---|---|---|---|---|---|---|---|
| **Type** | **Connections** | **Beta** | **Std** | **t.value** | **p** | **$p_{corrected}$** | **Mean value of connection** | **95% CI of value of connection** | |
| **inter-hemisphere** | **left FPN - right FPN** | -0.040 | 0.016 | -2.493 | 1.27E-02 | 0.018 | 1.156 | 1.127 | 1.185 |
| | **right CON - left CON** | -0.063 | 0.016 | -3.923 | 8.89E-05 | 6.67E-04 | 0.379 | 0.356 | 0.402 |
| **CON - FPN** | **left CON - right FPN** | 0.034 | 0.016 | -2.106 | 3.52E-02 | 0.044 | -1.359 | -1.387 | -1.330 |
| | **right CON - left FPN** | 0.043 | 0.016 | -2.714 | 6.68E-03 | 0.011 | -2.088 | -2.122 | -2.054 |
| | **left CON - left FPN** | 0.044 | 0.016 | 2.732 | 6.33E-03 | 0.011 | 1.043 | 1.018 | 1.067 |
| | **right CON - right FPN** | 0.051 | 0.016 | 3.200 | 1.38E-03 | 0.005 | 0.648 | 0.620 | 0.676 |
| **DMN-related** | **left CON - DMN** | 0.061 | 0.016 | 3.824 | 1.33E-04 | 6.67E-04 | 0.675 | 0.652 | 0.698 |
| | **right CON - DMN** | -0.045 | 0.016 | 2.797 | 5.18E-03 | 0.011 | -0.275 | -0.300 | -0.250 |
| **EDUCATION** | | | | | | | | | |
| **Type** | **Connections** | **Beta** | **Std** | **t.value** | **p** | **$p_{corrected}$** | **Mean value of connection** | **95% CI of value of connection** | |
| **CON - FPN** | **right CON-right FPN** | 0.086 | 0.031 | 2.736 | 6.24E-03 | 0.021 | 0.648 | 0.620 | 0.676 |
| **DMN-related** | **right FPN - DMN** | 0.104 | 0.031 | -3.335 | 8.59E-04 | 0.004 | -0.710 | -0.738 | -0.682 |
| | **right CON - DMN** | -0.149 | 0.031 | 4.761 | 1.99E-06 | 1.99E-05 | -0.275 | -0.300 | -0.250 |

Table S7. Correlation matrix between average motion during resting-state assessment, first four genetic principal components, cognitive performance (VNR), educational attainment and household income. Motions and genetic principal components showed very weak correlations with VNR, educational attainment and household income.

| | **Age** | **Sex** | **Motion** | **VNR** | **Edu** | **Income** |
|---|---|---|---|---|---|---|
| **Age** | 1 | 0.085 | 0.155 | -0.061 | -0.021 | -0.28 |
| **Sex** | 0.085 | 1 | 0.147 | 0.081 | 0.071 | 0.079 |
| **Motion** | 0.155 | 0.147 | 1 | -0.085 | -0.094 | -0.113 |
| **VNR** | -0.061 | 0.081 | -0.085 | 1 | 0.257 | 0.202 |
| **Edu** | -0.021 | 0.071 | -0.094 | 0.257 | 1 | 0.237 |
| **Income** | -0.28 | 0.079 | -0.113 | 0.202 | 0.237 | 1 |

Table S8. Replication analyses on the (1) unrelated sample, which related people were removed (N=3,253), and (2) updated unrelated sample (N=7,144). Three connections turned null in both unrelated 4k sample and unrelated 7k sample, which takes up 4.05% of 74 significant connections found in the main results. None of the significant connections showed opposite direction of effect in the additional analyses.

| | | **Main model** | | | **Unrelated people (N~=4k)** | | **Unrelated people (N~=7k)** | |
|---|---|---|---|---|---|---|---|---|
| | Connection | Beta (std) | $P_{uncorrected}$ | $P_{corrected}$ | Beta (std) | $P_{uncorrected}$ | Beta (std) | $P_{uncorrected}$ |
| **VNR** | N17_N15 | 0.054 (0.016) | 6.73E-04 | 3.85E-02 | 0.053 (0.018) | 3.36E-03 | 0.049 (0.012) | 7.30E-05 |
| | N21_N7 | 0.097 (0.016) | 9.09E-10 | 1.35E-06 | 0.09 (0.018) | 5.38E-07 | 0.074 (0.012) | 2.71E-09 |
| | N21_N11 | 0.062 (0.016) | 9.72E-05 | 1.44E-02 | 0.067 (0.018) | 2.28E-04 | 0.058 (0.012) | 3.14E-06 |
| | N22_N1 | 0.061 (0.016) | 1.53E-04 | 1.77E-02 | 0.051 (0.018) | 4.99E-03 | 0.025 (0.012) | 4.66E-02 |
| | N24_N4 | -0.066 (0.016) | 4.37E-05 | 7.21E-03 | -0.064 (0.018) | 4.36E-04 | -0.052 (0.013) | 3.71E-05 |
| | N24_N9 | -0.083 (0.016) | 2.14E-07 | 1.59E-04 | -0.073 (0.018) | 6.33E-05 | -0.059 (0.012) | 2.45E-06 |
| | N25_N5 | -0.072 (0.016) | 7.39E-06 | 1.65E-03 | -0.084 (0.018) | 3.57E-06 | -0.057 (0.012) | 3.75E-06 |
| | N26_N12 | 0.081 (0.016) | 4.96E-07 | 2.45E-04 | 0.061 (0.018) | 7.47E-04 | 0.052 (0.012) | 2.57E-05 |
| | N28_N24 | 0.076 (0.016) | 2.25E-06 | 8.35E-04 | 0.081 (0.018) | 1.01E-05 | 0.074 (0.013) | 4.02E-09 |
| | N29_N11 | 0.059 (0.016) | 2.45E-04 | 2.14E-02 | 0.057 (0.018) | 1.71E-03 | 0.055 (0.013) | 9.99E-06 |
| | N31_N12 | -0.066 (0.016) | 4.06E-05 | 7.21E-03 | -0.079 (0.018) | 1.47E-05 | -0.074 (0.012) | 3.61E-09 |
| | N33_N13 | 0.06 (0.016) | 1.78E-04 | 1.77E-02 | 0.05 (0.018) | 5.90E-03 | 0.043 (0.012) | 5.67E-04 |
| | N33_N22 | 0.055 (0.016) | 6.52E-04 | 3.85E-02 | 0.055 (0.018) | 2.76E-03 | 0.055 (0.013) | 1.11E-05 |
| | N39_N33 | 0.074 (0.016) | 4.80E-06 | 1.43E-03 | 0.046 (0.018) | 1.23E-02 | 0.047 (0.013) | 1.78E-04 |
| | N42_N6 | -0.056 (0.016) | 4.43E-04 | 3.13E-02 | -0.057 (0.018) | 1.80E-03 | -0.044 (0.013) | 4.75E-04 |
| | N42_N18 | 0.055 (0.016) | 5.77E-04 | 3.73E-02 | **0.035 (0.018)** | **5.63E-02** | 0.025 (0.012) | 4.60E-02 |
| | N44_N17 | 0.054 (0.016) | 6.21E-04 | 3.84E-02 | 0.041 (0.018) | 2.33E-02 | **<0.001, >-0.001 (0.012)** | **9.68E-01** |
| | N44_N25 | 0.071 (0.016) | 7.78E-06 | 1.65E-03 | 0.057 (0.018) | 1.48E-03 | 0.054 (0.012) | 1.19E-05 |
| | N45_N5 | -0.058 (0.016) | 2.93E-04 | 2.42E-02 | -0.045 (0.018) | 1.28E-02 | -0.05 (0.012) | 7.09E-05 |
| | N45_N15 | 0.059 (0.016) | 2.34E-04 | 2.14E-02 | 0.037 (0.018) | 4.03E-02 | 0.039 (0.012) | 1.72E-03 |
| | N45_N44 | 0.055 (0.016) | 4.81E-04 | 3.25E-02 | **0.034 (0.018)** | **5.71E-02** | **0.019 (0.012)** | **1.27E-01** |

| | | Main model | | | Unrelated people (N~=4k) | | Unrelated people (N~=7k) | |
|---|---|---|---|---|---|---|---|---|
| | Connection | Beta (std) | $P_{uncorrected}$ | $P_{corrected}$ | Beta (std) | $P_{uncorrected}$ | Beta (std) | $P_{uncorrected}$ |
| | N46_N25 | -0.057 (0.016) | 4.00E-04 | 2.97E-02 | -0.039 (0.018) | 3.18E-02 | **-0.02 (0.012)** | **1.09E-01** |
| | N47_N31 | 0.059 (0.016) | 1.68E-04 | 1.77E-02 | 0.056 (0.018) | 1.87E-03 | 0.034 (0.012) | 5.23E-03 |
| | N48_N19 | 0.061 (0.016) | 1.59E-04 | 1.77E-02 | 0.046 (0.018) | 1.10E-02 | 0.041 (0.013) | 1.14E-03 |
| | N48_N21 | -0.061 (0.016) | 1.44E-04 | 1.77E-02 | -0.057 (0.018) | 1.75E-03 | -0.021 (0.012) | 8.73E-02 |
| | N50_N7 | 0.057 (0.016) | 3.33E-04 | 2.60E-02 | 0.059 (0.018) | 1.18E-03 | 0.057 (0.012) | 4.27E-06 |
| **Educational attainment** | N5_N4 | -0.103 (0.031) | 1.01E-03 | 4.54E-02 | -0.056 (0.018) | 2.28E-03 | -0.045 (0.013) | 3.91E-04 |
| | N8_N3 | -0.119 (0.031) | 1.42E-04 | 1.75E-02 | -0.056 (0.018) | 2.34E-03 | -0.036 (0.013) | 4.51E-03 |
| | N12_N5 | 0.132 (0.031) | 2.71E-05 | 6.71E-03 | 0.056 (0.018) | 2.25E-03 | 0.033 (0.013) | 8.67E-03 |
| | N12_N11 | 0.106 (0.031) | 6.94E-04 | 3.97E-02 | **0.032 (0.018)** | **7.50E-02** | 0.038 (0.012) | 2.24E-03 |
| | N15_N7 | 0.122 (0.031) | 7.96E-05 | 1.48E-02 | 0.041 (0.018) | 2.35E-02 | 0.044 (0.012) | 4.66E-04 |
| | N17_N15 | 0.121 (0.031) | 9.59E-05 | 1.53E-02 | 0.046 (0.018) | 1.21E-02 | 0.054 (0.012) | 1.65E-05 |
| | N19_N18 | -0.136 (0.031) | 1.47E-05 | 5.47E-03 | -0.058 (0.019) | 1.74E-03 | -0.039 (0.013) | 1.99E-03 |
| | N20_N10 | -0.109 (0.031) | 4.91E-04 | 3.80E-02 | -0.071 (0.018) | 1.28E-04 | -0.043 (0.013) | 6.06E-04 |
| | N24_N4 | -0.108 (0.031) | 6.15E-04 | 3.80E-02 | -0.049 (0.018) | 7.95E-03 | -0.038 (0.013) | 2.33E-03 |
| | N25_N3 | 0.137 (0.031) | 1.36E-05 | 5.47E-03 | 0.068 (0.018) | 2.36E-04 | 0.042 (0.013) | 8.17E-04 |
| | N25_N4 | -0.161 (0.031) | 2.73E-07 | 4.06E-04 | -0.081 (0.018) | 1.06E-05 | -0.077 (0.013) | 8.59E-10 |
| | N26_N12 | 0.108 (0.031) | 5.51E-04 | 3.80E-02 | **0.029 (0.018)** | **1.12E-01** | 0.032 (0.013) | 1.05E-02 |
| | N29_N25 | 0.108 (0.031) | 5.88E-04 | 3.80E-02 | 0.042 (0.018) | 2.29E-02 | 0.038 (0.013) | 2.75E-03 |
| | N31_N7 | 0.125 (0.031) | 6.57E-05 | 1.39E-02 | 0.039 (0.018) | 3.21E-02 | 0.038 (0.012) | 2.19E-03 |
| | N33_N2 | -0.103 (0.031) | 9.96E-04 | 4.54E-02 | -0.064 (0.018) | 5.00E-04 | **-0.024 (0.013)** | **6.05E-02** |
| | N34_N26 | -0.133 (0.031) | 2.14E-05 | 6.37E-03 | -0.051 (0.018) | 5.55E-03 | -0.059 (0.013) | 2.69E-06 |
| | N35_N33 | 0.108 (0.031) | 5.63E-04 | 3.80E-02 | 0.055 (0.019) | 3.26E-03 | 0.037 (0.013) | 3.41E-03 |
| | N36_N35 | 0.105 (0.031) | 7.79E-04 | 4.09E-02 | 0.055 (0.018) | 2.59E-03 | 0.027 (0.013) | 3.49E-02 |
| | N40_N7 | 0.118 (0.031) | 1.72E-04 | 1.96E-02 | 0.06 (0.018) | 1.24E-03 | **0.019 (0.013)** | **1.46E-01** |
| | N40_N34 | 0.122 (0.031) | 1.03E-04 | 1.53E-02 | 0.049 (0.018) | 7.75E-03 | 0.044 (0.013) | 4.62E-04 |
| | N42_N8 | -0.108 (0.031) | 5.89E-04 | 3.80E-02 | -0.052 (0.018) | 4.56E-03 | **-0.018 (0.013)** | **1.55E-01** |

| | | Main model | | | Unrelated people (N~=4k) | | Unrelated people (N~=7k) | |
|---|---|---|---|---|---|---|---|---|
| | Connection | Beta (std) | $P_{uncorrected}$ | $P_{corrected}$ | Beta (std) | $P_{uncorrected}$ | Beta (std) | $P_{uncorrected}$ |
| | N44_N25 | 0.112 (0.031) | 3.35E-04 | 2.93E-02 | 0.047 (0.018) | 9.83E-03 | **0.012 (0.012)** | **3.30E-01** |
| | N44_N36 | 0.139 (0.031) | 9.61E-06 | 5.47E-03 | 0.071 (0.018) | 1.09E-04 | 0.044 (0.013) | 4.38E-04 |
| | N45_N15 | 0.117 (0.031) | 2.05E-04 | 2.17E-02 | **0.028 (0.018)** | **1.33E-01** | 0.037 (0.013) | 3.59E-03 |
| | N45_N36 | 0.105 (0.031) | 8.20E-04 | 4.09E-02 | 0.061 (0.018) | 1.07E-03 | 0.031 (0.013) | 1.46E-02 |
| | N45_N44 | 0.105 (0.031) | 6.74E-04 | 3.97E-02 | **0.036 (0.018)** | **5.18E-02** | **0.008 (0.013)** | **5.02E-01** |
| | N46_N36 | 0.11 (0.031) | 4.54E-04 | 3.74E-02 | 0.047 (0.018) | 1.09E-02 | 0.029 (0.013) | 1.91E-02 |
| | N47_N36 | 0.105 (0.031) | 7.93E-04 | 4.09E-02 | 0.046 (0.018) | 1.29E-02 | 0.028 (0.013) | 2.42E-02 |
| | N47_N45 | 0.11 (0.031) | 3.35E-04 | 2.93E-02 | **0.029 (0.018)** | **1.02E-01** | **0.016 (0.012)** | **1.88E-01** |
| | N48_N5 | -0.114 (0.031) | 2.75E-04 | 2.72E-02 | -0.061 (0.018) | 8.06E-04 | -0.046 (0.013) | 2.78E-04 |
| | N50_N10 | -0.121 (0.031) | 1.15E-04 | 1.55E-02 | -0.059 (0.018) | 1.31E-03 | -0.029 (0.013) | 2.30E-02 |
| | N52_N37 | 0.104 (0.031) | 8.37E-04 | 4.09E-02 | 0.052 (0.018) | 4.74E-03 | 0.043 (0.013) | 5.31E-04 |
| | N55_N10 | -0.105 (0.031) | 8.53E-04 | 4.09E-02 | -0.074 (0.018) | 6.83E-05 | -0.027 (0.013) | 3.32E-02 |
| **Household income** | N12_N11 | 0.072 (0.017) | 2.64E-05 | 9.80E-03 | 0.063 (0.019) | 9.81E-04 | 0.043 (0.013) | 1.17E-03 |
| | N15_N11 | 0.082 (0.017) | 1.60E-06 | 2.38E-03 | 0.082 (0.019) | 1.91E-05 | 0.043 (0.013) | 1.21E-03 |
| | N18_N8 | 0.064 (0.017) | 2.02E-04 | 3.34E-02 | 0.06 (0.02) | 2.40E-03 | **0.019 (0.013)** | **1.50E-01** |
| | N18_N12 | 0.067 (0.017) | 9.42E-05 | 2.01E-02 | 0.047 (0.02) | 1.69E-02 | 0.035 (0.013) | 9.10E-03 |
| | N24_N4 | -0.067 (0.017) | 9.49E-05 | 2.01E-02 | -0.062 (0.02) | 1.65E-03 | -0.052 (0.013) | 1.23E-04 |
| | N25_N4 | -0.062 (0.017) | 2.88E-04 | 3.89E-02 | -0.065 (0.02) | 9.67E-04 | -0.056 (0.013) | 2.66E-05 |
| | N26_N12 | 0.078 (0.017) | 6.04E-06 | 4.49E-03 | 0.074 (0.019) | 1.54E-04 | 0.062 (0.013) | 3.55E-06 |
| | N30_N6 | 0.062 (0.017) | 2.83E-04 | 3.89E-02 | 0.049 (0.02) | 1.24E-02 | 0.039 (0.013) | 3.19E-03 |
| | N31_N7 | 0.062 (0.017) | 3.19E-04 | 3.94E-02 | 0.049 (0.019) | 1.09E-02 | 0.035 (0.013) | 7.45E-03 |
| | N34_N26 | -0.073 (0.017) | 2.01E-05 | 9.80E-03 | -0.079 (0.02) | 5.35E-05 | -0.071 (0.013) | 1.25E-07 |
| | N40_N2 | 0.06 (0.017) | 4.27E-04 | 4.23E-02 | 0.041 (0.019) | 3.63E-02 | **0.024 (0.013)** | **7.07E-02** |
| | N40_N19 | 0.06 (0.017) | 4.06E-04 | 4.23E-02 | 0.051 (0.019) | 8.10E-03 | 0.044 (0.013) | 8.49E-04 |
| | N40_N22 | -0.061 (0.017) | 3.84E-04 | 4.23E-02 | -0.073 (0.02) | 2.14E-04 | -0.051 (0.013) | 1.51E-04 |
| | N44_N40 | 0.065 (0.017) | 1.40E-04 | 2.59E-02 | 0.062 (0.019) | 1.58E-03 | 0.042 (0.013) | 1.58E-03 |

| | | **Main model** | | | **Unrelated people (N~=4k)** | | **Unrelated people (N~=7k)** | |
|---|---|---|---|---|---|---|---|---|
| | Connection | Beta (std) | $P_{uncorrected}$ | $P_{corrected}$ | Beta (std) | $P_{uncorrected}$ | Beta (std) | $P_{uncorrected}$ |
| | N47_N18 | 0.068 (0.017) | 7.42E-05 | 2.01E-02 | 0.053 (0.02) | 6.36E-03 | **0.024 (0.013)** | **7.24E-02** |

# References

Acosta-Cabronero J, Williams GB, Pengas G, Nestor PJ. 2010. Absolute diffusivities define the landscape of white matter degeneration in Alzheimer's disease. Brain. 133:529–539.

Alfaro-Almagro F, Jenkinson M, Bangerter NK, Andersson JLR, Griffanti L, Douaud G, Sotiropoulos SN, Jbabdi S, Hernandez-Fernandez M, Vallee E, Vidaurre D, Webster M, McCarthy P, Rorden C, Daducci A, Alexander DC, Zhang H, Dragonu I, Matthews PM, Miller KL, Smith SM. 2018. Image processing and Quality Control for the first 10,000 brain imaging datasets from UK Biobank. Neuroimage. 166:400–424.

Allan CL, Sexton CE, Filippini N, Topiwala A, Mahmood A, Zsoldos E, Singh-Manoux A, Shipley MJ, Kivimaki M, Mackay CE, Ebmeier KP. 2016. Sub-threshold depressive symptoms and brain structure: A magnetic resonance imaging study within the Whitehall II cohort. J Affect Disord. 204:219–225.

Almeida OP, Garrido GJ, Lautenschlager NT, Hulse GK, Jamrozik K, Flicker L. 2008. Smoking is associated with reduced cortical regional gray matter density in brain regions associated with incipient alzheimer disease. Am J Geriatr Psychiatry. 16:92–98.

Amico F., Meisenzahl E., Koutsouleris N., Reiser M., Möller H-J., Frodl T. 2011. Structural MRI correlates for vulnerability and resilience to major depressive disorder. J Psychiatry Neurosci. 36:15–22.

Andersson JLR, Jenkinson M, Smith S. 2007a. Non-linear registration aka Spatial normalisation FMRIB Technial Report TR07JA2. In Pract. 22.

Andersson JLR, Jenkinson M, Smith SM. 2007b. Non-linear optimisation. FMRIB technical report TR07JA1 [WWW Document]. In Pract. URL

http://fsl.fmrib.ox.ac.uk/analysis/techrep/tr07ja1/tr07ja1.pdf

Andersson JLR, Sotiropoulos SN. 2015a. An integrated approach to correction for off-resonance effects and subject movement in diffusion MR imaging. Neuroimage. 125:1063–1078.

Andersson JLR, Sotiropoulos SN. 2015b. Non-parametric representation and prediction of single- and multi-shell diffusion-weighted MRI data using Gaussian processes. Neuroimage. 122:166–176.

Anthofer JM, Steib K, Fellner C, Lange M, Brawanski A, Schlaier J. 2015. DTI-based deterministic fibre tracking of the medial forebrain bundle. Acta Neurochir (Wien). 157:469–477.

Anticevic A, Cole MW, Murray JD, Corlett PR, Wang X-J, Krystal JH. 2012. The role of default network deactivation in cognition and disease. Trends Cogn Sci. 16:584–592.

Arnone D, McIntosh AM, Ebmeier KP, Munafò MR, Anderson IM. 2012. Magnetic resonance imaging studies in unipolar depression: Systematic review and meta-regression analyses. Eur Neuropsychopharmacol. 22:1–16.

Bachmann RF, Schloesser RJ, Gould TD, Manji HK. 2005. Mood stabilizers target cellular plasticity and resilience cascades: Implications for the development of novel therapeutics. Mol Neurobiol. 32:173–202.

Bae JN, MacFall JR, Krishnan KRR, Payne ME, Steffens DC, Taylor WD. 2006. Dorsolateral Prefrontal Cortex and Anterior Cingulate Cortex White Matter Alterations in Late-Life Depression. Biol Psychiatry. 60:1356–1363.

Barbu MC, Zeng Y, Shen X, Cox SR, Clarke T, Adams MJ, Johnstone M, Haley CS, Lawrie SM, Ian J. 2018. Association of whole-genome and NETRIN1 signaling pathway-derived polygenic risk scores for Major Depressive Disorder and thalamic radiation

white matter microstructure in UK Biobank. bioRxiv.

Bartova L, Meyer BM, Diers K, Rabl U, Scharinger C, Popovic A, Pail G, Kalcher K, Boubela RN, Huemer J, Mandorfer D, Windischberger C, Sitte HH, Kasper S, Praschak-Rieder N, Moser E, Brocke B, Pezawas L. 2015. Reduced default mode network suppression during a working memory task in remitted major depression. J Psychiatr Res. 64:9–18.

Batty GD, McIntosh AM, Russ TC, Deary IJ, Gale CR. 2016. Psychological distress, neuroticism, and cause-specific mortality: Early prospective evidence from UK Biobank. J Epidemiol Community Health. 70:1136–1139.

Beaulieu C. 2002. The basis of anisotropic water diffusion in the nervous system - A technical review. NMR Biomed. 15:435–455.

Benedetti F, Yeh PH, Bellani M, Radaelli D, Nicoletti MA, Poletti S, Falini A, Dallaspezia S, Colombo C, Scotti G, Smeraldi E, Soares JC, Brambilla P. 2011. Disruption of white matter integrity in bipolar depression as a possible structural marker of illness. Biol Psychiatry. 69:309–317.

Benjamini Y, Hochberg Y. 2000. On the Adaptive Control of the False Discovery Rate in Multiple Testing With Independent Statistics. J Educ Behav Stat. 25:60–83.

Benjamini Y, Hochberg Y, Yoav Benjamini YH. 1995. Controlling the False Discovery Rate: A Practical and Powerful Approach to Multiple Testing. J R Stat Soc Ser B. 57:289–300.

Bero AW, Yan P, Roh JH, Cirrito JR, Stewart FR, Raichle ME, Lee JM, Holtzman DM. 2011. Neuronal activity regulates the regional vulnerability to amyloid-b deposition. Nat Neurosci. 14:750–756.

Bijsterbosch J, Harrison S, Duff E, Alfaro-Almagro F, Woolrich M, Smith S. 2017. Investigations into within- and between-subject resting-state amplitude variations.

Neuroimage. 159:57–69.

Bliese P. 2016. Multilevel Modeling in R (2.2)--A Brief Introduction to R, the multilevel package and the nlme package.

Bluhm RL, Clark CR, Mcfarlane AC, Moores KA, Shaw ME, Lanius RA. 2011. Default network connectivity during a working memory task. Hum Brain Mapp. 32:1029–1035.

Bora E, Fornito A, Pantelis C, Yucel M. 2012. Gray matter abnormalities in Major Depressive Disorder: A meta-analysis of voxel based morphometry studies. J Affect Disord. 138:9–18.

Botvinick MM, Cohen JD, Carter CS. 2004. Conflict monitoring and anterior cingulate cortex: An update. Trends Cogn Sci. 8:539–546.

Braun U, Plichta MM, Esslinger C, Sauer C, Haddad L, Grimm O, Mier D, Mohnke S, Heinz A, Erk S, Walter H, Seiferth N, Kirsch P, Meyer-Lindenberg A. 2012. Test-retest reliability of resting-state connectivity network characteristics using fMRI and graph theoretical measures. Neuroimage. 59:1404–1412.

Bressler SL, Menon V. 2010. Large-scale brain networks in cognition: emerging methods and principles. Trends Cogn Sci. 14:277–290.

Brown ES, Varghese FP, McEwen BS. 2004. Association of depression with medical illness: Does cortisol play a role? Biol Psychiatry. 55:1–9.

Broyd SJ, Demanuele C, Debener S, Helps SK, James CJ, Sonuga-Barke EJS. 2009. Default-mode brain dysfunction in mental disorders: A systematic review. Neurosci Biobehav Rev. 33:279–296.

Brunoni AR, Valiengo L, Baccaro A, Zanão TA, De Oliveira JF, Goulart A, Boggio PS, Lotufo PA, Benseñor IM, Fregni F. 2013. The sertraline vs electrical current therapy for

treating depression clinical study. JAMA Psychiatry. 70:383–391.

Buckner RL, Krienen FM. 2013. The evolution of distributed association networks in the human brain. Trends Cogn Sci. 17:648–665.

Buckner RL, Sepulcre J, Talukdar T, Krienen FM, Liu H, Hedden T, Andrews-Hanna JR, Sperling RA, Johnson KA. 2009. Cortical Hubs Revealed by Intrinsic Functional Connectivity: Mapping, Assessment of Stability, and Relation to Alzheimer's Disease. J Neurosci. 29:1860–1873.

Bulik-Sullivan B, Finucane HK, Anttila V, Gusev A, Day FR, Loh PR, Duncan L, Perry JRB, Patterson N, Robinson EB, Daly MJ, Price AL, Neale BM. 2015. An atlas of genetic correlations across human diseases and traits. Nat Genet. 47:1236–1241.

Bullmore E, Sporns O. 2012. The economy of brain network organization. Nat Rev Neurosci. 13:336–349.

Bunge SA, Wendelken C, Badre D, Wagner AD. 2005. Analogical reasoning and prefrontal cortex: Evidence for separable retrieval and integration mechanisms. Cereb Cortex. 15:239–249.

Bush G, Luu P, Posner MI. 2000. Cognitive and emotional influences in anterior cingulate cortex. Trends Cogn Sci. 4:215–222.

Button KS, Ioannidis JPA, Mokrysz C, Nosek BA, Flint J, Robinson ESJ, Munafò MR. 2013. Power failure: Why small sample size undermines the reliability of neuroscience. Nat Rev Neurosci. 14:365–376.

Bycroft C, Freeman C, Petkova D, Band G, Elliott LT, Sharp K, Motyer A, Vukcevic D, Delaneau O, O'Connell J, Cortes A, Welsh S, McVean G, Leslie S, Donnelly P, Marchini J. 2017a. Genome-wide genetic data on ~500,000 UK Biobank participants. bioRxiv. https://doi.org/10.1101/166298.

Bycroft C, Freeman C, Petkova D, Band G, Elliott LT, Sharp K, Motyer A, Vukcevic D, Delaneau O, O'Connell J, Cortes A, Welsh S, McVean G, Leslie S, Donnelly P, Marchini J. 2017b. Genome-wide genetic data on 500,000 UK Biobank participants. bioRxiv. 166298.

Bylsma LM, Morris BH, Rottenberg J. 2008. A meta-analysis of emotional reactivity in major depressive disorder ☆. Clin Psychol Rev. 28:676–691.

Cabeza R, Anderson ND, Locantore JK, Mcintosh AR. 2002. Aging Gracefully : Compensatory Brain Activity in High-Performing Older Adults. Neuroimage. 17:1394–1402.

Calvin CM, Batty GD, Der G, Brett CE, Taylor A, Pattie A, Čukić I, Deary IJ. 2017. Childhood intelligence in relation to major causes of death in 68 year follow-up: prospective population study. bmj. 357:1–13.

Centre W, Neuroimaging I, Centre TW, Genetics H. 2017. Genome-wide association studies of brain structure and function in the UK Biobank. bioRxiv.

Chatfield C, Zidek J, Lindsey J. 2010. An introduction to generalized linear models. Chapman and Hall/CRC.

Chen C. 1979. Sleep, depression and antidepressants. Br J Psychiatry. 135:385–402.

Chen G, Hu X, Li L, Huang X, Lui S, Kuang W, Ai H. 2016. Disorganization of white matter architecture in major depressive disorder : a meta-analysis of diffusion tensor imaging with tract- based spatial statistics. Sci Rep. 6:1–11.

Cheon KA, Kim YS, Oh SH, Park SY, Yoon HW, Herrington J, Nair A, Koh YJ, Jang DP, Kim YB, Leventhal BL, Cho ZH, Castellanos FX, Schultz RT. 2011. Involvement of the anterior thalamic radiation in boys with high functioning autism spectrum disorders: A Diffusion Tensor Imaging study. Brain Res. 1417:77–86.

Cipriani A, Furukawa TA, Salanti G, Chaimani A, Atkinson LZ, Ogawa Y, Leucht S, Ruhe HG, Turner EH, Higgins JPT, Egger M, Takeshima N, Hayasaka Y, Imai H, Shinohara K, Tajika A, Ioannidis JPA, Geddes JR. 2018. Comparative efficacy and acceptability of 21 antidepressant drugs for the acute treatment of adults with major depressive disorder: a systematic review and network meta-analysis. Lancet. 391:1357–1366.

Clarke T-K, Adams MJ, Davies G, Howard DM, Hall LS, Padmanabhan S, Murray AD, Smith BH, Campbell A, Hayward C, Porteous DJ, Deary IJ, McIntosh AM. 2017. Genome-wide association study of alcohol consumption and genetic overlap with other health-related traits in UK Biobank (N=112 117). Mol Psychiatry. 22:1376–1384.

Clarke T-K, Hall LS, Fernandez-Pujals AM, MacIntyre DJ, Thomson P, Hayward C, Smith BH, Padmanabhan S, Hocking LJ, Deary IJ, Porteous DJ, McIntosh AM. 2015. Major depressive disorder and current psychological distress moderate the effect of polygenic risk for obesity on body mass index. Transl Psychiatry. 5:e592.

Cocchi L, Zalesky A, Fornito A, Mattingley JB. 2013. Dynamic cooperation and competition between brain systems during cognitive control. Trends Cogn Sci. 17:493–501.

Coenen VA, Panksepp J, Hurwitz TA, Urbach H, Mädler B. 2012. Human medial forebrain bundle (MFB) and anterior thalamic radiation (ATR): imaging of two major subcortical pathways and the dynamic balance of opposite affects in understanding depression. J Neuropsychiatry Clin Neurosci. 24:223–236.

Cole MW, Yarkoni T, Repovs G, Anticevic A, Braver TS. 2012. Global Connectivity of Prefrontal Cortex Predicts Cognitive Control and Intelligence. J Neurosci. 32:8988–8999.

Cooney RE, Joormann J, Eugène F, Dennis EL, Gotlib IH. 2010. Neural correlates of rumination in depression. Cogn Affect Behav Neurosci. 10:470–478.

Corbetta M, Akbudak E, Conturo TE, Snyder AZ, Ollinger JM, Drury HA, Linenweber MR, Petersen SE, Raichle ME, Van Essen DC, Shulman GL. 1998. A Common Network of Functional Areas for Attention and Eye Movements. Neuron. 21:761–773.

Corbetta M, Patel G, Shulman GL. 2008. The Reorienting System of the Human Brain: From Environment to Theory of Mind. Neuron. 58:306–324.

Cox SR, Bastin ME, Ferguson KJ, Maniega SM, MacPherson SE, Deary IJ, Wardlaw JM, MacLullich AMJ. 2015. Brain white matter integrity and cortisol in older men: The Lothian Birth Cohort 1936. Neurobiol Aging. 36:257–264.

Cox SR, Dickie DA, Ritchie SJ, Karama S, Pattie A, Royle NA, Corley J, Aribisala BS, Valdés Hernández M, Muñoz Maniega S, Starr JM, Bastin ME, Evans AC, Wardlaw JM, Deary IJ. 2016. Associations between education and brain structure at age 73 years, adjusted for age 11 IQ. Neurology. 87:1820–1826.

Cox SR, MacPherson SE, Ferguson KJ, Royle NA, Maniega SM, Hernández M del CV, Bastin ME, MacLullich AMJ, Wardlaw JM, Deary IJ. 2015. Does white matter structure or hippocampal volume mediate associations between cortisol and cognitive ageing? Psychoneuroendocrinology. 62:129–137.

Cox SR, Ritchie SJ, Tucker-Drob EM, Liewald DC, Hagenaars SP, Davies G, Wardlaw JM, Gale CR, Bastin ME, Deary IJ. 2016. Ageing and brain white matter structure in 3,513 UK Biobank participants. Nat Commun. 7:1–34.

Cullen KR, Klimes-Dougan B, Muetzel R, Mueller B a, Camchong J, Houri A, Kurma S, Lim KO. 2010. Altered white matter microstructure in adolescents with major depression: a preliminary study. J Am Acad Child Adolesc Psychiatry. 49:173–183.e1.

Daducci A, Canales-Rodríguez EJ, Zhang H, Dyrby TB, Alexander DC, Thiran JP. 2015. Accelerated Microstructure Imaging via Convex Optimization (AMICO) from diffusion

MRI data. Neuroimage. 105:32–44.

Dalgleish T. 2004. The emotional brain. Nat Rev Neurosci. 5:583–589.

Davidson KW, Rieckmann N, Rapp MA. 2005. Definitions and distinctions among depressive syndromes and symptoms: Implications for a better understanding of the depression-cardiovascular disease association. Psychosom Med. 67.

Davies G, Marioni RE, Liewald DC, Hill WD, Hagenaars SP, Harris SE, Ritchie SJ, Luciano M, Fawns-Ritchie C, Lyall D, others. 2016. Genome-wide association study of cognitive functions and educational attainment in UK Biobank (N= 112 151). Mol Psychiatry. 21:1–10.

De Groot M, Vernooij MW, Klein S, Ikram MA, Vos FM, Smith SM, Niessen WJ, Andersson JLR. 2013. Improving alignment in Tract-based spatial statistics: Evaluation and optimization of image registration. Neuroimage. 76:400–411.

de Schotten MT, Dell'Acqua F, Forkel SJ, Simmons A, Vergani F, Murphy DGM, Catani M. 2011. A lateralized brain network for visuospatial attention. Nat Neurosci. 14:1245–1246.

Deary IJ. 2012. Intelligence. Annu Rev Psychol. 63:453–482.

Deary IJ. 2014. The Stability of Intelligence From Childhood to Old Age. Curr Dir Psychol Sci. 23:239–245.

Deary IJ, Penke L, Johnson W. 2010. The neuroscience of human intelligence differences. Nat Rev Neurosci. 11:201–211.

Deary IJ, Yang J, Davies G, Harris SE, Tenesa A, Liewald D, Luciano M, Lopez LM, Gow AJ, Corley J, Redmond P, Fox HC, Rowe SJ, Haggarty P, McNeill G, Goddard ME, Porteous DJ, Whalley LJ, Starr JM, Visscher PM. 2012. Genetic contributions to

stability and change in intelligence from childhood to old age. Nature. 482:212–215.

Denk W, Briggman KL, Helmstaedter M. 2012. Structural neurobiology: Missing link to a mechanistic understanding of neural computation. Nat Rev Neurosci. 13:351–358.

Denson TF, Pedersen WC, Ronquillo J, Nandy AS. 2009. The angry brain: Neural correlates of anger, angry rumination, and aggressive personality. J Cogn Neurosci. 21:737–744.

DeRubeis RJ, Siegle GJ, Hollon SD. 2008. Cognitive therapy versus medication for depression: Treatment outcomes and neural mechanisms. Nat Rev Neurosci. 9:788–796.

Dichter GS, Kozink R V., McClernon FJ, Smoski MJ. 2012. Remitted major depression is characterized by reward network hyperactivation during reward anticipation and hypoactivation during reward outcomes. J Affect Disord. 136:1126–1134.

Disner SG, Beevers CG, Haigh EAP, Beck AT. 2011. Neural mechanisms of the cognitive model of depression. Nat Rev Neurosci. 12:467–477.

Dolan RJ. 2002. Emotion, Cognition, and Behavior. Science (80- ). 298:1191–1194.

Dosenbach NUF, Fair DA, Miezin FM, Cohen AL, Wenger KK, Dosenbach RAT, Fox MD, Snyder AZ, Vincent JL, Raichle ME, Schlaggar BL, Petersen SE. 2007. Distinct brain networks for adaptive and stable task control in humans. Proc Natl Acad Sci. 104:11073–11078.

Edwards AC, Docherty AR, Moscati A, Bigdeli TB, Peterson RE, Webb BT, Bacanu SA, Hettema JM, Flint J, Kendler KS. 2018. Polygenic risk for severe psychopathology among Europeans is associated with major depressive disorder in Han Chinese women. Psychol Med. 48:777–789.

Elliott LT, Sharp K, Alfaro-Almagro F, Shi1 S, Miller K, Marchini GDJ, Smit S. 2018.

Genome-wide association studies of brain structure and function in the UK Biobank. Nature. 562:210–216.

Ensminger ME, Hanson SG, Riley AW, Juon H-S. 2003. Maternal psychological distress: adult sons' and daughters' mental health and educational attainment. J Am Acad Child Adolesc Psychiatry. 42:1108–1115.

Etkin A, Büchel C, Gross JJ. 2015. The neural bases of emotion regulation. Nat Rev Neurosci. 16:693–700.

Euesden J, Lewis CM, O'Reilly PF. 2015. PRSice: Polygenic Risk Score software. Bioinformatics. 31:1466–1468.

Eugène F, Joormann J, Cooney RE, Atlas LY, Gotlib IH. 2010. Neural correlates of inhibitory deficits in depression. Psychiatry Res - Neuroimaging. 181:30–35.

Fales CL, Barch DM, Rundle MM, Mintun MA, Snyder AZ, Cohen JD, Mathews J, Sheline YI. 2008. Altered Emotional Interference Processing in Affective and Cognitive-Control Brain Circuitry in Major Depression. Biol Psychiatry. 63:377–384.

Fava M, Kendler KS. 2000. Major Depressive Disorder Review. Neuron. 28:335–341.

Fehr E, Camerer CF. 2007. Social neuroeconomics: the neural circuitry of social preferences. Trends Cogn Sci. 11:419–427.

Fischer TZ, Waxman SG. 2010. Neuropathic pain in diabetes-evidence for a central mechanism. Nat Rev Neurol. 6:462–466.

Forbes EE, Dahl RE. 2012. Research Review: Altered reward function in adolescent depression: What, when and how? J Child Psychol Psychiatry Allied Discip. 53:3–15.

Fornito A, Zalesky A, Breakspear M. 2015. The connectomics of brain disorders. Nat Rev Neurosci. 16:159–172.

Fox MD, Buckner RL, White MP, Greicius MD, Pascual-Leone A. 2012. Efficacy of transcranial magnetic stimulation targets for depression is related to intrinsic functional connectivity with the subgenual cingulate. Biol Psychiatry. 72:595–603.

Fox MD, Corbetta M, Snyder AZ, Vincent JL, Raichle ME. 2006. Spontaneous neuronal activity distinguishes human dorsal and ventral attention systems. Proc Natl Acad Sci. 103:10046–10051.

Fried EI, Kievit RA. 2015. The volumes of subcortical regions in depressed and healthy individuals are strikingly similar: a reinterpretation of the results by Schmaal et al. Mol Psychiatry. 1:1–2.

Frodl T, Carballedo A, Fagan AJ, Lisiecka D, Ferguson Y, Meaney JF. 2012. Effects of early-life adversity on white matter diffusivity changes in patients at risk for major depression. J Psychiatry Neurosci. 37:37–45.

Fujino J, Yamasaki N, Miyata J, Kawada R, Sasaki H. 2014. Altered brain response to others ' pain in major depressive disorder. J Affect Disord. 165:170–175.

Gamazon ER, Wheeler HE, Shah KP, Mozaffari S V, Aquino-Michaels K, Carroll RJ, Eyler AE, Denny JC, Nicolae DL, Cox NJ, Im HK, Consortium GTe, Nicolae DL, Cox NJ, Im HK. 2015. A gene-based association method for mapping traits using reference transcriptome data. Nat Genet. 47:1091–1098.

Gandal MJ, Leppa V, Won H, Parikshak NN, Geschwind DH. 2016. The road to precision psychiatry: Translating genetics into disease mechanisms. Nat Neurosci. 19:1397–1407.

Gandy K, Kim S, Sharp C, Dindo L, Maletic-Savatic M, Calarge C. 2017. Pattern separation: A potential marker of impaired hippocampal adult neurogenesis in major depressive disorder. Front Neurosci. 11.

Gavin AR, Walton E, Chae DH, Alegria M, Jackson JS, Takeuchi D. 2010. The associations between socio-economic status and major depressive disorder among blacks, latinos, asians and non-hispanic whites: Findings from the collaborative psychiatric epidemiology studies. Psychol Med. 40:51–61.

Geddes JR, Carney SM, Davies C, Furukawa TA, Kupfer DJ, Frank E, Goodwin GM. 2003. Relapse prevention with antidepressant drug treatment in depressive disorders : a systematic review. Lancet. 361:653–661.

Gent TC, Bandarabadi M, Herrera CG, Adamantidis AR. 2018. Thalamic dual control of sleep and wakefulness. Nat Neurosci. 21:1–11.

Gerlach KD, Spreng RN, Gilmore AW, Schacter DL. 2011. Solving future problems: Default network and executive activity associated with goal-directed mental simulations. Neuroimage. 55:1816–1824.

Glahn DC, Thompson PM, Blangero J. 2007. Neuroimaging Endophenotypes: Strategies for Finding Genes Influencing Brain Structure and Function. Hum Brain Mapp. 28:488–501.

Glimcher PW, Rustichini A. 2004. Neuroeconomics: The consilience of brain and decision. Science (80- ). 306:447–452.

Goldin PR, McRae K, Ramel W, Gross JJ. 2008. The Neural Bases of Emotion Regulation: Reappraisal and Suppression of Negative Emotion. Biol Psychiatry. 63:577–586.

Gordon JL, Girdler SS, Meltzer-Brody SE, Stika CS, Thurston RC, Clark CT, Prairie BA, Moses-Kolko E, Joffe H, Wisner KL. 2015. Ovarian hormone fluctuation, neurosteroids, and HPA axis dysregulation in perimenopausal depression: A novel heuristic model. Am J Psychiatry. 172:227–236.

Gotlib IH, Krasnoperova E. 2004. Attentional Biases for Negative Interpersonal Stimuli in

Clinical Depression. J Abnorm Psychol. 113:127–135.

Gotts SJ, Jo HJ, Wallace GL, Saad ZS, Cox RW, Martin A. 2013. Two distinct forms of functional lateralization in the human brain. Proc Natl Acad Sci. 110:E3435–E3444.

Goulden N, Khusnulina A, Davis NJ, Bracewell RM, Bokde AL, McNulty JP, Mullins PG. 2014. The salience network is responsible for switching between the default mode network and the central executive network: Replication from DCM. Neuroimage. 99:180–190.

Gradin VB, Kumar P, Waiter G, Ahearn T, Stickle C, Milders M, Reid I, Hall J, Steele JD. 2011. Expected value and prediction error abnormalities in depression and schizophrenia. Brain. 134:1751–1764.

Greicius MD, Flores BH, Menon V, Glover GH, Solvason HB, Kenna H, Reiss AL, Schatzberg AF. 2007. Resting-state functional connectivity in major depression: abnormally increased contributions from subgenual cingulate cortex and thalamus. Biol Psychiatry. 62:429–437.

Greicius MD, Kiviniemi V, Tervonen O, Vainionpää V, Alahuhta S, Reiss AL, Menon V. 2008. Persistent default-mode network connectivity during light sedation. Hum Brain Mapp. 29:839–847.

Greicius MD, Supekar K, Menon V, Dougherty RF. 2009. Resting-state functional connectivity reflects structural connectivity in the default mode network. Cereb Cortex. 19:72–78.

Grimm S, Ernst J, Boesiger P, Schuepbach D, Northoff G, Grimm S, Ernst J, Boesiger P, Schuepbach D, Boeker H. 2011. Reduced negative BOLD responses in the default-mode network and increased self-focus in depression increased self-focus in depression. World J Biol Psychiatry. 12:627–637.

Gusnard DA, Akbudak E, Shulman GL, Raichle ME. 2001. Medial prefrontal cortex and self-referential mental activity: Relation to a default mode of brain function. Proc Natl Acad Sci. 98:4259–4264.

Gutman DA, Holtzheimer PE, Behrens TEJ, Johansen-Berg H, Mayberg HS. 2009. A Tractography Analysis of Two Deep Brain Stimulation White Matter Targets for Depression. Biol Psychiatry. 65:276–282.

Hagenaars SP, Harris SE, Davies G, Hill WD, Liewald DCM, Ritchie SJ, Marioni RE, Fawns-Ritchie C, Cullen B, Malik R, METASTROKE Consortium IC for BPG, SpiroMeta Consortium, CHARGE Consortium Pulmonary Group CCA and LG, Worrall BB, Sudlow CLM, Wardlaw JM, Gallacher J, Pell J, McIntosh AM, Smith DJ, Gale CR, Deary IJ. 2016. Shared genetic aetiology between cognitive functions and physical and mental health in UK Biobank (N=112 151) and 24 GWAS consortia. Mol Psychiatry. 21:031120.

Hahn A, Wadsak W, Windischberger C, Baldinger P, Hoflich AS, Losak J, Nics L, Philippe C, Kranz GS, Kraus C, Mitterhauser M, Karanikas G, Kasper S, Lanzenberger R. 2012. Differential modulation of the default mode network via serotonin-1A receptors. Proc Natl Acad Sci. 109:2619–2624.

Hall J, Whalley HC, McKirdy JW, Romaniuk L, McGonigle D, McIntosh AM, Baig BJ, Gountouna VE, Job DE, Donaldson DI, Sprengelmeyer R, Young AW, Johnstone EC, Lawrie SM. 2008. Overactivation of Fear Systems to Neutral Faces in Schizophrenia. Biol Psychiatry. 64:70–73.

Hamilton JP, Furman DJ, Chang C, Thomason ME, Dennis E, Gotlib IH. 2011. Default-mode and task-positive network activity in major depressive disorder: Implications for adaptive and maladaptive rumination. Biol Psychiatry. 70:327–333.

Han Y, Wang J, Zhao Z, Min B, Lu J, Li K, He Y, Jia J. 2011. Frequency-dependent changes

in the amplitude of low-frequency fluctuations in amnestic mild cognitive impairment: A resting-state fMRI study. Neuroimage. 55:287–295.

Hasin DS, Sarvet AL, Meyers JL, Saha TD, Ruan WJ, Stohl M, Grant BF. 2018. Epidemiology of adult DSM-5 major depressive disorder and its specifiers in the United States. JAMA Psychiatry. 75:336–346.

Hearne LJ, Mattingley JB, Cocchi L. 2016. Functional brain networks related to individual differences in human intelligence at rest. Sci Rep. 6:32328.

Heim C, Mletzko T, Purselle D, Musselman DL, Nemeroff CB. 2008. The Dexamethasone/Corticotropin-Releasing Factor Test in Men with Major Depression: Role of Childhood Trauma. Biol Psychiatry. 63:398–405.

Heim C, Nemeroff CB. 2002. Neurobiology of early life stress: clinical studies. Semin Clin Neuropsychiatry. 7:147–159.

Heim C, Newport DJ, Mletzko T, Miller AH, Nemeroff CB. 2008. The link between childhood trauma and depression: Insights from HPA axis studies in humans. Psychoneuroendocrinology. 33:693–710.

Heller AS, Johnstone T, Peterson MJ, Kolden GG, Kalin NH, Davidson RJ. 2013. Increased prefrontal cortex activity during negative emotion regulation as a predictor of depression symptom severity trajectory over 6 months. JAMA psychiatry. 70:1181–1189.

Heo M, Pietrobelli A, Fontaine KR, Sirey JA, Faith MS. 2006. Depressive mood and obesity in US adults: Comparison and moderation by sex, age, and race. Int J Obes. 30:513–519.

Higgins DM, Peterson JB, Pihl RO, Lee AGM. 2007. Prefrontal cognitive ability, intelligence, Big Five personality, and the prediction of advanced academic and workplace

performance. J Pers Soc Psychol. 93:298–319.

Hill WD, Davies G, Harris SE, Hagenaars SP, Liewald D, Penke L, Gale CR, Deary I. 2016. Molecular genetic aetiology of general cognitive function is enriched in evolutionarily conserved regions. Transl Psychiatry. 6:e980.

Hill WD, Hagenaars SP, Marioni RE, Harris SE, Liewald DCM, Davies G, Okbay A, McIntosh AM, Gale CR, Deary IJ. 2016. Molecular Genetic Contributions to Social Deprivation and Household Income in UK Biobank. Curr Biol. 26:3083–3089.

Ho TC, Sacchet MD, Connolly CG, Margulies DS, Tymofiyeva O, Paulus MP, Simmons AN, Gotlib IH, Yang TT. 2017. Inflexible functional connectivity of the dorsal anterior cingulate cortex in adolescent major depressive disorder. Neuropsychopharmacology. 42:2434–2445.

Howard DM, Adams MJ, Clarke T, Hafferty JD, Gibson J, Shirali M, Coleman JRI, Ward J, Wigmore EM, Alloza C, Shen X, Barbu MC, Xu EY, Whalley HC, Marioni RE, Porteous DJ, Davies G, Deary IJ, Hemani G, Tian C, Hinds DA, Team 23andMe Research, Consortium MDDWG of the PG, Trzaskowski M, Byrne EM, Ripke S, Smith DJ, Sullivan PF, Wray NR, Breen G, Lewis CM, McIntosh AM. 2018. Genome-wide meta-analysis of depression in 807,553 individuals identifies 102 independent variants with replication in a further 1,507,153 individuals. bioRxiv. 6288:433367.

Howard DM, Adams MJ, Shirali M, Clarke T-K, Marioni RE, Davies G, Coleman JRI, Alloza C, Shen X, Barbu MC, Wigmore EM, Gibson J, Hagenaars S, Lewis CM, Smith DJ, Sullivan PF, Haley CS, Breen G, Deary IJ, McIntosh AM. 2017. Genome-wide association study of depression phenotypes in UK Biobank (n = 322,580) identifies the enrichment of variants in excitatory synaptic pathways. bioRxiv. 6268:168732.

Howard DM, Adams MJ, Shirali M, Clarke TK, Marioni RE, Davies G, Coleman JRI, Alloza C, Shen X, Barbu MC, Wigmore EM, Gibson J, Hagenaars SP, Lewis CM, Ward J, Smith

DJ, Sullivan PF, Haley CS, Breen G, Deary IJ, McIntosh AM. 2018. Genome-wide association study of depression phenotypes in UK Biobank identifies variants in excitatory synaptic pathways. Nat Commun. 9:1–10.

Howard DM, Clarke T-K, Adams MJ, Hafferty JD, Wigmore EM, Zeng Y, Hall LS, Gibson J, Boutin TS, Hayward C, Thomson PA, Porteous DJ, Smith BH, Murray AD, Consortium MDDWG of the PG, Haley CS, Deary IJ, Whalley HC, McIntosh AM. 2017. The stratification of major depressive disorder into genetic subgroups David. bioRxiv.

Huang H, Fan X, Williamson DE, Rao U. 2011. White matter changes in healthy adolescents at familial risk for unipolar depression: a diffusion tensor imaging study. Neuropsychopharmacology. 36:684–691.

Hyde CL, Nagle MW, Tian C, Chen X, Paciga SA, Wendland JR, Tung JY, Hinds DA, Perlis RH, Winslow AR. 2016. Identification of 15 genetic loci associated with risk of major depression in individuals of European descent. Nat Genet. 48:1031–1036.

Hyodo K, Dan I, Kyutoku Y, Suwabe K, Byun K, Ochi G, Kato M, Soya H. 2016. The association between aerobic fitness and cognitive function in older men mediated by frontal lateralization. Neuroimage. 125:291–300.

International T, Consortium S. 2009. Common polygenic variation contributes to risk of schizophrenia and bipolar disorder. Nature. 460.

Jahanshad N, Kochunov P V, Sprooten E, Mandl RC, Nichols TE, Almasy L, Blangero J, Brouwer RM, Curran JE, Zubicaray GI De, Duggirala R, Fox PT, Hong LE, Landman BA, Martin NG, Mcmahon KL, Medland SE, Mitchell BD, Olvera RL, Peterson CP, Starr JM, Sussmann JE, Toga AW, Wardlaw JM, Wright MJ, Hulshoff HE, Bastin ME, Mcintosh AM, Deary IJ, Thompson PM, Glahn DC. 2013. NeuroImage Multi-site genetic analysis of diffusion images and voxelwise heritability analysis : A pilot project of the ENIGMA – DTI working group. Neuroimage. 81:455–469.

James MH, Dayas C V. 2013. What about me…? The PVT: a role for the paraventricular thalamus (PVT) in drug-seeking behavior. Front Behav Neurosci. 7:6–8.

Jenkinson M, Bannister P, Brady M, Smith S. 2002. Improved optimization for the robust and accurate linear registration and motion correction of brain images. Neuroimage. 17:825–841.

Jenkinson M, Smith SM. 2001. A global optimization method for robust affine registration of brain images. Med Imaging Anal. 5:143–156.

Jones DK, Knösche TR, Turner R. 2013. White matter integrity, fiber count, and other fallacies: The do's and don'ts of diffusion MRI. Neuroimage. 73:239–254.

Jylha P, Melartin T, Isometsa E. 2009. Relationships of neuroticism and extraversion with axis I and II comorbidity among patients with DSM-IV major depressive disorder. J Affect Disord. 114:110–121.

Kaiser RH, Andrews-Hanna JR, Wager TD, Pizzagalli DA. 2015. Large-scale network dysfunction in major depressive disorder: A meta-analysis of resting-state functional connectivity. JAMA Psychiatry. 72:603–611.

Kamagata K, Zalesky A, Hatano T, Ueda R, Di Biase MA, Okuzumi A, Shimoji K, Hori M, Caeyenberghs K, Pantelis C, Hattori N, Aoki S. 2017. Gray Matter Abnormalities in Idiopathic Parkinson's Disease: Evaluation by Diffusional Kurtosis Imaging and Neurite Orientation Dispersion and Density Imaging. Hum Brain Mapp. 38:3704–3722.

Kamourieh S, Braga RM, Leech R, Newbould RD, Malhotra P, Wise RJS. 2015. Neural systems involved when attending to a speaker. Cereb Cortex. 25:4284–4298.

Kanske P, Heissler J, Schönfelder S, Wessa M. 2012. Neural correlates of emotion regulation deficits in remitted depression: The influence of regulation strategy, habitual regulation use, and emotional valence. Neuroimage. 61:686–693.

Karlsgodt KH, van Erp TGM, Poldrack RA, Bearden CE, Nuechterlein KH, Cannon TD. 2008. Diffusion Tensor Imaging of the Superior Longitudinal Fasciculus and Working Memory in Recent-Onset Schizophrenia. Biol Psychiatry. 63:512–518.

Kastner S, De Weerd P, Desimone R, Ungerleider LG. 1998. Mechanisms of directed attention in the human extrastriate cortex as revealed by functional MRI. Science (80- ). 282:108–111.

Kendler KS, Gardner CO. 2011. A longitudinal etiologic model for symptoms of anxiety and depression in women. Psychol Med. 41:2035–2045.

Kendler KS, Gardner CO. 2016. Depressive vulnerability, stressful life events and episode onset of major depression: A longitudinal model. Psychol Med. 46:1865–1874.

Kendler KS, Kuhn J, Prescott CA. 2004. The interrelationship of neuroticism, sex and stressful life events in the prediction of episodes of major depression. Am J Psychiatry. 161:631–636.

Kessler RC, Berglund P, Demler O, Jin R, Koretz D, Merikangas KR, Rush AJ, Walters EE, Wang PS. 2003. The Epidemiology of Major. Am Med Assoc. 289:3095–3105.

Kessler RC, Berglund P, Demler O, Jin R, Koretz D, Merikangas KR, Rush AJ, Walters EE, Wang PS. 2014. The Epidemiology of Major Depressive Disorder. Am Med Assoc. 289:3095–3105.

Kessler RC, Nelson CB, McGonagle KA, Liu J, Al. E. 1996. Comorbidity of DSM-III--R major depressive disorder in the general population: Results from the US National Comorbidity Survey. Br J Psychiatry. 168:17–30.

Kessler RC, Sampson NA, Berglund P, Gruber MJ, Al-Hamzawi A, Andrade L, Bunting B, Demyttenaere K, Florescu S, De Girolamo G, Gureje O, He Y, Hu C, Huang Y, Karam E, Kovess-Masfety V, Lee S, Levinson D, Medina Mora ME, Moskalewicz J, Nakamura

Y, Navarro-Mateu F, Browne MAO, Piazza M, Posada-Villa J, Slade T, Ten Have M, Torres Y, Vilagut G, Xavier M, Zarkov Z, Shahly V, Wilcox MA. 2015. Anxious and non-anxious major depressive disorder in the World Health Organization World Mental Health Surveys. Epidemiol Psychiatr Sci. 24:210–226.

Keyes KM, Platt J, Kaufman AS, McLaughlin KA. 2016. Association of Fluid Intelligence and Psychiatric Disorders in a Population-Representative Sample of US Adolescents. JAMA Psychiatry. 57:1336–1346.

Khubchandani J, Brey R, Kotecki J, Kleinfelder JA, Anderson J. 2016. The Psychometric Properties of PHQ-4 Depression and Anxiety Screening Scale Among College Students. Arch Psychiatr Nurs. 30:457–462.

Kievit RA, Davis SW, Mitchell DJ, Taylor JR, Duncan J, Henson RNA. 2014. Distinct aspects of frontal lobe structure mediate age-related differences in fluid intelligence and multitasking. Nat Commun. 5:5658.

Kochunov P, Jahanshad N, Marcus D, Winkler A, Sprooten E, Nichols TE, Wright SN, Hong LE, Patel B, Behrens T, Jbabdi S, Andersson J, Lenglet C, Yacoub E, Moeller S, Auerbach E, Ugurbil K, Sotiropoulos SN, Brouwer RM, Landman B, Lemaitre H, Braber A Den, Zwiers MP, Ritchie S, Hulzen K Van, Almasy L, Curran J, Greig I, Duggirala R, Fox P, Martin NG, Mcmahon KL, Mitchell B, Olvera RL, Peterson C, Starr J, Sussmann J, Wardlaw J, Wright M, Boomsma DI, Kahn R, Geus EJC De, Williamson DE, Hariri A, Van D, Bastin ME, Mcintosh A, Deary IJ, Hulshoff HE, Blangero J, Thompson PM, Glahn DC, Essen DC Van. 2015. NeuroImage Heritability of fractional anisotropy in human white matter : A comparison of Human Connectome Project and ENIGMA-DTI data. Neuroimage. 111:300–311.

Koechlin E, Summerfield C. 2007. An information theoretical approach to prefrontal executive function. Trends Cogn Sci. 11:229–235.

Kohler S, Thomas AJ, Lloyd A, Barber R, Almeida OP, O'Brien JT. 2010. White matter hyperintensities, cortisol levels, brain atrophy and continuing cognitive deficits in late-life depression. Br J Psychiatry. 196:143–149.

Kolling N, Behrens TEJ, Wittmann MK, Rushworth MFS. 2016. Multiple signals in anterior cingulate cortex. Curr Opin Neurobiol. 37:36–43.

Kong L, Wu F, Tang Y, Ren L, Kong D, Liu Y, Xu K, Wang F. 2014. Frontal-subcortical volumetric deficits in single episode, medication-naïve depressed patients and the effects of 8 weeks fluoxetine treatment: A VBM-DARTEL study. PLoS One. 9:e79055.

Korgaonkar MS, Grieve SM, Koslow SH, Gabrieli JDE, Gordon E, Williams LM. 2011. Loss of white matter integrity in major depressive disorder: Evidence using tract-based spatial statistical analysis of diffusion tensor imaging. Hum Brain Mapp. 32:2161–2171.

Korgaonkar MS, Williams LM, Song YJ, Usherwood T, Grieve SM. 2014. Diffusion tensor imaging predictors of treatment outcomes in major depressive disorder. Br J Psychiatry. 205:321–328.

Krause AJ, Simon E Ben, Mander BA, Greer SM, Saletin JM, Goldstein-Piekarski AN, Walker MP. 2017. The sleep-deprived human brain. Nat Rev Neurosci. 18:404–418.

Kroenke K, Spitzer RL, Janet BW, Williams DSW, Lö B. 2009. An Ultra-Brief Screening Scale for Anxiety and Depression: The PHQ– 4. Psychosomatics. 50:613–621.

Lai CH, Wu YT. 2014. Alterations in white matter micro-integrity of the superior longitudinal fasciculus and anterior thalamic radiation of young adult patients with depression. Psychol Med. 44:2825–2832.

Lammel S, Lim BK, Malenka RC. 2014. Reward and aversion in a heterogeneous midbrain dopamine system. Neuropharmacology. 76:351–359.

Lawlor DA, Harbord RM, Sterne JAC, Timpson N, Davey Smith G. 2008. Mendelian randomization: Using genes as instruments for making causal inferences in epidemiology. Stat Med. 27:1133–1163.

LeDoux J. 2012. Rethinking the Emotional Brain. Neuron. 73:653–676.

Lee SH, Ripke S, Neale BM, Faraone S V., Purcell SM, Perlis RH, Mowry BJ, Thapar A, Goddard ME, Witte JS, Absher D, Agartz I, Akil H, Amin F, Andreassen OA, Anjorin A, Anney R, Anttila V, Arking DE, Asherson P, Azevedo MH, Backlund L, Badner JA, Bailey AJ, Banaschewski T, Barchas JD, Barnes MR, Barrett TB, Bass N, Battaglia A, Bauer M, Bayés M, Bellivier F, Bergen SE, Berrettini W, Betancur C, Bettecken T, Biederman J, Binder EB, Black DW, Blackwood DHR, Bloss CS, Boehnke M, Boomsma DI, Breen G, Breuer R, Bruggeman R, Cormican P, Buccola NG, Buitelaar JK, Bunney WE, Buxbaum JD, Byerley WF, Byrne EM, Caesar S, Cahn W, Cantor RM, Casas M, Chakravarti A, Chambert K, Choudhury K, Cichon S, Cloninger CR, Collier DA, Cook EH, Coon H, Cormand B, Corvin A, Coryell WH, Craig DW, Craig IW, Crosbie J, Cuccaro ML, Curtis D, Czamara D, Datta S, Dawson G, Day R, De Geus EJ, Degenhardt F, Djurovic S, Donohoe GJ, Doyle AE, Duan J, Dudbridge F, Duketis E, Ebstein RP, Edenberg HJ, Elia J, Ennis S, Etain B, Fanous A, Farmer AE, Ferrier IN, Flickinger M, Fombonne E, Foroud T, Frank J, Franke B, Fraser C, Freedman R, Freimer NB, Freitag CM, Friedl M, Frisén L, Gallagher L, Gejman P V., Georgieva L, Gershon ES, Geschwind DH, Giegling I, Gill M, Gordon SD, Gordon-Smith K, Green EK, Greenwood TA, Grice DE, Gross M, Grozeva D, Guan W, Gurling H, De Haan L, Haines JL, Hakonarson H, Hallmayer J, Hamilton SP, Hamshere ML, Hansen TF, Hartmann AM, Hautzinger M, Heath AC, Henders AK, Herms S, Hickie IB, Hipolito M, Hoefels S, Holmans PA, Holsboer F, Hoogendijk WJ, Hottenga JJ, Hultman CM, Hus V, Ingason A, Ising M, Jamain S, Jones EG, Jones I, Jones L, Tzeng JY, Kähler AK, Kahn RS, Kandaswamy R, Keller MC, Kennedy JL, Kenny E, Kent L, Kim Y, Kirov GK, Klauck SM, Klei L, Knowles JA, Kohli MA, Koller DL, Konte B, Korszun A, Krabbendam

L, Krasucki R, Kuntsi J, Kwan P, Landén M, Långström N, Lathrop M, Lawrence J, Lawson WB, Leboyer M, Ledbetter DH, Lee PH, Lencz T, Lesch KP, Levinson DF, Lewis CM, Li J, Lichtenstein P, Lieberman JA, Lin DY, Linszen DH, Liu C, Lohoff FW, Loo SK, Lord C, Lowe JK, Lucae S, Macintyre DJ, Madden PAF, Maestrini E, Magnusson PKE, Mahon PB, Maier W, Malhotra AK, Mane SM, Martin CL, Martin NG, Mattheisen M, Matthews K, Mattingsdal M, Mccarroll SA, Mcghee KA, Mcgough JJ, Mcgrath PJ, Mcguffin P, Mcinnis MG, Mcintosh A, Mckinney R, Mclean AW, Mcmahon FJ, Mcmahon WM, Mcquillin A, Medeiros H, Medland SE, Meier S, Melle I, Meng F, Meyer J, Middeldorp CM, Middleton L, Milanova V, Miranda A, Monaco AP, Montgomery GW, Moran JL, Moreno-De-Luca D, Morken G, Morris DW, Morrow EM, Moskvina V, Muglia P, Mühleisen TW, Muir WJ, Müller-Myhsok B, Murtha M, Myers RM, Myin-Germeys I, Neale MC, Nelson SF, Nievergelt CM, Nikolov I, Nimgaonkar V, Nolen WA, Nöthen MM, Nurnberger JI, Nwulia EA, Nyholt DR, O'dushlaine C, Oades RD, Olincy A, Oliveira G, Olsen L, Ophoff RA, Osby U, Owen MJ, Palotie A, Parr JR, Paterson AD, Pato CN, Pato MT, Penninx BW, Pergadia ML, Pericak-Vance MA, Pickard BS, Pimm J, Piven J, Posthuma D, Potash JB, Poustka F, Propping P, Puri V, Quested DJ, Quinn EM, Ramos-Quiroga JA, Rasmussen HB, Raychaudhuri S, Rehnström K, Reif A, Ribasés M, Rice JP, Rietschel M, Roeder K, Roeyers H, Rossin L, Rothenberger A, Rouleau G, Ruderfer D, Rujescu D, Sanders AR, Sanders SJ, Santangelo SL, Sergeant JA, Schachar R, Schalling M, Schatzberg AF, Scheftner WA, Schellenberg GD, Scherer SW, Schork NJ, Schulze TG, Schumacher J, Schwarz M, Scolnick E, Scott LJ, Shi J, Shilling PD, Shyn SI, Silverman JM, Slager SL, Smalley SL, Smit JH, Smith EN, Sonuga-Barke EJS, St. Clair D, State M, Steffens M, Steinhausen HC, Strauss JS, Strohmaier J, Stroup TS, Sutcliffe JS, Szatmari P, Szelinger S, Thirumalai S, Thompson RC, Todorov AA, Tozzi F, Treutlein J, Uhr M, Van Den Oord EJCG, Van Grootheest G, Van Os J, Vicente AM, Vieland VJ, Vincent JB, Visscher PM, Walsh CA, Wassink TH, Watson SJ, Weissman MM, Werge T, Wienker TF, Wijsman EM, Willemsen G, Williams N, Willsey AJ, Witt SH, Xu W, Young AH, Yu TW,

Zammit S, Zandi PP, Zhang P, Zitman FG, Zöllner S, Devlin B, Kelsoe JR, Sklar P, Daly MJ, O'donovan MC, Craddock N, Sullivan PF, Smoller JW, Kendler KS, Wray NR. 2013. Genetic relationship between five psychiatric disorders estimated from genome-wide SNPs. Nat Genet. 45:984–994.

Lencz T, Knowles E, Davies G, Guha S, Liewald DC, Starr JM, Djurovic S, Melle I, Sundet K, Christoforou a, Reinvang I, Mukherjee S, DeRosse P, Lundervold a, Steen VM, John M, Espeseth T, Räikkönen K, Widen E, Palotie a, Eriksson JG, Giegling I, Konte B, Ikeda M, Roussos P, Giakoumaki S, Burdick KE, Payton a, Ollier W, Horan M, Donohoe G, Morris D, Corvin a, Gill M, Pendleton N, Iwata N, Darvasi a, Bitsios P, Rujescu D, Lahti J, Hellard SL, Keller MC, Andreassen O a, Deary IJ, Glahn DC, Malhotra a K. 2014. Molecular genetic evidence for overlap between general cognitive ability and risk for schizophrenia: a report from the Cognitive Genomics consorTium (COGENT). Mol Psychiatry. 19:168–174.

Lenze E, Cross D, Mckeel D, Neuman RJ, Ph D, Sheline YI. 1999. White Matter Hyperintensities and Gray Matter Lesions in Physically Healthy Depressed Subjects. Am J Psychiatry. 156:1602–1607.

Leppa JM. 2006. Emotional information processing in mood disorders : a review of behavioral and neuroimaging findings. Curr Opin Psychiatry. 19:34–39.

Leskelä U, Rytsälä H, Komulainen E, Melartin T, Sokero P, Lestelä-Mielonen P, Isometsä ET. 2006. The influence of adversity and perceived social support on the outcome of major depressive disorder in subjects with different levels of depressive symptoms. Psychol Med. 36:779–788.

Lewinsohn PM, Olino TM, Klein DN. 2005. Psychosocial impairment in offspring of depressed parents. Psychol Med. 35:1493–1503.

Liao Y, Huang X, Wu Q, Yang C, Kuang W, Du M, Lui S, Yue Q, Chan R, Kemp G, Gong Q.

2013. Is depression a disconnection syndrome? Meta- analysis of diffusion tensor imaging studies in patients with MDD. J Psychiatry Neurosci. 38:49–56.

Lin Y, Huang S, Simon GE, Liu S. 2016. Mathematical Biosciences Analysis of depression trajectory patterns using collaborative learning. Math Biosci. 282:191–203.

Linden DEJ. 2012. The Challenges and Promise of Neuroimaging in Psychiatry. Neuron. 73:8–22.

Löwe B, Wahl I, Rose M, Spitzer C, Glaesmer H, Wingenfeld K, Schneider A, Brähler E. 2010. A 4-item measure of depression and anxiety: Validation and standardization of the Patient Health Questionnaire-4 (PHQ-4) in the general population. J Affect Disord. 122:86–95.

Lyall DM, Cullen B, Allerhand M, Smith DJ, Mackay D, Evans J, Anderson J, Fawns-Ritchie C, McIntosh AM, Deary IJ, Pell JP. 2016. Cognitive test scores in UK biobank: Data reduction in 480,416 participants and longitudinal stability in 20,346 participants. PLoS One. 11:1–10.

Ma Y. 2015. Neuropsychological mechanism underlying antidepressant effect: A systematic meta-analysis. Mol Psychiatry. 20:311–319.

MacDonald a W, Cohen JD, Stenger VA, Carter CS. 2000. Dissociating the role of the dorsolateral prefrontal and anterior cingulate cortex in cognitive control. Science. 288:1835–1838.

Mahoney CJ, Ridgway GR, Malone IB, Downey LE, Beck J, Kinnunen KM, Schmitz N, Golden HL, Rohrer JD, Schott JM, Rossor MN, Ourselin S, Mead S, Fox NC, Warren JD. 2014. Profiles of white matter tract pathology in frontotemporal dementia. Hum Brain Mapp. 35:4163–4179.

Maller JJ, Thomson RHS, Rosenfeld J V., Anderson R, Daskalakis ZJ, Fitzgerald PB. 2014.

Occipital bending in depression. Brain. 137:1830–1837.

Mamah D, Conturo TE, Harms MP, Akbudak E, Wang L, McMichael AR, Gado MH, Barch DM, Csernansky JG. 2010. Anterior thalamic radiation integrity in schizophrenia: A diffusion-tensor imaging study. Psychiatry Res - Neuroimaging. 183:144–150.

Maniega SM, Valdés Hernández MC, Clayden JD, Royle NA, Murray C, Morris Z, Aribisala BS, Gow AJ, Starr JM, Bastin ME, Deary IJ, Wardlaw JM. 2015. White matter hyperintensities and normal-appearing white matter integrity in the aging brain. Neurobiol Aging. 36:909–918.

Marcus M, Yasamy MT, Ommeren M van, Chisholm D, Saxena S. 2012. Depression: A Global Public Health Concern.

Maret S, Faraguna U, Nelson AB, Cirelli C, Tononi G. 2011. Sleep and waking modulate spine turnover in the adolescent mouse cortex. Nat Neurosci. 14:1418–1420.

Marioni RE, Davies G, Hayward C, Liewald D, Kerr SM, Campbell A, Luciano M, Smith BH, Padmanabhan S, Hocking LJ, Hastie ND, Wright AF, Porteous DJ, Visscher PM, Deary IJ. 2014. Molecular genetic contributions to socioeconomic status and intelligence. Intelligence. 44:26–32.

Matthews PM, Sudlow C. 2015. The UK Biobank. Brain. 138:3463–3465.

Mazza E, Poletti S, Bollettini I, Locatelli C, Falini A, Colombo C, Benedetti F. 2017. Body mass index associates with white matter microstructure in bipolar depression. Bipolar Disord. 19:116–127.

McFarland BR, Klein DN. 2009. Emotional reactivity in depression: Diminished responsiveness to anticipated reward but not to anticipated punishment or to nonreward or avoidance. Depress Anxiety. 26:117–122.

McIntosh AM, Hall LS, Zeng Y, Adams MJ, Gibson J, Wigmore E, Hagenaars SP, Davies G, Fernandez-Pujals AM, Campbell AI, Clarke TK, Hayward C, Haley CS, Porteous DJ, Deary IJ, Smith DJ, Nicholl BI, Hinds DA, Jones A V., Scollen S, Meng W, Smith BH, Hocking LJ. 2016. Genetic and Environmental Risk for Chronic Pain and the Contribution of Risk Variants for Major Depressive Disorder: A Family-Based Mixed-Model Analysis. PLoS Med. 13:1–17.

Meng C, Brandl F, Tahmasian M, Shao J, Manoliu A, Scherr M, Schwerthoffer D, Bauml J, Forstl H, Zimmer C, Wohlschlager AM, Riedl V, Sorg C. 2014. Aberrant topology of striatum's connectivity is associated with the number of episodes in depression. Brain. 137:598–609.

Meyer-Lindenberg A, Tost H. 2012. Neural mechanisms of social risk for psychiatric disorders. Nat Neurosci. 15:663–668.

Meyer-lindenberg AS, Olsen RK, Kohn PD, Brown T, Egan MF, Weinberger DR, Faith K. 2005. Regionally Specific Disturbance of Hippocampal - Dorsolateral Prefrontal Functional Connectivity in Schizophrenia. Arch Gen Psychiatry. 62.

Miller EK. 2000. The prefrontal cortex and cogitive control. Nat Rev neu. 1:59–65.

Miller KL, Alfaro-Almagro F, Bangerter NK, Thomas DL, Yacoub E, Xu J, Bartsch AJ, Jbabdi S, Sotiropoulos SN, Andersson JLR, Griffanti L, Douaud G, Okell TW, Weale P, Dragonu I, Garratt S, Hudson S, Collins R, Jenkinson M, Matthews PM, Smith SM. 2016. Multimodal population brain imaging in the UK Biobank prospective epidemiological study. Nat Neurosci.

Mistry S, Harrison JR, Smith DJ, Escott-Price V, Zammit S. 2018. The use of polygenic risk scores to identify phenotypes associated with genetic risk of bipolar disorder and depression: A systematic review. J Affect Disord. 234:148–155.

Mitterschiffthaler MT, Williams SCR, Walsh ND, Cleare AJ, Donaldson C. 2008. Neural basis of the emotional Stroop interference effect in major depression. Psychol Med. 38:247–256.

Mogg K, Bradbury KE, Bradley BP. 2006. Interpretation of ambiguous information in clinical depression. Behav Res Ther. 44:1411–1419.

Mohr H, Wolfensteller U, Betzel RF, Mišić B, Sporns O, Richiardi J, Ruge H. 2016. Integration and segregation of large-scale brain networks during short-term task automatization. Nat Commun. 7.

Mori S, Kaufmann WE, Davatzikos C, Stieltjes B, Amodei L, Fredericksen K, Pearlson GD, Melhem ER, Solaiyappan M, Raymond G V., Moser HW, Van Zijl PCM. 2002. Imaging cortical association tracts in the human brain using diffusion-tensor-based axonal tracking. Magn Reson Med. 47:215–223.

Moser JS, Huppert JD, Foa EB, Simons RF. 2012. Interpretation of ambiguous social scenarios in social phobia and depression : Evidence from event-related brain potentials. Biol Psychol. 89:387–397.

Muñoz M, Pong-Wong R, Canela-Xandri O, Rawlik K, Haley CS, Tenesa A. 2016. Evaluating the contribution of genetics and familial shared environment to common disease using the UK Biobank. Nat Genet. 48:980–983.

Murphy ML, Frodl T. 2011. Meta-analysis of diffusion tensor imaging studies shows altered fractional anisotropy occurring in distinct brain areas in association with depression. Biol Mood Anxiety Disord. 1:1–12.

Musliner KL, Seifuddin F, Judy JA, Pirooznia M, Goes FS, Zandi PP. 2015. Polygenic risk, stressful life events and depressive symptoms in older adults: a polygenic score analysis. Psychol Med. 45:1709–1720.

Navrady LB, Adams MJ, Chan SWY, Ritchie SJ, Mcintosh AM. 2018. Genetic risk of major depressive disorder: The moderating and mediating effects of neuroticism and psychological resilience on clinical and self-reported depression. Psychol Med. 48:1890–1899.

Nebes RD, Ph D, Vora IJ, Meltzer CC, Fukui MB, Williams RL, Kamboh MI, Ph D, Saxton J, Ph D, Houck PR, Dekosky ST, Iii CFR. 2001. Relationship of Deep White Matter Hyperintensities and Apolipoprotein E Genotype to Depressive Symptoms in Older Adults Without Clinical Depression. Am J Psychiatry. 158:878–884.

Nelder JA, Baker RJ. 2004. Generalized linear models. Encycl Stat Sci. 4.

Nemeroff CB, Vale WW. 2005. The neurobiology of depression: inroads to treatment and new drug discovery. J Clin Psychiatry. 66 Suppl 7:5–13.

Nugent AC, Davis RM, Zarate CA, Drevets WC. 2013. Reduced thalamic volumes in major depressive disorder. Psychiatry Res - Neuroimaging. 213:179–185.

Oberski DL. 2014. lavaan.survey: An R ackage for complex survey analysis of structural equation models. J Stat Softw. 57:1–27.

Okbay A, Baselmans BML, De Neve J-E, Turley P, Nivard MG, Fontana MA, Meddens SFW, Linnér RK, Rietveld CA, Derringer J, Gratten J, Lee JJ, Liu JZ, de Vlaming R, Ahluwalia TS, Buchwald J, Cavadino A, Frazier-Wood AC, Furlotte NA, Garfield V, Geisel MH, Gonzalez JR, Haitjema S, Karlsson R, van der Laan SW, Ladwig K-H, Lahti J, van der Lee SJ, Lind PA, Liu T, Matteson L, Mihailov E, Miller MB, Minica CC, Nolte IM, Mook-Kanamori D, van der Most PJ, Oldmeadow C, Qian Y, Raitakari O, Rawal R, Realo A, Rueedi R, Schmidt B, Smith A V, Stergiakouli E, Tanaka T, Taylor K, Wedenoja J, Wellmann J, Westra H-J, Willems SM, Zhao W, Amin N, Bakshi A, Boyle PA, Cherney S, Cox SR, Davies G, Davis OSP, Ding J, Direk N, Eibich P, Emeny RT, Fatemifar G, Faul JD, Ferrucci L, Forstner A, Gieger C, Gupta R, Harris TB, Harris JM, Holliday EG,

Hottenga J-J, De Jager PL, Kaakinen MA, Kajantie E, Karhunen V, Kolcic I, Kumari M, Launer LJ, Franke L, Li-Gao R, Koini M, Loukola A, Marques-Vidal P, Montgomery GW, Mosing MA, Paternoster L, Pattie A, Petrovic KE, Pulkki-Råback L, Quaye L, Räikkönen K, Rudan I, Scott RJ, Smith JA, Sutin AR, Trzaskowski M, Vinkhuyzen AE, Yu L, Zabaneh D, Attia JR, Bennett DA, Berger K, Bertram L, Boomsma DI, Snieder H, Chang S-C, Cucca F, Deary IJ, van Duijn CM, Eriksson JG, Bültmann U, de Geus EJC, Groenen PJF, Gudnason V, Hansen T, Hartman CA, Haworth CMA, Hayward C, Heath AC, Hinds DA, Hyppönen E, Iacono WG, Järvelin M-R, Jöckel K-H, Kaprio J, Kardia SLR, Keltikangas-Järvinen L, Kraft P, Kubzansky LD, Lehtimäki T, Magnusson PKE, Martin NG, McGue M, Metspalu A, Mills M, de Mutsert R, Oldehinkel AJ, Pasterkamp G, Pedersen NL, Plomin R, Polasek O, Power C, Rich SS, Rosendaal FR, den Ruijter HM, Schlessinger D, Schmidt H, Svento R, Schmidt R, Alizadeh BZ, Sørensen TIA, Spector TD, Steptoe A, Terracciano A, Thurik AR, Timpson NJ, Tiemeier H, Uitterlinden AG, Vollenweider P, Wagner GG, Weir DR, Yang J, Conley DC, Smith GD, Hofman A, Johannesson M, Laibson DI, Medland SE, Meyer MN, Pickrell JK, Esko T, Krueger RF, Beauchamp JP, Koellinger PD, Benjamin DJ, Bartels M, Cesarini D. 2016. Genetic variants associated with subjective well-being, depressive symptoms, and neuroticism identified through genome-wide analyses. Nat Genet. 48:624–633.

Palm U, Schiller C, Fintescu Z, Obermeier M, Keeser D, Reisinger E, Pogarell O, Nitsche MA, Möller HJ, Padberg F. 2012. Transcranial direct current stimulation in treatment resistant depression: A randomized double-blind, placebo-controlled study. Brain Stimul. 5:242–251.

Pariante CM. 2006. The glucocorticoid receptor: part of the solution or part of the problem? Psychopharmacology (Berl). 20:79–84.

Pariante CM. 2009. Risk factors for development of depression and psychosis: Glucocorticoid receptors and pituitary implications for treatment with antidepressant

and glucocorticoids. Ann N Y Acad Sci. 1179:144–152.

Pariante CM, Lightman SL. 2008. The HPA axis in major depression: classical theories and new developments. Trends Neurosci. 31:464–468.

Parr A, Cusack R, Thompson R, Nimmo-smith I, Torralva T, Roca M, Antoun N, Manes F, Woolgar A, Parr A, Cusack R, Thompson R, Nimmo-smith I, Torralva T. 2015. Fluid intelligence loss linked to restricted regions of damage within frontal and parietal cortex. Proc Natl Acad Sci U S A. 112:E4969.

Patenaude B, Smith SM, Kennedy DN, Jenkinson M. 2011. A Bayesian model of shape and appearance for subcortical brain segmentation. Neuroimage. 56:907–922.

Pechtel P, Dutra SJ, Goetz EL, Pizzagalli DA. 2013. Blunted reward responsiveness in remitted depression. J Psychiatr Res. 47:1864–1869.

Penke L, Maniega SM, Bastin ME, Valdés Hernández MC, Murray C, Royle N a, Starr JM, Wardlaw JM, Deary IJ. 2012. Brain white matter tract integrity as a neural foundation for general intelligence. Mol Psychiatry. 17:1026–1030.

Penke L, Maniega SM, Murray C, Gow AJ, Valdes Hernandez MC, Clayden JD, Starr JM, Wardlaw JM, Bastin ME, Deary IJ. 2010. A General Factor of Brain White Matter Integrity Predicts Information Processing Speed in Healthy Older People. J Neurosci. 30:7569–7574.

Petersen SE, Posner MI. 2012. The Attention System of the Human Brain: 20 Years After. Annu Rev Neurosci. 35:73–89.

Peyrot WJ, Van der Auwera S, Milaneschi Y, Dolan C V., Madden PAF, Sullivan PF, Strohmaier J, Ripke S, Rietschel M, Nivard MG, Mullins N, Montgomery GW, Henders AK, Heat AC, Fisher HL, Dunn EC, Byrne EM, Air TA, Wray NR, Ripke S, Mattheisen M, Trzaskowski M, Byrne EM, Abdellaoui A, Adams MJ, Agerbo E, Air TM, Andlauer

TFM, Bacanu SA, Bækvad-Hansen M, Beekman ATF, Bigdeli TB, Binder EB, Blackwood DHR, Bryois J, Buttenschøn HN, Bybjerg-Grauholm J, Cai N, Castelao E, Christensen JH, Clarke TK, Coleman JRI, Colodro-Conde L, Couvy-Duchesne B, Craddock N, Crawford GE, Davies G, Deary IJ, Degenhardt F, Derks EM, Direk N, Dolan C V., Dunn EC, Eley TC, Escott-Price V, Farnush, Kiadeh FH, Finucane HK, Forstner AJ, Frank J, Gaspar HA, Gill M, Goes FS, Gordon SD, Grove J, Hall LS, Hansen CS, Hansen TF, Herms S, Hicki IB, Hoffmann P, Homuth G, Horn C, Hottenga JJ, Hougaard DM, Ising M, Jansen R, Jorgenson E, Knowles JA, Kohane IS, Kraft J, Kretzschmar WW, Krogh J, Kutalik Z, Li Y, Lind PA, MacIntyre DJ, MacKinnon DF, Maier RM, Maier W, Marchini J, Mbarek H, McGrath P, McGuffin P, Medland SE, Mehta D, Middeldorp CM, Mihailov E, Milaneschi Y, Milani L, Mondimore FM, Montgomery GW, Mostafavi S, Mullins N, Nauck M, Ng B, Nivard MG, Nyholt DR, O'Reilly PF, Oskarsson H, Owen MJ, Painter JN, Pedersen CB, Pedersen MG, Peterson RE, Pettersson E, Peyrot WJ, Pistis G, Posthuma D, Quiroz JA, Qvist P, Rice JP, Riley BP, Rivera M, Mirza SS, Schoevers R, Schulte EC, Shen L, Shi J, Shyn SI, Sigurdsson E, Sinnamon GCB, Smit JH, Smith DJ, Stefansson H, Steinberg S, Streit F, Strohmaier J, Tansey KE, Teismann H, Teumer A, Thompson W, Thomson PA, Thorgeirsson TE, Traylor M, Treutlein J, Trubetskoy V, Uitterlinden AG, Umbricht D, Van der Auwera S, van Hemert AM, Viktorin A, Visscher PM, Wang Y, Webb BT, Weinsheimer SM, Wellmann J, Willemsen G, Witt SH, Wu Y, Xi HS, Yang J, Zhang F, Arolt V, Baune BT, Berger K, Boomsma DI, Cichon S, Dannlowski U, de Geus EJC, DePaulo JR, Domenici E, Domschke K, Esko T, Grabe HJ, Hamilton SP, Hayward C, Heath AC, Kendler KS, Kloiber S, Lewis G, Li QS, Lucae S, Madden PAF, Magnusson PK, Martin NG, McIntosh AM, Metspalu A, Mors O, Mortensen PB, Müller-Myhsok B, Nordentoft M, Nöthen MM, O'Donovan MC, Paciga SA, Pedersen NL, Penninx BWJH, Perlis RH, Porteous DJ, Potash JB, Preisig M, Rietschel M, Schaefer C, Schulze TG, Smoller JW, Stefansson K, Tiemeier H, Uher R, Völzke H, Weissman MM, Werge T, Lewis CM, Levinson DF, Breen G, Børglum AD, Sullivan PF, Baune BT, Breen G,

Levinson DF, Lewis CM, Martin NG, Nelson EN, Boomsma DI, Grabe HJ, Wray NR, Penninx BWJH. 2018. Does Childhood Trauma Moderate Polygenic Risk for Depression? A Meta-analysis of 5765 Subjects From the Psychiatric Genomics Consortium. Biol Psychiatry. 84:138–147.

Phillips ML, Ladouceur CD, Drevets WC. 2008. A neural model of voluntary and automatic emotion regulation: Implications for understanding the pathophysiology and neurodevelopment of bipolar disorder. Mol Psychiatry. 13:833–857.

Pinheiro J, Bates D, DebRoy S, Sarkar D. 2007. nlme: Linear and Nonlinear Mixed Effects Models. R Packag version 3. 1–97.

Polter AM, Kauer J a. 2014. Stress and VTA synapses: implications for addiction and depression. Eur J Neurosci. 39:1179–1188.

Posner J, Cha J, Wang Z, Talati A, Warner V, Gerber A, Peterson BS, Weissman M. 2015. Increased Default Mode Network Connectivity in Individuals at High Familial Risk for Depression. Neuropsychopharmacology. 1–9.

Posner MI, Rothbart MK. 2000. Developing mechanisms of self-regulation. Dev Psychopathol. 12:427–441.

Power JD, Cohen AL, Nelson SM, Wig GS, Barnes KA, Church JA, Vogel AC, Laumann TO, Miezin FM, Schlaggar BL, Petersen SE. 2011. Functional Network Organization of the Human Brain. Neuron. 72:665–678.

Proudfit GH, Bress JN, Foti D, Kujawa A, Klein DN. 2015. ScienceDirect Depression and event-related potentials : emotional disengagement and reward insensitivity. Curr Opin Psychol. 4:110–113.

Rae CL, Davies G, Garfinkel SN, Gabel MC, Dowell NG, Cercignani M, Seth AK, Greenwood KE, Medford N, Critchley HD. 2017. Deficits in Neurite Density Underlie White Matter

Structure Abnormalities in First-Episode Psychosis. Biol Psychiatry. 82:716–725.

Raichle ME. 2015. The Brain's Default Mode Network. Annu Rev Neurosci. 413–427.

Raichle ME, MacLeod a M, Snyder a Z, Powers WJ, Gusnard D a, Shulman GL. 2001. A default mode of brain function. Proc Natl Acad Sci U S A. 98:676–682.

Ray Ochsner, K.N., Cooper, J.C., Robertson, E.R., Gabrielle, J.D.E. & Gross, J.J. RD. 2000. Individual differendes in trait rumination and the neural systems supporting cognitive reappraisals. Cogn Affect Behav Neurosci. 5:156–168.

Reineberg AE, Andrews-Hanna JR, Depue BE, Friedman NP, Banich MT. 2015. Resting-state networks predict individual differences in common and specific aspects of executive function. Neuroimage. 104:69–78.

Rilling JK. 2013. Neuropsychologia The neural and hormonal bases of human parental care. Neuropsychologia. 51:731–747.

Ritsher JEB, Warner V, Johnson JG, Dohrenwend BP. 2001. Inter-generational longitudinal study of social class and depression: a test of social causation and social selection models. Br J Psychiatry. 178:84s–90.

Rosenberg MD, Finn ES, Scheinost D, Papademetris X, Shen X, Constable RT, Chun MM. 2016. A neuromarker of sustained attention from whole-brain functional connectivity. Nat Neurosci. 19.

Rosenblau G, Sterzer P, Stoy M, Park S, Friedel E, Heinz A, Pilhatsch M, Bauer M, Ströhle A. 2012. Functional neuroanatomy of emotion processing in major depressive disorder is altered after successful antidepressant therapy. J Psychopharmacol. 26:1424–1433.

Rosseel Y. 2012. lavaan : an R package for structural equation modeling and more Version 0 . 5-12 ( BETA ). J Stat Softw. 48:1–36.

Royall DR, Lauterbach EC, Cummings JL, Reeve A, Rummans TA, Kaufer DI, LaFrance WC, Coffey CE. 2002. Executive control function: A review of its promise and challenges for clinical research. J Neuropsychiatry Clin Neurosci. 14:377–405.

Rubinov M, Bullmore E. 2013. Fledgling pathoconnectomics of psychiatric disorders. Trends Cogn Sci. 17:641–647.

Russ TC, Hannah J, Batty GD, Booth CC, Deary IJ, Starr JM. 2017. Childhood Cognitive Ability and Incident Dementia. Epidemiology. 28:361–364.

Russo SJ, Nestler EJ. 2013. The brain reward circuitry in mood disorders. Nat Rev Neurosci. 14:609–625.

Sacchet MD, Livermore EE, Iglesias JE, Glover GH, Gotlib IH. 2015. Subcortical volumes differentiate Major Depressive Disorder, Bipolar Disorder, and remitted Major Depressive Disorder. J Psychiatr Res. 68:91–98.

Sämann PG, Wehrle R, Hoehn D, Spoormaker VI, Peters H, Tully C, Holsboer F, Czisch M. 2011. Development of the brain's default mode network from wakefulness to slow wave sleep. Cereb Cortex. 21:2082–2093.

Sambataro F, Murty VP, Callicott JH, Tan HY, Das S, Weinberger DR, Mattay VS. 2010. Age-related alterations in default mode network: Impact on working memory performance. Neurobiol Aging. 31:839–852.

Sambataro F, Wolf ND, Pennuto M, Vasic N, Wolf RC. 2014. Revisiting default mode network function in major depression: Evidence for disrupted subsystem connectivity. Psychol Med. 44:2041–2051.

Scheiermann C, Kunisaki Y, Frenette PS. 2013. Circadian control of the immune system. Nat Rev Immunol. 13:190–198.

Schmaal L, Veltman DJ, van Erp TGM, Sämann PG, Frodl T, Jahanshad N, Loehrer E, Tiemeier H, Hofman A, Niessen WJ, Vernooij MW, Ikram MA, Wittfeld K, Grabe HJ, Block A, Hegenscheid K, Völzke H, Hoehn D, Czisch M, Lagopoulos J, Hatton SN, Hickie IB, Goya-Maldonado R, Krämer B, Gruber O, Couvy-Duchesne B, Rentería ME, Strike LT, Mills NT, de Zubicaray GI, McMahon KL, Medland SE, Martin NG, Gillespie NA, Wright MJ, Hall GB, MacQueen GM, Frey EM, Carballedo A, van Velzen LS, van Tol MJ, van der Wee NJ, Veer IM, Walter H, Schnell K, Schramm E, Normann C, Schoepf D, Konrad C, Zurowski B, Nickson T, McIntosh AM, Papmeyer M, Whalley HC, Sussmann JE, Godlewska BR, Cowen PJ, Fischer FH, Rose M, Penninx BWJH, Thompson PM, Hibar DP. 2016. Subcortical brain alterations in major depressive disorder: findings from the ENIGMA Major Depressive Disorder working group. Mol Psychiatry. 21:806–812.

Schmaal L, Yücel M, Ellis R, Vijayakumar N, Simmons JG, Allen NB, Whittle S. 2017. Brain Structural Signatures of Adolescent Depressive Symptom Trajectories: A Longitudinal Magnetic Resonance Imaging Study. J Am Acad Child Adolesc Psychiatry. 56:593–601.e9.

Schreiter S, Pijnenborg GHM. 2013. Empathy in adults with clinical or subclinical depressive symptoms. J Affect Disord. 150:1–16.

Sexton CE, Allan CL, Masurier M Le. 2012. Magnetic Resonance Imaging in Late-Life Depression. Arch Gen Psychiatry. 69:680–689.

Sexton CE, Mackay CE, Ebmeier KP. 2009. A Systematic Review of Diffusion Tensor Imaging Studies in Affective Disorders. Biol Psychiatry. 66:814–823.

Shapira-Lichter I, Oren N, Jacob Y, Gruberger M, Hendler T. 2013. Portraying the unique contribution of the default mode network to internally driven mnemonic processes. Proc Natl Acad Sci. 110:4950–4955.

Sharpe M, Hawton K, House A, Molyneux A, Sandercock P, Bamford J, Warlow C. 1990. Mood disorders in long-term survivors of stroke: Associations with brain lesion location and volume. Psychol Med. 20:815–828.

Sheffield JM, Repovs G, Harms MP, Carter CS, Gold JM, MacDonald AW, Daniel Ragland J, Silverstein SM, Godwin D, Barch DM. 2015. Fronto-parietal and cingulo-opercular network integrity and cognition in health and schizophrenia. Neuropsychologia. 73:82–93.

Sheline YI, Price JL, Vaishnavi SN, Mintun MA, Barch DM, Epstein AA, Wilkins CH, Snyder AZ, Couture L, Schechtman K, McKinstry RC. 2008. Regional white matter hyperintensity burden in automated segmentation distinguishes late-life depressed subjects from comparison subjects matched for vascular risk factors. Am J Psychiatry. 165:524–532.

Shen X, Cox SR, Adams MJ, Howard DM, Lawrie SM, Ritchie SJ, Bastin ME, Deary IJ, McIntosh AM, Whalley HC. 2018. Resting-state connectivity and its association with cognitive performance, educational attainment, and household income in UK Biobank. Biol Psychiatry Cogn Neurosci Neuroimaging. 1–9.

Shen X, Reus LM, Cox SR, Adams MJ, Liewald DC, Bastin ME, Smith DJ, Deary IJ, Whalley HC, McIntosh AM. 2017. Subcortical volume and white matter integrity abnormalities in major depressive disorder: Findings from UK Biobank imaging data. Sci Rep. 7:1–10.

Shou H, Yang Z, Satterthwaite TD, Cook PA, Bruce SE, Shinohara RT, Rosenberg B, Sheline YI. 2017. Cognitive behavioral therapy increases amygdala connectivity with the cognitive control network in both MDD and PTSD. NeuroImage Clin. 14:464–470.

Smith DJ, Nicholl BI, Cullen B, Martin D, Ul-Haq Z, Evans J, Gill JMR, Roberts B, Gallacher J, Mackay D, Hotopf M, Deary I, Craddock N, Pell JP. 2013. Prevalence and characteristics of probable major depression and bipolar disorder within UK biobank:

cross-sectional study of 172,751 participants. PLoS One. 8:e75362.

Smith SM. 2002. Fast robust automated brain extraction. Hum Brain Mapp. 17:143–155.

Smith SM, Nichols TE. 2018. Statistical Challenges in “Big Data” Human Neuroimaging NeuroView. Neuron. 97:263–268.

Smith SM, Nichols TE, Vidaurre D, Winkler AM, Behrens TEJ, Glasser MF, Ugurbil K, Barch DM, Van Essen DC, Miller KL, J Behrens TE, Glasser MF, Ugurbil K, Barch DM, Van Essen DC, Miller KL. 2015. A positive-negative mode of population covariation links brain connectivity, demographics and behavior. Nat Neurosci. 18:1–7.

Snyder HR. 2013. Major depressive disorder is associated with broad impairments on neuropsychological measures of executive function: a meta-analysis and review. Psychol Bull. 139:81–132.

Soares JC, Mann JJ. 1997. The anatomy of mood disorders—review of structural neuroimaging studies. Biol Psychiatry. 41:86–106.

Soriano-Mas C, Hernndez-Ribas R, Pujol J, Urretavizcaya M, Deus J, Harrison BJ, Ortiz H, Lpez-Sol M, Menchn JM, Cardoner N. 2011. Cross-sectional and longitudinal assessment of structural brain alterations in melancholic depression. Biol Psychiatry. 69:318–325.

Spasojević J, Alloy LB. 2001. Rumination as a common mechanism relating depressive risk factors to depression. Emotion. 1:25–37.

Sporns O. 2014. Contributions and challenges for network models in cognitive neuroscience. Nat Neurosci. 17:652–660.

Spreng RN, Grady CL. 2010. Patterns of Brain Activity Supporting Autobiographical Memory, Prospection, and Theory of Mind, and Their Relationship to the Default Mode Network.

J Cogn Neurosci. 22:1112–1123.

Spreng RN, Stevens WD, Chamberlain JP, Gilmore AW, Schacter DL. 2010. Default network activity, coupled with the frontoparietal control network, supports goal-directed cognition. Neuroimage. 53:303–317.

Sprooten E, Lymer GKS, Maniega SM, McKirdy J, Clayden JD, Bastin ME, Porteous D, Johnstone EC, Lawrie SM, Hall J, McIntosh AM. 2009. The relationship of anterior thalamic radiation integrity to psychosis risk associated neuregulin-1 variants. Mol Psychiatry. 14:237–238.

Stanek KM, Grieve SM, Brickman AM, Korgaonkar MS, Paul RH, Cohen RA, Gunstad JJ. 2011. Obesity is associated with reduced white matter integrity in otherwise healthy adults. Obesity. 19:500–504.

Starkstein SE, Robinson RG, Price TR. 1987. Comparison of cortical and subcortical lesions in the production of poststroke mood disorders. Brain. 110:1045–1059.

Stetler C, Miller GE. 2011. Depression and hypothalamic-pituitary-adrenal activation: A quantitative summary of four decades of research. Psychosom Med. 73:114–126.

Stickgold RJ, Alsop D, Gaab N, Schlaug G, Born J, Cirelli C, Greenspan RJ, Tononi G, Armstrong JD, Shaw PJ, Winther a ME, Acebes A, Ramanan N, Gutierrez CM, Heller E a, Pack a I, Abel T, Robinson DF, Suzuki Y, Vine L, Gottschalk L, Donlea JM, Hall JC, Jackson FR, Siegel RW. 2011. Sleep and Synaptic Homeostasis : Science (80- ). 1576–1581.

Sudlow C, Gallacher J, Allen N, Beral V, Burton P, Danesh J, Downey P, Elliott P, Green J, Landray M, Liu B, Matthews P, Ong G, Pell J, Silman A, Young A, Sprosen T, Peakman T, Collins R. 2015. UK Biobank: An Open Access Resource for Identifying the Causes of a Wide Range of Complex Diseases of Middle and Old Age. PLoS Med.

12:1–10.

Sullivan PF, Daly MJ, O'Donovan M. 2012. Genetic architectures of psychiatric disorders: the emerging picture and its implications. Nat Rev Genet. 13:537–551.

Sullivan PF, Neale MC, Kendler KS. 2000. Genetic Epidemiology of Major Depression: Review and Meta-Analysis. Am J Psychiatry. 157:1552–1562.

Sullivan E V., Rosenbloom MJ, Serventi KL, Deshmukh A, Pfefferbaum A. 2003. Effects of alcohol dependence comorbidity and antipsychotic medication on volumes of the thalamus and pons in schizophrenia. Am J Psychiatry. 160:1110–1116.

Szikla G, Bouvier G, Hori T, Petrov V. 2012. Angiography of the human brain cortex: atlas of vascular patterns and stereotactic cortical localization. Springer Science & Business Media.

Taylor WD, Macfall JR, Ph D, Payne ME, Mcquoid DR, Provenzale JM, Steffens DC, Krishnan KRR. 2004. Late-Life Depression and Microstructural Abnormalities in Dorsolateral Prefrontal Cortex White Matter. Am J Psychiatry. 161:1293–1296.

Toga AW, Thompson PM. 2003. Mapping brain asymmetry. Nat Rev Neurosci. 4:37–48.

Turk-Browne NB. 2013. Functional interactions as big data in the human brain. Science (80- ). 342:580–584.

Turner AD, Furey ML, Drevets WC, Zarate C, Nugent AC. 2012. Association between subcortical volumes and verbal memory in unmedicated depressed patients and healthy controls. Neuropsychologia. 50:2348–2355.

Uhr M, Tontsch A, Namendorf C, Ripke S, Lucae S, Ising M, Dose T, Ebinger M, Rosenhagen M, Kohli M, Kloiber S, Salyakina D, Bettecken T, Specht M, Pütz B, Binder EB, Müller-Myhsok B, Holsboer F. 2008. Polymorphisms in the Drug

Transporter Gene ABCB1 Predict Antidepressant Treatment Response in Depression. Neuron. 57:203–209.

van den Heuvel MP, Hulshoff Pol HE. 2010. Exploring the brain network: A review on resting-state fMRI functional connectivity. Eur Neuropsychopharmacol. 20:519–534.

van den Heuvel MP, Stam CJ, Boersma M, Hulshoff Pol HE. 2008. Small-world and scale-free organization of voxel-based resting-state functional connectivity in the human brain. Neuroimage. 43:528–539.

van den Heuvel MP, Stam CJ, Kahn RS, Hulshoff Pol HE. 2009. Efficiency of Functional Brain Networks and Intellectual Performance. J Neurosci. 29:7619–7624.

van Eijndhoven P, van Wingen G, van Oijen K, Rijpkema M, Goraj B, Jan Verkes R, Oude Voshaar R, Fernández G, Buitelaar J, Tendolkar I. 2009. Amygdala Volume Marks the Acute State in the Early Course of Depression. Biol Psychiatry. 65:812–818.

van Erp TGM, Hibar DP, Rasmussen JM, Glahn DC, Pearlson GD, Andreassen O a, Agartz I, Westlye LT, Haukvik UK, Dale a M, Melle I, Hartberg CB, Gruber O, Kraemer B, Zilles D, Donohoe G, Kelly S, McDonald C, Morris DW, Cannon DM, Corvin A, Machielsen MWJ, Koenders L, de Haan L, Veltman DJ, Satterthwaite TD, Wolf DH, Gur RC, Gur RE, Potkin SG, Mathalon DH, Mueller B a, Preda A, Macciardi F, Ehrlich S, Walton E, Hass J, Calhoun VD, Bockholt HJ, Sponheim SR, Shoemaker JM, van Haren NEM, Pol HEH, Ophoff R a, Kahn RS, Roiz-Santiañez R, Crespo-Facorro B, Wang L, Alpert KI, Jönsson EG, Dimitrova R, Bois C, Whalley HC, McIntosh a M, Lawrie SM, Hashimoto R, Thompson PM, Turner J a. 2016. Subcortical brain volume abnormalities in 2028 individuals with schizophrenia and 2540 healthy controls via the ENIGMA consortium. Mol Psychiatry. 21:547–553.

Veer IM. 2010. Whole brain resting-state analysis reveals decreased functional connectivity in major depression. Front Syst Neurosci. 4:1–10.

Vigo D, Thornicroft G, Atun R. 2018. Estimating the true global burden of mental illness. The Lancet Psychiatry. 3:171–178.

Voineskos AN, Rajji TK, Lobaugh NJ, Miranda D, Shenton ME, Kennedy JL, Pollock BG, Mulsant BH. 2012. Age-related decline in white matter tract integrity and cognitive performance: A DTI tractography and structural equation modeling study. Neurobiol Aging. 33:21–34.

Vos T, Flaxman AD, Naghavi M, Lozano R, Michaud C, Ezzati M, Shibuya K, Salomon JA, Abdalla S, Aboyans V, Abraham J, Ackerman I, Aggarwal R, Ahn SY, Ali MK, Alvarado M, Anderson HR, Anderson LM, Andrews KG, Atkinson C, Baddour LM, Bahalim AN, Barker-Collo S, Barrero LH, Bartels DH, Basáñez MG, Baxter A, Bell ML, Benjamin EJ, Bennett D, Bernabé E, Bhalla K, Bhandari B, Bikbov B, Abdulhak A Bin, Birbeck G, Black JA, Blencowe H, Blore JD, Blyth F, Bolliger I, Bonaventure A, Boufous S, Bourne R, Boussinesq M, Braithwaite T, Brayne C, Bridgett L, Brooker S, Brooks P, Brugha TS, Bryan-Hancock C, Bucello C, Buchbinder R, Buckle G, Budke CM, Burch M, Burney P, Burstein R, Calabria B, Campbell B, Canter CE, Carabin H, Carapetis J, Carmona L, Cella C, Charlson F, Chen H, Cheng ATA, Chou D, Chugh SS, Coffeng LE, Colan SD, Colquhoun S, Colson KE, Condon J, Connor MD, Cooper LT, Corriere M, Cortinovis M, De Vaccaro KC, Couser W, Cowie BC, Criqui MH, Cross M, Dabhadkar KC, Dahiya M, Dahodwala N, Damsere-Derry J, Danaei G, Davis A, De Leo D, Degenhardt L, Dellavalle R, Delossantos A, Denenberg J, Derrett S, Des Jarlais DC, Dharmaratne SD, Dherani M, Diaz-Torne C, Dolk H, Dorsey ER, Driscoll T, Duber H, Ebel B, Edmond K, Elbaz A, Ali SE, Erskine H, Erwin PJ, Espindola P, Ewoigbokhan SE, Farzadfar F, Feigin V, Felson DT, Ferrari A, Ferri CP, Fèvre EM, Finucane MM, Flaxman S, Flood L, Foreman K, Forouzanfar MH, Fowkes FGR, Franklin R, Fransen M, Freeman MK, Gabbe BJ, Gabriel SE, Gakidou E, Ganatra HA, Garcia B, Gaspari F, Gillum RF, Gmel G, Gonzalez-Medina D, Gosselin R, Grainger R, Grant B, Groeger J, Guillemin F, Gunnell D, Gupta R, Haagsma J, Hagan H, Halasa YA, Hall W, Haring D,

Haro JM, Harrison JE, Havmoeller R, Hay RJ, Higashi H, Hill C, Hoen B, Hoffman H, Hotez PJ, Hoy D, Huang JJ, Ibeanusi SE, Jacobsen KH, James SL, Jarvis D, Jasrasaria R, Jayaraman S, Johns N, Jonas JB, Karthikeyan G, Kassebaum N, Kawakami N, Keren A, Khoo JP, King CH, Knowlton LM, Kobusingye O, Koranteng A, Krishnamurthi R, Laden F, Lalloo R, Laslett LL, Lathlean T, Leasher JL, Lee YY, Leigh J, Levinson D, Lim SS, Limb E, Lin JK, Lipnick M, Lipshultz SE, Liu W, Loane M, Ohno SL, Lyons R, Ma J, Mabweijano J, MacIntyre MF, Malekzadeh R, Mallinger L, Manivannan S, Marcenes W, March L, Margolis DJ, Marks GB, Marks R, Matsumori A, Matzopoulos R, Mayosi BM, McAnulty JH, McDermott MM, McGill N, McGrath J, Medina-Mora ME, Meltzer M, Mensah GA, Merriman TR, Meyer AC, Miglioli V, Miller M, Miller TR, Mitchell PB, Mock C, Mocumbi AO, Moffitt TE, Mokdad AA, Monasta L, Montico M, Moran A, Morawska L, Mori R, Murdoch ME, Mwaniki MK, Naidoo K, Nair MN, Naldi L, Narayan KMV, Nelson PK, Nelson RG, Nevitt MC, Newton CR, Nolte S, Norman P, Norman R, O'Donnell M, O'Hanlon S, Olives C, Omer SB, Ortblad K, Osborne R, Ozgediz D, Page A, Pahari B, Pandian JD, Rivero AP, Patten SB, Pearce N, Padilla RP, Perez-Ruiz F, Perico N, Pesudovs K, Phillips D, Phillips MR, Pierce K, Pion S, Polanczyk G V., Polinder S, Pope CA, Popova S, Porrini E, Pourmalek F, Prince M, Pullan RL, Ramaiah KD, Ranganathan D, Razavi H, Regan M, Rehm JT, Rein DB, Remuzzi G, Richardson K, Rivara FP, Roberts T, Robinson C, De Leòn FR, Ronfani L, Room R, Rosenfeld LC, Rushton L, Sacco RL, Saha S, Sampson U, Sanchez-Riera L, Sanman E, Schwebel DC, Scott JG, Segui-Gomez M, Shahraz S, Shepard DS, Shin H, Shivakoti R, Singh D, Singh GM, Singh JA, Singleton J, Sleet DA, Sliwa K, Smith E, Smith JL, Stapelberg NJC, Steer A, Steiner T, Stolk WA, Stovner LJ, Sudfeld C, Syed S, Tamburlini G, Tavakkoli M, Taylor HR, Taylor JA, Taylor WJ, Thomas B, Thomson WM, Thurston GD, Tleyjeh IM, Tonelli M, Towbin JA, Truelsen T, Tsilimbaris MK, Ubeda C, Undurraga EA, Van Der Werf MJ, Van Os J, Vavilala MS, Venketasubramanian N, Wang M, Wang W, Watt K, Weatherall DJ, Weinstock MA, Weintraub R, Weisskopf MG, Weissman MM, White RA, Whiteford H, Wiebe N,

Wiersma ST, Wilkinson JD, Williams HC, Williams SRM, Witt E, Wolfe F, Woolf AD, Wulf S, Yeh PH, Zaidi AKM, Zheng ZJ, Zonies D, Lopez AD, Murray CJL, Moradi-Lakeh M. 2012. Years lived with disability (YLDs) for 1160 sequelae of 289 diseases and injuries 1990-2010: A systematic analysis for the Global Burden of Disease Study 2010. Lancet. 380:2163–2196.

Vossel S, Geng JJ, Fink GR. 2014. Dorsal and Ventral Attention Systems. Neurosci. 20:150–159.

Vythilingam M, Vermetten E, Anderson GM, Luckenbaugh D, Anderson ER, Snow J, Staib LH, Charney DS, Bremner JD. 2004. Hippocampal volume, memory, and cortisol status in major depressive disorder: Effects of treatment. Biol Psychiatry. 56:101–112.

Wager TD, Davidson ML, Hughes BL, Lindquist MA, Ochsner KN. 2008. Prefrontal-Subcortical Pathways Mediating Successful Emotion Regulation. Neuron. 59:1037–1050.

Wagner AD, Maril A, Bjork RA, Schacter DL. 2001. Prefrontal contributions to executive control: fMRI evidence for functional distinctions within lateral prefrontal cortex. Neuroimage. 14:1337–1347.

Wagner G, Koch K, Schachtzabel C, Schultz CC, Sauer H, Schl??sser RG. 2011. Structural brain alterations in patients with major depressive disorder and high risk for suicide: Evidence for a distinct neurobiological entity? Neuroimage. 54:1607–1614.

Wakana S, Jiang H, Nagae-Poetscher LM, van Zijl PCM, Mori S. 2004. Fiber tract-based atlas of human white matter anatomy. Radiology. 230:77–87.

Walsh ND, Williams SCR, Brammer MJ, Bullmore ET, Kim J, Suckling J, Mitterschiffthaler MT, Cleare AJ, Pich EM, Mehta MA, Fu CHY. 2007. A Longitudinal Functional Magnetic Resonance Imaging Study of Verbal Working Memory in Depression After

Antidepressant Therapy. Biol Psychiatry. 62:1236–1243.

Weissman DH, Roberts KC, Visscher KM, Woldorff MG. 2006. The neural bases of momentary lapses in attention. Nat Neurosci. 9:971–978.

Weissman MM. 1996. Cross-National Epidemiology of Major Depression and Bipolar Disorder. JAMA J Am Med Assoc. 276:293.

Wen MC, Steffens DC, Chen MK, Zainal NH. 2014. Diffusion tensor imaging studies in late-life depression: systematic review and meta-analysis. Int J Geriatr Psychiatry. 29:1173–1184.

Wen T, Liu DC, Hsieh S. 2018. Connectivity patterns in cognitive control networks predict naturalistic multitasking ability. Neuropsychologia. 114:195–202.

Whalley H, Harris M, Shen X, Gibson J, Lawrie S, McIntosh1 A. 2018. S130. Dissecting the Neuroimaging Phenotype of Major Depressive Disorder Based on Genetic Loading for Schizophrenia. Biol Psychiatry. 83:S398.

Whalley HC, Sprooten E, Hackett S, Hall L, Blackwood DH, Glahn DC, Bastin M, Hall J, Lawrie SM, Sussmann JE, McIntosh AM. 2013. Polygenic risk and white matter integrity in individuals at high risk of mood disorder. Biol Psychiatry. 74:280–286.

Wheeler AL, Chakravarty MM, Lerch JP, Pipitone J, Daskalakis ZJ, Rajji TK, Mulsant BH, Voineskos AN. 2014. Disrupted prefrontal interhemispheric structural coupling in Schizophrenia related to working memory performance. Schizophr Bull. 40:914–924.

Whitton AE, Treadway MT, Pizzagalli DA. 2015. Reward processing dysfucntion in major depression bipolar disorder and schizophrenia. Curr Opin Psychiatry. 28:7–12.

Winokur A, DeMartinis NA, McNally DP, Gary EM, Cormier JL, Gary KA. 2003. Comparative effects of mirtazapine and fluoxetine on sleep physiology measures in patients with

major depression and insomnia. J Clin Psychiatry. 64:1224–1229.

World Health Organization. 2017. Depression and other common mental disorders: global health estimates, World Health Organization.

Wray NR, Lee SH, Mehta D, Vinkhuyzen AAE, Dudbridge F, Middeldorp CM. 2014. Research Review: Polygenic methods and their application to psychiatric traits. J Child Psychol Psychiatry. 55:1068–1087.

Wray NR, Maier R. 2014. Genetic Basis of Complex Genetic Disease: The Contribution of Disease Heterogeneity to Missing Heritability. Curr Epidemiol Reports. 1:220–227.

Wray NR, Ripke S, Mattheisen M, Trzaskowski M, Byrne EM, Abdellaoui A, Adams MJ, Agerbo E, Air TM, Andlauer TMF, Bacanu SA, Bækvad-Hansen M, Beekman AFT, Bigdeli TB, Binder EB, Blackwood DRH, Bryois J, Buttenschøn HN, Bybjerg-Grauholm J, Cai N, Castelao E, Christensen JH, Clarke TK, Coleman JIR, Colodro-Conde L, Couvy-Duchesne B, Craddock N, Crawford GE, Crowley CA, Dashti HS, Davies G, Deary IJ, Degenhardt F, Derks EM, DIrek N, Dolan C V., Dunn EC, Eley TC, Eriksson N, Escott-Price V, Kiadeh FHF, Finucane HK, Forstner AJ, Frank J, Gaspar HA, Gill M, Giusti-Rodríguez P, Goes FS, Gordon SD, Grove J, Hall LS, Hannon E, Hansen CS, Hansen TF, Herms S, Hickie IB, Hoffmann P, Homuth G, Horn C, Hottenga JJ, Hougaard DM, Hu M, Hyde CL, Ising M, Jansen R, Jin F, Jorgenson E, Knowles JA, Kohane IS, Kraft J, Kretzschmar WW, Krogh J, Kutalik Z, Lane JM, Li Y, Li Y, Lind PA, Liu X, Lu L, MacIntyre DJ, MacKinnon DF, Maier RM, Maier W, Marchini J, Mbarek H, McGrath P, McGuffin P, Medland SE, Mehta Di, Middeldorp CM, Mihailov E, Milaneschi Y, Milani L, Mill J, Mondimore FM, Montgomery GW, Mostafavi S, Mullins N, Nauck M, Ng B, Nivard MG, Nyholt DR, O'Reilly PF, Oskarsson H, Owen MJ, Painter JN, Pedersen CB, Pedersen MG, Peterson RE, Pettersson E, Peyrot WJ, Pistis G, Posthuma D, Purcell SM, Quiroz JA, Qvist P, Rice JP, Riley BP, Rivera M, Saeed Mirza S, Saxena R, Schoevers R, Schulte EC, Shen L, Shi J, Shyn SI, Sigurdsson E,

Sinnamon GBC, Smit JH, Smith DJ, Stefansson H, Steinberg S, Stockmeier CA, Streit F, Strohmaier J, Tansey KE, Teismann H, Teumer A, Thompson W, Thomson PA, Thorgeirsson TE, Tian C, Traylor M, Treutlein J, Trubetskoy V, Uitterlinden AG, Umbricht D, Van Der Auwera S, Van Hemert AM, Viktorin A, Visscher PM, Wang Y, Webb BT, Weinsheimer SM, Wellmann J, Willemsen G, Witt SH, Wu Y, Xi HS, Yang J, Zhang F, Arolt V, Baune BT, Berger K, Boomsma DI, Cichon S, Dannlowski U, De Geus ECJ, Depaulo JR, Domenici E, Domschke K, Esko T, Grabe HJ, Hamilton SP, Hayward C, Heath AC, Hinds DA, Kendler KS, Kloiber S, Lewis G, Li QS, Lucae S, Madden PFA, Magnusson PK, Martin NG, McIntosh AM, Metspalu A, Mors O, Mortensen PB, Müller-Myhsok B, Nordentoft M, Nöthen MM, O'Donovan MC, Paciga SA, Pedersen NL, Penninx BWJH, Perlis RH, Porteous DJ, Potash JB, Preisig M, Rietschel M, Schaefer C, Schulze TG, Smoller JW, Stefansson K, Tiemeier H, Uher R, Völzke H, Weissman MM, Werge T, Winslow AR, Lewis CM, Levinson DF, Breen G, Børglum AD, Sullivan PF. 2018. Genome-wide association analyses identify 44 risk variants and refine the genetic architecture of major depression. Nat Genet.

Wray NR, Yang J, Hayes BJ, Price AL, Goddard ME, Visscher PM. 2013. Pitfalls of predicting complex traits from SNPs. Nat Rev Genet. 14:507–515.

Wu QZ, Li DM, Kuang WH, Zhang TJ, Lui S, Huang XQ, Chan RCK, Kemp GJ, Gong QY. 2011. Abnormal regional spontaneous neural activity in treatment-refractory depression revealed by resting-state fMRI. Hum Brain Mapp. 32:1290–1299.

Wunderlich K, Beierholm UR, Bossaerts P, O'Doherty JP. 2011. The human prefrontal cortex mediates integration of potential causes behind observed outcomes. J Neurophysiol. 106:1558–1569.

Xu J, Li Y, Lin H, Sinha R, Potenza MN. 2013. Body mass index correlates negatively with white matter integrity in the fornix and corpus callosum: A diffusion tensor imaging study. Hum Brain Mapp. 34:1044–1052.

Yehuda R, Halligan SL, Golier JA, Grossman R, Bierer LM. 2004. Effects of trauma exposure on the cortisol response to dexamethasone administration in PTSD and major depressive disorder. Psychoneuroendocrinology. 29:389–404.

Yirmiya R, Rimmerman N, Reshef R. 2015. Depression as a Microglial Disease. Trends Neurosci. 38:637–658.

Young KA, Manaye KF, Liang CL, Hicks PB, German DC. 2000. Reduced number of mediodorsal and anterior thalamic neurons in schizophrenia. Biol Psychiatry. 47:944–953.

Young KA, Ph D, Holcomb LA, Ph D, Yazdani U, Hicks PB, Ph D, German DC, Ph D. 2004. Elevated Neuron Number in the Limbic Thalamus in Major Depression. Am J Psychiatry. 161:1270–1277.

Zhang H, Schneider T, Wheeler-Kingshott CA, Alexander DC. 2012. NODDI: Practical in vivo neurite orientation dispersion and density imaging of the human brain. Neuroimage. 61:1000–1016.

Zhang Y, Brady M, Smith S. 2001. Segmentation of brain MR images through a hidden Markov random field model and the expectation-maximization algorithm. Med Imaging, IEEE Trans. 20:45–57.

Zheng Z, Shemmassian S, Wijekoon C, Kim W, Bookheimer SY, Pouratian N. 2014. DTI correlates of distinct cognitive impairments in Parkinson’s disease. Hum Brain Mapp. 35:1325–1333.

Zhu CZ, Zang YF, Cao QJ, Yan CG, He Y, Jiang TZ, Sui MQ, Wang YF. 2008. Fisher discriminative analysis of resting-state brain function for attention-deficit/hyperactivity disorder. Neuroimage. 40:110–120.

Zou QH, Zhu CZ, Yang Y, Zuo XN, Long XY, Cao QJ, Wang YF, Zang YF. 2008. An

improved approach to detection of amplitude of low-frequency fluctuation (ALFF) for resting-state fMRI: Fractional ALFF. J Neurosci Methods. 172:137–141.